GETTING BELOW THE SURFACE: DENSITY ESTIMATION METHODS FOR DEEP DIVING ANIMALS USING SLOW AUTONOMOUS UNDERWATER VEHICLES

Kalliopi Charitomeni Gkikopoulou

A Thesis Submitted for the Degree of PhD
at the
University of St Andrews

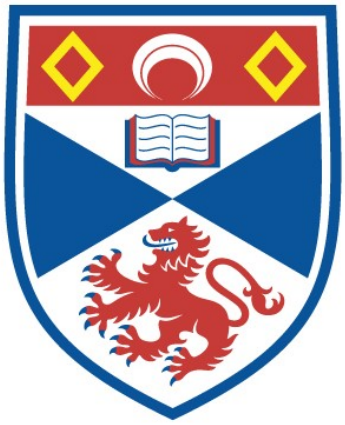

2018

Getting below the surface: density estimation methods for deep diving animals using slow autonomous underwater vehicles

Kalliopi Charitomeni Gkikopoulou

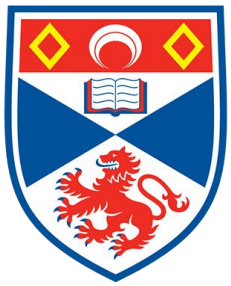

University of
St Andrews

This thesis is submitted in partial fulfilment for the degree of

Doctor of Philosophy (PhD)

at the University of St Andrews

November 2017

Free education for all…

Candidate's declaration

I, Kalliopi Charitomeni Gkikopoulou, do hereby certify that this thesis, submitted for the degree of PhD, which is approximately 51,000 words in length, has been written by me, and that it is the record of work carried out by me, or principally by myself in collaboration with others as acknowledged, and that it has not been submitted in any previous application for any degree.

I was admitted as a research student at the University of St Andrews in March 2013.

I, Kalliopi Charitomeni Gkikopoulou, received assistance in the writing of this thesis in respect of grammar, spelling and syntax, which was provided by Carl Robert Donovan, Esther Lane Jones.

I received funding from an organisation or institution and have acknowledged the funder(s) in the full text of my thesis.

Date Kalliopi Charitomeni Gkikopoulou

Supervisor's declaration

I hereby certify that the candidate has fulfilled the conditions of the Resolution and Regulations appropriate for the degree of PhD in the University of St Andrews and that the candidate is qualified to submit this thesis in application for that degree.

Date

Prof. Peter L. Tyack Dr. Douglas M. Gillespie

Dr. Mark Johnson Dr Sophie Smout

Permission for publication

In submitting this thesis to the University of St Andrews we understand that we are giving permission for it to be made available for use in accordance with the regulations of the University Library for the time being in force, subject to any copyright vested in the work not being affected thereby. We also understand, unless exempt by an award of an embargo as requested below, that the title and the abstract will be published, and that a copy of the work may be made and supplied to any bona fide library or research worker, that this thesis will be

electronically accessible for personal or research use and that the library has the right to migrate this thesis into new electronic forms as required to ensure continued access to the thesis.

I, Kalliopi Charitomeni Gkikopoulou, confirm that my thesis does not contain any third-party material that requires copyright clearance.

The following is an agreed request by candidate and supervisor regarding the publication of this thesis:

Printed copy and Electronic copy

Embargo on all of print copy for a period of 1 year on the following ground(s):

- Publication would preclude future publication

Title and Abstract

- I agree to the title and abstract being published.

Date Kalliopi Charitomeni Gkikopoulou

Prof Peter L. Tyack Dr. Douglas M. Gillespie

Dr. Mark Johnson Dr. Sophie Smout

Underpinning Research Data or Digital Outputs

Candidate's declaration

I, Kalliopi Charitomeni Gkikopoulou, hereby certify that no requirements to deposit original research data or digital outputs apply to this thesis and that, where appropriate, secondary data used have been referenced in the full text of my thesis.

Date Kalliopi Charitomeni Gkikopoulou

Abstract

Underwater gliders can provide an alternative cost-effective platform for passive acoustic monitoring surveys, compared to boat surveys, for abundance estimation and to collect high resolution environmental data for habitat studies. Gliders are usually equipped with one acoustic sensor, which limits the methods available for abundance estimation from acoustic data. Estimation of parameters used in distance sampling methodology, such as the detection function and cue rates, must be estimated separately from the glider deployment. A methodology for deriving the acoustic detection function of vocal animals is demonstrated in chapter 2with a combined biologging and passive acoustic experiment. The methodology consists of distance estimation of the clicks produced by the tagged animal and detected at acoustic receivers placed at different depths, using surface bounce detections to estimate range. In addition, different detection algorithms were tested for the detectability of Blainville's beaked whales. Detectability was found to vary with depth for Blainville's beaked whales in the area of El Hierro (Canary Islands). The depth dependent detectability for this species was tested further in chapter 3 with a wider dataset from two different geographic populations of Blainville's beaked whales, those of El Hierro and the Bahamas. Differences in detectability were found using depth and animal movement data as recorded on the DTAG in a simulated network of receivers placed at different depths. In addition, sequences of clicks, called click scans, were tested as an additional "cue" for cue counting methodology. The high directionality of beaked whale regular clicks leads to reduced detection ranges for receivers close to the surface or for receivers placed much deeper than the foraging depths of the whales and this reduction translates into varying lengths and numbers of detected click clusters as a function of distance and receiver depth. Chapter 4 presents a method for estimating density of animals from underwater gliders and tests the method in a simulated glider survey using different distribution and density scenarios using clicks and click scans as cue for density estimation.

Acknowledgements

I am grateful to my supervising team; Peter Tyack, Doug Gillespie, Mark Johnson and Sophie Smout (and Phil Hammond who was initially in the team and during the PhD candidate interview). I want to thank Peter Tyack in particular for his great spirit, uplifting discussions and always bringing inspiration, especially at the start of my PhD where motivation was hiding under my desk and for transforming my unconnected thoughts to an interesting story. His positivity and help was indispensable. Next, I would like to thank Mark Johnson for just being Mark Johnson, a diamond: tough and pure. Our journey was like climbing a mountain without the right boots … at the start almost bleeding due to my incapability of being a "right" student and feeling intimidating from his mask of "grumpy pants" that soon realized that is just a way to reserve priceless time for good work and unique ideas. I am grateful to Doug Gillespie for being a unique combination of a neural computer and caring and understanding human being. His ability to see mistakes in my code helped me a lot (of course). His physicists way of thinking keep me grounded, just like gravity. I want to thank him as well for giving me the opportunity to allow me to swear, making life easier as a Greek. A "reality check" from now on will be my friend… Thank you Sophie, for coming to the supervising team and bring the glue that at the beginning was missing, for your continuously positive vibes and wiliness to help.

Thanks to

Natacha Aguilar de Soto, for providing me with her valuable dataset that derived from her passion for science, life and creativity.

Rene Swift, Franscesco and Mark Johnson for building the recorders that were going to bring valuable data. Poseidon as always had other plans than the ones that humans expected and most of our glider deployments were unsuccessful, but like any other innovative idea and technology there are always failures and I am more than ok with failure.

Prof. Jason Matthiopoulos, because he was the reason I entered SMRU 8 years ago, providing me with a great supervision time and an opportunity to continue my studies. Alexandros Frantzis being the first person to give me the opportunity to see and work with marine mammals, another passionate soldier of marine mammal science, I am grateful to him and I hope to bring some of the gained knowledge back to the sunny and blue seas.

Esther Lane Jones for being my PhD partner during the last months of the PhD and with the everyday communication and updates she kept the spirit going.

those that gave me the opportunity to do fieldwork that was not part of my PhD, Mark Jonson and Natacha Aguilar de Soto, Luke Rendel, Alexis Frantzis, Esmeralda Quiros Guerrero and those that conversations started with “Lets imagine that you have a glider… or that there is a whale in the water”, Iosu Paradinas, Carl Donovan and Jamie MacAulay.

all my computer power fairies, Carl Donovan, Debbie Russel, Esther Jones, Doug Gillespie, Guest SMRU, Claire Elvins for providing with RAM and processors to run again and again the simulations, without them I would have finished maybe never.
Carl Donovan and Len Thomas for giving me a quiet space in CREEM for writing and being away for social biologists and being closer to anti-social statisticians.
Lastly I want to thank chaos is everywhere around us, yet things still keep going, thanks SUN for exploding and giving life and consciousness to amazing evolving earthlings… and to all my friends that are mostly aliens - Debbie, Esme, Heather, Joao, Iosu, Trias, Rich, Matt, Carl, Charles, Luca, Joao, Heather! And at specific second JESS my rainbow unicorn… Lammas and hobbits… and the last hobbit for all his support … “sup.. port ?!”

Lastly, every word that is written in the thesis is dedicated to every hour that I have spent with Lucia.
And every letter for every hour that I will spend in the future

Just because magic is possible.

Funding

This work was supported by the Natural Environment Research Council (NERC) [grant number NE/J020176/1] project name “Monitoring Marine Mammals from Autonomous Underwater Vehicles”.

and the Office of Naval Research (ONR) [grant number N000141612973] as part of the project “Estimating beaked whale density from passive acoustic recordings”.

Preface

"Ever tried. Ever failed. No matter. Try Again. Fail again. Fail better." Samuel Becket. Scientific experiments could not have been described better than by an Irish playwright.

Failure is an unavoidable aspect of trying new experimental techniques, exploring new grounds, and testing new ideas. Here, a failure to deliver on the initial proposal for a PhD, which derived from adapting to a continuous lack of data, transformed into an equally useful project (at least as I see it) exploring the use of gliders as a new platform for density estimation and habitat preference studies.

The initial PhD plan derived as an outcome of NERC's call for incorporating different types of sensors on already existing autonomous vehicles, underwater gliders. A successful proposal to incorporate acoustic recorders into gliders for the passive acoustic detection of marine mammals led to the initial proposal for the PhD: "Getting below the surface: modelling marine mammal habitat use using deep water oceanographic parameters". The detected sounds from the planned deployments would have been used to develop statistical models of habitat use for the species detected in the area where the gliders were deployed. Through the course of the PhD the plan changed a couple of times, with the final title of the PhD being: "Getting below the surface: density estimation methods for marine mammals using underwater autonomous gliders."

The change to the content of the PhD resulted from the lack of data from several glider deployments. The 6-month duration of glider deployments was dictated by the glider operator, SAMs, and trial deployments were not possible to test the sound recording system on the glider platforms before a long-term deployment. As a consequence, the first couple of deployments came back with no more than few days of data due to a software bug on the recording system that was triggered by the depth trajectory of the glider. More extensive tests of the recording equipment would have been desirable, but limitations in time and communication didn't allow that. The "Lack of data" can be seen as a result of human and random factors. Within the human factors, I consider "communication", "responsibility" and "project owning". Communication between the different institutes should have been tighter, though I initially, as a new PhD student, thought the main responsibility for keeping communication between the glider owners and ourselves was more the responsibility of people more senior than myself. Within the random factors of course comes whatever we cannot predict, and that is battery and recorder explosions, caused by incorrect cable

connections and battery failure. Again, the duration of the gliders, which was 6 months each, would not allow for rapid recovery from such mistakes.

If it was to repeat everything again, I would make sure that someone from our project was present with the glider group to install and test equipment prior to deployments. I would hope that more extensive tests of our equipment would allow to capture some of the bugs though not all. If it was to repeat again. I would Try again. No matter what. I would fail again. I would fail better.

CHAPTER 1

General introduction

1.1 PhD Overview

The increasing use of underwater gliders for oceanographic research in combination with the increasing storage capabilities of acoustic sensors has resulted in a rising usage of underwater autonomous vehicles for marine mammal research (Baumgartner et al., 2008). The use of any new platform for passive acoustic monitoring for marine mammals requires assessment. Gliders survey at a range of depths where many cetaceans produce vocalizations in order to forage, navigate and communicate. By contrast, traditional surveys use boats that tow arrays close to the surface or use fixed sensors to sample at one predefined depth. The vertical excursion of gliders gives the opportunity to sample a range of depths, extending the methodology to estimate density, but the slow speed of gliders may violate assumptions of standard line transect or point sampling methods for estimating density.

This thesis investigates the use of underwater gliders as a platform for passive acoustic density estimation for cetaceans. Specifically, it considers the Blainville's beaked whale, *Mesoplodon densirostris* as an animal model, due to the deep diving behaviour and acoustically distinctive characteristics of the vocalizations of this species. The thesis then examines parameters required to use gliders as a platform for density estimation, such as the acoustic detection function and cue rates. Finally, a method for estimating density from acoustic data collected from gliders is proposed and the method is tested in simulation framework.

This chapter introduces the motivations for surveying marine mammals, such as population estimation and conservation. Then methods to estimate abundance methods based on acoustic data are presented. Then factors influencing density estimation from acoustic data are given, with presentations on detection theory and the passive sonar equation. Finally, an overview of the use of gliders as a passive acoustic platform is

presented. The introduction finishes with the PhD thesis objectives and a short summary of each of the following chapters.

1.2 Motivation

Surveys are an important tool to inform management about the status of wildlife populations, whether the management goal is to maintain sustainable yields of exploited species or to identify risk to protected populations. Many survey methods are based on visual sightings of animals, but some animals are more easily heard than seen, so methods have been recently developed to adapt passive acoustic monitoring (PAM) for surveys (Mellinger et al., 2007). This thesis explores the use of PAM on underwater autonomous vehicles for surveys of vocal marine mammals.

The motivation for this thesis is to evaluate slow autonomous vehicles (AUVs) as acoustic platforms for abundance estimation of marine mammals. The specific AUV considered throughout this thesis is the *glider*, which is described in Section 1.4. I derive analytical methods for abundance estimation using acoustic detection data from gliders, identify the key parameters and then also the means to estimate these parameters in the field. The methodology and its efficacy are illustrated for Blainville's beaked whales.

Acoustic monitoring can be a cheap, efficient way to derive estimates of population size, especially for highly vocal animals such as marine mammals and more specifically the cetaceans. Slow-moving AUVs pose challenges for line transect methods, but they also offer advantages, such as low flow noise. Gliders in particular have low self-noise in comparison to ships or faster AUVs that produce propeller noise. Gliders also give the opportunity to survey large spatial and temporal scales by remaining in the water for long periods of up to months at a time. This persistence of gliders and their low noise make them a promising potential cost-effective tool to sample animals that spend most of their time underwater.

In this chapter, I present the historical development of population estimation methods, particularly in the context of marine mammals, which are challenging because they are not visible for much of the time when they submerge. Included in this review are biological motivations for estimating the population size of a species. Following this, I

introduce abundance estimation methods, focusing on PAM surveys applied to marine mammals. Finally, factors that influence the density estimated from acoustic methods are considered – factors such as vocalization rates of marine mammals, equipment and detection methods, and characteristics of sound transmission in the water.

1.2.1 Drivers for population estimation

Fishing is a major source of food for humans and, since ancient times, has provided employment and economic benefits. It was thought for centuries that marine fisheries could not be exhausted, but the advent of steam trawlers led fishers to complain about declining fish stocks. This led in the 1880s to collection of statistics on the amount of fish landed and the fishing effort (Thurstan et al., 2010). Changes in the catch per unit effort are important for the classic management of fisheries. Records of whaling catches assisted efforts to maximize catches, and documented shifts in the catch from the most profitable species to less profitable as it became harder to catch the most profitable species (Rocha et al., 2015). This process reduced some cetacean populations down to 14% of their pre-industrial levels (Springer et al., 2003).

Recognition of the impact of whaling on cetacean populations led to the creation of International Whaling Commission (IWC), primarily to assist in decisions for catch limits through the Regulation of Whaling (1946). The process for managing the take of whales was progressively changed through time to reflect environmental concerns of a number of the IWC member states, moving away from its original role of sustainable harvesting. This eventually led to the proposal and implementation of the commercial whaling moratorium from 1985\1986, which is still in place today. A major contributor to the recovery of whale populations was the banning of commercial whaling. However, with the loss of catch statistics, sighting-survey methods became more important for obtaining abundance estimates of whale stocks (Freeman, 2008).

Another factor that reduces cetacean populations is the interaction of marine mammals with fisheries, either by physical contact with fishing gear or interaction through trophic levels (Read et al., 2006). Bycatch (Alverson et al., 1994), from fishing activities has been described as the most serious direct threat to cetaceans globally, now that whaling is reduced (IWC 2001). Cetacean bycatch is mainly caused by entanglement in fishing

gear, affecting cetaceans from small species such as vaquita (D'Agrosa et al., 2000) and Hector's dolphin (Rayment et al., 2011) up to large whales, and from local fisheries up to large scale industrial operations. Global bycatch estimates of marine mammals reveal the importance of the issue and the need for conservation planning (Read et al., 2006).

Recognition that marine mammal populations might be reduced by both whaling and interaction with fisheries demonstrates the need for improved management strategies. However, there are substantive challenges in estimating the actual scale of population reduction from whaling and bycatch – due partly to incomplete and even falsified whaling records (Rocha et al., 2015) or from a general lack of reporting for bycatch events (Read et al., 2006).

1.2.2 Conservation of marine mammals

One of the main goals of conservation biology is to maintain biodiversity and prevent the extinction of species. Globally, the International Union for Conservation of Nature (IUCN) has the leading role for identifying and documenting species that are in need of protection and for providing an index of biodiversity globally and locally. The importance of marine mammal conservation is further supported by national governmental institutions such as the Joint Nature Conservation Committee (JNCC), which supplies the UK government with advice for the protection of marine mammals. In the U.S. the Marine Mammal Protection Act (MMPA) mandates protection and conservation of all marine mammals nationally and internationally (NMFS, 2012). Two agreements under the Bonn Convention protect cetaceans: the ACCOBAMS agreement for the Mediterranean Sea and Contiguous Atlantic Area, and the ASCOBANS agreement for the Baltic, North East Atlantic, Irish and North Seas. European programs for the protection of species such as the Habitats Directive (1992 Council Directive 92/43/EEC) also have been established for the conservation of both natural habitats and of wild fauna and flora. This directive aims to promote the maintenance of biodiversity, whilst taking in to account economic, social, cultural and regional requirements. Cetaceans are protected under Annex IV of the Habitats Directive.

Meeting the conservation mandates of national and international organisations requires estimates of the size of marine mammal populations. The IUCN assessment of the status

of all mammals depends upon information about their population abundance (Schipper et al., 2008). The regulations for establishing allowable incidental takes of marine mammals in the US also require estimates of minimum population size (Wade, 1998). Knowledge of population size also assists with research on population dynamics and species interactions (Hammond, 2010). Estimating the number of animals in an area is important for ecology and conservation biology Hammond, 2010), and information on trends in population size supports efforts to quantify the impact of anthropogenic activities on a wildlife population. The ability to identify which marine mammal populations are at risk from hazards such as pollution or noise depends upon comparing the geographical distribution of the hazard with that of the population (Harwood 2000). This makes it crucial to have a clear understanding of wildlife habitat and to model and predict animal distribution and abundance. Therefore, the ability to manage and conserve wildlife depends heavily on knowledge of where the animals are, why they are there, and how many there are. In particular, the abundance of a species is needed to assess conservation status and prioritize management actions (Hammond, 2010).

1.3 Animal abundance and distance sampling theory

There are various methods of estimating population size, from counting animals or their cues, catch-effort models, capture-recapture methods, to more sophisticated analytical methods that take into account the detectability of animals and their signals as a function of the environment and/or how animals are actually detected (Schwarz & Seber, 1999). Distance sampling is a widely used technique for estimating the size or density of biological populations (Thomas et al., 2010) and an overview of the method will be presented below.

1.3.1 Quadrat method

Ideally, to estimate the size of a population one would count all the animals that occupy the area of interest, though that is almost impossible for most species. If the number of animals in an area A cannot be counted, then it is possible to count the number of

animals in a sample of that area, a; this is known as the quadrat method. Then the estimated density D becomes

$$\hat{D} = \frac{n}{a} \tag{1.1}$$

Where n is the number of animals detected in each quadrat, and a is the area sampled. Similar to the quadrat method is the strip transect sampling and the point counts.

1.3.2 Strip transect sampling

Strip transect sampling is similar to the quadrat method, but the quadrats are long strips, where the observer travels along the centreline of the strip. For an area *A*, there is a number of strips, *k*, where an observer counts everything on the strips. Each strip has a half-strip of size *w*, which is also known as the truncation distance. Then the estimated density can be estimated by

$$\hat{D} = \frac{n}{2wkL} \tag{1.2}$$

where *n* is the number of animals detected in all the strips, *L* is the total length of the strips and $2wL$ is the area surveyed.

1.3.3 Point counts

Point counts out to a maximum distance *w* (as in strip transect sampling) are a form of quadrat sampling, assuming that all objects within w of each point are detected. For *k* points placed randomly in an area *A*, then density can be estimated by

$$\hat{D} = \frac{n}{k\pi w^2} \tag{1.3}$$

where *n* is the number of objects detected over the *k* points, out to a distance *w* from each point, giving a sampled area of $k\pi w^2$.

1.3.4 Distance sampling

For both strip transect sampling and point counts, there is a strong assumption that all objects inside the strips and maximum distance are counted. This assumption is not

realistic for most surveys, as some objects may be missed during the survey. A statistical method to account for the number of objects missed inside the survey area, either $2wL$ for strip transect sampling or $k\pi w^2$ for point counts, is the distance sampling approach. As is indicated by its name, distance sampling makes use of the distances to the detected objects to account for detectability from the centreline of the strip or centre of the area sampled under point sampling (Buckland et al., 2001).

When it is not possible to count all the animals along a strip transect or within the area of a point count, the proportion of missed animals must be estimated to derive estimates of the density within the sampling area and hence within the total area of interest *A*. To do so, a parameter *P* must be estimated that represents the proportion of all animals in the sampling area that were detected. This can be used to account for the proportion of animals that were missed in the strip or in the area around the point, for strip and point sampling (Fig 1.1). The parameter *P* can be estimated through distance sampling approach.

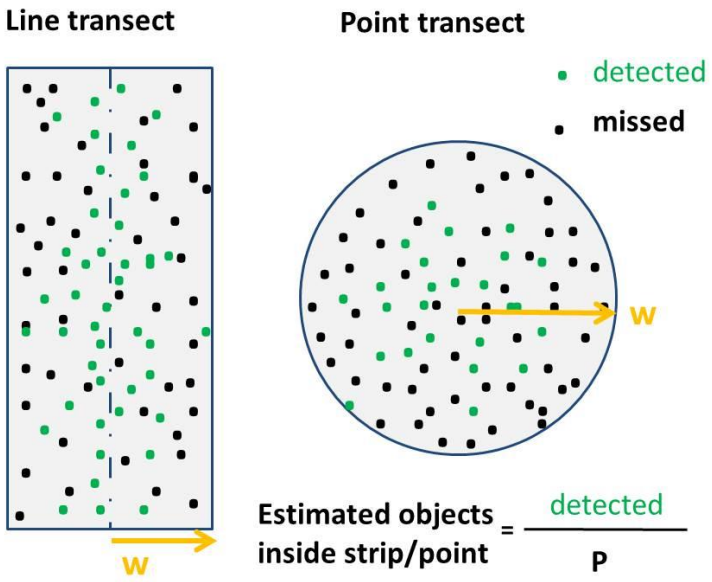

Figure 1.1 Line transect and Point sampling. Green dots are the objects detected and black dots are the objects missed, w is the half strip width for line-transect and maximum distance for point-transect sampling. The parameter P is the proportion of detected animals out of the total number of animals in the area.

In distance sampling methodology, an observer estimates the distances from the line or centre point out to detected animals, clusters of animals or their cues. The estimated distances then can be used to model the probability of detection as a function of distance from the line or point, which eventually can be used for population size estimation

(Buckland et al., 2001; Schwarz & Seber, 1999). For both line and point sampling three assumptions are required:

1) All the animals are detected along the line and on the point which means that the probability of detection at zero distance from the line and the point equals 1, *g(0)=1* where *g(x)* is the detection function i.e. the probability of detection as a function of distance *x*.

2) Animals are detected at their initial location, prior to any movement in relation to the observer or observation platform

3) Distances are measured accurately.

All the three assumptions listed above are important for estimating the detection function, which is the central concept of distance sampling (Buckland et al., 2001). The detection function is used to estimate the parameter *P*, which is the proportion of animals missed in either case of strip-transect survey and point counts (Fig. 1.1).

The most common form of distance sampling is line transect sampling (Thomas et al., 2010), in which a survey region is sampled by sighting along a number of lines placed randomly or systematically within the surveyed area. The perpendicular distances measured from the line to the animals can be used to estimate the proportion of animals in the strip that is detected and further to estimate animal density and abundance. The density then is estimated by

$$\hat{D} = \frac{n}{2wL\hat{P}_a} \tag{1.4}$$

where n is the number of detected objects, *L* is the length of the lines, *w* is the truncation distance and $\hat{P}_a$ is the proportion of objects detected from the population. For line transects the $\hat{P}_a$ is estimated by

$$P_a = \int_0^w xg(x)dx \tag{1.5}$$

where *g(x)* is the detection function at horizontal distance *x* (Buckland et al., 2001) i.e. the probability of detecting an object as a function of distance given that the object is there.

Point transect sampling is similar to line transect sampling, except the observer samples the surveyed area based on a set of random or systematically placed points instead of lines (Buckland et al., 2001). Point transect sampling is common for bird surveys

(Buckland, 2006) and for cryptic animals in terrain that is difficult to access (Ruette, et al., 2003). In point-transect sampling an observer measures the distance r_i from the point to each of the objects detected. For a *k* number of points and a maximum distance *w* (for distances further away from w objects are assumed not detectable) the surveyed area a becomes $k\pi w^2$ and density estimation is given by

$$\hat{D} = \frac{n}{kpw^2 \hat{P}_a} \tag{1.6}$$

where *n* is the number of detected objects and $\hat{P}_a$ is the expected proportion of objects (animals, group of animals) detected within radius w.

P_a is also called the average detection probability and is estimated by $\int_0^w g(x)h(x)dx$

where *g(x)* is the detection function and *h(x)* is the distribution of animals about the observation point (Marques et al., 2013), which is assumed homogeneous.

Another method for estimating the density of animals based on distance sampling is the cue counting method (Hiby, 1985). Instead of detection of animals, in cue counting the observer or the acoustic recording system can detect cues from the species of interest. The cues can be visual, such as blows of a whale, acoustic cues such as the vocalization of a frog (Driscoll, 1998), or other objects that are produced by the animal and whose production can be assumed linearly related to animal abundance (Buckland et al., 2001). Cue counting was initially developed as an alternative to line transect sampling for estimating whale abundance from sighting surveys by detecting the whale's blows (Hiby & Hammond, 1989). The cue counting method is very similar to point-transect sampling (Buckland et al., 2001) although instead of counting animals, their cues are counted. In this method, the observed number of cues can be translated to density of cues per unit time per unit area using a point transect modelling framework. The number of cues per individual per unit time or cue rate can be estimated as well by an independent survey (Buckland et al., 2001). The density of animals then is estimated by

$$D = \frac{n}{\pi w^2 \hat{P} T \hat{r}} \tag{1.7}$$

Where n is the number of detected cues, $\hat{P}$ is the expected number of cues per unit area, *T* is the time that an observer was searching, and *r* is the cue rate, the number of cues

produced by one animal per unit time. The time of observation T is similar to the length of the transect in line-transect sampling.

1.4 Estimating the abundance of marine mammals

Estimating the population size of marine mammal species can be challenging and costly. Marine mammals either spend all of their lives in water, as is the case with cetaceans and sirenians, or a considerable amount of their time at sea, as is the case for pinnipeds. The methods for estimating marine mammal abundance broadly use the sampling of animals (Hammond 1986), sampling of space (Burnham et al., 1980; Buckland et al., 2001) and/or spatial density models (Hedley & Buckland, 2004; Gomez de Segura et al., 2007; Buckland et al., 2016).

Density estimation based on sampling animals, and the use of capture-recapture techniques, has been used extensively in marine mammal science (Hammond, 2010), either by capturing animals by means of photography (Hammond, 1986) or genetic samples (Lukacs & Burnham, 2005). This method was initially used to estimate the effect of plague and the size of the human population of England in the 1600s (Hald, 1990) and later the population of France.

Density estimation based on distance sampling techniques, as described earlier, is the most common method used to survey marine mammals. Methods based on line-transects (Burnham et al., 1980; Buckland et al., 2001; Buckland et al., 2004) for estimating density have been adapted to boats (Hammond et al., 2002; Hammond et al., 2013), and aerial surveys (Hammond et al., 2013), where visual observers record distances and angles from their platforms to detected animals along with other environmental parameters (e.g. wind, waves and lighting conditions) that may influence their visual detectability. A function accounting for the decreasing visual detectability of animals when further away from the platform corrects for animals that were not detected during the survey (Buckland et al., 2001). A combination of methods such as line-transect and mark-recapture (Buckland et al., 2010) can also account for movement of animals due to vessel presence. Availability in the detection process is the amount of time that an animal is available for detection, and perception bias (the ability to observed/detect) arises for environmental or species-specific parameters that affect the

detectability of the species. To account for availability bias, distance sampling with hidden Markov models (Borchers & Samara, 2007) and visual surveys from dual platforms (Buckland et al., 2010; Hammond et al., 2002) have been in used in the past.
For land-based surveys or offshore platforms, point sampling is a method that can be used for estimating density of marine mammals around the area of an observation point; a land station can be treated as point-transect method (Arranz et al., 2014). Visual methods for estimating the density of marine mammals are influenced by the low visual detection probability due to the limited time that animals spend on the surface (Mellinger & Barlow, 2003). The ability of observers to detect animals during the survey is influenced by a variety of conditions, including weather (Palka, 1996), light availability and perhaps seasonality (Mellinger et al., 2007). This often limits visual methods to daytime and calm conditions, which often restricts visual surveys to summertime, when conditions are most often fair enough to allow vessels to operate and observers to see well at sea.

1.5 Animal abundance using passive acoustic methods

The density of vocal animals can be achieved by counting their vocalizations, along with measures of vocal production rate and detectability of the vocal signals. Some species for which vocalizations have been used for population estimation are birds (Buckland, 2006; Dawson et al., 2009), elephants (*Loxodonta Africana cyclotis*) (Thompson et al., 2010), gibbons (*Nomascus annamensis*) (Kidney et al., 2016), frogs (*Arthroleptalla lightfooti*) (Stevenson et al., 2015) and marine mammals (Lewis et al., 2007; Marques et al., 2013). Many marine mammals use sound for foraging, navigation and communication purposes. As some marine mammals spend most of their time underwater, visual detection is characterized by relatively low availability. Therefore, an acoustic means of detection for many marine mammal species can be a more efficient way to detect them (Mellinger et al., 2007). Studies that have compared visual detection with acoustic detection have yielded higher detection range of acoustic cues for species such as the sperm whales (Barlow & Taylor, 2005) and higher detection probabilities for porpoises (Gillespie et al., 2005; Boisseau et al., 2007).

To derive estimates of population size from acoustic cues, methodologies based upon distance-sampling have mostly been used, using line transect or point sampling, cue-counting methods and a combination of mark recapture with distance sampling. Depending on whether the acoustic sensor used to sample the animal's sounds is a towed array or a fixed sensor, line or point-transect sampling may be applied respectively. In the point-transect method, observations are made from a random set of fixed points, while a line-transect involves an observation platform moving along random survey lines. Point-transect methods have been used to estimate the abundance of songbirds (Buckland et al., 2002; 2006) and of marine mammals (Gkikopoulou et al., 2013).

Line-transects for acoustic cues need to estimate the distance between the vocalizing animal and the receiver. Multi-hydrophone ranging can be used to locate the animal based on differences in sound arrival times (Spiesberg & Fristrup, 1990). Time difference of arrival (TDOA) can give bearings to the vocalizing animal and in the case of fast moving platforms and a regularly vocalizing animal, could give information about its distance through target motion analysis. Lewis et al., (2007) estimated the abundance of sperm whales in the Mediterranean. When only one acoustic receiver is available, then distance from the vocal animal can be estimated by acoustic propagation models in some situations (Tiemann et al., 2004).

Cue-counting methods have been widely applied to fixed sensors used for echolocating animals (Akamatsu et al., 2008; Marques et al., 2009; Kusel et al., 2011; Moretti et al., 2010; Frasier et al., 2016). Cue density (the number of cues per unit of space and unit of time) can only be translated to animal density if there is a cue rate (number of cues produced by an individual per unit of time) available otherwise estimates of cues per unit area are estimated.

There are some methods in addition to distance sampling that are based on sampling space and that account for animal movement. These include spatially explicit capture recapture models (SECR) (Efford, 2004; Efford et al., 2009). SECR models allow detectability to change in relation to spatial information and animal movement. When different traps or recorders are used, detectability can change as a function of trap type (Efford, 2011). Acoustic detectors can be thought as proximity detectors ("traps" that record an individual's presence but leave the animal free to be detected by other

detectors within any occasion). This approach can be used with multiple fixed acoustic arrays such as the bottom mounted hydrophones in AUTEC (Atlantic Undersea Test and Evaluation Center) for density of animals in the area.

1.5.1 Factors influencing marine mammal abundance estimation from acoustic cues

Several factors should be taken into account for estimating density from acoustic cues. These can be split into species-specific animal factors, environmental factors and equipment-specific factors. The intervals between marine mammal vocalizations will influence the vocal rates used for a particular species, as well the variability of the type of vocalizations. Other influences arise from the type of receiver, the algorithms used for detection as well as environmental factors such as the ambient noise and the receiver depth.

1.5.2 Animal vocalization

Animals produce signals to i) communicate with conspecifics, ii) detect and/or influence the behaviour of prey, and iii) navigate and orient in their environment (Krebs & Davies, 1981). The marine environment favours the acoustic channel for rapid transmission of information ranging from a few meters to many kilometres of distance (Tyack, 1998). The range of frequencies that cetaceans use to vocalize varies greatly among species and depends on the size of the animal (Fletcher 2004), its foraging strategies and social structure.

Baleen whales are mostly migratory, and some species travel thousands of kilometres between the productive high latitude summer feeding grounds and warmer oligotrophic mating/breeding waters in winter (Norris, 1967). Baleen whale vocalizations consist mostly of communication signals (Tyack & Clark, 2000), though some could be used for identifying echo returns from large ocean features such as the sea-surface and seamounts (Tyack 2000; Tyack & Clark, 2000).

Baleen whale vocalizations, as for bird vocalizations (Catchpole & Slater, 1995), can be divided into two general categories:

i) Songs: tend to be long, complex vocalizations repeated by males in the breeding season and

ii) Calls: tend to be shorter, simpler and produced by both sexes throughout the year.

For example, fin whale songs are produced by males (Croll et al., 2002) and humpback whale and bowhead whale songs are well-known reproductive advertisement displays produced primarily during the breeding season (Tyack, 2000). In contrast, calls are produced by whales of different age-sex classes during many seasons (Clark, 1983) and usually occur in particular contexts (Catchpole & Slater, 1995), e.g. southern right whale "up calls" are produced more from single animals (Clark, 1983). As a further example, the low frequency vocalization of sei whale is believed to function as a "contact call" (Baumgartner et al., 2008) in order to allow dispersed animals to coordinate activities such as feeding or breeding.

Low frequency sound can propagate over great distances in the ocean (Urick, 1983) and baleen whale vocalizations are mostly low frequency, ranging from the 15-20 Hz calls of blue whales (Mellinger & Clark 2003) and 20-Hz calls of fin whales (Watkins et al., 1987) up to the 4 kHz upper frequency of humpback whale vocalisations (Tyack & Clark, 2000). Differences in the frequency of vocalization may result from different strategies of baleen whales. For example, humpback and bowhead whales have vocalizations 4 octaves higher in frequency than those of blue and fin whales (Tervo et al., 2012), and the "active space" of these songs is estimated to be between 40-130 km, an order of magnitude smaller than the estimated active space of blue and fin whale songs (Tervo et al., 2012). The potentially long range of low-frequency vocalizations of baleen whales coupled with potential variability in range of detection can be problematic for PAM-based distance sampling (Marques et al., 2011)

One of the differences between baleen whales and odontocetes is the use of echolocation by odontocetes. The term echolocation was first defined by Griffin (1944) to describe the use of echoes from a sound emitted by a bat to estimate the location, range and direction of an object. Echolocation clicks are highly directional (Au, 2004; Zimmer et al., 2005), and directionality is physically determined by the ratio between the size of the transmitting organ and the wavelength of the projected sound. Species-

specific differences can be found in bandwidth and peak frequency of the clicks for odontocetes (Au 2004) and bats (Jones & Holderied, 2007). Sperm whale (Mohl et al., 2003) and delphinid clicks are broadband (Au 2004), in comparison to the echolocation signals of beaked whales which are narrow band over the short term and unique among the toothed whales in their frequency modulation (Zimmer et al., 2005). Another type of echolocation click is the Narrow Band High Frequency (NBHF) clicks that have evolved in 4 different taxonomic groups, Delphinids of the genus *Cephalorhynchus*, phocoenids, pygmy sperm whale (*Kogia simus*) and Fransciscana river dolphin (*Pontoporia blainvillei*) (Mohl & Andersen 1973; Kyhn et al., 2013).

Other sounds emitted by the odontocetes are whistles, burst pulses and patterned sequences of clicks which are produced for social interaction (Tyack & Clark 2000). Whistles (frequency modulated sounds that are narrow band over the short term) are typically categorized by the frequency modulation contour over time (Au, 1993). A specific type of whistle, called the "signature whistle," seems to encode individual information (Tyack & Clark, 2000; Sayigh & Janik, 2009) and remains stable for many years in most individuals. Burst pulses are distinguished from echolocation clicks by their use in communication, with different patterns of repetition rate than clicks used for echolocation (Arranz et al., 2016). Species that don't produce whistles – such as the porpoises (Clausen et al., 2010) and sperm whale – are believed to alter their echolocation clicks in order to communicate (Moore et al., 1993; Madsen et al., 2002; Watkins & Schevill, 1977).

Whether they are used for communication purposes or navigation and foraging, these vocal signals can provide cues for acoustic detection of animals and then, if cue rates are available, to convert density of acoustic cues to density of animals (Marques et al., 2009), either for baleen whales (Harris et al., 2013; Marques et al., 2011) or odontocetes (Marques et al., 2009). When cue rates for animal vocalisations are not available, then detection of cues can be used for cue density estimation (Martin et al., 2013). Yet the type of vocalization will set the limits on the conclusions that can be derived regarding population size, as well as the uncertainty around the estimates. Characteristics that favour use of a vocalisation for density estimation include ease of detection and classification and regular production by all age and sex classes.

Here I select echolocation clicks of Blainville's beaked whale as a detection cue for PAM-based distance sampling because the signal can easily be detected and classified with confidence. The click cue rates of Blainville's beaked whales are well established (Warren et al., 2017) and similar across age and sex classes, and as a result, the detection function can be defined either by sound propagation models (Zimmer et al., 2008) or experiments in the sea (Marques et al., 2009). The deep diving behaviour of Blainville's beaked whales makes them a model species to test the performance of gliders that sample a range of depths from the surface down to ~1000m depth. This depth range samples most of the foraging layers of Blainville's beaked whales (200-1200 m) (Johnson et al., 2006).

1.6 Detection theory

The task of detecting signals in noise arises in many areas of scientific research as well as in technological systems including radar, communications, speech recognition, sonar, image processing, biomedicine, controls and seismology (Kay, 1993). Detection theory, also known as hypothesis testing and decision theory, is concerned with how best to make detections and how to quantify detector performance. This field incorporates ideas from mathematics, statistics and engineering. The simplest detection problem is to decide whether a signal, embedded in noise, is present. In this simple binary hypothesis testing problem, there are only two possible scenarios: the data contain both signal and noise, or just noise. The goal is to make the best decision given the observed dataset and given the application-dependent costs of making an error. The basis of signal detection theory is that all decision making takes place in the presence of some uncertainty. The event of interest (the signal), the channel through which the signal is transmitted, and the noise, all have a component of randomness and hence a statistical approach is required.

For a binary problem (i.e., one in which a decision must be made as to whether an event is there or not) there are four different outcomes from a detection system: i) a hit, i.e., the signal was there and was detected, ii) a correct rejection, in which the signal was not there and it was not detected, iii) a miss, in which the signal was there but was missed by the detector and iv) a false alarm, in which the detector reported a signal when none

was present. Those outcomes are based on at least one criterion, which can be a detection threshold i.e. the minimum level of a measurement upon which a decision is made. The performance of the detector for a given detection threshold can be expressed by its sensitivity and specificity. Sensitivity (true positive rate) is the proportion of signals or events that are correctly detected (i.e. the number of hits divided by the total number of signals available for detection), while specificity (true negative rate) is the proportion of correct rejections.

The overall efficiency of a detector can be represented by its receiver operating characteristics (ROC) curve which displays the sensitivity and specificity as the detection threshold is varied from a low value (giving high sensitivity) to a high value (giving high specificity). For each threshold value, the sensitivity and specificity are presented in the y-axis and x-axis of the plot, respectively. The ROC curve can be used to determine a suitable operating point for the detector, i.e., a detection threshold that gives an acceptable trade-off between sensitivity and specificity. Although it is desirable for a detector to simultaneously have high specificity and high sensitivity, the ROC curve precisely defines the trade-off between these two qualities for a given detector; to improve both qualities simultaneously, the detector algorithm itself must be enhanced so as to search more effectively for the required signal. Such a modified detector will have a ROC curve that passes deeper into the top left-hand corner of the plot (Fig. 1.2 – orange curve) providing increased sensitivity for a given level of specificity. In mitigation surveys of rare species, it is desirable to make sure that all animals are detected, so a detection system for this task should have high sensitivity. On the other hand, for surveys of density estimation of abundant species, high sensitivity is not necessary as long as the false alarm rate of the detection system is known.

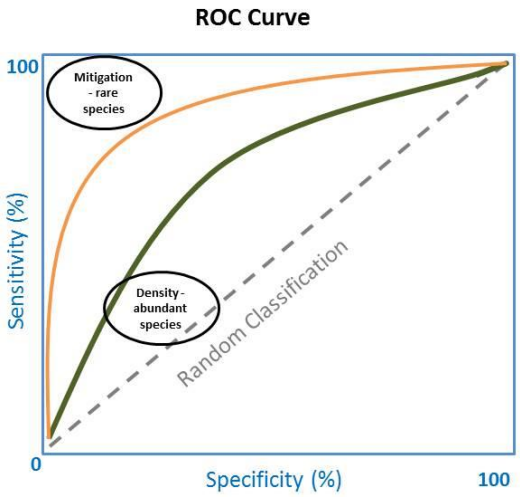

Figure 2 Receiver Operator Characteristics Curve – Sensitivity (y-axis) percentage of hit rate in relation to true number of signals and Specificity (x-axis) percentage of false alarm rate in relation to true number of misses. A classification system with higher efficiency is shown in orange and a worse classification system is shown in dark green. The two ovals show examples of desired locations in the plot when dealing with mitigation of rare species (high sensitivity) or a density estimation survey of an abundant species.

A major factor limiting detector performance in the biological sciences, and especially in passive acoustic detection of animal vocalizations, is that the signals being detected are not stable and can vary by individual, location, time of year, amongst many other factors. This variability means that the detector must contend with a wide spread of possible signals and performance will inevitably be poorer than for detectors in technological systems where the signal is completely known. In the following, I discuss the parameters that influence the detection of signals in the sea and I introduce the passive sonar equation as a means for summarizing these factors. In addition, I present detection algorithms specifically designed for marine mammal vocalizations such as click and whistle detectors.

1.6.1 Underwater sound propagation and the passive sonar equation

Sound travels much faster in water, with a speed of about 1500m s^{-1}, than in air, with a speed of about 340m s^{-1}, and marine mammals have adapted to use sound as the most effective sense for long-range communication, navigation and foraging. For every active sonar system, either biological or man-made, acoustic energy is generated from a "projector" (Urick, 1983). A parameter that specifies the amount of sound radiated by a projector is the source level (SL), which is defined as the intensity of sound recorded at a point 1 m from the acoustic centre of the projector on the axis of the beam pattern (Urick, 1983). When expressed in decibels, the source level is referred to the intensity of a plane wave having an rms pressure of 1 μPa. Another important characteristic of active sonar is the transmitting directivity index, which is the difference, measured at a point on the axis of the beam pattern, between the level of the sound generated by the projector and the level that would be produced by a omnidirectional projector radiating the same total amount of acoustic power (Urick, 1983).

In order to detect a signal (positive detection) – a signal-to-noise ratio (SNR) should be above a pre-specified threshold. A basic passive sonar equation is the following (Urick, 1983):

$$SNR\ (R) = ASL(\theta) - TL(R) - NL + AG + PG \qquad (1.8)$$

Where ASL(θ): is the apparent source level of the sound source (dB// 1μPa @ 1 m), TL(R) is the transmission loss (range and frequency dependent), NL is the background noise level masking the signal, AG is the gain of the receiving hydrophone array and PG is the gain of the processing system, which includes any sophisticated system which the detection process is conducted i.e. type of detection algorithm.

Whereas ASL is a property of the target acoustic source (the distribution of signal's source level and directionality), the TL is dependent on the sound speed profile, bathymetry, sea state, frequency of the source and range from the receiver. Attenuation of an acoustic signal increases exponentially with the frequency (Urick 1983); low frequency calls of some baleen whale species can be detected several hundreds of kilometres away from the source (Spiesberger & Fristrup, 1990) and high frequency echolocation clicks of a porpoise can be detected only within a few hundreds of meters.

1.6.2 Underwater ambient noise

Underwater ambient noise is the consequence of a number of physical, biological and anthropogenic sources and varies widely with location and time. The principal non-anthropogenic noise sources are rain, waves, turbulent flow, underwater earthquakes and sounds from fish, marine mammals and invertebrates. Although wave and seismic noises are generally low frequency, rain can generate noise that covers a wide spectrum (Urick, 1983). Fish choruses are also typically low in frequency, but in tropical shallow waters, sounds from snapping shrimp can dominate the mid-frequency ambient noise (Cato, 1993) causing a significant source of interference for passive acoustic monitoring. Anthropogenic noise sources include ship traffic, underwater construction, airguns used in oil exploration, echo sounders and sonar, and animal deterrence devices. Ship noise dominates the low frequency ambient noise in many locations and close passes of vessels can produce noise that covers the entire frequency range used by marine mammals (Dyndo et al., 2015; Hermannsen et al., 2014). In shallow coastal waters, the ambient noise is more temporally and spatially variable than in deep waters, due both to complex sound propagation and local concentrations of biotic noise sources (Urick, 1983). As human presence is often also greater in shallow waters, the contribution of anthropogenic noise in these environments can be significant. In contrast, in deep water locations with little ship traffic, the ambient noise level at high frequencies can be so low that it falls below the electronic noise of a hydrophone preamplifier (Johnson et al., 2011). In this case the total noise of a sound recorder will be limited by the "self-noise" of the system, rather than the environmental ambient noise. As the system noise is constant, this can result in a more predictable noise environment for evaluating detector performance.

1.6.3 Detection in marine mammals

The ability to extract a signal from background noise can be improved with filtering and pattern recognition algorithms. Filtering algorithms for marine mammals depend on the type of the vocalization, which can be tonal (Roch et al, 2011; Mellinger et al., 2011) or transient sounds (Roch et al., 2007; 2011), and on the background noise (Zimmer et al., 2011). Automatic or semi-automatic algorithms for the detection of species' calls have

numerous applications such as characterization of the vocalization, localization and density estimation (Marques et al., 2013).

Marine bioacoustics often involves large-scale data sets recorded over long recording periods and/or from many hydrophones, so the analysis often requires automatic methods for extracting the desired signal (Mellinger et al., 2016). The matched filter is an ideal detector for well-known signals (whose waveform as a function of time is completely defined) in Gaussian noise (Urick, 1983). However, in reality cetacean signals are only partially known systems and the environmental noise seldom fits a Gaussian distribution (Mellinger & Clark, 2000).

The best detector to use depends heavily upon the type of signal and the type of noise. Systems for the detection, classification and localization (DCL) of marine mammals from passive acoustics include: automatic, semi-automated (supervised) or manual methods (Mellinger et al., 2007). Spectrogram correlation techniques have been used for detection of blue and fin whale calls (Mellinger & Clark, 2000), right whale 'up calls' (Mellinger et al., 2004) and highly stereotyped vocalizations such as those of fin whale populations (Mellinger et al., 2007).

For echolocation clicks a number of detection methods are available: detector threshold, a sequential detector that implements a sequential probability ratio test (Wald, 1947), energy summation detectors, and energy ratio mapping algorithms (Klinck & Mellinger 2011). Frequency modulated click detectors (FMCD) have also been used for detecting the frequency modulated clicks of beaked whales (Yack et al., 2010). Furthermore, statistical techniques for classification of odontocete clicks are available such as those used by Gillespie and Caillat (2008), where the extracted click's parameters were analysed with two different methods; multivariate analysis of variance and tree classifiers. Roch et al., (2011) classified nine odontocete species from the cepstral features of their echolocation clicks using a Gaussian Mixture Model detector (Roch et al., 2008).

For tonal frequency-modulated signals such as delphinid whistles and some baleen whale calls, edge detection techniques have been used for locating the whistle segments in a spectrogram (Datta & Sturtivant, 2002) and for detecting calls of baleen whales such as right whales (Gillespie, 2004). Edge-detection here encompasses methods that use pixel contrast to define the boundaries of shapes in an image – here being

spectrograms that include animal calls. A generalized baleen whale call detector has been developed by Baumgartner and Mussoline (2011) based on pitch-tracking, allowing estimation of complex frequency modulation. Mellinger et al., (2011) used a method based on frequency contour and peak frequency tracking in order to detect tonal calls, which worked well for delphinid whistles and minke "boing" calls. Bayesian filter-based methods (Johansson & White, 2011; Roch et al., 2011) and graph representation algorithms (Roch et al., 2011) have also been used for automatic whistle extraction. Gillespie et al., (2013) have developed a method based on partial detection of frequency contours.

Neural networks have been used by several scientists for marine mammal classification (Potter et. al. 1994; Mellinger & Clark, 2000; Mellinger 2004; Gillespie, 2004) but drawbacks are the large amount of data required and the uncertainty about the underlying function used for the classification (Mellinger & Clark, 2000).

The critical parameters describing any detection system are its efficiency (specificity and sensitivity as described on section 1.6) and false alarm rate (Gillespie 2004; Mellinger et al., 2007). False alarm rate is based on a test dataset (Mellinger et al., 2011), where training data should be representative and not biased. When multiple species are included in transect data, absolute abundance estimates should not be based on a detector's click counts unless the false detection rates are determined for all the species present in the data (Yack et al., 2010). Depending on the application of a detector, different trade-offs can be accomplished by changing the characteristics of the detector such as the false alarm rate. For example, if a detector is used to detect a rare species in a mitigation process then the false positive rate should be increased enough to make sure that if an animal is in the area it will be detected.

1.6.4 PAM receivers

Early detections of baleen whale sounds used underwater acoustic receivers deployed by geophysicists for the detection and the localization of low-frequency seismic signals. Watkins et al., (1987) analysed data for fin whale 20 Hz pulses recorded from seismometers cabled to shore in Bermuda from 1951- 1982. Byrne et al., (1987) deployed the first analog recorder that could record continuously for 66 days and the

first whale sounds recorded from bottom mounted autonomous recorders were described by Duennebier et al., (1987) from fin whales (Au & Lammers, 2016).

For more than 50 years now, passive acoustic recorders have been specialized for the recording of marine mammal vocalizations (Sousa-Lima et al., 2013). Nowadays these passive acoustic recorders can be grouped in four categories, (1) stationary/fixed acoustic receivers, (2) moving receivers that are towed from or attached to moving platforms, (3) drifters, or (4) animal-born acoustic tags. All of the above types can range in sampling frequency, duration of recording, and self-noise levels, depending on the species of interest, the duration of the study, and the equipment used.

Stationary fixed receivers can either be mounted on the bottom of the sea or fixed at a predefined depth. Bottom-mounted receivers can be autonomous or cabled to a land station. The latter are usually found in naval undersea ranges such as the AUTEC in the Bahamas, for monitoring Naval activities such as submarine movements. Early autonomous fixed receivers include Cornell Pop-Ups, ARP (Acoustic Recording Package) for baleen whale calls and HARP (High-frequency Acoustic Recording Package) for high-frequency signals (Wiggins & Hildebrand 2007). Other receivers are specialized for high-frequency signals and record and store acoustic features of the signal rather than the signal itself (C-PODs and T-PODs (http://www.chelonia.co.uk/). Fixed receivers have the advantage of acoustic monitoring for long period of times (Hildebrand et al., 2015), depending on the power capabilities of the system.

Arrays of hydrophones are commonly towed from vessels for distribution and density estimation studies in marine mammal science (Leaper et al., 2000; Lewis et al., 2007). Towed arrays can localize signals from time difference of arrival of acoustic signals to the different elements of the towed array (Zimmer, 2011).

Drifting acoustic recorders, either arrays of hydrophones (Griffiths & Barlow, 2016) or single recorders are useful in areas with strong high tidal currents (Macaulay et al., 2017) and provide relatively easy deployment. Drifters can be deployed in areas with differentiated habitats to investigate the presence of species in different habitats (Griffiths & Barlow, 2016),

Autonomous animal-borne acoustic tags can record vocalization rates produced by the tagged animal in addition to measurements of ambient noise and other physiological measures, such as parameters of diving capabilities and fluke rates (Johnson et al.,

2009; Martin Lopez et al., 2015). The first acoustic recording tag was the compact acoustic probe (CAP) introduced in 1997 by Burgess et al. (1998), which was attached on elephant seals. This tag had low-frequency recording capabilities along with a depth sensor and was capable of deployments up to 2000m depth. A more advanced version was the Bprobe (Burgess et al., 2000). These days, a more sophisticated acoustic tag is the DTAG (Digital Acoustic Recording Tag) (Johnson & Tyack, 2003), which is able to record acceleration, depth, temperature, orientation and magnetic field, and has been deployed on many species. The DTAG has been instrumental in assisting density estimation from acoustic cues, first of all by characterizing the signal produced by the whales and secondly by extracting click rates of several species. By extracting the click rates from echolocating animals along with information on location and seasonality, more accurate click rates can be used when density estimation is conducted in various areas and seasons.

1.7 PAM underwater gliders

The idea of an ultra-low powered buoyancy underwater driven vehicle was first proposed by Stommel (1989) with only a decade elapsing before its realization (Eriksen et al., 2001; Rudnick et al., 2004; Rudnick, 2016). Since then, oceanographers have increased their subsurface presence in the open oceans and collected long time series of data (Schofield et al., 2007) using either autonomous vehicles or profiling drifters (Barron et al., 2007).

Glider applications in oceanographic research vary over wide temporal scales, from weeks to months, and spatial scales from ocean basin to mesoscale and sub-mesoscale, with capabilities to measure small-scale internal waves and the microscale (Rudnick, 2016). This increased usage of autonomous platforms in the open sea provides opportunities to deploy acoustic sensors and to gather information about marine mammals where the platforms operate.

Underwater gliders are low power, comparatively quiet and capable of multiple dives to 1000m over distances of tens to thousands of kilometres (Moore et al., 2008). Recent glider developments have the potential for diving to deeper waters, such as 2000m or deeper, though these deep applications are not yet widely available due to

hydrodynamic and construction limitations (Osse & Eriksen, 2007). Additionally, the low self-noise generated from the automated underwater glider gives the opportunity to integrate an acoustic sensor to the existing glider sensors, resulting in a new acoustic platform for surveying marine mammals. Platforms such as gliders also offer the advantage of sampling the full range of depths to which cetaceans dive (Rudnick, 2016). Much of the use of gliders for marine mammal PAM has involved the detection, identification and classification of species in real, or near-real, time (Baumgartner et al., 2013), mainly to assist boat surveys, test autonomous detection and classification systems, or to assist avoidance of ship-marine mammal strikes. Gliders have also been used in marine mammal science for surveys that have been conducted for a broad taxonomic range, from mysticetes (Baumgartner & Fratantoni, 2008; Baumgartner et al., 2008; Baumgartner & Mussolini, 2011; Fucile et al., 2006; Baumgartner et al., 2013; Moore et al., 2008) to odontocetes (Klinck et al., 2012; Arima et al., 2014) and pinnipeds (Baumgartner et al., 2014). Their usage has expanded exploration into areas that were previously difficult to study, for example: the Arctic (Baumgartner et al., 2014), diurnal patterns of mysticete vocal activity in relation to prey vertical migration (Baumgartner & Fratantoni, 2008), or the assessment of risk for marine mammals and resulting mitigation measures (Haun et al., 2008). In addition, if recording systems are available on board a glider, there is the opportunity of assessing underwater noise, such as airgun pulses, in areas where the glider operates (Baumgartner et al., 2014).

As underwater gliders are a new platform for passive acoustic monitoring, their usage has not been established exclusively for specific ecological research targets for marine mammals. Analysis methods established for previous traditional survey modes such as line-transect or point-sampling, are required to evolve in order to make use of the data collected from gliders. One distinction between different PAM glider surveys distinguishes between surveys conducted mainly for oceanographic research or those conducted to study marine mammals, such as density and habitat estimation. The long durations during which gliders can be deployed in waters where many marine mammals vocalize make gliders a particularly useful acoustic platform for surveying marine mammals for density estimation. However, if only single hydrophones are used on a glider, this can restrict the ability to estimate range to the calling animal, thereby limiting applicable methodologies for distance sampling. This makes it essential to

develop independent methods to estimate the detection functions of different species to apply distance sampling approaches to glider surveys.

1.8 PhD Objectives and overview of the chapters

The main objective of this thesis is to investigate the use of underwater gliders as a PAM platform for estimating marine mammal abundance from acoustic cues. To use underwater gliders for abundance estimation of marine mammals, analytical methods are derived for generating population size estimates, along with estimating key parameters underpinning the methods.

The objectives of the thesis are to:

- Derive a method for estimating the detection function of vocal marine mammals in the field.
- Test different acoustic detectors for Blainville's beaked whale echolocation clicks.
- Investigate acoustic cues for deep diving echolocating animals and estimate their detection function as a function of receiver's depth.
- Derive a method to estimate abundance from underwater gliders.
- Assess the method with a simulated glider survey, under different animal density scenarios.
- Investigate biases arising from the simulated glider surveys.

The thesis objectives are distributed in the following four chapters of the thesis. A brief summary of each chapter follows:

Chapter 2 presents a field method for extracting the acoustic detection function of echolocating animals. The method combines passive acoustic monitoring with a biologging experiment in the field to extract the probability of detecting an echolocation click as a function of distance. The method is applied to Blainville's beaked whales in the area of El Hierro (Canary Islands, Spain). Passive acoustic recorders are deployed in acoustic proximity to a whale tagged with a DTAG and a synchronized plot is used to identify the clicks produced by the tagged animal and their distance to the passive

acoustic receiver based on time of arrival methods. A model fits the detection probability with parameters such as range and depth.

Chapter 3 considers two different acoustic cues for density estimation of Blainville's beaked whales: single regular clicks and click scans (sequences of detected clicks). To estimate the statistical parameters of the two acoustic cues, a simulation study places a network of theoretical receivers at different depths around a diving animal. The clicks to be detected from simulated whales are derived from movement and acoustic production information from DTAG datasets.

Chapter 4 investigates underwater gliders as platforms for density estimation of echolocating animals. A mathematical equation for estimating density of deep diving echolocating animals from acoustic data is derived. The method is validated with a simulation survey of a passive acoustic underwater glider in different scenarios of animal density and distributions, and abundance estimates are extracted based on click cue counting and click scan cue counting methods. Variance estimations are derived from the simulations.

1.9 References

Akamatsu, T., Wang, D., Wang, K., Li, S., Dong, S., Zhao, X., Barlow, J., Stewart, B.S. & Richlen, M. (2008) Estimation of the detection probability for Yangtze finless porpoises (*Neophocaena phocaenoides asiaeorientalis*) with a passive acoustic method. Journal of the Acoustical Society of America, 123, 4403-4411.

Alverson, D.L., Freeberg, M.H., Pope, J.G. & Murawski S.A. (1994) A Global Assessment of Fisheries Bycatch and Discards. FAO, Rome.

Arima, M., Tonai, H., Akamatsu, T. & Minakuchi, H. (2014) Feasibility Study of Underwater Passive Acoustic Observations of Killer Whales using A-tag. In World Automation Congress (*Wac*), 2014, 291-296.

Arranz, P., DeRuiter, S.L., Stimpert, A.K., Neves, S., Friedlaender, A.S., Goldbogen, J.A., Visser, F., Calambokidis, J., Southall, B.L. & Tyack, P.L. (2016) Discrimination of fast click-series produced by tagged Risso's dolphins (*Grampus griseus*) for echolocation or communication. Journal of Experimental Biology, 219, 2898-2907.

Au, W.W.L. (2004) Echolocation signals of wild dolphins. Acoustical Physics, 50, 454-462.

Barlow, J. & Taylor, B.L. (2005) Estimates of sperm whale abundance in the northeastern temperate Pacific from a combined acoustic and visual survey. Marine Mammal Science, 21, 429-445.

Barron, C.N., Smedstad, L.F., Dastugue, J.M. and Smedstad, O.M., 2007. Evaluation of ocean models using observed and simulated drifter trajectories: Impact of sea surface height on synthetic profiles for data assimilation. Journal of Geophysical Research: Oceans, 112, (C7).

Baumgartner, M.F. & Fratantoni, D.M. (2008) Diel periodicity in both sei whale vocalization rates and the vertical migration of their copepod prey observed from ocean gliders. Limnology and Oceanography, 53, 2197-2209.

Baumgartner, M.F. & Mussoline, S.E. (2011) A generalized baleen whale call detection and classification system. Journal of the Acoustical Society of America, 129, 2889-2902.

Baumgartner, M.F., Stafford, K.M., Winsor, P., Statscewich, F. & Fratantoni, D.M. (2014) Glider-based passive acoustic monitoring in the Arctic. Marine Technology Society Journal, 48, 40-51.

Baumgartner, M.F., Van Parijs, S.M., Wenzel, F.W., Tremblay, Carter Esch, H.C. & Warde, A.M. (2008) Low frequency vocalizations attributed to sei whales (*Balaenoptera borealis*). The Journal of the Acoustical Society of America, 124, 1339-1349.

Boisseau, O., Matthews, J., Gillespie, D., Lacey, C., Moscrop, A. & Ouamari, N. E. (2007) A visual and acoustic survey for harbour porpoises off North-West Africa: further evidence of a discrete population. African Journal of Marine Science, 29, 403-410.

Borchers, D.L. & Samara, F.I.P. (2007) Accommodating availability bias on line transect surveys using hidden Markov models. Technical Report, pp. 13. Centre for Research into Ecological and Environmental Modelling, St Andrews.

Buckland, S.T. (2006) Point-transect surveys for songbirds: Robust methodologies. Auk, 123, 345-357.

Buckland, S.T., Anderson, D.R., Burnham, K.P., Laake, J.L., D.L., B. & Thomas, L. (2001) Introduction to Distance Sampling: Estimating abundance of biological populations. Oxford University Press, Oxford, United Kingdom.

Buckland, S.T., Laake, J.L. & Borchers, D.L. (2010) Double-observer line transect methods: levels of independence. Biometrics, 66, 169-177.

Buckland, S.T., Oedekoven, C.S. & Borchers, D.L. (2016) Model-based distance sampling. Journal of Agricultural Biological and Environmental Statistics, 21, 58-75.

Burgess, W.C. (2000) The bioacoustic probe: A general purpose acoustic recording tag. The Journal of the Acoustical Society of America, 108, 2583-2583.

Burnham, K.P., Anderson, D.J. & Laake, J.L. (1980) Estimation of density from line transect sampling of biological populations. Wildlife Monographs, 72, 3-202.

Catchpole, C.K. & Slater, P.J.B. (1995) Bird song; Biological themes and variations. Cambridge University Press, Cambridge, United Kingdom.

Cato, D.H. (1998) Simple methods of estimating source levels and locations of marine animal sounds. The Journal of the Acoustical Society of America, 104, 1667-1678.

Clark, C.W. (1983) Acoustic communication and behavior of the Southern Right Whale (*Eubalaena australis*). In Communication and Behavior of Whales, edited by R. Payne (Westview, Boulder), 163-198.

Clausen, K.T., Wahlberg, M., Beedholm, K., Deruiter, S. & Madsen, P.T. (2010) Click communication in harbour porpoises *Phocoena phocoena*. Bioacoustics, 20, 1-28.

Croll, D.A., Clark, C.W., Acevedo, A., Tershy, B., Flores, S., Gedamke, J. & Urban, J. (2002) Bioacoustics: Only male fin whales sing loud songs. Nature, 417, 809-809.

D'Agrosa, C., Lennert-Cody, C.E. & Vidal, O. (2000) Vaquita bycatch in Mexico's artisanal gillnet fisheries: driving a small population to extinction. Conservation Biology, 14, 1110-1119.

Datta, S. & Sturtivant, C. (2002) Dolphin whistle classification for determining group identities. Signal Processing, 82, 251-258.

Dawson, D.K. & Efford, M.G. (2009) Bird population density estimated from acoustic signals. Journal of Applied Ecology, 46, 1201-1209.

Driscoll, D.A. (1998) Counts of calling males as estimates of population size in the endangered frogs *Geocrinia alba* and *G. vitellina*. Journal of Herpetology, 32, 475-481.

Duennebier, F.K., Anderson, P.N. and Fryer, G.J., 1987. Azimuth determination of and from horizontal ocean bottom seismic sensors. Journal of Geophysical Research: Solid Earth, 92(B5), 3567-3572.

Dyndo, M., Wisniewska, D.M., Rojano-Donate, L. & Madsen, P.T. (2015) Harbour porpoises react to low levels of high frequency vessel noise. Scientific Reports, 5, 11083.

Efford, M. (2004) Density estimation in live-trapping studies. Oikos, 106, 598-610.

Efford, M.G. (2011) Estimation of population density by spatially explicit capture-recapture analysis of data from area searches. Ecology, 92, 2202-2207.

Efford, M.G., Dawson, D.K. & Borchers, D.L. (2009) Population density estimated from locations of individuals on a passive detector array. Ecology, 90, 2676-2682.

Eriksen, C.C., Osse, T.J., Light, R.D., Wen, T., Lehman, T.W., Sabin, P.L., Ballard, J.W. & Chiodi, A.M. (2001) Seaglider: A long-range autonomous underwater vehicle for oceanographic research. IEEE Journal of Oceanic Engineering, 26, 424-436.

Frasier, K.E., Wiggins, S.M., Harris, D., Marques, T.A., Thomas, L. & Hildebrand, J.A. (2016) Delphinid echolocation click detection probability on near-seafloor sensors. The Journal of the Acoustical Society of America, 140, 1918-1930.

Freeman, M.M. (2008) Challenges of assessing cetacean population recovery and conservation status. Endangered Species Research, 6, 173-184.

Fucile, P.D., Singer, R.C., Baumgartner, M. & Ball, K. (2006) A self contained recorder for acoustic observations from AUV's. In OCEANS 2006,1-4. IEEE.

Gillespie, D., P. Brown, S. Kuklik, I., Lacey, C. Lewis, T., Matthews, J., (2005) Relative abundance of harbour porpoises (*Phocoena phocoena*) from acoustic and visual surveys of the Baltic Sea and adjacent waters during 2001 and 2002. Journal of Cetacean Research and Management, 7, 51.

Gillespie, D. (2004) Detection and classification of right whale calls using an 'edge' detector operating on a smoothed spectrogram. Canadian Acoustics, 32, 39-47.

Gillespie, D., Caillat, M., Gordon, J. & White, P. (2013) Automatic detection and classification of odontocete whistles. The Journal of the Acoustical Society of America, 134, 2427-2437.

Gordon, J., Gillespie, D., Potter, J., Frantzis, A., Simmonds, M.P., Swift, R. & Thompson, D. (2003) A review of the effects of seismic surveys on marine mammals. Marine Technology Society Journal, 37, 16-34.

Gomez de Segura, A.G., Hammond, P.S., Canadas, A. & Raga, J.A. (2007) Comparing cetacean abundance estimates derived from spatial models and design-based line transect methods. Marine Ecology Progress Series, 329, 289-299.

Griffiths, E.T. & Barlow, J. (2016) Cetacean acoustic detections from free-floating vertical hydrophone arrays in the southern California Current. The Journal of the Acoustical Society of America, 140 (5), 399-404.

Hald, A. (1990) A history of probability and statistics and their applications before 1750. Vol. 501. John Wiley & Sons, New York.

Hammond, P.S. (1986) Estimating the size of naturally marked whale populations using capture-recapture techniques. Reports of the International Whaling Commission, 8, 253-282.

Hammond, P.S., Berggren, P., Benke, H., Borchers, D.L., Collet, A., Heide-Jorgensen, M.P., Heimlich, S., Hiby, A.R., Leopold, M.F. & Oien, N. (2002) Abundance of harbour porpoise and other cetaceans in the North Sea and adjacent waters. Journal of Applied Ecology, 39, 361-376.

Hammond, P.S. (2010) Estimating the abundance of marine mammals. In Boyd, I.L., Bowen, W.D. and Iverson S.J. (Eds). Marine Mammal Ecology and Conservation (pp 42-67). Oxford University Press, Oxford, United Kingdom.

Hammond, P.S., Macleod, K., Berggren, P., Borchers, D.L., Burt, L., Canadas, A., Desportes, G., Donovan, G.P., Gilles, A., Gillespie, D., Gordon, J., Hiby, L., Kuklik, I., Leaper, R., Lehnert, K., Leopold, M., Lovell, P., Oien, N., Paxton, C.G.M., Ridoux, V., Rogan, E., Samarra, F., Scheidat, M., Sequeira, M., Siebert, U., Skov, H., Swift, R., Tasker, M.L., Teilmann, J., Van Canneyt, O. & Vazquez, J.A. (2013) Cetacean abundance and distribution in European Atlantic shelf waters to inform conservation and management. Biological Conservation, 164, 107-122.

Harris, D., Matias, L., Thomas, L., Harwood, J. & Geissler, W.H. (2013) Applying distance sampling to fin whale calls recorded by single seismic instruments in the northeast Atlantic. The Journal of the Acoustical Society of America, 134, 3522-3535.

Haun, J., Ryan, K. & Portunato, N. (2008) Marine mammal risk mitigation using passive acoustic technologies. In New Trends for Environmental Monitoring Using Passive Systems, 2008, 1-5. IEEE.

Heazle, M. (2004) Scientific uncertainty and the International Whaling Commission: an alternative perspective on the use of science in policy making. Marine Policy, 28, 361-374.

Hedley, S.L. & Buckland, S.T. (2004) Spatial models for line transect sampling. Journal of Agricultural Biological and Environmental Statistics, 9, 181-199.

Hermannsen, L., Beedholm, K., Tougaard, J. & Madsen, P.T. (2014) High frequency components of ship noise in shallow water with a discussion of implications for

harbor porpoises (*Phocoena phocoena*). The Journal of the Acoustical Society of America, 136, 1640-1653.

Hilby, A.R. (1985) An approach to estimate population densities of great whales from sighting survey. Mathematical Medicine and Biology: A Journal of the IMA, 2, 201-220.

Hiby, A.R. & Hammond, P. (1989) Survey techniques for estimating abundance of cetaceans. Report of the International Whaling Commission, 11, 47-80.

Hildebrand, J.A., Baumann-Pickering, S., Frasier, K.E., Trickey, J.S., Merkens, K.P., Wiggins, S.M., McDonald, M.A., Garrison, L.P., Harris, D., Marques, T.A. & Thomas, L. (2015) Passive acoustic monitoring of beaked whale densities in the Gulf of Mexico. Scientific Reports, 5, 16343.

Johansson, A.T. & White, P.R. (2011) An adaptive filter-based method for robust, automatic detection and frequency estimation of whistles. The Journal of the Acoustical Society of America, 130, 893-903.

Johnson, M., Madsen, P.T., Zimmer, W.M.X., de Soto, N.A. & Tyack, P.L. (2006) Foraging Blainville's beaked whales (*Mesoplodon densirostris*) produce distinct click types matched to different phases of echolocation. Journal of Experimental Biology, 209, 5038-5050.

Jones, G. & Holderied, M.W. (2007) Bat echolocation calls: adaptation and convergent evolution. Proceedings of the Royal Society B-Biological Sciences, 274, 905-912.

Kidney, D., Rawson, B.M., Borchers, D.L., Stevenson, B.C., Marques, T.A. & Thomas, L. (2016) An efficient acoustic density estimation method with human detectors applied to gibbons in Cambodia. PloS one, 11, 5, e0155066.

Kay, S.M., 1993. Fundamentals of statistical signal processing. Prentice Hall PTR, Upper Saddle River, New Jersey.

Klinck, H. & Mellinger, D.K. (2011) The energy ratio mapping algorithm: A tool to improve the energy-based detection of odontocete echolocation clicks. The Journal of the Acoustical Society of America, 129, 1807-1812.

Klinck, H., Mellinger, D.K., Klinck, K., Bogue, N.M., Luby, J.C., Jump, W.A., Shilling, G.B., Litchendorf, T., Wood, A.S., Schorr, G.S. & Baird, R.W. (2012) Near-real-time acoustic monitoring of beaked whales and other cetaceans using a Seaglider^{TM}. PloS one, 7, 5, e36128.

Kusel, E.T., Mellinger, D.K., Thomas, L., Marques, T.A., Moretti, D. & Ward, J. (2011) Cetacean population density estimation from single fixed sensors using passive acoustics. The Journal of the Acoustical Society of America, 129, 3610-3622.

Kyhn, L.A., Tougaard, J., Beedholm, K., Jensen, F.H., Ashe, E., Williams, R. & Madsen, P.T. (2013) Clicking in a killer whale habitat: narrow-band, high-frequency biosonar clicks of harbour porpoise (*Phocoena phocoena*) and Dall's porpoise (*Phocoenoides dalli*). PloS one, 8, 5, e63763.

Leaper, R., Douglas, G. and Papastavrou V. (2000) Results of passive acoustic surveys for odontocetes in the Southern Ocean. Journal of Cetacean Research and Management, 2, 187-196.

Lewis, T., Gillespie, D., Matthews, L.J., Danbolt, M., Leaper, R., McLanaghan, R. & Moscrop, A. (2007) Sperm whale abundance estimates from acoustic surveys of the Ionian Sea and Straits of Sicily in 2003. Journal of the Marine Biological Association of the United Kingdom, 87, 353-357.

Lukacs, P.M. & Burnham, K.P. (2005) Review of capture-recapture methods applicable to noninvasive genetic sampling. Molecular Ecology, 14, 3909-3919.

Macaulay, J., Gordon, J., Gillespie, D., Malinka, C. & Northridge, S. (2017) Passive acoustic methods for fine-scale tracking of harbour porpoises in tidal rapids. The Journal of the Acoustical Society of America, 141, 1120-1132.

Madon, B., Gimenez, O., McArdle, B., Baker, C.S. & Garrigue, C. (2011) A new method for estimating animal abundance with two sources of data in capture-recapture studies. Methods in Ecology and Evolution, 2, 390-400.

Madsen, P.T., Payne, R., Kristiansen, N.U., Wahlberg, M., Kerr, I. & Møhl, B. (2002) Sperm whale sound production studied with ultrasound time/depth-recording tags. Journal of Experimental Biology, 205, 1899-1906.

Marques, T.A., Munger, L., Thomas, L., Wiggins, S. & Hildebrand, J. A. (2011) Estimating North Pacific right whale *Eubalaena japonica* density using passive acoustic cue counting. Endangered Species Research, 13, 163-172.

Marques, T.A., Thomas, L., Martin, S.W., Mellinger, D.K., Ward, J.A., Moretti, D.J., Harris, D. & Tyack, P.L. (2013) Estimating animal population density using passive acoustics. Biological Reviews, 88, 287-309.

Marques, T.A., Thomas, L., Ward, J., DiMarzio, N. & Tyack, P.L. (2009) Estimating cetacean population density using fixed passive acoustic sensors: An example with Blainville's beaked whales. The Journal of the Acoustical Society of America, 125, 1982-1994.

Martin, S.W., Marques, T.A., Thomas, L., Morrissey, R.P., Jarvis, S., DiMarzio, N., Moretti, D. & Mellinger, D.K. (2013) Estimating minke whale (*Balaenoptera acutorostrata*) boing sound density using passive acoustic sensors. Marine Mammal Science, 29, 142-158.

Madsen, P.T., Payne, R., Kristiansen, N.U., Wahlberg, M., Kerr, I. and Møhl, B., 2002. Sperm whale sound production studied with ultrasound time/depth-recording tags. Journal of Experimental Biology, 205(13), 1899-1906.

Mellinger, D. & Barlow, J. (2003) Future Directions for Acoustic Marine Mammal Surveys: Stock Assessment and Habitat Use. NOAA OAR Special Report (ed. NOAA), pp. 1-38. Pacific Marine Environmental Laboratory.

Mellinger, D.K. & Clark, C.W. (2000) Recognizing transient low-frequency whale sounds by spectrogram correlation. The Journal of the Acoustical Society of America, 107, 3518-3529.

Mellinger, D.K., Martin, S.W., Morrissey, R.P., Thomas, L. & Yosco, J.J. (2011) A method for detecting whistles, moans, and other frequency contour sounds. The Journal of the Acoustical Society of America, 129, 4055-4061.

Mellinger, D.K., Nieukirk, S.L., Matsumoto, H., Heimlich, S.L., Dziak, R.P., Haxel, J., Fowler, M., Meinig, C. & Miller, H.V. (2007) Seasonal occurrence of North Atlantic right whale (*Eubalaena glacialis*) vocalizations at two sites on the Scotian Shelf. Marine Mammal Science, 23, 856-867.

Mellinger, D.K., Stafford, K.M., Moore, S.E., Dziak, R.P. & Matsumoto, H. (2007) An overview of fixed passive acoustic observation methods for cetaceans. Oceanography, 20, 36-45.

Mellinger, D.K., Stafford, K.M., Moore, S.E., Munger, U. & Fox, C.G. (2004) Detection of North Pacific right whale (*Eubalaena japonica*) calls in the Gulf of Alaska. Marine Mammal Science, 20, 872-879.

Møhl, B., Wahlberg, M., Madsen, P.T., Heerfordt, A. & Lund, A. (2003) The monopulsed nature of sperm whale clicks. The Journal of the Acoustical Society of America, 114, 1143-1154.

Moore, S.E., Howe, B.M., Stafford, K.M., Boyd, M.L. (2008) Including whale call detection in standard ocean measurements: Application of acoustic Seagliders. Marine Technology Society Journal, 41, 53-57.

Moretti, D., Marques, T.A., Thomas, L., DiMarzio, N., Dilley, A., Morrissey, R., McCarthy, E., Ward, J. & Jarvis, S. (2010) A dive counting density estimation method for Blainville's beaked whale (*Mesoplodon densirostris*) using a bottom-mounted hydrophone field as applied to a Mid-Frequency Active (MFA) sonar operation. Applied Acoustics, 71, 1036-1042.

Osse, T.J. & Eriksen, C.C. (2007) The Deepglider: A full ocean depth glider for oceanographic research. In Oceans 2007, 1-12. IEEE.

Palka, D.L. (1996) Effects of Beaufort sea state on the sightability of harbour porpoise in the Gulf of Maine. Reports of the International Whaling Commission, 575-582.

Potter, J.R., Mellinger, D.K. & Clark, C.W. (1994) Marine mammal call discrimination using artificial neural networks. The Journal of the Acoustical Society of America, 96, 1255-1262.

Rayment, W., Clement, D., Dawson, S., Slooten, E. & Secchi, E. (2011) Distribution of Hector's dolphin (*Cephalorhynchus hectori*) off the west coast, South Island, New Zealand, with implications for the management of bycatch. Marine Mammal Science, 27, 398-420.

Rayment, W. & Webster, T. (2009) Observations of Hector's dolphins (*Cephalorhynchus hectori*) associating with inshore fishing trawlers at Banks Peninsula, New Zealand. New Zealand Journal of Marine and Freshwater Research, 43, 911-916.

Read, A.J., Drinker, P. & Northridge, S. (2006) Bycatch of marine mammals in US and global fisheries. Conservation Biology, 20, 163-169.

Rocha Jr, R.C, Clapham, P.J. & Ivashcenko, Y.V. Emptying the oceans: a summary of industrial whaling catches in the 20th Century. Marine Fisheries Review, 76, 37-48.

Roch, M.A., Brandes, T.S., Patel, B., Barkley, Y., Baumann-Pickering, S. & Soldevilla, M.S. (2011) Automated extraction of odontocete whistle contours. The Journal of the Acoustical Society of America, 130, 2212-2223.

Roch, M.A., Klinck, H., Baumann-Pickering, S., Mellinger, D.K., Qui, S., Soldevilla, M.S. & Hildebrand, J.A. (2011) Classification of echolocation clicks from odontocetes in the Southern California Bight. The Journal of the Acoustical Society of America, 129, 467-475.

Roch, M.A., Soldevilla, M.S., Burtenshaw, J.C., Henderson, E.E. & Hildebrand, J.A. (2007) Gaussian mixture model classification of odontocetes in the Southern California Bight and the Gulf of California. The Journal of the Acoustical Society of America, 121, 1737-1748.

Ruette, S., Stahl, P. and Albaret, M., 2003. Applying distance-sampling methods to spotlight counts of red foxes. Journal of Applied Ecology, *40*(1), pp.32-43.

Rudnick, D.L. (2016) Ocean research enabled by underwater gliders. Annual Review of Marine Science, 8, 519-541.

Rudnick, D.L., Davis, R.E., Eriksen, C.C., Fratantoni, D.M. & Perry, M.J. (2004) Underwater gliders for ocean research. Marine Technology Society Journal, 38, 73-84.

Sato, K., Watanuki, Y., Takahashi, A., Miller, P.J.O., Tanaka, H., Kawabe, R., Ponganis, P.J., Handrich, Y., Akamatsu, T., Watanabe, Y., Mitani, Y., Costa, D.P., Bost, C.A., Aoki, K., Amano, M., Trathan, P., Shapiro, A. & Naito, Y. (2007) Stroke frequency, but not swimming speed, is related to body size in free-ranging seabirds, pinnipeds and cetaceans. Proceedings of the Royal Society B-Biological Sciences, 274, 471-477.

Sayigh, L.S. & Janik, V.M. (2009) Signature Whistles. In Perrin, W.F., Würsig, B. & Thewissen, J.G.M. (Eds). Encyclopedia of Marine Mammals, 2nd Edition, (pp.1014-1016) Academic Press.

Schipper, J., Chanson, J.S., Chiozza, F., Cox, N.A., Hoffmann, M., Katariya, V., Lamoreux, J., Rodrigues, A.S.L., Stuart, S.N., Temple, H.J., Baillie, J., Boitani, L., Lacher, T.E., Mittermeier, R.A., Smith, A.T., Absolon, D., Aguiar, J.M., Amori, G., Bakkour, N., Baldi, R., Berridge, R.J., Bielby, J., Black, P.A., Blanc, J.J., Brooks, T.M., Burton, J.A., Butynski, T.M., Catullo, G., Chapman, R.,

Cokeliss, Z., Collen, B., Conroy, J., Cooke, J.G., da Fonseca, G.A.B., Derocher, A.E., Dublin, H.T., Duckworth, J.W., Emmons, L., Emslie, R.H., Festa-Bianchet, M., Foster, M., Foster, S., Garshelis, D.L., Gates, C., Gimenez-Dixon, M., Gonzalez, S., Gonzalez-Maya, J.F., Good, T.C., Hammerson, G., Hammond, P.S., Happold, D., Happold, M., Hare, J., Harris, R.B., Hawkins, C.E., Haywood, M., Heaney, L.R., Hedges, S., Helgen, K.M., Hilton-Taylor, C., Hussain, S.A., Ishii, N., Jefferson, T.A., Jenkins, R.K.B., Johnston, C.H., Keith, M., Kingdon, J., Knox, D.H., Kovacs, K.M., Langhammer, P., Leus, K., Lewison, R., Lichtenstein, G., Lowry, L.F., Macavoy, Z., Mace, G.M., Mallon, D.P., Masi, M., McKnight, M.W., Medellin, R.A., Medici, P., Mills, G., Moehlman, P.D., Molur, S., Mora, A., Nowell, K., Oates, J.F., Olech, W., Oliver, W.R.L., Oprea, M., Patterson, B.D., Perrin, W.F., Polidoro, B.A., Pollock, C., Powel, A., Protas, Y., Racey, P., Ragle, J., Ramani, P., Rathbun, G., Reeves, R.R., Reilly, S.B., Reynolds, J.E., Rondinini, C., Rosell-Ambal, R.G., Rulli, M., Rylands, A.B., Savini, S., Schank, C.J., Sechrest, W., Self-Sullivan, C., Shoemaker, A., Sillero-Zubiri, C., De Silva, N., Smith, D.E., Srinivasulu, C., Stephenson, P.J., van Strien, N., Talukdar, B.K., Taylor, B.L., Timmins, R., Tirira, D.G., Tognelli, M.F., Tsytsulina, K., Veiga, L.M., Vie, J.C., Williamson, E.A., Wyatt, S.A., Xie, Y. & Young, B.E. (2008) The status of the world's land and marine mammals: Diversity, threat, and knowledge. Science, 322, 225-230.

Schwarz, C.J. & Seber, G.A.F. (1999) Estimating animal abundance: review III. Statistical Science, 14, 427-456.

Sousa-Lima, R.S., Norris, T.F., Oswald, J.N. & Fernandes, D.P. (2013) A review and inventory of fixed autonomous recorders for passive acoustic monitoring of marine mammals. Aquatic Mammals, 39, 205-210.

Spiesberger, J.L. & Fristrup, K.M. (1990) Passive localization of calling animals and sensing of their acoustic environment using acoustic tomography. The American Naturalist, 135, 107-153.

Springer, A.M., Estes, J.A., Van Vliet, G.B., Williams, T.M., Doak, D.F., Danner, E.M., Forney, K.A. & Pfister, B. (2003) Sequential megafaunal collapse in the North Pacific Ocean: An ongoing legacy of industrial whaling? Proceedings of the National Academy of Sciences, 100, 12223-12228.

Stevenson, B.C., Borchers, D.L., Altwegg, R., Swift, R.J., Gillespie, D.M. & Measey, G.J. (2015) A general framework for animal density estimation from acoustic detections across a fixed microphone array. Methods in Ecology and Evolution, 6, 38-48.

Stommel, H.M. (1989) The Slocum mission. Oceanus, 32, 93-96.

Tervo, O.M., Christoffersen, M.F., Simon, M., Miller, L.A., Jensen, F.H., Parks, S.E. & Madsen, P.T. (2012) High source levels and small active space of high-pitched song in bowhead whales (*Balaena mysticetus*). PloS one, 7, 12, e52072.

Thomas, L., Buckland, S.T., Rexstad, E.A., Laake, J.L., Strindberg, S., Hedley, S.L., Bishop, J.R.B., Marques, T.A. & Burnham, K.P. (2010) Distance software: design and analysis of distance sampling surveys for estimating population size. Journal of Applied Ecology, 47, 5-14.

Thompson, M.E., Schwager, S.J. & Payne, K.B. (2010) Heard but not seen: an acoustic survey of the African forest elephant population at Kakum Conservation Area, Ghana. African Journal of Ecology, 48, 224-231.

Thurstan, R.H., Brockington, S. & Roberts, C.M. (2010) The effects of 118 years of industrial fishing on UK bottom trawl fisheries. Nature Communications, 1, 15.

Tiemann, C.O., Porter, M.B. & Frazer, L.N. (2004) Localization of marine mammals near Hawaii using an acoustic propagation model. The Journal of the Acoustical society of America, 115, 2834-2843.

Tyack, P.L. (1998) Acoustic communication under the sea. In Hopp, S.L., Owren, M.J. & Evans, C.S. (Eds). Animal acoustic communication, sound analysis and research methods (pp. 163-220). Springer Sciences & Business Media.

Tyack, P.L. (2000) Functional aspects of cetacean communication. In Cetacean Societies: field studies of dolphins and whales. The University of Chicago Press.

Tyack, P.L., & Clark, C.W. (2000) Communication and acoustic behavior of dolphins and whales. In Au, W.L., Popper, A.N., and Fay, R.R. (Eds), Hearing by whales and dolphins (pp. 156-224). Springer New York.

Urick, R.J. (1983) Principles of underwater sound. Peninsula Publishing, Los Altos.

Wade, P.R. (1998) Calculating limits to the allowable human-caused mortality of cetaceans and pinnipeds. Marine Mammal Science, 14, 1-37.

Warren, V.E., Marques, T.A., Harris, D., Thomas, L., Tyack, P.L., de Soto, N.A., Hickmott, L.S. & Johnson, M.P. (2017) Spatio-temporal variation in click production rates of beaked whales: implications for passive acoustic density estimation. The Journal of the Acoustical Society of America, 141, 1962-1974.

Watkins, W.A., Tyack, P., Moore, K.E. & Bird, J.E. (1987) The 20-Hz signals of finback whales (*Balaenoptera physalus*). The Journal of the Acoustical Society of America, 82, 1901-1912.

Wiggins, S. M. and J. A. Hildebrand (2007) "High-frequency Acoustic Recording Package (HARP) for broad-band, long-term marine mammal monitoring", Symposium on Underwater Technology and Workshop on Scientific Use of Submarine Cables and Related Technologies, 17–20 Apr, IEEE, Tokyo, p 551–557.

Yack, T.M., Barlow, J., Roch, M.A., Klinck, H., Martin, S., Mellinger, D.K. & Gillespie, D. (2010) Comparison of beaked whale detection algorithms. Applied Acoustics, 71, 1043-1049.

Zimmer, W.M.X. (2011) Passive acoustic monitoring of cetaceans. Cambridge University Press, New York.

Zimmer, W.M.X., Harwood, J., Tyack, P.L., Johnson, M.P. & Madsen, P.T. (2008) Passive acoustic detection of deep-diving beaked whales. The Journal of the Acoustical Society of America, 124, 2823-2832.

Zimmer, W.M.X., Johnson, M.P., Madsen, P.T. & Tyack, P.L. (2005) Echolocation clicks of free-ranging Cuvier's beaked whales (*Ziphius cavirostris*). The Journal of the Acoustical Society of America, 117, 3919-3927.

Chapter 2

Field measurements of the detection function of Blainville's beaked whale (*Mesoplodon densirostris*) using passive acoustic sensing

2.1 Introduction

Reliable methods for detecting cetaceans at sea are needed for abundance surveys to inform population management and for mitigation procedures to reduce the impact of human disturbance. Abundance surveys and mitigation protocols have traditionally relied on visual sightings (Hiby & Hammond 1989), the efficacy of which is heavily dependent on weather and light conditions (Palka, 1996), transit speed (Barlow, 1999; Evans & Hammond, 2004) and platform height, as well as the surfacing behaviour of the species (Mellinger & Barlow, 2003) and the ability of the observers (Borchers et al., 2010; Williams et al., 2007). As many cetacean species vocalize frequently, passive acoustic methods have started to be used either stand-alone (Marques et al., 20011; Mellinger et al., 2007; Kyhn et al., 2012) or in combination with visual observations (Barlow & Taylor, 2005; Rankin et al., 2007). Acoustic methods may depend less than visual surveys on environmental conditions (Mellinger et al., 2007) although both methods are strongly affected by animal behaviour. In both visual and acoustic surveys, distance sampling methods (Buckland et al., 2001) are widely used to estimate abundance, accounting for imperfect detectability (Johnson et al., 2008) and as a formalism for translating detections into abundance estimates. Distance sampling requires information about the proportion of time that animals are available for detection and the detection function, i.e., the probability of detecting an individual that is available for detection, as a function of distance from the observer or acoustic receiver (Buckland et al., 2001). Similar information is also required for real-time mitigation to ensure that the risk of undetected animals occurring within the mitigation zone is sufficiently low (e.g. JNCC- ANNEX A, 2008). In both cases, knowledge of the

detector performance is critical beforehand to design effective surveys or mitigation protocols, and afterwards for interpreting results.

There are two main sources of bias in animal detection methods: the availability bias (McLaren, 1961) and the perception bias, i.e., whether or not the animal is detected given that it is available. For cetaceans the availability bias refers to periods when animals are not at the surface available for visual detection or are not vocal in the case of acoustic surveys (Barlow et al., 2013). Bias can be reduced by appropriate survey design and, in some cases, in post-survey analysis. Availability bias can be reduced by choosing a survey method that exploits abundant and reliable cues (MacCarthy et al., 2013); for example, animals that vocalize frequently may be more available acoustically than visually. Post-survey methods, such as Mark-Recapture Line Transect (Borchers et al., 1998) and Hidden Markov Models (HMM, e.g. Borchers et al., 2013) can account for availability bias using correcting estimators. Availability bias is greatly influenced by the behaviour of animals (Richman et al., 2014); e.g. spatially varying diving patterns may lead to differences in the available time for visual or acoustic detection.

Perception bias is influenced by species-specific factors as well as characteristics of the environment and detector. For visual detection of cetaceans, species-specific characteristics include the percentage of the body visible at the surface and the blow size. Environmental factors include the light and sea-state conditions, while the height of the observation platform and the duration of observation shifts influence the performance of observers. Likewise, for acoustic surveys perception bias is influenced by the characteristics of individual vocal cues (i.e., source level, frequency, beampattern, duration), as well as by behaviour, e.g. foraging groups can have larger detectability than travelling groups in some cases (Nuuttila et al., 2013).

The primary environmental factor influencing acoustic detection is ambient noise, which comprises physical (e.g., wind-driven surface waves, rain), biological (e.g., snapping shrimp) and, increasingly, human noise sources such as from shipping, construction and seismic surveys. When performing passive acoustic monitoring, ambient noise can potentially mask vocalizations of the species of interest (Parks et al., 2007), while discrete sounds from other cetacean species can trigger false detections and so may be a source of misclassification bias (Caillat et al., 2013; Ou et al., 2012; Zimmer & Pavan, 2008). The physical characteristics of the water (i.e. salinity and

temperature depth profiles of the water column, water depth and substrate type) also affect sound propagation and absorption, and hence the transmission of acoustic cues.

In addition to environmental factors, the detectability of acoustic cues can be limited by the characteristics of the recording system, in particular the hydrophone and recorder self-noise, the processing bandwidth, and the depth of the receiver (Zimmer et al., 2008), as well as the algorithm used to detect specific sounds (Yack et al., 2010). Although detection is a stochastic process that depends on the instantaneous values of noise and signal, the average detectability of an acoustic signal is conventionally modelled by the sonar equation (Urick, 1983), which incorporates factors such as ambient noise, sound source parameters, transmission loss and characteristics of the detection system. This provides a simplified and consistent model with which to evaluate the impact of each component and therefore the consequences of different survey and receiver designs. In acoustic surveys, testing the performance of different detectors allows researchers to choose the detector better suited to the target species and environmental conditions. As with visual surveys (Palka et al., 1996) estimates of the acoustic false alarm rate and detection probability can be used in post-processing to improve abundance estimates (Marques et al., 2013).

The characteristics of the vocal cues have a major influence both on detectability and on detector design, with tonal frequency modulated signals, such as whistles, requiring different detection methods than do short transients, such as echolocation clicks. Toothed whales produce echolocation transients for foraging and navigation, and tonal and/or transient sounds for social communication (Aguilar de Soto et al., 2012; Dunn et al., 2013; Tyack, 1986). While sound production for communication occurs irregularly in most species, echolocation behaviour is more stereotypical, especially for deep diving whales such as beaked whales. Several beaked whale species have been tagged with sound recording tags (Tyack et al., 2006; Johnson et al., 2006; Miller et al., 2015; Stimpert et al., 2014). The two most studied species of beaked whales are the Cuvier's and Blainville's beaked whales (*Ziphius cavirostris* and *Mesoplodon densirostris*, respectively). These whales typically spend only some 2 to 8 minutes at the surface per dive which can last 20-80 minutes (Tyack et al., 2006; Barlow et al., 2013) rendering a very low probability of visual detection (Barlow, 1999; Barlow & Gisiner, 2006). In contrast, they produce echolocation clicks almost continuously when foraging at depth

(Tyack et al., 2006; Aguilar de Soto et al., 2012). Both species spend approximately 20% of their total time echolocating in deep foraging dives, producing approximately 3500 clicks in a 20-30-minute bout per dive (Tyack et al., 2006, Arranz et al., 2011). Blainville´s beaked whale usual clicks, when recorded on the acoustic axis, have distinctive frequency upsweeps with a mean duration of 271μs (219-321μs durations corresponding to 5-95% of cumulative energy) and centre frequencies between 35 and 42 kHz (Johnson et al., 2006). Clicks from Cuvier's beaked whales also have an upsweep but with a slightly higher centre frequency and shorter duration (Zimmer et al., 2005). Similar observations have been made for clicks from Northern bottlenose whales (*Hyperoodon ampullatus*) (Wahlberg et al., 2011) and Sowerby's beaked whales (*Mesoplodon bidens*) (Cholewiak et al., 2013), suggesting that the frequency modulated sweep and relatively long duration may be common features of beaked whale echolocation clicks. Both of these features are very different from the usual clicks produced by other toothed whales, making beaked whale clicks a promising cue for taxa detection and tracking (Roch et al., 2011; Yack et al., 2010). Although few verified recordings are available, clicks from some beaked whale species, although superficially similar, may also be mutually distinguishable (Baumann-Pickering et al., 2013; Gillespie et al., 2009; Wahlberg et al., 2011) hinting at the possibility of species-level acoustic surveys. However definitive recordings of most of the 22 currently recognized species of beaked whales have yet to be obtained.

Passive acoustic detection functions for beaked whale clicks have been estimated for both Blainville's beaked whale (Moretti et al., 2006; Marques et al., 2009, 2013; Moretti et al., 2010) and for Cuvier's beaked whale (Zimmer et al., 2008) using a variety of methods. Zimmer et al., (2008) inferred the detection function of Cuvier's beaked whale from the predicted transmission loss, combined with general information about the sound source and a simplified model of detector operation. This physical modelling approach provides an indication of how the sound source and environmental parameters impact the detection function but requires many simplifying assumptions. Thus, independent measurements under authentic conditions are important to qualify this approach. The fixed hydrophone network of the U.S. Navy's Atlantic Undersea Test and Evaluation Center (AUTEC) in the Bahamas, has been used for several studies on beaked whale detection (Moretti et al., 2006; Marques et al., 2009; 2013; Moretti et

al., 2010; Ward et al., 2011). The network consists of 82 bottom-mounted hydrophones placed at approx. 2000m depth. Combining this array with on-animal sound recordings using the DTAG (Johnson & Tyack, 2003) has enabled tracking of individual animals within the array, giving a precise distance between the animal and a receiving hydrophone for each echolocation click. This provides a direct connection between range and detectability, which can be used to derive an empirical detection function for specific detectors (Marques et al., 2009; Ward et al., 2011). This method also allows direct comparison of different detector designs with the same signals (Ward et al., 2008). Although this approach provides arguably the most precise measurement of the detection function, it has a number of drawbacks. Hydrophone array installations such as AUTEC are extremely expensive and exist in only a few locations in the world. Thus, a method anchored to this type of infrastructure provides little opportunity to compare detection probability in different regions or to measure the detectability of other species that are not common in locations with fixed arrays.

As the detection function is dependent on detector design, a comparative assessment of different detectors is essential. Sophisticated passive acoustic detection systems may include several layers of detectors and classifiers to reduce false alarms and to categorize sounds into different classes (i.e. call types/species). Several detector algorithms for beaked whale clicks have been proposed that exploit different characteristics of these signals but are therefore vulnerable to any changes in these characteristics. Matched filters exploit the relatively large time-bandwidth product of beaked whale clicks but may be less effective when the signal is altered by absorption or by reception at an angle well away from the acoustic axis (Ward et al., 2008). Coherent demodulation (FMCD, by Steve Martin in Yack et al., 2010) takes advantage of the distinctive upsweep present in on-axis clicks but this feature can be absent in off-axis clicks. Spectral correlation (Moretti et al., 2006; Zimmer & Pavan, 2008) and the energy ratio mapping algorithm (Klinck & Mellinger 2011; Matsumoto et al., 2013) take advantage of the spectral distribution of energy in the clicks which also changes substantially with aspect and distance. Proposed classifiers of beaked whale echolocation clicks include a Gaussian mixture model (GMM) method from Roch (in Yack et al., 2010) and a two stage-process classification using a Teager energy envelope for click identification (Roch et. al., 2011). The two-stage classification first detects

echolocation clicks based on their high frequency content, and then cepstral features of the detected clicks, i.e the inverse Fourier transform of the logarithm of the click power spectra, are classified by the GMM to differentiate species (Roch et al., 2011).

The performance of a detector or classifier depends on the robustness of the cue to the prevailing environmental conditions and behaviour of the animals. For this reason, it is desirable to compare detector efficiency with the same validated dataset and under a range of real environmental conditions; however, few such studies have been attempted. This is principally because of the difficulty in obtaining recordings in which the large majority of potentially detectable sounds can be classified to species level to provide a calibrated test set. Ideally such a test set should represent a variety of ambient conditions and should include target and non-target species to allow quantification of detection rates and false positives. Studies comparing detection algorithms, such as Yack et al., (2010) have been conducted using data from the field. However, studies using field data from passive acoustic recorders seldom have information about the distance at which sounds were received. Distance information is essential, especially if sound samples are available from a variety of distances, both to establish detectability as a function of range and to assess whether the signal characteristics exploited by detectors/classifiers are robust to sound propagation over different distances.

Here we present a transportable field method for evaluating and comparing detector performance and estimating an acoustic detection function for beaked whales using a combination of sound recording tags and rapidly-deployable drifting sound recorders. The method comprises two steps. First, we estimate the range from the tagged whale to each drifting recorder at the time it produces each click. We then extract waveforms from the far-field recordings corresponding to each reception and pass these through a bank of detectors. We use this method to estimate the detection function of five detector designs for Blainville's beaked whale clicks under real environmental conditions. The results provide insight into how detector design, receiver depth and range together influence detectability for the ultrasonic clicks of Blainville's beaked whales. Being readily transportable, the new detection function method can be applied in different locations and on different species to determine regional and behavioural detectability.

2.2 Materials and Methods

2.2.1 Study area

Field work took place off the island of El Hierro in the Canary Islands (approx. 27.67° N, 18.02° W). This steep-sloped volcanic island has deep waters close to shore with year-round populations of Cuvier's and Blainville's beaked whales (Aguilar de Soto, 2006). Due to the extreme bathymetric slopes adjacent to the island, these deep-diving whales are visible from a shore station at 120 m altitude on a coastal cliff and during field work four observers scan the area with 15x and 7x binoculars to locate animals (Arranz et al., 2014) and guide two small vessels to them. A 4.5m rigid hulled inflatable boat is used to approach and tag whales while a 6m vessel is used to follow tagged whales, deploy sound recording buoys and perform CTD profiles. Field work took place when sea state was a Beaufort 2 or less.

In 2008 and 2010 five animals were tagged with DTAG Version 2 sound and orientation-recording tags, which are attached to the animals with suction cups (Johnson & Tyack, 2003). Sensors in the tags include temperature, pressure for measuring depth, and a 3-axis accelerometer and a 3-axis magnetometer for orientation, all sampled at 50 Hz per channel. Sound is recorded from two spherical hydrophones in the front of the tag and sampling rate was set at 192 kHz per channel. A VHF beacon is incorporated in the tag for tracking and retrieval. Flotation in the rear of the tag ensures that the tag floats with its antenna free of the water after release. Photo-identification is attempted with all animals approached and a catalogue of identified animals is maintained (**www.cetabase.info**).

Prior to each tag deployment, a drifting receiving system was deployed in the area. This consisted of a buoy with a GPS logger and a weighted cable to which 1-3 autonomous recorders were attached at depths ranging from 20 m to 300 m (Table 1). The autonomous recorders were modified DTAGs (Johnson & Tyack, 2003) in 2008 and DMONs (an autonomous passive acoustic monitor developed at Woods Hole Oceanographic Institution) in 2010. The sampling rate of the DTAG was set to 96 kHz with a 0.4-46kHz bandwidth and approximate noise floor of 40 dB re μPa/$\sqrt{\text{Hz}}$ RMS at 30 kHz. The DMONs sampled at 120 kHz and had a bandwidth of 0.1-

52kHz, with a system noise floor at 30 kHz of 32 dB re μPa/$\sqrt{Hz}$. Both DTAG and DMON recorders sampled a single hydrophone. Autonomous recorders deployed at the same time were not synchronized and so were not used as an array.

2.2.2 Data analysis

For each of the five tag deployments, echolocation clicks from the tagged whale were located in the on-animal DTAG sound recording using a supervised click detector. Clicks from the tagged animal were distinguished from those of other nearby whales in two ways (Johnson et al., 2006). Clicks from the tagged whale have low-frequency energy (below 25kHz) that is absent in clicks recorded from non-tagged whales (Johnson et al., 2009) and a consistent angle of arrival, θ, computed from $\theta=\sin^{-1}(\tau c/d)$, where c is the speed of sound in seawater, d is the hydrophone separation (0.025 m), and τ is the time delay between the two hydrophone signals, measured by cross-correlation. The arrival angle of clicks from the tagged whale, when corrected for the tag orientation on the whale, will be consistently close to zero, as the sound source from the tagged animal is directly in front of the tag, while those from other whales will vary widely as the tagged whale manoeuvres.

Blainville's beaked whales produce two types of clicks; frequency modulated (FM) usual clicks of duration 271 μs (219-321 μs 5-95%), that are used to search for prey, and wide-bandwidth pulses of duration 104 μs (73-120 μs 5-95%) produced at a high rate during prey capture attempts, i.e. buzzes (Johnson et al., 2006). These buzz clicks have a source level some 15 dB lower than usual clicks (Madsen et al., 2005) and so are less likely to be detected in a PAM system. For this reason, here we only analyse usual FM clicks. An inter-click-interval (ICI) threshold of 0.1 s was used to distinguish usual from buzz clicks (Johnson et al., 2006).

The sound recordings from the autonomous recorders contain clicks from the tagged animal as well as other whales in the vicinity. To identify the clicks from the tagged whale, a synchronized envelope plot was used (Fig. 2.1, Johnson et al., in prep). In this display, segments of sound from the receiver, synchronized to the timing of clicks emitted by the tagged whale, are displayed as envelopes in a stack plot. A band-pass filter broadly matched to the -10 dB bandwidth of Blainville's beaked

whale FM clicks (26-51 kHz) was applied prior to forming the envelopes. The tags deployed on the whales and the autonomous recorders had free-running clocks which were synchronized to within +/- 2 s before deployment but which drifted over the course of the deployment. A tool in Matlab called *crosstool* was created by Mark Johnson and was used to identify the arrival time of clicks from the tagged animal at the autonomous recorder, the time offset between the click production times as reported by the tag on the animals and the start time of the sound segments used in the synchronized plot was adjusted manually until a near-vertical line appeared in the stacked envelope display, representing the direct arrival of clicks (Fig. 2.1). This line shows the precise received times on the autonomous recorder of the clicks from the tagged whale, relative to their transmission time as recorded by the tag. The time offset between the clicks on the tag and the received times at the autonomous recorder is the 'apparent time of flight', i.e., the sum of the actual time of flight (the time taken for sound to travel from the whale to the receiver) plus the clock offset between the two devices. The vertical line appears because the apparent time of flight varies little over a sequence of tens of clicks because both the distance between tag and receiver, and the clock offset vary relatively slowly with time.

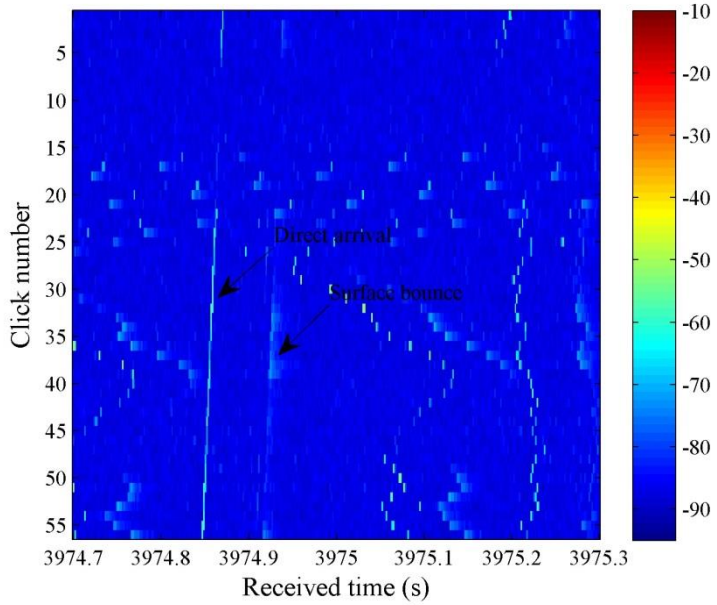

Figure 2.1 Synchronized plot used to identify sounds arriving from the tagged whale on each autonomous recorder. 0.6 s blocks of sound from the autonomous recorder are synchronized with clicks from the tagged whale and the relative time delay between tag and receiver is

adjusted until a vertical line appears in the display. The arrival times with respect to the clock on the autonomous recorder are then collected from the display using a supervised peak extractor. Colour represents the intensity of the received signal in dB re 1 V. In this display the surface bounce of the direct arrival can be seen as a parallel line to the right of the stronger direct arrival line. The surface bounce has the same clock offset with the direct arrival but a longer path so it arrives with a longer but consistent apparent time of flight that can be seen as a parallel line to the direct arrival on the plot.

2.2.3 Distance Estimation

To estimate the acoustic time of flight, and therefore the distance between whale and receiver, the clock offset between the two devices must first be estimated. This can then be subtracted from the apparent time of flight to estimate the acoustic time of flight. The clocks in the recorders and tags drift with time and temperature. To estimate the clock offset as a function of time, we first estimated the range from the whale to the receiver in a subset of clicks in which the surface bounce was detected in addition to the direct arrival, allowing range estimation independent of the local clocks due to the tag recording the depth of the whale (Cato, 1998). The time difference, τ, between the direct and surface bounce arrivals for a whale (Fig. 2.2) at depth d_t and a receiver at depth d_r is:

$$\text{TDOA } \tau = \frac{\text{surface bounce}}{\text{path integrated speed}(\bar{s}_{sb})} - \frac{\text{direct path length}}{\text{path integrated speed}(\bar{s}_{d})} \tag{2.1}$$

$$= \frac{r_{sb}}{\bar{s}_{sb}} - \frac{r_d}{\bar{s}_d} \tag{2.2}$$

$$r_d{}^2 = h^2 + (d_t - d_r)^2,\ r_{sb}{}^2 = h^2 + (d_r + d_t)^2 \tag{2.3}$$

$$\begin{aligned} r_{sb}{}^2 &= r_d{}^2 - (d_t - d_r)^2 + (d_r + d_t)^2 \\ &= r_d{}^2 + 4d_r d_t \end{aligned} \tag{2.4}$$

$$\tau = \frac{1}{\bar{s}_{sb}}\sqrt{r^2 + 4d_r d_t} - \frac{r_d}{\bar{s}_d} \tag{2.5}$$

$$\left(\tau + \frac{r_d}{\bar{s}_d}\right)^2 = \frac{1}{\bar{s}_{sb}^{\,2}}\left(r_d^{\,2} + 4d_r d_t\right) \tag{2.6}$$

$$r_d^{\,2}\left(\frac{1}{\bar{s}_d^{\,2}} - \frac{1}{\bar{s}_{sb}^{2}}\right) + \frac{2\tau}{\bar{s}_d} r_d + \tau^2 - \frac{4d_r d_t}{\bar{s}_{sb}^{2}} = 0 \tag{2.7}$$

r_d is the maximum root of this polynomial

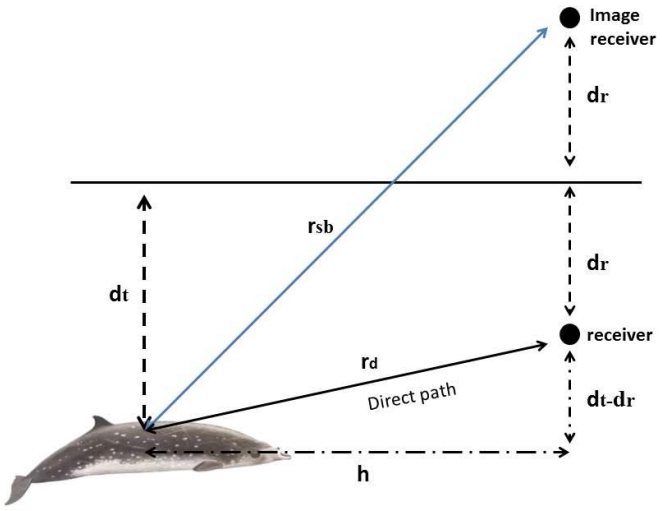

Figure 2.2 Schematic representation for distance calculation from the vocalizing animal. The tag records the depth of the whale transmitting clicks, dt, while the receiver is deployed to a known depth, dr. There is therefore only one unknown distance (h) which can be estimated from the time difference of the direct and surface bounce arrivals.

For the path integrated sound speeds, CTD profiles (Fig. 2.3) were used to estimate sound speeds in the area. The sound speed profiles vary relatively little with season and location within the study site. The variability of up to 5 m/s apparent in Fig. 2.3 amounts to some 0.3% of sound speed. Given the minor impact of this variability on the derived distance estimates, a single representative sound speed profile was used (solid green line Fig. 2.3). A robustness check was then made to assess the differences in distance estimate that would result from choosing a different one of the curves in Fig. 2.3.

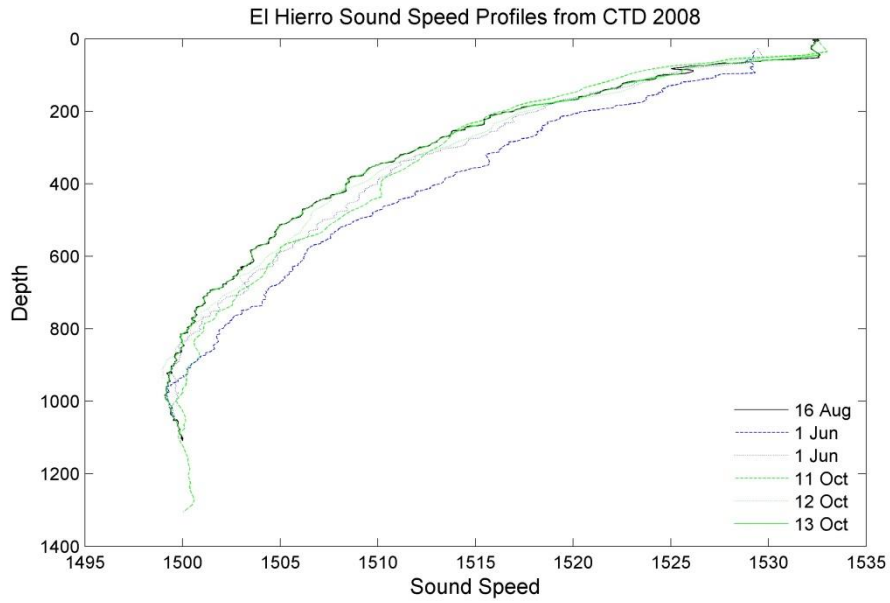

Figure 2.3 Representative sound speed profiles for the field site off El Hierro, for the year 2008. The different colours correspond to sound speed profiles from different dates spanning the times of year that tags were deployed (solid black- August, dashed blue June, dotted blue June from a different location within the fieldsite, dashed green 11 October, dotted green 12 October and solid green 13 October).

These estimated ranges were then converted into time of flight by dividing by the path integrated sound speed for the direct path. The estimated times of flight were subtracted from the apparent time of flight of the direct arrival to give an estimate of the clock offset at the time of the click. The resulting clock offset estimates were collected throughout the recording and used to fit a simple model for the clock offset for each dive containing three parameters: the initial time offset (seconds), the drift rate (seconds per second) and the temperature coefficient (seconds per cumulative degree Celsius). The temperature was obtained from the DTAG and the receiver. Once fitted, this model was used to predict the clock offset at times during the dive when surface bounces were not detected, allowing the time of flight and therefore the range of the animal to be estimated for all clicks received at the recorders. A Kalman Filter (KF) was used to smooth the range estimates and to predict ranges at times when the animals produced clicks, recorded in the tag, that were not detected in the synchronized envelope display. The KF range estimates were then used to deduce the

expected arrival time of all clicks produced by the whale, increasing the data set of click waveforms for detector testing.

2.2.4 Click waveforms

The Kalman Filter distance predictions for each click produced by the whale were converted into expected arrival times at the recorders by dividing the range by the path integrated sound speed and adding the predicted clock offset. Clicks for which the Kalman state covariance estimate implied a timing error greater than 1.3 ms, which is half the duration of the analysis block used for testing the detectors, were eliminated because their arrival time was too uncertain. The state covariance estimate becomes larger (implying more uncertain estimation) as the time between measurements increases, hence extended periods with undetected clicks will have more uncertain time estimates. Sound extracts 2.6ms long, starting 1.3ms before the predicted arrival time, were extracted from the recordings of the autonomous recorders. These full bandwidth sound extracts contained varying levels of ambient noise, especially at low frequencies due to differing sea conditions and boat traffic. In order to provide a controlled environment (i.e., a relatively constant noise spectrum) for the detector comparison study I adopted a suggestion of thesis supervisor M. Johnson and applied a whitening filter to the sound extracts. The objective of the whitening filter was to reduce the variance in the ambient noise segments and to provide a controlled environment for the detector comparison study. The whitening filter coefficients for each receiver deployment were based on a 10^{th} order forward linear predictor calculated with the autocorrelation method i.e. Levinson-Durbin recursion (Jackson, 1989 pp. 244-257). The whitening filter was calculated from ambient noise sampled at the start of each recorder deployment so as to be specific to the environmental conditions during each deployment. In all cases, the whitening filter was a high-pass filter with steep attenuation between 1-10 kHz and fairly flat response at higher frequencies in which the system noise of the recorders dominates the total noise (Johnson et al., 2011). The sound extracts are about 6 times longer than the duration of a Blainville's beaked whale FM click to allow both for error in the arrival time estimates and for filter time constants in the detectors that will be run over each extract. The energy level and root-

mean-square (RMS) sound pressure level of each extract were calculated over the smallest window covering 90% of the energy in the 2.6ms block to capture the arrival of the click. The sensitivity of the hydrophone, preamplifier and acquisition circuits in the recorders was subtracted from this level in dB to estimate the click received level (RL) in dB re 1μPa RMS. To estimate the contemporaneous noise level, a 5 ms segment of whitened audio was taken starting 7ms prior to each click, leaving a 2ms gap before the nominal click arrival time to ensure that the click energy did not impinge on the noise interval. The RMS level of the noise sample was calculated and compared against the click levels to estimate the whitened signal-to-noise ratio (SNR). Clicks with received SNR<0dB were not used for detector testing but were used in the modelling of the final detection function to account for the total number of clicks produced. Due to the number of clicks in the dataset, the noise segments were not examined individually to check if they contained a click e.g., from a whale other than the tagged whale. The presence of a click in a noise segment would lead to a lower calculated SNR and may have led to a small number of detectable clicks being excluded from the analysis. However, clicks should occur rarely in the short noise segments and this source of bias is unlikely to greatly impact the results.

2.2.5 Detector simulation

Five different detectors exploiting different characteristics of beaked whale clicks were compared. These comprised two correlation detectors, two energy detectors and an energy ratio detector. The correlation detectors filter the input signal with a time-reversed waveform, called a template, which is similar to the signals of interest. If the template is identical to the received signal, this process is called matched filtering. Given the variability in click waveforms and the random orientation of animals with respect to the receiver, perfect matching is not realistic for PAM and, instead, templates must be selected that are a reasonable match to the expected waveforms. Here, two different templates were used. The first was based on an exemplar on-axis click from a nearby conspecific recorded at high SNR by a tag on a Blainville's beaked whale (Johnson et al., 2006). The second template was created from both on- and off-axis clicks from nearby conspecifics recorded in tag deployments on 10 Blainville’s

beaked whales in the study area. This template was the mean of 100 randomly selected clicks from each tag deployment resulting in 1000 clicks in total, time aligned by cross correlation.

A band-pass energy detector calculates the energy of the signal in the frequency band of interest and so ignores phase information. Here I used two band-pass energy detectors. The first is an 8^{th} order 27-40 kHz Butterworth bandpass filter with energy summed over a 220 μs rectangular window corresponding to the approximate bandwidth and 95% energy duration of an on-axis beaked whale click (Johnson et al., 2006). The second energy detector is an 8^{th} order 27-37 kHz Butterworth bandpass filter with energy summed in a 430 μs rectangular window corresponding to the bandwidth and duration of a moderately off-axis beaked whale click.

The fifth detector is an energy ratio detector (Klinck and Mellinger, 2011) which compares the energy in two frequency bands: one overlapping the click frequency range and the other chosen to contain little click energy. Frequency bands of 27-37 kHz (in band) and 13–23 kHz (out of band) were used with 8th order bandpass filters and energy summed over 430 μs rectangular windows.

For each detector, a threshold that gave a false alarm rate of 10^{-6} (i.e., an average of one false alarm per one million 2.6 ms sound blocks equivalent to a false alarm rate of about 1 per 40 minutes when processing continuous audio) was chosen to allow comparison between the different detectors. This choice of false alarm rate may be fairly realistic for abundance surveys although a lower rate may be preferred for mitigation. Here, the choice defines the number of repetitions of the algorithm needed to determine the detection threshold and a relatively high false alarm rate was selected to minimise processing time. The false alarm rate was evaluated with a set of approximately 54000 whitened noise segments of 2.6ms duration each taken from the receiver recordings. As there was typically only one group of beaked whales within several kilometers of the buoys, the noise segments were taken during the time intervals in which this group was not foraging. Spot checks (1% of the noise samples were selected by random number generation) for clicks from other animals during these intervals were made using spectrograms on a subsample of the data.

2.2.6 Simulation Distance Adjustment (SDA) of clicks

Because of the narrow biosonar beam of beaked whales (Madsen et al., 2013; Johnson et al., 2006), clicks are detectable from an decreasing range of aspects as distance increases. As a result, the data set for detector testing contains relatively few click waveforms at long ranges. To overcome this, I used a Simulation Distance Adjustment (SDA) approach to generate longer range click waveforms based on the signals recorded from close animals. A two-way manipulation of the click waveforms was made. First, a low-pass filter was applied to the click waveforms to account for the greater relative absorption of sound at high frequencies at the simulated increased propagation range. The absorption coefficient was calculated based on standard absorption curves (Kinsler & Frey, pp.159-160), which are temperature and frequency dependent. To simulate the increased high frequency absorption, a symmetric FIR filter derived from the inverse Fourier transform of the absorption frequency response was used. The second step was to adjust the SNR to reflect the increased transmission loss. This was achieved by adding whitened noise samples from the same receiver recording to the whitened and filtered click so that the SNR was reduced by $20\log10(r/r_0)$ where r_0 is the original recording range of the click and r is the new range to simulate. The composite signal was then attenuated to match the total noise power to the ambient noise level used to calibrate the detection threshold. For simplicity, transmission loss was based on spherical spreading and absorption was calculated for an average 450 m path depth and 12.3º C water temperature, values which are reasonably close to experimental values.

2.2.7 Detection function

Multi-covariate models have been used to derive the detection function of birds (Marques et al., 2007), and to identify covariates that may influence detectability. Here, the acoustic detection function of beaked whale clicks was analysed using a

binomial approach within a generalized estimating equation (GEE) using the package geepack (Hojsgaard et al., 2006) in R (www.r-project.org) combined with Generalized Additive Models (GAMs) to account for non-linear relationships between the response and the predictors. GEEs take into account the serial autocorrelation existing in the data (GEEs; Liang & Zeger 1985), which translates into generally larger variance estimates than with a linear regression (for positive correlation). Here, the model comprised a logit link function predicting the binary detection status of each click from a set of covariates.

A binomial-response GAM with logit link function has the following form:

$$g(\mu_i) = \eta_i = \log\left(\frac{p_i}{1-p_i}\right) = \beta_o + \sum_{j=1}^{p} f_j(X_j) \qquad (2.8)$$

Where $g(\mu_i)$ is the link function η_i is the additive predictor and the f_j are the smooth functions acting on each covariate, *Xj*. GAMs usually assume independence in the model errors, which is not true for the sequential data here (i.e., series of clicks from an animal with slowly varying distance and aspect). The correlations existing in the repeated observations are accounted for in the GEE through a correlation structure matrix. This allows the independence assumption between single observations to be relaxed and an independence assumption is only required between blocks of observations, where the block is chosen to reflect a natural scale of decorrelation in the data (Liang & Zeger, 1986). The block variance covariance structure takes the form:

$$R = \begin{pmatrix} R_1 & 0 & 0 & 0 \\ 0 & R_{\cdots} & 0 & 0 \\ 0 & 0 & R\ldots & 0 \\ 0 & 0 & 0 & R_n \end{pmatrix} \qquad (2.9)$$

Where $R_1 \ldots R_n$ are sub-matrices of correlations corresponding to each block, and have dimension equal to the size of the block (i.e., the number of consecutive clicks) that the sub-matrix represents. The zeros represent the assumed zero correlation between blocks of data. The correlation values within the sub-matrices $R1\ldots n$ are estimated by the GEE and so add additional parameters to the problem. To reduce the number of correlation parameters, GEE solvers support several different matrix structures in addition to the worst-case unstructured design (Liang & Zeger, 1986).

Examples are: exchangeable, auto-regressive, M-dependent and fixed. Here, a simple working independence (WI) structure was used for model fitting. The blocking structure was that of the outcome of the 5 different detectors for each set of visually detected clicks, taking in to account that the same click was used from the five different detectors.

The covariates incorporated in the model were: i) estimated slant range distance between the receiver and the animal, ii) depth of the receiver, iii) type of receiver (DTAG or DMON) and iv) detector algorithm. First-order interactions between the covariates, i.e., distance with type of detector, distance with receiver depth, and depth with type of detector, were also explored. All of the variables were entered in the model as factors except distance, which participated as a continuous variable. The depth of the receiver varied between 20, 200, 250 and 300 meters depth and so was grouped into two categories: "shallow" which consists of the 20m receivers, and "deep" corresponding to receiver depths of 200, 250 and 300 m.

As the purpose of the model was description, a parsimonious model was chosen by backwards model selection based on marginal p-values from the GEE fit. A *p*-value of 0.05 was used as the threshold defining significance of a covariate. The full model was initially fitted, followed by iteratively dropping the least significant model term and then refitting, until all terms were significant. The *p*-values were calculated using *getPvalues* in package MuMIn (Barton, 2015) in R (R Core Team, 2015). A parametric bootstrapping approach was used to estimate the 95% confidence intervals for the predicted means. The bootstrap used 1000 realizations of the model coefficients based on the GEE-derived standard errors for each model term. Goodness of fit was checked by 10-fold cross validation which comprises dividing the data into 10 equal but random subsets and using one subset in turn for validation and the remaining 9 for fitting the model (Hastie et al, 2009). This results in 10 measures of predictive accuracy for each model considered. A Receiver Operating Characteristic (ROC) curve was used to assess the model adequacy for each iteration of the cross-validation, with the Area Under the Curve (AUC) used as a measure of the model fit (Boyce et al., 2002). The contribution of the explanatory variables in the final model was visualised by means of partial residual plots of the estimated relationship between the response (on the link scale) and each predictor, coupled with confidence

intervals based on the GEE standard errors. The raw click dataset and the augmented dataset after the SDA (Simulation Distance Adjustment) were modelled separately, and two different detection functions were obtained. These detection functions were then adjusted for the total number of clicks produced by the animal to account for the clicks that were produced but were missed. The resulting detection functions were parameterized by their effective radius, $\hat{e}_r$, i.e., the distance at which as many objects beyond $\hat{e}_r$ are detected as are missed within $\hat{e}_r$ (Buckland et al., 2001). This is estimated by

$$\hat{e}_r = \sqrt{\hat{P}w^2} \qquad (2.10)$$

where $\hat{P}$ is the average probability of detecting a click of a Blainville's beaked whale within a distance of 0 to w, i.e., $\hat{P} = \int_0^w \frac{2xg(x)dx}{w^2}$ and $g(x)$ is the detection function at distance *x* from the receiver with a truncation distance *w*.

To test if receiver type, independent of detector algorithm, influences detectability of clicks, a Generalized Linear Model (GLM) with a logit-link and binomial errors was used. This model predicted which clicks would be visually detected from the synchronized plot. A GLM is an extension of a linear regression model that allows the distribution of the response to be from the exponential family such as Gaussian, Binomial, Poisson or Gamma. In this case, the detection probability was modelled as a binary response variable (with a Bernoulli distribution). A formula for this GLM is as follows:

$$g(\mu_i) = \log\left(\frac{m_i}{1-m_i}\right) = \eta_i = \beta_0 + \beta_1 \text{distance}_i + \beta_2 \text{depth}_i + \beta_3 \text{ReceiverType}_i \quad (2.11)$$

where i is the *i*-th observation ($i = 1, \ldots, n$), m is the probability of detection, $g(\mu_i)$ is the link function and η_i is the resulting linear predictor. The covariates that participated in the model are distance, depth of the receiver and type of receiver. A backwards selection was used to find the model which described the data most parsimoniously.

2.3 Results

Five Blainville's beaked whales were tagged in proximity of acoustic recorders, 3 in 2008 and 2 in 2010 (Table 1), resulting in 9 deep foraging dives recorded by the autonomous recorders. Animals were vocal during the deeper part of deep dives, producing echolocation clicks for an average of 24 min (16–29 min) per deep dive as reported elsewhere (Table 1, Aguilar de Soto et al., 2012). Figure 2.3 shows the typical characteristics of the regular clicks recorded from Blainville's beaked whales for an on-axis and an off-axis click.

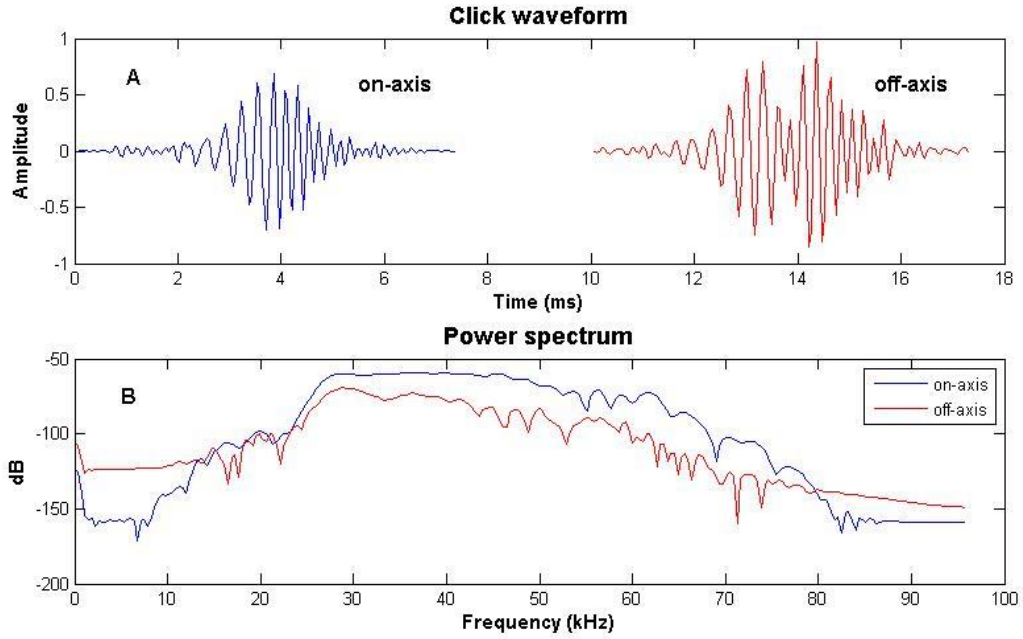

Figure 2.4 A) FM Click waveforms and B) Power spectrum, for an approximately on-axis (blue) and off axis (red) click from a Blainville's beaked whale as recorded by a DTAG for two non-focal animals in close proximity to the tagged animal. Note that the amplitude of the clicks in (A) is arbitrary: they have been amplified by different amounts to improve clarity.

Animal id	Year	DTAG recording (hours)	# Dives	# Clicks per dive	# Direct arrivals				# Surface bounce Clock offset r^2 std(r)				# Kalman Filter (SNR >0)			
					Depth of receiver											
					20	200	250	300	20	200	250	300	20	200	250	300
md08_289a/MdH22-08	2008	19.5	3	4992 4425 3868	187 1977 2522	230 1934 2314	141 2790 950	224 1750 1961	53 507 1466	44 116 243	37 218 123	110 164 188	0.8 (33) 1.0 (12.9) 1.0 (162)	0.7 (1.7) 1.0 (2.5) 1.0 (1.8)	1.0 (8) 1.0 (1.5) 0.9 (1.9)	1.0 (8) 1.0 (2.1) 1.0 (1.5)	689 (1) 2673 (2) 3183 (3)	499 (1) 2812 (2) 3309 (3)	512(1) 2772 (2) 1205 (3)	886 (1) 2681 (2) 3214 (3)
md08_142a/MdH74	2008	1.8	1	3192		888	801	776		213	174	91		0.7 (3)	0.41 (3.4)	0.3 (2.5)		1586	1504	1403
md08_148a/MdHC1-08	2008	6.2	1	3042		2102	2035	2059		197	178	132		1.0 (2.3)	0.8 (1.9)	0.8 (1.6)		1743	1651	1752
md10_146a/MdHX33	2010	2.9	1	3104	884 2295	2220 1069			343 1466	451 167			1.0 (8.3) 1.0 (10)	1.0 (2.1) 1.0 (1.8)			2691 1816	2664 1500		
md10_163a/MdH86-10	2010	18.1	3	3895 2710 2269	1577 91 280 2453 629 856	1625 98 342 2742 947 1071			676 40 51 1675 161 426	716 24 44 1559 58 315			0.9 (20), 0.2 (17), 0.3 (9.1) 0.9 (10) 0.9 (9.7) 0.9 (23.1)	0.9 (13), 0.8 (9.8), 0.1 (166.5) 0.9 (5) 0.8 (88) 1.0 (22.1)			2591 (1) 3441 (1)	1352 (1) 445 (2) 3496 (1) 1650 (2)		

Table 1 DTAG deployments and the corresponding autonomous recorder deployments. The table shows the Animal id: The code comprises the species initials, the year (two digits), the Julian day, and the tag deployment of the day (a single letter), the second code refers to individuals in the photo-ID catalogue at http://www.cetabase.info, followed by the year (two digits) of the deployment, duration of each DTAG deployment, the number of dives analysed, the number of non-buzz clicks produced in each dive, the number of direct and surface bounce detections from the synchronized plot, the clock offset estimate from the linear regression for each dive and the number of positive SNR signals extracted after the Kalman filter arrival time estimation. The standard deviation for the clock offset is in milliseconds. Dives with insufficient data for clock offset estimation were excluded from further analysis (shaded cells).

Table 1 shows the number of clicks produced, received and the number of surface bounce receptions for each dive and animal. During dives in which the tagged whales were within 6km of the recorders, 42% of clicks were detected in the autonomous recordings using synchronized plots and an average of 0.11% of clicks had a detectable surface bounce from which range and clock offset could be estimated.

2.3.1 Clock offset and distance estimation

The clock offset was estimated independently for each dive and recorder. The number of direct path - surface bounce pairs used to estimate the clock offset parameters varied from 24 to 1675 (Table 1). Dives with insufficient data for clock offset estimation were excluded from further analysis (shaded cells in Table 1). For the 25 dives in which the clock offset could be estimated, the r^2 of the linear regression was greater than 0.9 in 19 cases and for the remaining 6 had a mean value of 0.33 ranging between 0.1-0.7 and these dives were not used in the analysis (shaded cells on Table 1). An example of the clock offset prediction model fit is given in Fig. 2.5.

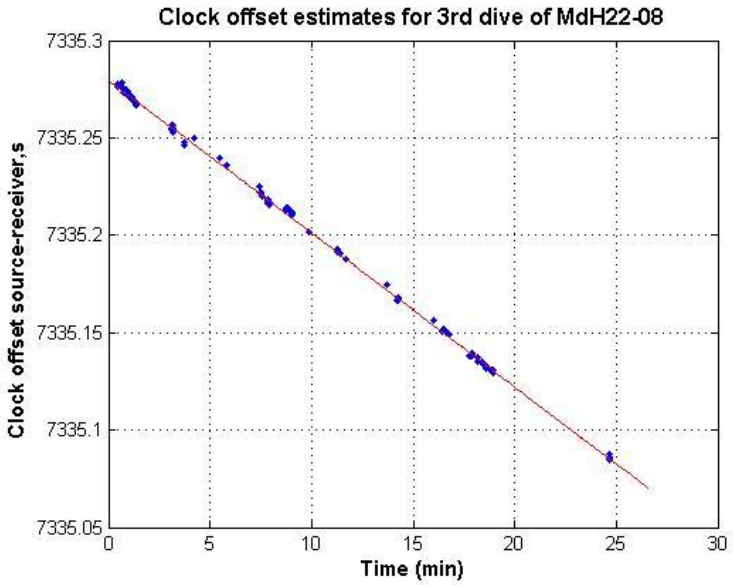

Figure 2.5 Clock offset estimate (R^2=1.0) for the third dive of animal MdH22-08 with a receiver depth of 300m depth. Clock offset estimates from individual clicks are shown with blue dots and the regression fit is shown by the red line as a function of time (in min) since the start of the dive.

The slant ranges between whale and recorder, derived from the surface bounce arrivals varied from 0.42 km to 4.2 km with fairly uniform coverage out to 3 km but few data points beyond this. The Kalman Filter interpolation increased the number of clicks with a range

estimate but the distribution of distances covered by the resulting extended dataset was much the same (Fig. 2.6).

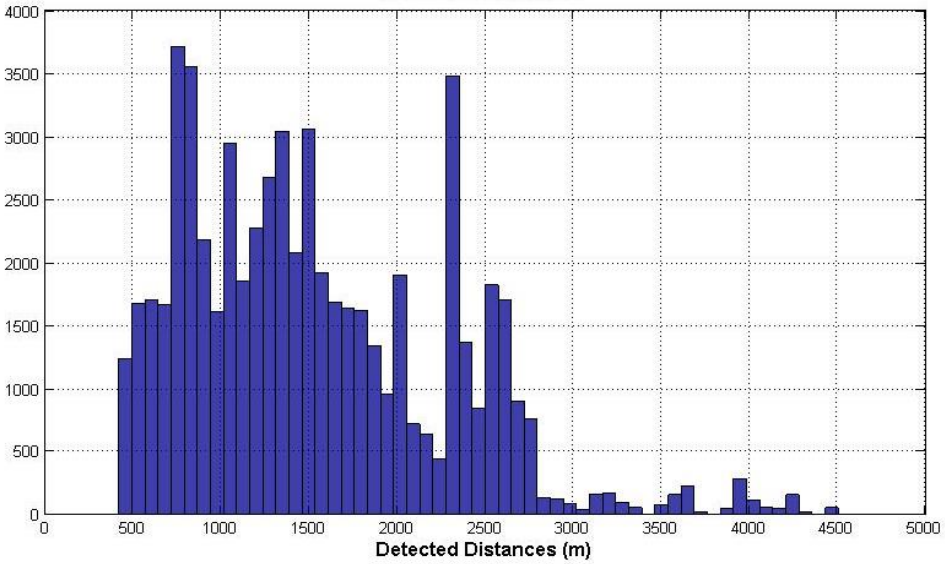

Figure 2.6 Histogram of clicks received at different distances (direct distance between the whale and the receiver) from KF estimation.

The number of clicks detected visually in the autonomous recorders using synchronized plots was 40807 (46% of generated clicks). Using the expected times of arrival from the Kalman Filter, the number of clicks with reliable arrival times increased to 61120, of which 52032 had a positive SNR and were kept for the detection function analysis. For the SDA dataset distances of up to 6 km were simulated.

With detection thresholds adjusted for a false alarm rate of 1 per 10^6 of 2.6 ms extracts, the number of clicks detected by the 5 different detectors for the raw and the simulated distance dataset is given in Table 2. Detection rates are expressed in two ways: (i) as percentages of clicks tested, i.e., out of 52032 for the actual receptions and out of 246281 for the SDA signals, and (ii) as percentages of clicks actually produced by the whale (442670 for raw receptions and 2462815 for SDA).

Table 2 Percentage of clicks detected by the 5 different detectors for the raw click dataset and the simulated distance adjustment (SDA) click dataset. Percentages are shown with respect to the number of clicks extracted and the total number of clicks produced. The detectors comprise a correlation detector based on an exemplar on-axis click (MF1), a correlation detector based on a set of on- and off-axis clicks (MF2), an energy detector based on a 27-40 kHz bandpass filter with energy summed over a 220 µs rectangular window(EN1), an Energy detector based on 27-37 kHz bandpass filter with energy summed over a 430 µs rectangular window (EN2) and an Energy ratio (ENRAT) detector, comparing the frequency bands of 27-37 kHz and 13-23 kHz.

% of Clicks detected with respect to:	SOURCE DATA	DETECTOR				
		MF1	MF2	EN1	EN2	ENRAT
# Extracted	Raw	51.41	53.72	56.56	56.72	43.79
	SDA	13.30	15.01	15.65	15.09	10.85
# Produced	Raw	28.12	29.38	30.94	31.03	23.95
	SDA	7.74	8.75	9.12	8.79	6.32

2.3.2 Detection function model

The covariates that significantly influenced the probability of click detection comprise distance, receiver depth, detector type, and a three-way interaction between distance, receiver depth and detector type. The final models for the two datasets (Raw clicks and SDA simulated clicks, Table 3) have an area under the curve (AUC) of 0.7 and 0.8, respectively (Table 3). The predictive ability of the models was assessed with a 10-fold cross validation giving a mean AUC of 0.65 (Raw) and 0.83 (SDA).

Table 3 Significant covariates (p<0.05) in models of acoustic detection probability of raw Blainville's beaked whale clicks, i.e., taken directly from recordings, and the same clicks with simulated distance adjustment (SDA). The p-values and X^2 are based on generalised estimating equations. The area under the curve (AUC), a measure of the predicting power for the final model for each dataset, is the mean of the AUC values from the 10 fold cross-validation.

Model	Covariate	P	X^2	AUC_{10F}
	Distance	<0.0001	18.76	
	Detector	<0.0001	125.54	
Raw	Depth	0.39	0.74	0.66
	Distance:Detector	<0.0001	24.61	
	Detector:Depth	<0.0001	33.69	
	Distance:Depth	<0.0001	1.27	
	Distance:Depth:Detector	<0.0001	29.29	
	Distance	<0.0001	274.88	
	Detector	<0.0001	491.03	
SDA	Depth	0.08	3.03	0.85
	Distance:Detector	<0.0001	519.29	
	Distance:Depth	0.06	1.57	
	Detector:Depth	<0.0001	110.81	
	Distance:Depth:Detector	<0.0001	44.06	

The estimated probability of detection as a function of distance for the 5 different detectors and for the two different receiver depth groups (shallow and deep) is given in figure 2.7 for the raw model and the simulated distance adjustment (SDA) model. The probabilities take into account the total number of clicks produced. The covariates retained in these models are distance, depth, detector type and the three-way interaction between these covariates (Table 3).

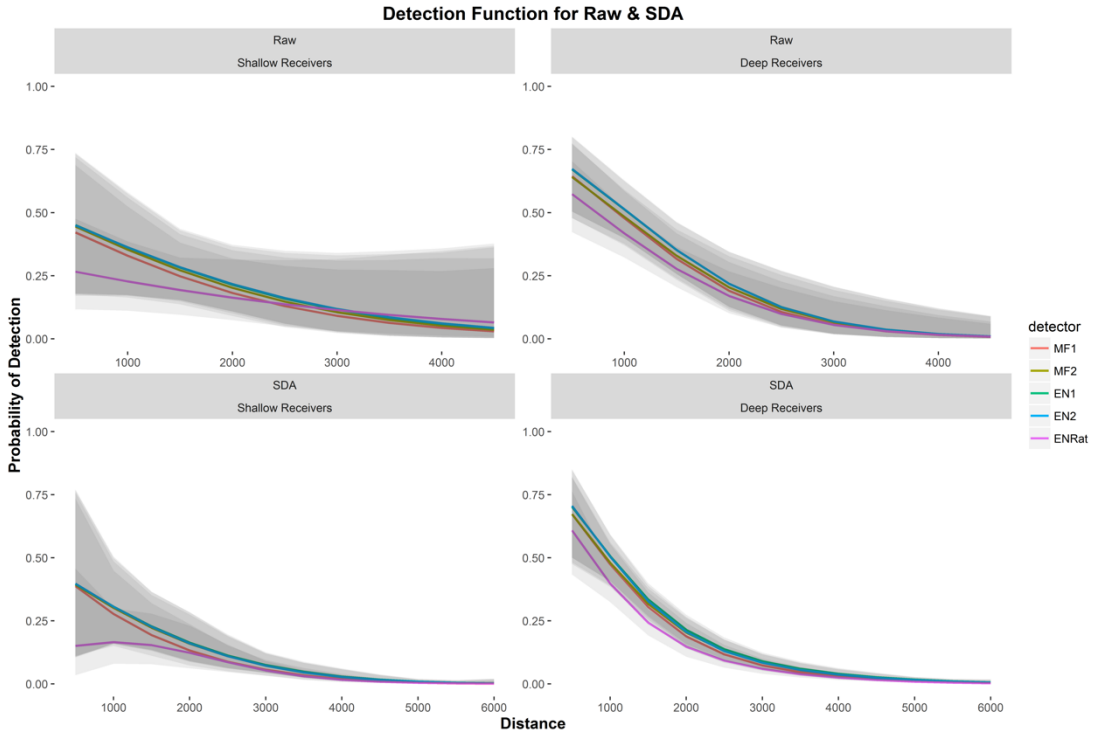

Figure 2.7 Detection functions (i.e., probability of detection as a function of slant distance) for the model using actual received clicks (Raw) for a shallow receiver (20 m) and for a deep receiver (200-300m), and for the model using simulated distance adjusted (SDA) clicks for shallow receiver (20m) and for a deep receiver (200-300m). Grey areas indicate the 95% CI in the detection function for each detector. The probabilities are corrected for the total number of clicks produced by the animal. Note the longer slant distance displayed for the SDA functions.

Detection performance differed markedly between the deep and shallow recording depths with uniformly higher detection probabilities for the deep recordings. Detection rates for the five detectors differed more subtly. The most noteworthy difference is in the energy ratio detector which shows significantly poorer performance at short ranges, especially with a shallow receiver. However, this detector offered slightly better performance than the other detectors at long ranges with the raw data and with a shallow receiver. The detectors based on off-axis signals show marginally better performance at short ranges than the ones based on on-axis clicks but detector performance is remarkably similar beyond about 2km. The influence of receiver type (DTAG or DMON) on the detection probability was tested in a separate model taking into account only the number of clicks visual detected using the synchronized plots (without additional automatic detection) in relation to the number of clicks produced. A Generalized Linear Model (GLM) was used to test if probability of

detection differed between the receiver types. The model with the lowest AIC had a three-way interaction between distance, depth and receiver type Fig. 2.8.

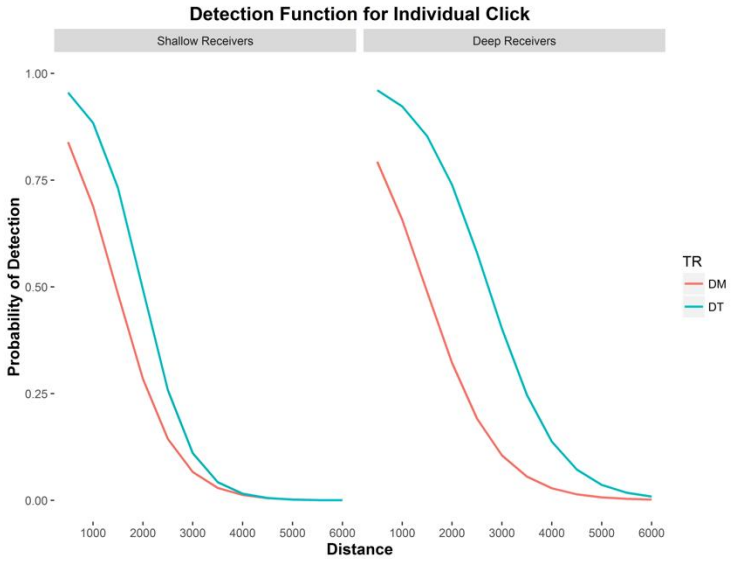

Figure 2.8 Detection function of individual Blainville's beaked whales clicks recorded by shallow and deep receivers, modelled separately for two different recorder types, DMON based (red line) and DTAG based (blue line).

Receivers based on the DTAG showed higher detection probability than receivers based on the DMON (Figure 2.8) despite the lower self-noise of the latter device. However, it must be borne in mind that this result is based on only 2 tagged individuals for the DTAG and 3 for the DMON.

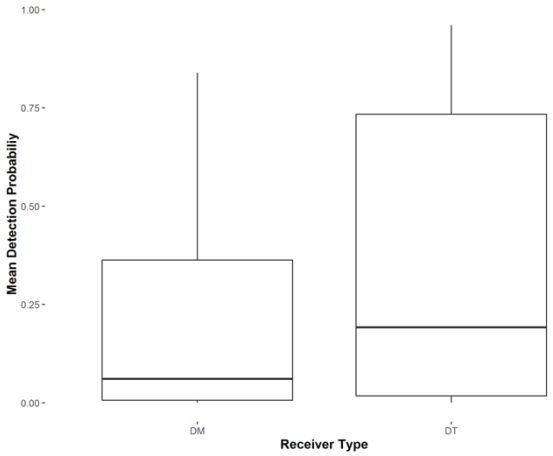

Figure 2.9 Mean detection probability for the two different types of receivers, DMON (DM) and DTAG (DT) as predicted by a generalized linear model.

Table 4 Effective Radius for the five different detectors, pooling both receiver types.

DT	Effective Radius	
	Shallow Waters (20m)	**Deep Waters (200-300m)**
MF1	1535	2357
MF2	1626	2472
EN1	1681	2543
EN2	1696	2565
ENRat	1572	2486

The effective detection radius, i.e. the distance at which the cumulative density function reached 0.5 can be seen in Table 4. Estimation of the effective radius gives a single parameter with which to compare different detection systems. The effective radius is a useful measure of survey effort as the spatial coverage can then be estimated. Our results show that receivers placed in deep waters have an average 35% higher effective radius than shallow receivers. The effective radius for the shallow receivers ranges between 1535 to 1696 m dependent on the receiver, and for the deep receivers from 2357 to 2565 m. For both shallow and deep receivers, the matched filter detector based on on-axis clicks (MF1) had the lowest effective radius while the energy detector, which calculates the energy between 27-37 kHz over a 430 μs window, had the highest. However, the relatively small difference in performance of these detectors was likely within the confidence intervals of the effective radius estimation.

When comparing the two different recording systems, the receivers based on the DTAG design appeared to facilitate detection of a higher proportion of clicks than the ones based on the DMON design, for both the shallow and deep receivers (Fig. 2.7). The effective radii of the DMON and DTAG receivers was 1779 m vs 2165 m at shallow depths and 1899 m vs 2900 m for deep receivers.

2.4 Discussion

Designing effective abundance surveys and mitigation protocols using passive acoustic detection of cetacean vocalizations requires information about the detection function, i.e., the probability of detecting a cue as a function of distance. In acoustic surveys, the detection function is dependent on the detection algorithm used and thus testing different algorithms is important to guide survey design.

Here I present a method for deriving the acoustic detection function of animals that vocalize frequently and apply the technique to study the detectability of Blainville's beaked whale echolocation clicks in an area in the Canary Islands where this species is frequent. In particular, I studied the impact of different detector algorithms and receiver depths on the detection function. The method requires the attachment of a sound recording tag to an animal in the vicinity of one or more acoustic receivers. Vocalizations and ambient noise recorded on the tags and at the receivers are used both to assess detectability and to determine the distance from the animal to the receiver. The tag attached to the animal ensures that all vocalizations are counted whether or not they are detected at the receiver, enabling the absolute detection rate to be estimated. The animal will vocalize at a variety of distances from the receivers as it ranges freely, allowing the detection function to be approximated from a set of point measurements. Here I show that a simulation method based on recorded vocalizations can also be used to expand the range of distances over which the detection function is predicted. Compared to the large-scale arrays of fixed hydrophones that have been used previously to estimate detectability (Moretti et al., 2010; Marques et al., 2009; Ward et al., 2010), the new method is cost-effective and mobile, giving the opportunity to investigate how detectability varies with location and population.

Beaked whale echolocation clicks are highly directional (Madsen et al., 2013; Zimmer et al., 2005), so the probability of detecting a click depends on the orientation of the animal with respect to the receiver. As a result, click arrivals identified in the receiver recordings using synchronized plots will favour on-axis clicks especially at greater ranges, due to the lower apparent source level of off-axis clicks. In an effort to obtain a wider set of click distances for testing the detectors, I used a Kalman Filter (KF) to predict the arrival time of all clicks, regardless of whether they were detected in the synchronized plot. Using the predicted arrival times of all clicks as analysis blocks containing possible clicks, the detectors have a higher opportunity of detecting signals with lower received level, which are not visible in the synchronized plot.

Errors in range estimation will arise from unmodeled variations in the clock offset between the tag and recorder and from inaccuracies in the sound speed profile, as CTD measurements were not always possible at the same time as the tagging event. Sound speed profiles inferred from CTD measurements made in the general area in which animals were tagged and at different months of the year show differences of less than 5 m/s or 0.3% (Fig. 2.3). To evaluate the potential error resulting from using a profile from the wrong time of year, consider the case of an animal at 2000m range and 600m depth with the receiver at 200m depth. The time difference between the direct and surface bounce arrival will be 69.3 ms using the 1 June sound speed profile from Fig. 2.3. If the faster 18 Oct profile was assumed in the analysis, the measured arrival time difference would lead to an inferred slant range of 2013 m, an error of 1.3% compared to the true slant range of 2039.6 m. This would in turn lead to a predicted time of flight of 1.334 s (true value 1.348 s) and therefore a clock offset error of about 14 ms. The error in clock offset and sound speed will combine to give errors of about 1% in the range estimates for clicks received at similar distances without a surface bounce. These incorrect ranges are smoothed by the KF allowing prediction of the range of the animal when clicks are not received. However, because the same clock offset and sound speed values are then used to calculate arrival time from the range predictions, the errors in clock offset and sound speed cancel out. Thus, the KF arrival time predictions for clicks are independent of errors in the sound speed profile. In effect, the KF is smoothing and predicting arrival times, but is doing so by processing the estimated ranges (which are just a linear transformation of the arrival times). This has the benefit that the dynamic model and state noise in the KF have a more intuitive relation to animal movement.

Although errors in the sound speed profile do not affect the quality of arrival time predictions, they do affect the range estimates. However, likely errors of order 1% translate into errors of less than 50 m for the maximum distance detected in this study 4700 m. As the estimated distances were grouped in bins of 500 meters for computation of the detection function, errors of this magnitude have no impact on the estimated detection function. Range errors will also arise if the sound propagation path is not straight, e.g., due to refraction, and this will have a greater impact for longer ranges. However, the magnitude of error from this source will also be small compared to the bin size used in the analysis.

Errors in the KF range and therefore arrival time predictions can have a direct impact on the detection function if they are large enough. Arrival time errors only affect the results in the extreme case in which the 2.6 ms analysis window does not contain a click (i.e., an arrival time error of > 1.3 ms). Such large errors could occur if clicks are not received for an interval

because the animal changed direction. This problem was minimized by choosing a relatively large analysis window compared to the click duration and by excluding clicks for which the KF range covariance indicated that the arrival time was too uncertain. Clicks with a range standard deviation (the square-root of the error covariance produced by the KF) larger than about 2 meters were excluded to keep timing errors below 1.3 ms. This condition led to an average of 46% (10.6 – 92.1%) of the clicks produced being excluded. To further minimize ranging errors, I only analysed clicks from dives for which the clock offset regression r^2 was greater than 0.8 (leaving three foraging dives out of the final dataset). Nonetheless, a small proportion of click extracts may be have timing errors large enough that they do not contain an actual click which would lead to a slight underestimation of the detection rate. Nevertheless, the two criteria used to accept click extracts, i.e., that the KF covariance is below a threshold and that the signal to noise ratio is positive, should eliminate most samples with high uncertainty of containing a signal.

Our results demonstrate that a Blainville's beaked whale echolocation click in quiet ambient noise conditions such as those off El Hierro can be detected at a distance of at least 4.7 km. This is the furthest distance at which a click from a tagged animal was ranged using the synchronized plot method in our study. Simulating waveforms from greater ranges suggests that detection at up to 6 km may be possible, but the probability of detection is very small. On-axis clicks of Blainville's beaked whales have been detected at ranges of up to 5500 m (Ward et al., 2011) to 6500 m on the low-noise bottom-mounted (1630 m mean depth) receivers at AUTEC (Ward et al., 2008). Receivers at these depths receive lower surface-generated ambient noise (i.e., from wind and rain) and are likely closer to the foraging depth of the animal, hence can detect animals at larger distances. In comparison, a maximum detectable distance of 4 km was predicted by Zimmer (2008) for a Cuvier's beaked whale and a 100 m depth receiver using a theoretical detection function based on the passive sonar equation. Thus, detection distances of 4-6 km seem to be achievable for these beaked whale species in low noise conditions. In fact, the lowest predicted deep water ambient noise levels (i.e., corresponding to a sea-state of 0 and no shipping noise) in the 25-50 kHz frequency range of beaked whale clicks are so low (Urick, 1983) that it is difficult to produce a battery-powered receiver with a comparable self-noise. As a result, the system noise of the recorder will likely dominate the total noise at beaked whale frequencies in quiet conditions and so set the maximum detection range. The system noise of the receivers used in this study was 10-20 dB above the lowest ambient noise at 30 kHz reported by Cato (1998) suggesting that longer detection ranges may be possible with lower noise devices. However, at ranges of multiple

kilometers, absorption is a major contributor to the transmission loss, and so a 10 dB improvement in system noise does not translate into a 3-fold increase in detection range as would be expected for spherical spreading. For example, if a signal at 40 kHz is just detectable at 5 km on a self-noise limited receiver, a 10 dB reduction in system noise would extend the detection range to only 6 km. At these ranges, the broadband beaked whale clicks become narrowband transients completely lacking the distinguishing FM sweep and so are difficult to classify. Thus, improving the self-noise of recorders beyond a certain level may have very little impact on effective radius. Interestingly, in this study the receivers based on DTAGs have a slightly higher effective radius than receivers based on DMONs despite an almost 10 dB poorer self-noise and further study is needed to understand this although it may be simply a consequence of varying detectability of individual animals (e.g., due to behaviour or source characteristics) coupled with the small numbers of individuals associated with each receiver type.

As expected, our results indicate that the probability of detecting echolocation clicks from Blainville's beaked whales decreases rapidly at ranges larger than a couple of kilometres. However, less expected is the similarity in performance of the different detector methods examined here. The energy ratio detector performs significantly worse at small ranges (probability of detection smaller than the rest of the detectors at ranges of 500m), but it shows a slightly better performance than the other detectors at long ranges. Otherwise, the detectors provide almost indistinguishable performance. This is surprising because the distinctive features of beaked whale clicks, i.e., their long duration and FM upsweep, seem to make them ideal candidates for matched filter detection. However, there are two problems with applying matched filter processing to animals recorded at random aspects. The first is that clicks from nearby animals will be received with sufficient SNR for detection from a range of aspects. As click waveforms vary widely with aspect, the on-axis click, representing only a narrow set of aspects, is not an effective template for a matched filter detector. In our study, the MF2 detector which used a template derived from on- and off-axis clicks did slightly better than MF1 which had an on-axis template showing that the high processing gain of on-axis clicks confers no advantage for short-range detection. The second problem with matched filter detectors pertains to animals at large distances. As distance increases, only clicks from a narrow range of aspects around the acoustic axis will have SNR sufficient to be detectable. These clicks should therefore match well an on-axis template in a matched filter. However, differential absorption of high frequencies over the long transmission path reduces the bandwidth of the clicks and so reduces their processing gain. For example, an on-axis click

from a close Blainville's beaked whale has an RMS bandwidth of about 7 kHz (Johnson et al., 2006) but this drops to some 3.6 kHz at a distance of 4 km, halving the time-bandwidth product and therefore the processing gain for the same click duration. As a consequence, there appears to be no advantage to the 'coherent' processing that a MF offers over a bandpass energy detector and this conclusion is borne out by our detector performance results. An additional factor affecting matched filter detectors is that clicks detected on shallow receivers from animals foraging at greater depths will tend to come disproportionately from aspects well away from the narrow acoustic beam, at least when the horizontal range is short. For example, if there is an 800 m difference between the receiver and foraging depths, on-axis clicks will only be received when the animal pitches up by 39º at a 1 km horizontal range or by 22º at 2 km. For an animal foraging in a horizontal layer, these pitch angles may be relatively infrequent. Thus, a detector designed to integrate power in the bandwidth of off-axis or long-range beaked whale clicks, over the duration of off-axis clicks, may provide the simplest and most robust detector design.

This analysis shows a considerable difference in detectability between shallow receivers (placed at 20m) and deep receivers (placed at 200-300m). Depth dependence in detectability is expected, as surface-generated noise attenuates with depth (Lurton, 2002; Zimmer et al., 2008) while deeper receivers are also closer to the depths at which beaked whales vocalize. Beaked whales produce echolocation clicks while foraging, starting at depths ranging from 200-500m (Johnson et al., 2004; Johnson et al., 2006). In this study whales started clicking at depths ranging from 194-502 m, so receivers placed in deep waters were more likely to intercept clicks from aspects close to the acoustic axis during the mostly horizontal foraging phase, than receivers placed at shallow depths (20 m). Although distortion of signals due to multipath interference can contribute to the lower detectability of shallow receivers, this is not likely a problem for the short transients and deep water studied here. The only path detected other than the direct path was the surface bounce, which was detected well after the direct arrival.

The depth dependency of the detection function will lead to varying effective radii around receivers, which needs to be taken into account in survey designs. The effective area of detection is a useful measurement as it takes into account the proportion of animals that remained undetected (Buckland et al., 2001) and can be used to convert a relative index of abundance to an absolute density (Kyhn et al., 2010). To estimate the absolute density, i.e., the number of animals per spatial unit, a measurement of spatial coverage is required, which can be derived from the effective radius. In addition, the effective radius enables direct

comparison of surveys made with different systems and that cover different behaviours of a species (Nuuttila et al., 2013). The effective radius also gives the opportunity of investigating if detectability is influenced by other factors such as changes in vocalization patterns due to differences in habitat or prey type, or changes in sound propagation characteristics. In comparison, the maximum detection distance is more sensitive to environmental conditions, receiver characteristics, and the precise orientation of the animal. Moreover, a small change in the number of detected clicks in the tail of the detection function can have a large impact on the maximum detection distance, whereas the effective radius is dependent on the shape of the entire detection function and is therefore both more robust and more informative as a measure of effort.

The novel method described here allowed us to estimate the detection function of Blainville's beaked whales and test the performance of different click detectors for the FM echolocation signal of the species. The method relies on the capability to tag animals that will then vocalize in the proximity of one or more acoustic receivers while maneuvering so as to allow recording from different aspects. This must be repeated for a sufficient number of individuals so that the accumulated detection function is representative of the population. The dataset of 5 animals available for this study is on the low side and a larger data set would have certainly given a more robust result. The study also was only able to consider two receiver depths, neither of which were close to the depth at which beaked whales vocalize. A follow-up study exploring a range of receiver depths from 10-1000 m would provide a more definitive guide for the optimal design of passive acoustic monitors for beaked whales. Finally, the study was not able to explore the impact of elevated ambient noise due to wind and wave noise as tagging could only be performed at low sea-states. This limitation could be overcome by recording separately the ambient noise at varying sea-states with the same receivers at the same depths. These ambient noise recordings could be mixed with the low-noise recordings from the tagging trials to simulate detectability at higher noise levels. If data regarding higher ambient noise measurements are not available, then a theoretical model for the effect of noise on detection could be constructed (Ward et al., 2011). This approach could also be used to study discrimination of non-target species, such as dolphins, which may generate a large number of false alarms unless a classifier is added to the detector. Despite these limitations, the study demonstrates the efficacy of the method and provides an indication of how detection performance depends on receiver placement but largely not on detector algorithm, and these preliminary results will be used in the remainder of the thesis.

Compared to the fixed hydrophone array installations used previously to obtain detection functions for beaked whales, the new method is both low cost and highly portable. Acoustic recording tags like the DTAG can be leased for about $3000USD per month while a drifting acoustic recorder can be produced using, for example, a Soundtrap autonomous recorder for about $5000USD. The tagging and recorder deployment can both be performed from a small boat in the case of coastal animals. The entire equipment can be shipped in a small box to new field sites. This makes it possible to estimate the detection function in the area of an acoustic survey prior to the survey itself. The importance of using a site and temporal specific detection function has been noted by Marques et al., (2013) and Warren et al., (2017). The portability of the method also allows comparison between detectability of different populations of the same species in different environmental conditions. The performance of different detection algorithms can be tested as a function of distance, receiver depth, and as a function of varying ambient noise levels, giving the opportunity to take in to account different detectability in each case. Although specifically designed for echolocating animals, the method could be used to investigate the detection function of social signals as well, provided that these are produced frequently enough to be able to track the distance of the animal. For odontocete species, such as the bottlenose dolphin, that spend a significant amount of time socializing, a comparison between detectability of their communication signals and that of echolocation signals would be of interest to determine which signal provides the most effective passive acoustic cue. The detection function of acoustic cues for baleen whales could also be determined in the same way but the long propagation ranges and relative infrequency of their vocalizations would require deployment of acoustic receivers for long enough to cover long range movements of a tagged whale and to acquire sufficient vocalizations for statistical analysis. In this case, moored receivers may be preferred to prevent receivers from drifting far away from tagged animals.

Knowing the performance of the detection system in a particular environment is critical to inform survey design, where the detection coverage preferably should be known prior to survey (Thomas et al., 2010). Measurements of coverage and effort are essential for comparing studies, equipment, spatio-temporal differences, and as an essential step towards density estimation. The method presented in this study gives the opportunity to compare the performance of different detectors and recording systems under real environmental conditions and can be applied to any frequently vocalizing species. In the case of beaked whales, these results indicate that detector choice has little impact on performance and the design factor that has the most impact is receiver depth. In future work, it will be important to explore this

dependency more as well as the impact of different ambient noise levels and interference sources.

2.5 References

Aguilar de Soto, N., (2006). Acoustic and diving behaviour of the short-finned pilot whale (*Globicephala macrorhynchus*) and Blainville's beaked whale (*Mesoplodon densirostris*) in the Canary Islands. Implications on the effects of man-made noise and boat collisions (Doctoral dissertation, Ph. D. thesis, Universidad de La Laguna, La Laguna, Spain).

Aguilar de Soto, N.A., Madsen, P.T., Tyack, P., Arranz, P., Marrero, J., Fais, A., Revelli, E. & Johnson, M. (2012) No shallow talk: Cryptic strategy in the vocal communication of Blainville's beaked whales. Marine Mammal Science, 28, E75-E92.

Arranz, P., de Soto, N.A., Madsen, P.T., Brito, A., Bordes, F. & Johnson, M.P. (2011) Following a foraging fish-finder: Diel habitat use of Blainville's beaked whales Revealed by Echolocation. Plos One, 6, e28353.

Arranz, P., DeRuiter, S.L., Stimpert, A.K., Neves, S., Friedlaender, A.S., Goldbogen, J.A., Visser, F., Calambokidis, J., Southall, B.L. & Tyack, P.L. (2016) Discrimination of fast click-series produced by tagged Risso's dolphins (*Grampus griseus*) for echolocation or communication. Journal of Experimental Biology, 219, 2898-2907.

Barlow, J. (1999) Trackline detection probability for long-diving whales. Marine Mammal Survey and Assessment Methods, 209-221.

Barlow, J. & Taylor, B.L. (2005) Estimates of sperm whale abundance in the northeastern temperate Pacific from a combined acoustic and visual survey. Marine Mammal Science, 21, 429-445.

Barlow, J., Tyack, P.L., Johnson, M.P., Baird, R.W., Schorr, G.S., Andrews, R.D. & de Soto, N.A. (2013) Trackline and point detection probabilities for acoustic surveys of Cuvier's and Blainville's beaked whales. Journal of the Acoustical Society of America, 134, 2486-2496.

Barlow, J. (2006) Mitigating, monitoring and assessing the effects of anthropogenic sound on beaked whales. Journal of Cetacean Research and Management, 7, 239-249.

Baumann-Pickering, S., McDonald, M.A., Simonis, A.E., Berga, A.S., Merkens, K.P.B., Oleson, E.M., Roch, M.A., Wiggins, S.M., Rankin, S., Yack, T.M. & Hildebrand, J.A.

(2013) Species-specific beaked whale echolocation signals. Journal of the Acoustical Society of America, 134, 2293-2301.

Baumgartner, M.F. & Fratantoni, D.M. (2008) Diel periodicity in both sei whale vocalization rates and the vertical migration of their copepod prey observed from ocean gliders. Limnology and Oceanography, 53, 2197-2209.

Borchers, D., Marques, T., Gunnlaugsson, T. & Jupp, P. (2010) Estimating distance sampling detection functions when distances are measured with errors. Journal of Agricultural Biological and Environmental Statistics, 15, 346-361.

Borchers, D.L., Laake, J.L., Southwell, C. & Paxton, C.G.M. (2006) Accommodating unmodeled heterogeneity in double-observer distance sampling surveys. Biometrics, 62, 372-378.

Borchers, D.L., Zucchini, W., Heide-Jorgensen, M.P., Canadas, A. & Langrock, R. (2013) Using hidden Markov models to deal with availability bias on line transect surveys. Biometrics, 69, 703-713.

Borchers, D. L., Zucchini, W. and Fewster,EWSTER, R. M. (1998). Mark-recapture models for line transect surveys. Biometrics 54 1207-1220

Buckland, S.T., Anderson, D.R., Burnham, K.P., Laake, J.L., D.L., B. & Thomas, L. (2001) Introduction to Distance Sampling: Estimating abundance of biological populations. Oxdord University Press, Oxford.

Caillat, M., Thomas, L. & Gillespie, D. (2013) The effects of acoustic misclassification on cetacean species abundance estimation. Journal of the Acoustical Society of America, 134, 2469-2476.

Cato, D.H. (1998) Simple methods of estimating source levels and locations of marine animal sounds. Journal of the Acoustical Society of America, 104, 1667-1678.

Dunn, C., Hickmott, L., Talbot, D., Boyd, I. & Rendell, L. (2013) Mid-frequency broadband sounds of Blainville's beaked whales. Bioacoustics the International Journal of Animal Sound and Its Recording, 22, 153-163.

Evans, P.G.H. & Hammond, P.S. (2004) Monitoring cetaceans in European waters. Mammal Review, 34, 131-156.

Gillespie, D., Dunn, C., Gordon, J., Claridge, D., Embling, C. & Boyd, I. (2009) Field recordings of Gervais' beaked whales *Mesoplodon europaeus* from the Bahamas. Journal of the Acoustical Society of America, 125, 3428-3433.

Hiby, A.R. & Hammond, P. (1989) Survey techniques for estimating abundance of cetaceans. Report of the International Whaling Commission, 11, 47-80.

Johnson, M., de Soto, N.A. & Madsen, P.T. (2009) Studying the behaviour and sensory ecology of marine mammals using acoustic recording tags: a review. Marine Ecology Progress Series, 395, 55-73.

Johnson, M., Madsen, P.T., Zimmer, W.M.X., de Soto, N.A. & Tyack, P.L. (2004) Beaked whales echolocate on prey. Proceedings of the Royal Society B-Biological Sciences, 271, S383-S386.

Johnson, M., Madsen, P.T., Zimmer, W.M.X., de Soto, N.A. & Tyack, P.L. (2006) Foraging Blainville's beaked whales (*Mesoplodon densirostris*) produce distinct click types matched to different phases of echolocation. Journal of Experimental Biology, 209, 5038-5050.

Johnson, M.P. & Tyack, P.L. (2003) A digital acoustic recording tag for measuring the response of wild marine mammals to sound. IEEE Journal of Oceanic Engineering, 28, 3-12.

Klinck, H. & Mellinger, D.K. (2011) The energy ratio mapping algorithm: A tool to improve the energy-based detection of odontocete echolocation clicks. Journal of the Acoustical Society of America, 129, 1807-1812.

Kyhn, L.A., Jensen, F.H., Beedholm, K., Tougaard, J., Hansen, M. & Madsen, P.T. (2010) Echolocation in sympatric Peale's dolphins (*Lagenorhynchus australis*) and Commerson's dolphins (*Cephalorhynchus commersonii*) producing narrow-band high-frequency clicks. Journal of Experimental Biology, 213, 1940-1949.

Kyhn, L.A., Tougaard, J., Thomas, L., Duve, L.R., Stenback, J., Amundin, M., Desportes, G. & Teilmann, J. (2012) From echolocation clicks to animal density-Acoustic sampling of harbor porpoises with static dataloggers. Journal of the Acoustical Society of America, 131, 550-560.

Liang, K.Y. & Zeger, S.L. (1986) Longitudinal data-analysis using Generalized Linear-Models. Biometrika, 73, 13-22.

Madsen, P.T., de Soto, N.A., Arranz, P. & Johnson, M. (2013) Echolocation in Blainville's beaked whales (*Mesoplodon densirostris*). Journal of Comparative Physiology A - Neuroethology Sensory Neural and Behavioral Physiology, 199, 451-469.

Madsen, P.T., Johnson, M., de Soto, N.A., Zimmer, W.M.X. & Tyack, P. (2005) Biosonar performance of foraging beaked whales (*Mesoplodon densirostris*). Journal of Experimental Biology, 208, 181-194.

Marques, T.A., Munger, L., Thomas, L., Wiggins, S. Hildebrand J. A, (2011) Estimating North Pacific right whale *Eubalaena japonica* density using passive acoustic cue counting. Endangered Species Research, 13, 163-172.

Marques, T.A., Thomas, L., Martin, S.W., Mellinger, D.K., Ward, J.A., Moretti, D.J., Harris, D. & Tyack, P.L. (2013) Estimating animal population density using passive acoustics. Biological Reviews, 88, 287-309.

Marques, T.A., Thomas, L., Fancy, S.G. & Buckland, S.T. (2007) Improving estimates of bird density using multiple-covariate distance sampling. Auk, 124, 1229-1243.

Marques, T.A., Thomas, L., Ward, J., DiMarzio, N. & Tyack, P.L. (2009) Estimating cetacean population density using fixed passive acoustic sensors: An example with Blainville's beaked whales. Journal of the Acoustical Society of America, 125, 1982-1994.

Matsumoto, H., Jones, C., Klinck, H., Mellinger, D.K., Dziak, R.P. & Meinig, C. (2013) Tracking beaked whales with a passive acoustic profiler float. Journal of the Acoustical Society of America, 133, 731-740.

McCarthy, M.A., Moore, J.L., Morris, W.K., Parris, K.M., Garrard, G.E., Vesk, P.A., Rumpff, L., Giljohann, K.M., Camac, J.S., Bau, S.S., Friend, T., Harrison, B. & Yue, B. (2013) The influence of abundance on detectability. Oikos, 122, 717-726.

Mellinger, D.K., Stafford, K.M., Moore, S.E., Dziak, R.P. & Matsumoto, H. (2007) An overview of fixed passive acoustic observation methods for cetaceans. Oceanography, 20, 36-45.

Moretti, D., DiMarzio, N., Morrissey, R., Ward, J. & Jarvis, S. (2006) Estimating the density of Blainville's beaked whale (*Mesoplodon densirostris*) in the Tongue of the Ocean (TOTO) using passive acoustics. Oceans 2006, Vols 1-4, 313-317.

Moretti, D., Marques, T.A., Thomas, L., DiMarzio, N., Dilley, A., Morrissey, R., McCarthy, E., Ward, J. & Jarvis, S. (2010) A dive counting density estimation method for Blainville's beaked whale (*Mesoplodon densirostris*) using a bottom-mounted hydrophone field as applied to a Mid-Frequency Active (MFA) sonar operation. Applied Acoustics, 71, 1036-1042.

Nuuttila, H.K., Thomas, L., Hiddink, J.G., Meier, R., Turner, J.R., Bennell, J.D., Tregenza, N.J.C. & Evans, P.G.H. (2013) Acoustic detection probability of bottlenose dolphins, *Tursiops truncatus*, with static acoustic dataloggers in Cardigan Bay, Wales. Journal of the Acoustical Society of America, 134, 2596-2609.

Ou, H., Au, W.W.L. & Oswald, J.N. (2012) A non-spectrogram-correlation method of automatically detecting minke whale boings. Journal of the Acoustical Society of America, 132, El317-El322.

Palka, D.L. (1996) Effects of Beaufort sea state on the sightability of harbour porpoise in the Gulf of Maine. Report of the International Whaling Commission, 46, 575-582.

Parks, S.E., Clark, C.W. & Tyack, P.L. (2007) Short- and long-term changes in right whale calling behavior: The potential effects of noise on acoustic communication. Journal of the Acoustical Society of America, 122, 3725-3731.

Rankin, S. & Barlow, J. (2007) Sounds recorded in the presence of Blainville's beaked whales, *Mesoplodon densirostris*, near Hawai'i (L). Journal of the Acoustical Society of America, 122, 42-45.

Richman, N.I., Gibbons, J.M., Turvey, S.T., Akamatsu, T., Ahmed, B., Mahabub, E., Smith, B.D. & Jones, J.P.G. (2014) To see or not to see: investigating detectability of Ganges river dolphins using a combined visual-acoustic survey. Plos One, 9, e96811.

Roch, M.A., Klinck, H., Baumann-Pickering, S., Mellinger, D.K., Qui, S., Soldevilla, M.S. & Hildebrand, J.A. (2011) Classification of echolocation clicks from odontocetes in the Southern California Bight. Journal of the Acoustical Society of America, 129, 467-475.

Stimpert, A.K., DeRuiter, S.L., Southall, B.L., Moretti, D.J., Falcone, E.A., Goldbogen, J.A., Friedlaender, A., Schorr, G.S. & Calambokidis, J. (2014) Acoustic and foraging behavior of a Baird's beaked whale, *Berardius bairdii*, exposed to simulated sonar. Scientific Reports, 4, 7031.

Thomas, L., Buckland, S.T., Rexstad, E.A., Laake, J.L., Strindberg, S., Hedley, S.L., Bishop, J.R.B., Marques, T.A. & Burnham, K.P. (2010) Distance software: design and analysis of distance sampling surveys for estimating population size. Journal of Applied Ecology, 47, 5-14.

Tyack, P. (1986). Whistle repertoires of two bottlenosed dolphins, *Tursiops truncatus*: mimicry of signature whistles? Behavioral Ecology and Sociobiology, 18, 251-257.

Tyack, P.L., Johnson, M., Soto, N.A., Sturlese, A. & Madsen, P.T. (2006) Extreme diving of beaked whales. Journal of Experimental Biology, 209, 4238-4253.

Tyack, P.L., Johnson, M.P., Zimmer, W.M.X., de Soto, N.A. & Madsen, P.T. (2006) Acoustic behavior of beaked whales, with implications for acoustic monitoring. Oceans 2006, Vols 1-4, 509-514.

Urick, R.J. (1983) Principles of underwater sound. Peninsula Press, Los Altos.

Wahlberg, M., Beedholm, K., Heerfordt, A. & Mohl, B. (2011) Characteristics of biosonar signals from the northern bottlenose whale, *Hyperoodon ampullatus*. Journal of the Acoustical Society of America, 130, 3077-3084.

Ward, J., Jarvis, S., Moretti, D., Morrissey, R., DiMarzio, N., Johnson, M., Tyack, P., Thomas, L. & Marques, T. (2011) Beaked whale (*Mesoplodon densirostris*) passive

acoustic detection in increasing ambient noise. Journal of the Acoustical Society of America, 129, 662-669.

Ward, J.M., R. Moretti, D., DiMarzio N., Jarvis S., Johnson, M. Tyack, P. and White C. (2008) Passive acoustic detection and localization of *Mesoplodon densirostris* (Blainville's beaked whale) vocalizations using distributed bottom-mounted hydrophones in conjunction with a Digital Tag (DTag) recording. Canadian. Acoustics, 36, 60-66

Warren, V.E., Marques, T.A., Harris, D., Thomas, L., Tyack, P.L., de Soto, N.A., Hickmott, L.S. & Johnson, M.P. (2017) Spatio-temporal variation in click production rates of beaked whales: Implications for passive acoustic density estimation. Journal of the Acoustical Society of America, 141, 1962-1974.

Williams, R., Leaper, R., Zerbini, A.N. & Hammond, P.S. (2007) Methods for investigating measurement error in cetacean line-transect surveys. Journal of the Marine Biological Association of the United Kingdom, 87, 313-320.

Yack, T.M., Barlow, J., Roch, M.A., Klinck, H., Martin, S., Mellinger, D.K. & Gillespie, D. (2010) Comparison of beaked whale detection algorithms. Applied Acoustics, 71, 1043-1049.

Zimmer, W.M.X., Harwood, J., Tyack, P.L., Johnson, M.P. & Madsen, P.T. (2008) Passive acoustic detection of deep-diving beaked whales. Journal of the Acoustical Society of America, 124, 2823-2832.

Zimmer, W.M.X., Johnson, M.P., Madsen, P.T. & Tyack, P.L. (2005) Echolocation clicks of free-ranging Cuvier's beaked whales (*Ziphius cavirostris*). Journal of the Acoustical Society of America, 117, 3919-3927.

Zimmer, W.M.X. & Pavan, G. (2008) Context driven detection/classification of Cuvier's beaked whale (*Ziphius cavirostris*). Passive '08: 2008 New Trends for Environmental Monitoring Using Passive Systems, 111-116.

APPENDIX I: Detection Function and underlying data

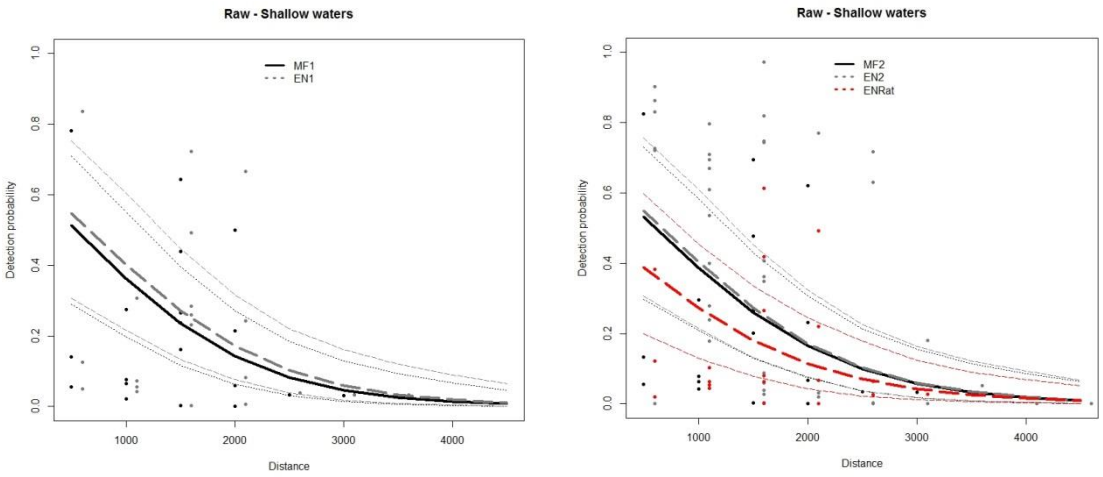

Appendix Figure 1 Detection function for shallow waters (20m) for acoustic detectors designed Left - based on on-axis click of Blainville's beaked whales, Solid black line shows the detection function of the correlation detector (MF1) based on on-axis echolocation click and 95% CI (dotted line) - Grey long-dashed line shows the detection function of an energy detector based on a 27-40 kHz bandpass filter with energy summed over a 200 µs rectangular window (EN1) and the 95% CI (grey dashed line). Black points are the percentage of clicks detected in relation to the ones produced at each distance bin for MF1 detector and grey dots are the percentage of clicks detected in relation to the ones produced for the EN1 detector. Right – detection function for detectors based on off-axis click MF2 (solid black line) and energy detector based on based on 27-37 kHz bandpass filter with energy summed over a 430 µs rectangular window (EN2 – grey dashed line) and energy ration (ENRat – red dashed line).

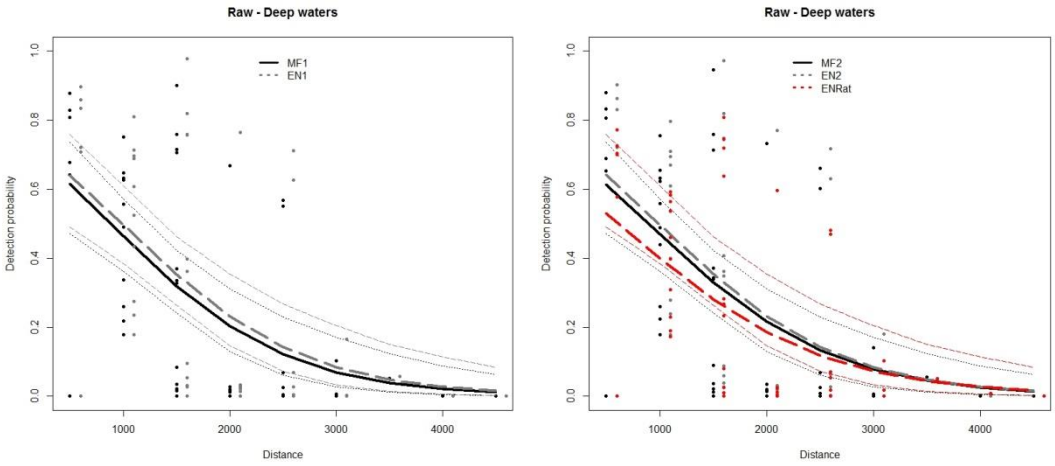

Appendix Figure 2 Detection function for deep waters (200-300m) for acoustic detectors designed Left - based on on-axis click of Blainville's beaked whales, Solid black line shows the detection function of the correlation detector (MF1) based on on-axis echolocation click and 95% CI (dotted line) - Grey long-dashed line shows the detection function of an energy detector based on a 27-40 kHz bandpass filter with energy summed over a 200 µs rectangular window (EN1) and the 95% CI (grey dashed line). Black points are the percentage of clicks detected in relation to the ones produced at each distance bin for MF1 detector and grey dots are the percentage of clicks detected in relation to the ones produced for the EN1 detector. Right – detection function for detectors based on off-axis click MF2 (solid black line) and energy detector based on based on 27-37 kHz bandpass filter with energy summed over a 430 µs rectangular window (EN2 – grey dashed line) and energy ration (ENRat – red dashed line).

Chapter 3

The use of Blainville's beaked whales' (*Mesoplodon densirostris*) clicks and click scans as acoustic cues for abundance estimation

3.1 Introduction

A first step required for any method to estimate the density of wildlife is to detect some sign of an individual animal that can be classified to the species of interest. The classic way to detect wildlife is through visual observation. However, due to the small fraction of their body that is exposed above the surface when they breathe, beaked whales have a reduced probability of visual detection (Barlow et al., 1999; Barlow et al., 2013; Tyack et al., 2006), which is also dependent on light and weather conditions, so acoustic means of detection for beaked whales have been also been explored (Barlow et al., 2013; Ward et al., 2008). Deep-diving odontocetes such as beaked whales spend most of their time underwater. Barlow et al., (1999) used a modelling approach to estimate that Blainville's beaked whales are available for visual detection for about 14% of their time, and recent tag techniques have estimated this number at around 8% (Aguilar de Soto, personal communication), due to the high proportion of time spent underwater and not available for sighting. By contrast, their highly vocal behaviour, which is used for foraging, navigation, echolocation and communication, suggests better opportunities for acoustic detection.

Deep divers, such as the beaked whales, need to echolocate for a relatively large proportion of dive duration, to search, select and capture their prey, and orientate themselves at depths where there is no light. The use of acoustic and movement recording tags such as DTAGs (Johnson & Tyack, 2003) has given insights into the acoustic production mechanisms and foraging behaviour of these species (Johnson et al., 2006; Tyack et al., 2006; Madsen et al., 2013). For example, Blainville's beaked whales spend 20% of their time actively searching for prey by echolocating, but are silent during the ascent phase of the foraging dive and the consecutive shallower dives of their stereotyped dive cycle (Aguilar de Soto et al., 2012). During deep dives, Blainville's beaked whales are known to hunt mostly at depths of 600-800 m (Johnson et al., 2006), near the scattering layer or seafloor (Arranz et al., 2011). Echolocation typically starts at 400 m depth and ends at ~700 m during the start of ascent (Arranz et al., 2011), with maximum diving depths at around 800 m (Arranz et al., 2011;

Johnson et al., 2006) for data collected in El Hierro (Canary Islands). The production of acoustic cues at depth raises the question of which depth is optimal for receivers of passive acoustic surveys – this will be estimated in this chapter using acoustic propagation modelling and data from tagged whales.

While visual methods for surveying cetaceans often identify the "blow" as the cue that can be detected, the observer must usually identify other field marks to classify species, such as blow shape, which can be species-specific (e.g. the slanted blow of sperm whales). Similarly, one of the most common cues used to detect odontocetes acoustically is echolocation clicks. Some odontocete species click so regularly over time that echolocation clicks are a particularly good detection cue. Typically, an automated detection algorithm is used to identify clicks on the recordings. However, it can often be difficult to classify individual clicks to species (Caillat et al., 2013; Roch et al., 2011), and other transient sounds can often trigger click detectors (e.g. Hildebrand et al., 2015). Errors in the detection system can result either from false detections of an unwanted signal or failure of the detector to detect the signal. For the species of interest in this thesis, Blainville's beaked whales, there are several detection algorithms (Chapter 2; Yack et al., 2010), which base their detection criteria on different signal characteristics. The various detection algorithms each have their corresponding false alarm rates for a given dataset, which can be as high as 52% (Yack et al., 2010). Errors in automated detection algorithms can be introduced due to features other than the signal of interest that share similar characteristics, such other species in the area, other biological sounds, transient sounds or vessels. The false alarm rate of a single click detector is a critical feature of the detection system representing a key type of error in detection. When a detector is used, automated or not, in acoustic density estimation methods, the false alarm rate should be known in order to correct the number of detections (Marques et al., 2013). As the false alarm rate is an unavoidable characteristic of any detection and classification system, additional treatment of the detections is usually required in an effort to minimize false positives, of which examples are described below.

When passive acoustic devices listen for beaked whales, they often receive a short sequence of clicks as the whale scans past the hydrophone with its directional sonar beam. The length of scans or click sequences depends on the: 1) scanning behaviour of the animal, 2) effective beam pattern of the sound production, 3) relative speed between the animal and the receiver, either a stationary hydrophone with a moving animal, or a moving hydrophone with a moving animal 4) distance between the receiver and animal (Rayment et al., 2009) and 5) diving behaviour. In addition, inter-click interval (ICI) distributions vary by species, allowing ICI

measures to be assigned to species. When beaked whales are in echolocation search mode, they have a relatively stable ICI of approximately 0.29-0.32 s for Blainville's beaked whales (Ward et al., 2008). Zimmer et al., (2005) report similarly stable 0.38s ICI for Cuvier's beaked whale recorded in the Ligurian Sea.

Click detections and their ICIs can be used to determine species presence and distinguish between false alarms deriving from other species in the area such as delphinids and sperm whales. For a species with well-defined ICI, a click sequence then becomes the detection cue with a potential to minimize false detections of single clicks. Matsumoto et al., (2013) reduced the large number of false positive detections of individual clicks for beaked whales by rejecting bouts of fewer than 5 clicks. A "beaked whale likelihood value" was calculated using the ICIs of the clicks detected in the bout, when ICI measurements fell between 0.2-0.5s.

The ICI between detected regular clicks has been incorporated in automated click train detectors such as in T-PODs (Timing Porpoise Detector; Chelonia Ltd UK), where ICI values of the detected regular clicks can be a criterion of certainty for species identification. When T-PODs were used to detect Hector's dolphins in New Zealand (NZ), longer click trains (greater than 20 clicks) with smaller mean ICI (less than 0.4s) were treated as true detections as opposed to shorter click trains (less than 10 clicks) with longer ICIs (greater than 0.6s) that possibly correspond to boat sonar or an unknown source (Rayment et al., 2009). All these uses of ICI information from click scans as a detection and classification cue lead me to explore the use of click scans as a cue for detecting beaked whales.

There are unexploited opportunities to evaluate the clustering behaviour of single click detections as a potential cue for the cue counting method and for extraction of any species-specific information from the clusters of individual clicks. Click trains are sequences of ultrasonic clicks emitted by porpoises and dolphins to orient in their environment and capture prey (Au, 1993). Click trains have been used as cues for abundance estimation for Yangtze finless porpoises (Kimura et al., 2010), though the individual production rate varies considerable (Kimura et al., 2013) and abundance estimates are prone to large variance (Kimura et al., 2013). In this chapter, a

(CS) is defined as a series of clicks detected on a passive acoustic recorder with ICI between 0.1 to 1 s, as clicks with ICIs less than 0.1 s are found in buzzes, and clicks with ICIs longer than 1 s correspond to situations where one or more clicks were undetected, or the animal

paused its echolocation. Here, we investigate the clustering nature of individual click detections and the potential use of click scans as an acoustic cue for cue counting methods.

Beaked whales have a stereotyped diving pattern in which they are silent when near the surface and they produce thousands of distinctive echolocation clicks during their foraging dives (Johnson et al., 2004; Tyack et al., 2006). A vocal period is defined as the duration between the beginning and end of clicking during a foraging dive. This has been determined as 23-33 min (Johnson et al., 2006) during foraging dives lasting about 48 min (Arranz et al., 2011) and whales spent about 90 min performing shallow silent dives between deep foraging ones (Arranz et al., 2011). While foraging, beaked whales produce thousands of echolocation clicks that can often be identified to species-level (Gillespie et al., 2009). Blainville's beaked whales produce broad-band frequency-modulated clicks with a centroid frequency of 38 kHz (see Chapter 2) in a highly directional signal beam (Au, 1993; Au 2002; Zimmer et al., 2005). The high directionality of beaked whale clicks (Madsen et al., 2013; Johnson et al., 2006; Shaffer et al., 2013), with a directivity index of 23 dB (Shaffer et al., 2013), translates to a rapid reduction of the signal energy for off-axis angles. Echoes from clicks produced by tagged animals, and recorded on the DTAG, suggest a beamwidth of +/- 10° (Madsen et al., 2013). A -3dB beamwidth of ~13° was estimated from field acoustic recordings by Shaffer et al., (2013) for Blainville's beaked whales in the Bahamas.

Click trains are consecutive regular clicks which are produced by the animal between buzzes or pauses and have clicking intervals between 0.1 s and 1 s (Johnson et al., 2006). Buzzes, rapid clicks produced during the last phase of foraging attempts (Miller et al., 2004), typically last about 2.9 s (Johnson et al., 2006) and approximately 27 foraging attempts occur per foraging dive (Johnson et al., 2006; Madsen et al., 2013). Click trains that correspond to searching for prey last for about 62 s (Madsen et al., 2013) with a first prey capture attempt occurring only 2 min on average after the start of echolocation for Blainville's beaked whales (Arranz et al., 2011). Beaked whales have adapted to hunt at depth and only begin searching for prey with echolocation as they approach depth at which prey are expected (Arranz et al., 2011). This is in contrast to some other deep divers such as the sperm whales that start clicking earlier on descent (Watwood et al., 2006), leading to longer durations of echolocation during their foraging dives.

Knowledge about beaked whales' vocal period (duration between start and end of clicking during a foraging dive) and silent period (descent/ascent phase of a foraging dive) is crucial for converting the number of clicks produced by the animals during their foraging dives to the expected number of clicks per unit time at any location for passive acoustic monitoring. A

third parameter is the click rate, which is the average number of clicks produced by the animal per unit time (Marques et al., 2009, 2013; Kusel et al., 2011). Estimated click rates for Blainville's beaked whales take into account the total time of a full dive cycle – foraging dive and the consecutive shallow silent dives (Marques et al., 2009; Kusel et al., 2011; Hildebrand et al., 2015). As click rates are a basic part of the cue counting methodology using acoustic data, an unbiased estimate of this parameter is required. To do so, click rates have been estimated taking into account the whole dive duration and correcting the available time by excluding clicks made by the animal during foraging attempts - "buzzes". Exclusion of clicks with low-amplitude such as the clicks during buzzes is considered during the click rate estimation, as those clicks will be less or even undetectable from a passive acoustic receiver.

While there is flexibility in the definition of "cue" for cue-counting, the idea behind the different versions of a "cue" is based on identifying a cue rate for a predefined time period. For counting clicks as cues, click rates can be extracted from acoustic tags (Kusel et al., 2011, Marques et al., 2009), where a ground truth of the number of clicks produced by the animal is provided by the acoustic tag recordings. The translation of detected cue numbers to number of animals takes place with a statistical method based on distance sampling methodology (Buckland et al 2001), termed the "cue counting" approach. Cue counting from acoustic detections is well established (Marques et al., 2013), and this methodology has been widely used in numerous studies (Hildebrand et al., 2015; Kusel et al., 2011; Kusel et al., 2016; Marques et al., 2011; Martin et al., 2013). Individual regular echolocation clicks have been used extensively in acoustic cue counting methods; the click rate of beaked whales has been used to translate the density of regular clicks to an animal density (Marques et al., 2009; Kusel et al., 2011; Hildebrand et al., 2015) using a cue counting approach (Buckland et al., 2001), where the regular click during foraging dive forms a cue. Another cue of a whole foraging dive, requires detection of an "acoustic event" which is the onset of clicks at the beginning of a foraging dive (Moretti et al., 2010). The cue rate for foraging dive cue counting (Moretti et al., 2010) has also been extracted from acoustic tags, where the average number of foraging dives per hour is estimated. Foraging dive was used as a cue using the extended network of receivers (AUTEC) given the high probability of detecting a foraging dive in the surveyed area (Moretti et al., 2010) and the ability to extract the foraging dive rates from acoustic tags. The configuration of receivers at AUTEC permits the estimation of the start of clicking during a foraging dive as an indicator of the cue (Moretti et al., 2010). The ability to derive the cue rate from a method that provides ground truth of the produced

cues is important as cue rate should be an unbiased parameter, which allows the translation of number of cues to number of animals.

Even though the acoustic production and behaviour of a species might be well known, in cases where acoustic cues have low availability as in the 18% of their total time Blainville's beaked whales are vocal (Arranz et al., 2011), detecting an animal can be still challenging. Identifying factors affecting detectability of a cue can help correct potential biases in subsequent analysis. The detection of a signal depends on sufficient signal-to-noise ratio, which in turn depends on source level, the off-axis attenuation of the signal, the transmission loss, noise in the environment and the characteristics of the recording system used (Zimmer et al., 2011).

Off-axis attenuation of the signal is a function of directionality for echolocating species. Directionality benefits the animal by concentrating energy in the direction of echolocation, enabling a higher on-axis source level (SL), which reduces clutter and reflection from the surface. However, from the perspective of Passive Acoustic Monitoring (PAM), directional signals lead to low detection probability relative to more omni-directional sources (Marques et al., 2009; Zimmer et al., 2005). The narrow beamwidth of beaked whales in combination with changes of orientation during foraging dives due to behavioural factors, translates in the field to acoustic recordings that contain short sequences of detected clicks and gaps of silence.

Another factor affecting the detectability of the signal is the foraging depth of the species in relation to the depth of the receiver. When a clicking animal is at a different depth than the receiver, the closest they can be is the difference in depths. This results in lower detectability of acoustic cues for receivers at depths that are different to the foraging depths of the whale. Larger distances, in combination with the high frequency characteristics of the signal and the changing orientation of the animals during foraging translate to a reduction of signal energy due to transmission loss and off-axis attenuation. Transmission loss and off-axis attenuation are in addition frequency dependent (Urick, 1983). On the other hand, receivers placed close to the depths of the sound source have the advantage of larger detection ranges, resulting in higher numbers of detections.

The number of clicks detected is influenced by the receiver noise floor, noise that is introduced by the acoustic system and the pre-amplifiers (Urick, 1983) and ambient noise, which is defined as noise that is in the environment. Noisy receivers will detect fewer clicks than a receiver with less noise, as the signal to be detected needs to be some dB higher than the ambient noise and the floor noise of the receiver, an increment called the Detection

Threshold. Much of the ambient noise is generated by ships and waves at the surface, which means that deeper receivers often have lower ambient noise. In addition to the recording system and the ambient noise, the number of true detections depends also on algorithms used for automated detection (Chapter 2, Yack et al., 2010), as different algorithms may need a higher threshold for defining a detection.

To estimate the number of animals using an area, a function relating the detection of the animal with distance is essential. Understanding the acoustic and foraging behaviour of beaked whales has assisted in establishing methodologies for abundance estimation using acoustic cues for specific species (Marques et al., 2013). The first step towards abundance estimation is to identify the probability of detection for a specific cue as a function of distance in an area, although the definition of cues may be study-specific (Marques et al., 2013). For approaches based on distance sampling, detection probability of an acoustic cue is described as a detection function, which is based on distances between the vocalizing animal and the receiver, coupled with estimation of the cue production rate over a time period (Buckland et al., 2001).

The objective of this chapter is to investigate two different acoustic cues for estimating the abundance of beaked whales for acoustic surveys. This is done for individual clicks, which have already been used in density estimation, and using a new approach involving sequences of clicks or Click Scans (CS). In addition, I investigate the effect of receiver depth on the detectability of cues as a function of distance. To do so, I use data from DTAGs in conjunction with a simulated network of receivers placed around the animal at different water depths. The use of DTAGs provides the opportunity to record animal movement during concurrent sound production. Here, I investigate the use of: 1) a single receiver at different depths with the probability of detecting a click and CS as a function of horizontal distance, 2) the distribution of CS length as a function of distance and depth and 3) number of CS detected as a function of distance and receiver depth.

3.2 Material and Methods

Here, I present a simulation study to assess the number of clicks and click scans as cues for a cue counting method. I use animal movement data and sound production times, as recorded on DTAG devices, from two different geographical locations to investigate the influence of relative receiver position on the number and nature of detected click scans. The proportion of cues detected at each receiver from those produced were used to estimate a detection function

for each cue, as a function of distance and receiver depth. From these, parameters such as the average detection probability, were estimated from the derived detection function.

I used data collected from DTAG deployments from the El Hierro and the Bahamas Islands to extract movement data and the clicking events' relative timing. I estimated a theoretical beam pattern to model the sound production from the animal, giving further estimates of the received level for each hydrophone in the theoretical network of receivers. Click times, as recorded on the DTAGs, were used to produce clicking events with realistic intervals to simulate the time of click production. Finally, I used depth data recorded on the DTAG for the distribution of the animal in the water column as well as deriving the orientation of the animal at the time of each click. The detection of clicks and click scans on the theoretical receivers was assessed with a simple energy detector and detection threshold *Td*.

The methodology that follows is divided into:

1. the data collection and click identification on DTAG for the clicking time events,
2. an estimation of the click beam pattern based on a piston model,
3. the design of the theoretical network of receivers.

To estimate the probability of detection for the two different acoustic cues of Blainville's beaked whales, the DTAG data were used in a simulation framework to identify the received level of clicks based on orientation and depth distribution.

Key assumptions of the following methodology were i) a constant source level for the sound production of Blainville's beaked whales, ii) sound production based on a piston model, iii) sound propagation based on spherical spreading and iv) a constant detection threshold based on a simple energy detector.

3.2.1 Data collection

The dataset used for analysis was derived from 19 tagging deployments on Blainville's beaked whales; 14 animal deployments between 2003-2013 off the island of El Hierro in the Canary Islands where there is a resident population of Blainville's beaked whales close to shore, and 5 animals east of Andros Island in the Bahamas, where Blainville's beaked whales are the most common species of beaked whales in the area (Gillespie et al., 2009). Animals were tagged with suction-cup DTAGs (Johnson & Tyack 2003) collecting sound, tri-axial acceleration, tri-axial magnetic field and depth of the tagged animal. Acoustic data were

sampled at 96 kHz in 2003 and at 192 kHz from 2004 onwards. Depth and orientation data were sampled at 50 Hz and decimated in post-processing to a 25 Hz sampling rate.

3.2.2 Click identification on the DTAG.

Echolocation clicks from tagged whales were detected in the DTAG sound recordings using a supervised click detector, consisting of a band-pass energy detector to identify the clicks. Clicks from tagged whales were distinguished from those of other nearby whales in two ways as described in Johnson et al., (2006). Clicks from the tagged whale have a low-frequency energy component below 25 kHz, which is absent from the nearby untagged whales, and clicks from the tagged whale have a more consistent angle of arrival on the DTAG hydrophones than those from untagged whales.

Blainville's beaked whales produce two types of clicks: frequency-modulated (FM) clicks with duration of 270 μs, used for prey search, and short-duration, 105μs, wide bandwidth pulses produced at a high rate during prey capture attempts (Johnson et al., 2006). For the analysis here, we consider only the long-duration FM clicks with inter-click-interval (ICI) greater than 0.1 s, as clicks during prey capture attempts have lower amplitude and hence are less detectable from a passive acoustic receiver.

3.2.3 Click beam pattern

To model the beam pattern of the regular echolocation click of the Blainville's beaked whales, we used an equation for a flat circular piston oscillating in an infinite baffle (Au et al., 1978).

$$P(x) = P_0 \frac{2J_1(x)}{x} \tag{3.1}$$

$$x = ka\sin\theta = 2\pi \frac{\alpha \sin(\theta)}{c} f \tag{3.2}$$

Where P_o is the source level, α is the radius of the piston (assumed aperture for Blainville's beaked whales), c is the speed of sound in the water, θ is the off-axis angle, f is the frequency of the signal and J_1 is the Bessel function of the first kind.

Due to the broadband frequency characteristics of the Blainville's beaked whale clicks (Johnson et al., 2006) the beam pattern estimation was based on a broadband piston model B(θ), previously applied in Cuvier beaked whales (Zimmer et al., 2005).

$$B(\theta) = \frac{\int_{-\infty}^{\infty} P^2(\theta, f) W^2(f) df}{\int_{-\infty}^{\infty} W^2(f) df} \tag{3.3}$$

The broadband piston model is approximated by integrating P(x) for the different frequencies of the Blainville's click by a weighted function W(f) to account for the varied frequency components of the signal. Following Zimmer et al., (2005), adapting the assumption that the power spectrum of the Blainville's beaked whale can be approximated by a Gaussian function, the weighting function is as follows

$$W(f) = \exp\left\{-\frac{1}{2}\left(\frac{f - f_o}{b}\right)^2\right\} \tag{3.4}$$

With f_o representing the centroid frequency of the regular FM echolocation click and b denoting the root mean squared bandwidth of the signal. A Gaussian approximated power spectrum, which averaged the frequency specific piston models across all frequencies existing in the signal of Blainville's beaked whales, was tested as well.

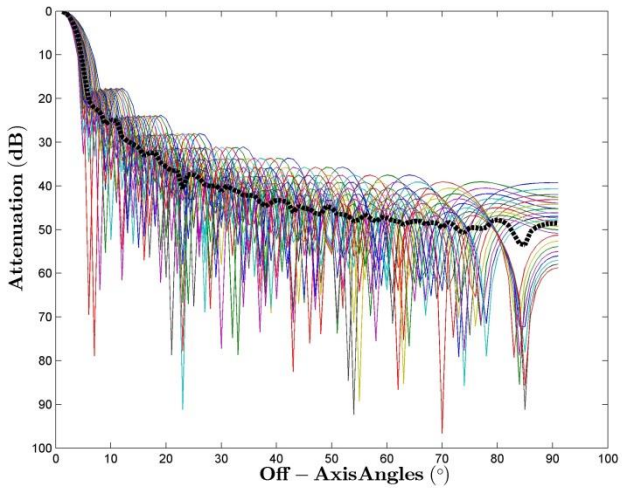

Figure 3.1 Off-axis attenuation of a Blainville's beaked whale click. Coloured lines are the signal attenuation for different frequencies of the signal based on a piston model and black the mean signal attenuation of all the different frequencies.

For broadband signals such as the frequency modulated echolocation signal of Blainville's beaked whales, it is important to take into account the range of frequencies for the piston model because averaging over a range of frequencies produces a smoother function for representing the sound production of the whale. In simulation studies this is important as a piston model from one frequency would lead to abrupt fluctuations of the sound energy with increasing off-axis angles (Fig. 3.1).

3.2.4 Received Level of Clicks and Click Scans as estimated for the modelled receivers.

I define a click scan (CS) as the number of sequential clicks, with ICI smaller than 1 s, that a single acoustic receiver fixed at a certain depth will detect by remaining within the animal's beam. ICI values longer than 1 s could correspond to pauses by the animal or missed detections. The number and the length of the CS that a single receiver will detect is the result of the behaviour of the whale, its effective acoustic beam pattern (the functional effective search volume as a function of angle (Madsen et al., 2013)), its orientation, and finally the distance between the animal and the receiver.

To estimate the duration a receiver will remain in the effective acoustic beam of the animal, 1) movement and 2) acoustic data recorded on DTAG and 3) an estimate of the effective acoustic beam pattern of the animal are required. The effective acoustic beam pattern is estimated as described above in section C. Movement data were used to identify the position and orientation of the whale with respect to the receiver to estimate the received level of clicks produced by the animal. To do so, a coordinate system was created to place the receivers and the animal.

A coordinate system [x, y, z] is defined, with the centre of the axis being at a point on the sea surface, to place the receivers and the animal. A theoretical equally spaced horizontal grid of receivers was placed around the centre of the axis in different depths. The grid is 12 km x 12 km and the receivers are spaced every 150 m. The whale changes position along the z axis only, which represents its depth as recorded on the pressure sensor on the DTAG. In this case, ignoring the [x,y] displacement of the whale does not affect detectability as receivers are placed uniformly around the whale. The orientation of the whale at each echolocation event is extracted from the accelerometer and magnetometer. As the tag usually is placed in varying orientation on the whale and away from the animal's centre of gravity, to measure the orientation of the animal and not the orientation of the tag we work with the animal or whale

frame, which is different from the tag frame. The whale frame is related to the tag frame with the rotation matrix Ψ, which is constant and depends only on how the tag is oriented on the whale. A Matlab tool, *prhpredictor*, has been created by Mark Johnson to estimate the orientation of the tag on the whale's body. The rotation angles r_o, p_o, γ_o in the rotation matrix Ψ relate the tag frame to the body frame. The tool *prhpredictor* predicts the tag position on the whale by parameterizing r_o, p_o, γ_o and defines how to rotate the sensor measurements so as to coincide with the principal axes of the whale. The rotation matrix Ψ is estimated at periods when the orientation of the whale is approximately known, such as surfacing periods before the tagged whale dives. Then the rotation matrix Ψ is multiplied by the tag orientation to create the orientation matrix A_w. The tri-axial acceleration matrix in the whale frame $\mathbf{A_w}$ (3x3xn - where n is the number of samples during the tag deployment) is combined with the tri-axial magnetometer matrix in the whale frame $\mathbf{M_w}$ (3x3xn) to calculate the body-axis bases (caudal-rostral, transverse and ventral-dorsal axes), $\mathbf{W_w}$ (3x3xn), of the animal. The caudal-rostral axis of the animal is a vector with 3 elements and defines the orientation of the animal in space. We calculate the minimum specific acceleration (MSA) (Simon et al., 2012) to exclude samples with extreme specific acceleration values, which would be problematic when calculating the position of the whale. Defining the position of the whale, $[0, 0, z_a]$ for each sampling time and the orientation of the whale from the $\mathbf{W_w}$ we can calculate the angle between the animal and receiver, θ (Fig. 3.2). For every sampling point in time, the angle θ is calculated as the inverse cosine of the dot product of the unit vector of animal position and orientation and the unit vector of receiver position (x_r, y_r, z_r).

$$\theta = arc\cos\left(\frac{W_{ti} \cdot R}{|W_{ti}| \cdot |R|}\right) \tag{3.5}$$

Where W_{ti} is the unit vector of the body-axis of the animal at time t_i and R is the unit vector from the whale to the receiver. Having the angle θ between animal and receiver, and their positions in the grid, I estimate the received level for each click at each of the receivers, for all the clicks during the foraging dive.

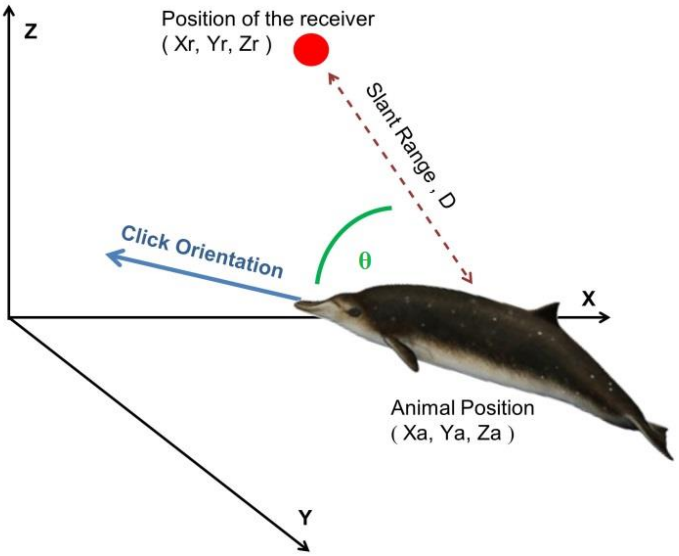

Figure 3.2 The slant range D, between the animal and the receiver was used to calculate the transmission loss of the signal. The angle θ between the echolocation axis of the animal during the vocalizing event and the receiver was used to calculate the off-axis attenuation.

The received level (RL) of each click is calculated for each receiver taking in to account the orientation of the whale, the transmission loss based on spherical spreading and absorption taking into account the main frequency of the Blainville's beaked whale click. The absorption coefficient **a**, was calculated based on standard absorption curves (Kinsler & Frey, pp. 159-160), for the centroid frequency of the broadband click.

$$RL_i = SL + B(\theta) - 20\log_{10} \mathrm{D}_i - aD_i \qquad (3.6)$$

Where SL is the source level of the Blainville's beaked whale, D_i is the direct distance (slant range) between the animal and the receiver for the i^{th} regular click event.

The process described above was repeated for all the DTAG deployments and for different receiver positions around the animal. An inter CS interval (ICSI) is defined as the time between two consecutive CS.

3.2.5 Threshold for detection

The positive detection of a click signal is defined as a function of the signal to noise ratio (SNR) between the signal and the ambient noise. This SNR is called the detection threshold, DT, and the signal will be detected if the RL is equal to or greater than the ambient noise level NL plus DT. The number of CS and the length of the CS will differ in varying ambient noise levels, but for simplicity here we will consider NL as a constant. In the frequency range

of Blainville's beaked whale echolocation clicks (26-51 kHz), a typical spectrum level for ocean noise is 40 dB re $1\mu Pa\sqrt{Hz}$ for sea state 4 (Urick 1983, fig. 7.5). The noise level over the 25 kHz click band would thus be expected to be the spectrum level of 40 dB plus 10 $\log_{10}$ (25,000) or 40+44 = 84 dB re 1 μPa.

Here, the detection of individual clicks is considered with one detection threshold criterion which includes both processing gain and a reception threshold (Lurton, 2002). To determine if a click is detected, the detection threshold is chosen to be 16 dB, following Ward et al., (2011) who used a processing gain of 11 dB and a reception threshold of 5 dB for detecting beaked whale clicks on the AUTEC range. For simplicity, a constant noise level plus a constant detection threshold of 16 dB for the clicks and CS received is considered for the receivers at all depths. Here we assume that the signal is detected if the received level of the click is greater than the ambient noise level plus the detection threshold, i.e. RL > NL +DT = 84 + 16 = 100 dB.

The first criterion is a simple energy detector for both individual clicks and CS. For the detection of CS, a timing criterion is added to that of the detection threshold where individual clicks with less than 1s ICI are considered to be the same CS (Table 1).

Table 1 Detection Criterion for clicks and click scans (CS).

Detection Criterion	Click	Click Scan
Detection Threshold (> 100 dB)	✓	✓
Timing (ICI) (< 1s)		✓

3.2.6 Probability of detection

In distance sampling, detection distances are used to estimate the area of effective search, or equivalently the average probability of detection within some distance, *w*, where no detection is assumed possible further away (Buckland et al., 2001; 2004; Marques et al., 2013).

For acoustic surveys, density estimation of an object of interest (e.g. animal, cue) is given by $\hat{D} = \frac{n(1-f)}{\hat{p}a\hat{r}}$ (Marques et al., 2013), where n is the number of objects detected, f is the false detection rate, p is the average detection probability of an object within the area a, and r is the

estimated rate of objects produced over a unit of time, which in our case is the number of clicks or click scans produced by the animal over a time unit.

As the probability of detection usually depends on the distance from the sound source to the acoustic sensor, a probability of detection function of distance is required. In our study the detection function is estimated as a function of horizontal distance, where clicks detected on the receivers are recorded as presences and the clicks not detected as absences, with an empirical detection function calculated by dividing the number of clicks detected by the total number of the clicks produced. The horizontal distance is used instead of the slant range, as it is integrates different slant ranges for animals vocalizing at different depths. For example, a receiver near the surface will never have a detected slant range of 100 m as Blainville's beaked whales start echolocating at depths of around 400m depth.

The average detection probability, $\hat{P}$, is given by $\hat{P} = \int_0^w \hat{g}(x)h(x)dx$, where $\hat{g}(x)$ is the estimated detection function, h(x) is the distribution of available distances regardless of detection of the object/cue, and w is the truncation distance to which the integration is calculated. The h(x) – the distribution of distances to objects/cues for the point and cue counting method is calculated by $2x/w^2$ where x is distance. A truncation distance w should be chosen to define the maximum distance at which clicks are detectable. A value of w corresponding to a maximum distance that an on-axis click could be detected is given by 20log10(w)+a*w=DT, where DT is the detection threshold. The average detection probability represents the area of effective search and is a measure of detectability (Buckland et al., 2001; Marques et al., 2013).

3.3 Results

The dataset used for the analysis consists of DTAG data from 19 animal deployments (13 from El Hierro and 6 from the Bahamas), with a total number of 71 deep foraging dives (42 from El Hierro and 29 from the Bahamas). A total number of 265,711 clicks were detected from all the whales together (151,263 from El Hierro and 114,448 from the Bahamas) with 259,871 (147,740 - El Hierro and 112,131 - Bahamas) corresponding to regular clicks – defined as ICI larger than 0.1s. Table 2 shows the number of foraging dives for each animal and the corresponding number of clicks produced, number of regular clicks and depth information for each foraging dive in the two different locations, El Hierro and Bahamas.

Animals in the Bahamas were performing foraging dives in deeper layers of the sea column, mean depth of 833m, in relation to El Hierro animals, where the mean depth was 698m.

Table 2 Click and dive data for the tagged animals used in the simulation, 13 animals (42 dives) from the area of El Hierro and 6 animals (29 dives) from the Bahamas. For each tag deployment the number of dives is shown and for each dive the number of clicks produced, the number of regular clicks, the mean depth of the foraging dive and the 5% - 95% quantiles of depth during echolocation events.

Area	Animal id	Dive #	# Clicks Produced	# Reg. Clicks	Depth (m)		
					Mean	5%	95%
El Hierro	md03_284a	1	4262	4235	639	586	790
		2	4326	4300	673	593	752
		3	4265	4254	740	638	835
		4	2625	2392	458	241	633
		5	3691	3545	624	311	777
	md03_298a	1	3329	3305	644	488	806
		2	3924	3887	677	540	727
	md04_287a	1	3909	3870	657	554	960
		2	3751	3736	758	590	914
		3	3547	3520	618	585	663
		4	4401	4315	929	600	1229
	md05_277a	1	3585	3562	739	547	929
		2	4119	4088	704	562	829
		3	3412	3377	657	547	883
	md05_285a	1	4303	4229	653	609	684
		2	3439	3428	798	591	986
		3	3518	3504	733	544	820
		4	5751	4588	646	360	745
	md05_294a	1	3070	3052	600	572	627
	md05_294b	1	2643	2620	597	574	624
		2	3367	2954	589	564	613
		3	3718	3352	741	626	783
	md08_136a	1	4171	4084	670	475	773
	md08_137a	1	4009	3944	1110	712	1308
		2	3195	3150	763	697	832
		3	3537	3470	1100	706	1326
		4	3458	3433	435	330	499
		5	3997	3976	477	355	547
		6	4189	4149	846	740	928
		7	4204	4160	711	341	958
	md08_142a	1	3042	3017	663	584	798
	md08_148a	1	3192	3183	827	605	994
		2	4295	4274	655	545	789
	md10_146a	1	3104	3052	825	641	900
	md10_163a	1	3895	3853	713	615	797
		2	2710	2696	743	580	843
		3	2269	2241	710	545	797
		4	3245	3228	667	486	791
		5	3039	3002	719	549	783
		6	3953	3931	646	399	797
		7	2565	2554	586	284	802
		8	2239	2230	596	281	770
Total	13	42	151263	147740	698	531	825

Area	Animal id	Dive #	# Clicks Produce	# Reg. Clicks	Depth (m)		
					Mean	5%	95%
BAHAMAS	md06_296a	1	5797	5788	962	780	1031
		2	4903	4890	938	699	1058
		3	4556	4551	904	677	990
		4	7564	7557	740	597	861
	md07_227a	1	773	757	1190	602	1377
		2	1619	1617	894	638	986
		3	1568	1562	1059	623	1334
		4	1373	1370	978	588	1293
		5	1585	1579	763	591	817
		6	1544	1542	1082	472	1337
	md07_245a	1	6679	6552	954	812	1001
		2	2855	2832	934	716	998
		3	2429	2419	898	650	1004
		4	4151	4147	1151	650	1331
	md07_248a	1	4267	4021	847	685	942
		2	4399	4144	870	700	933
		3	4659	4517	848	689	982
		4	4488	4393	820	671	910
	md07_248b	1	5128	4570	846	677	1002
		2	6277	6230	804	711	877
		3	5722	5711	800	592	1047
		4	6818	6333	792	553	1013
	md08_289a	1	4992	4950	611	571	644
		2	4425	4397	618	594	644
		3	3868	3847	621	588	667
		4	4522	4518	461	365	514
		5	2488	2465	609	326	857
		6	1213	1100	392	282	470
		7	3786	3772	767	450	945
Total	6	29	114448	112131	833	605	961

The off-axis attenuation of Blainville's beaked whales' regular clicks was calculated based on a circular piston model taking in to account the broad band nature of Blainville's beaked whale clicks as in Zimmer et al., (2005). I assume that for angles larger than 90° the whale will be undetectable, an assumption that is not true for short distances between the animal and

the receiver. Fig. 3.3 shows the sound level attenuation as a function of angle based on a circular piston model with diameter a= 0.25m (assumed aperture for Blainville's beaked whales, Madsen et al., 2013), and a weighted function based on the bandwidth of the echolocation signal of Blainville's beaked whales. The beam pattern can alternatively be estimated as a simple or weighted mean, by the energy in each frequency band. The three functions are very similar (Fig. 3.3) suggesting a robust prediction of the off-axis attenuation of the signal regardless type of weighting function used.

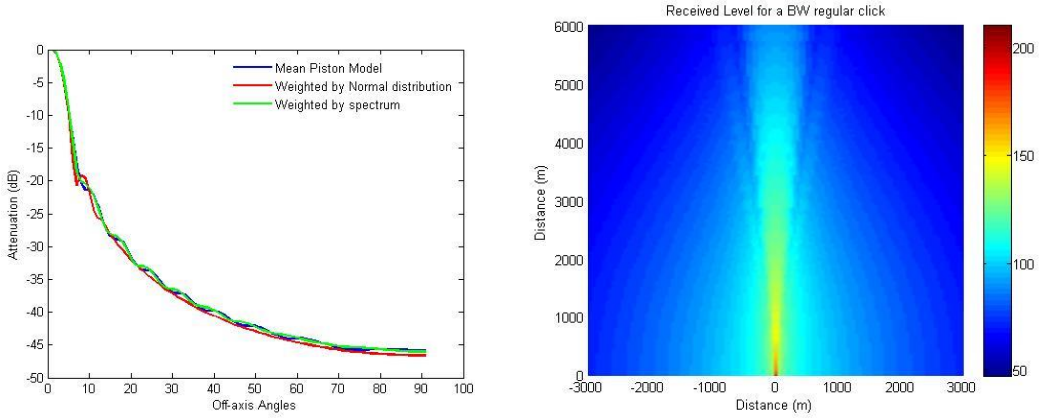

Figure 3.3 Off-axis attenuation of a Blainville's beaked whale click based on three different models – Mean beam pattern based on the piston model for frequencies 26 kHz – 51 kHz (blue line), weighted by normal distribution (red line) and weighted by the actual spectrum measured from an on-axis click (green line). Received level of a click as a function of distance in front and beside the animal.

The tagged whales started vocalizing at depths ranging from 178 m to 643 m, with maximum depths ranging from 530 m to 1390 m for the different dives. The mean foraging depth of the whales during regular clicking was at 698 m (range 435 m – 1110 m) for the animals from El Hierro and 833 m (range 392 m – 1190 m) for the animals from the Bahamas (Table 2). Whales' depth during vocalization periods (Fig. 3.4 and 3.5) had a mean value of 753 m (561 m – 880 m 5 - 95 % quantiles).

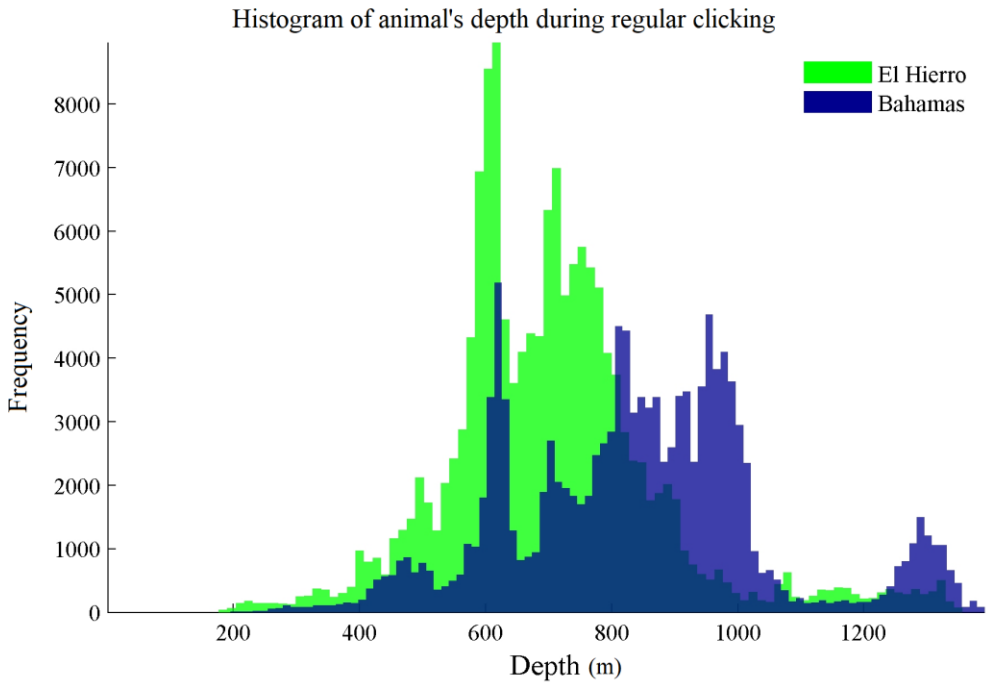

Figure 3.4 Histogram of animals' depth during regular clicking, animals from El Hierro (Canary Islands) in green and from the Bahamas in blue.

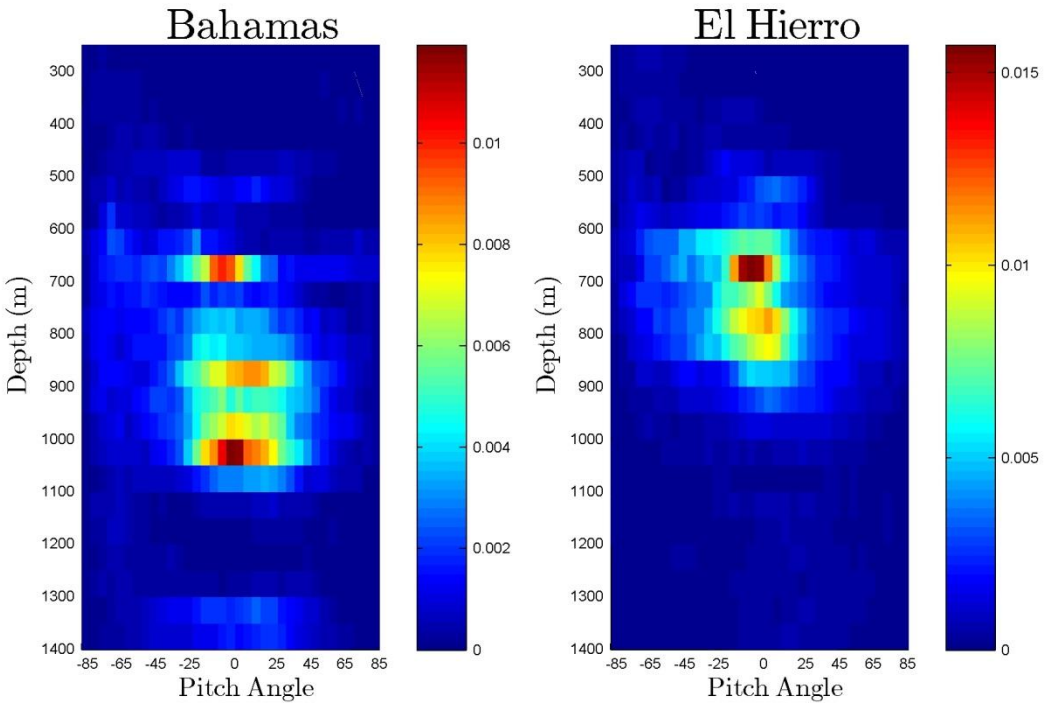

Figure 3.5 Proportion of clicks produced (colour bar) at different depths and their orientation. Pitch angle of animal's orientation during echolocation events for different depths bins during deep foraging dives of Blainville's beaked whales for two different locations: El Hierro (Canary Islands) on the left, and Andros Island (Bahamas) on the right. The El Hierro dataset comprise data derived from 13 animals performing 42 deep foraging dives. For Andros Island (Bahamas) on the right, data derived from 19 animals performing 29 foraging dives.

3.3.1 Clicks

The detection probability of individual clicks as a function of horizontal distance was considerably different for receivers placed at different depths. Fig. 3.6 shows the detection functions for receivers placed at 20 m and 100m depths, which are often used for towed hydrophones, at 300m depth, at 600m and 1000m depths, where the detection function had the largest average detection probability, and of deep receivers of 2000m depth that can be found on bottom mounted hydrophones such as those in the AUTEC in the Bahamas.

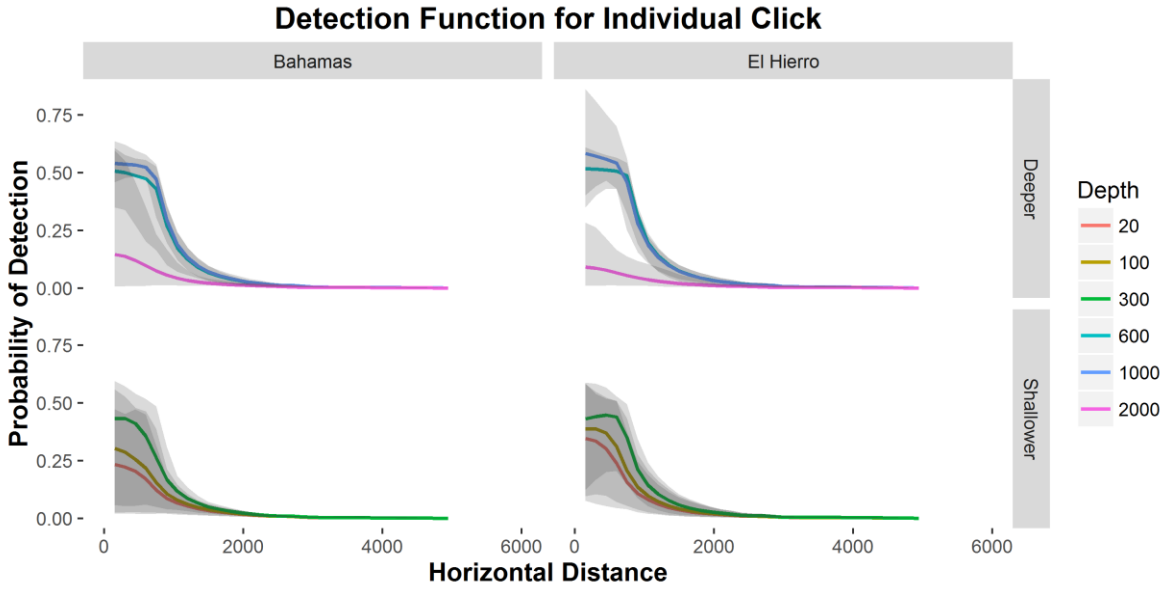

Figure 3.6 Probability of detection of an individual Blainville's click as a function of horizontal distance, at different receiver depths. Curves correspond to receivers placed in: 20m, 100m, 300m ("Shallower") and 600m, 1000m and 2000m depth ("Deeper").

The probability of click detection differs among receivers placed in different depths (Fig. 3.6). Depth dependent detectability was derived from the simulation based on the number of clicks detected in different receivers placed at different depths ranging from 10 m to 2000 m, with approximately 200 m depth separation except the shallow receivers which were placed at 20 and 100 meters depth. Lower detectability was found at receivers between 1600 and 2000 m depth, followed by receivers close to the surface (20 m, 100 m and 200 m). Detectability then increases for receivers placed at 200-400 m with peak detection-at-zero-distance (g(0)) for receivers placed between 800 m and 1200 m. The g(0) here has a mean value of 0.52 (0.41 to 0.66 with 95% confidence) for the Bahamas, and a mean value of 0.56 (0.37 – 0.75 with 95% confidence) for the El Hierro.

This result is expected as beaked whales vocalize at depths of 600-800 m (Johnson et al., 2006) in addition to the high directionality of their echolocation signal (Fig. 3.3) and the distribution of pitch angles during their foraging behaviour (Fig. 3.5).

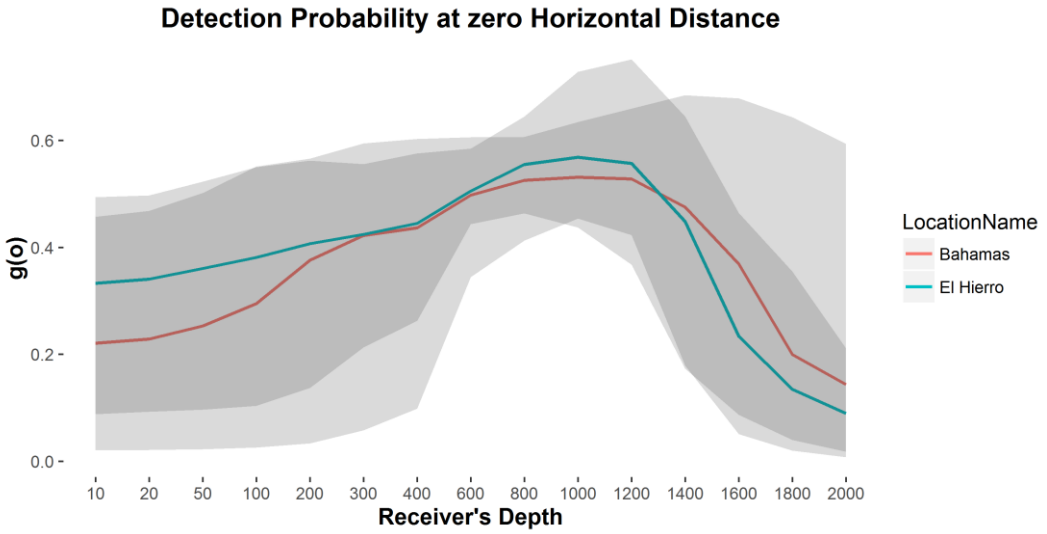

Figure 3.7 Detection probability at zero horizontal distance – g(0) as a function of receiver depth for two different locations. Red line for the Bahamas dataset (29 dives) and blue line for the El Hierro dataset (42 dives) and grey area 95% confidence intervals.

The probability of detection at zero horizontal distance *g(0)* differs as a function of receiver depth (Fig. 3.7) and between the two different geographical locations. El Hierro has larger *g(0)* for receivers up to 1400 m depth whereas for receivers deeper than that the Bahamas have greater detectability as a result of the deeper foraging depths of the animals in that area. The maximum detection probability at zero horizontal distance is found on receivers that are located at 1000 m depth for the El Hierro area and at 800-1200m depth range for receivers for the Bahamas area.

The optimal depth of the receiver is influenced from the mean foraging dive of the animal and the orientation of the produced clicks during the depths where the animal is placed. The foraging depth and the orientation of the animal are influenced by the three-dimensional prey distribution, which will vary as a function of location and season.

3.3.2 Probability of detection

The average detection probability, $\hat{P}_a$, differs as a function with receiver depth and location due to the foraging depth of the two different populations.

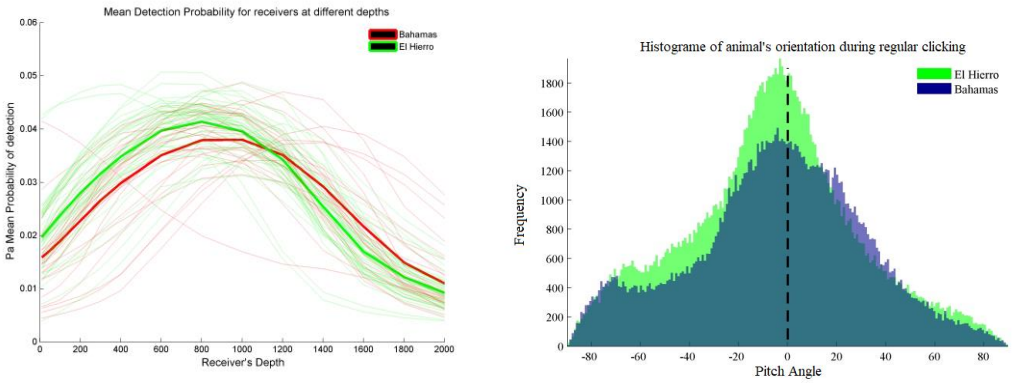

Figure 3.8 (Left) Average probability of detection (P_a) for receivers at different depths. Estimated P_a taking into account the available distances for individual clicks – different colours represent the Pa for the different dataset, that of El Hierro (green) and that of Bahamas (red). Thinner lines correspond to P_a for each individual dive. A truncation point w of 4.8 km was chosen to calculate the Pa for each different depth of receiver. (Right) Histogram of whale pitch angle during all foraging dives.

The depth at which the receiver has higher average detection probability is determined by the foraging depth and orientation of the animal during echolocation events. In Fig. 3.8 the average detection probability is maximized at receivers placed at 1000 m for the Bahamas dataset (29 dives) with a value of 0.038 (std 0.0059) and 800 m depth for the El Hierro dataset (42 dives) with a value of 0.041 (std 0.0046). The mean pitch angle of the whale during regular clicking was -4.2° (std 35.5) and -6.5° (std 34.9) for Bahamas and El Hierro respectively.

A GAM (Generalized Additive Model) model was fitted to the average probability of detection (P_a) for the two locations to identify if differences in the observed *Pa* were statistically significant. The mgcv library in R (Wood, 2006) was used to fit a GAM model (Gaussian errors, log-link), modelling the average probability of detection as a function of receiver's depth and location. The systematic component was therefore:

$$\eta_i = \beta_0 + f(Depth_i, Location)$$

Where η provides the link-scale predictions, which is a function of: β_0 the intercept, and f a spline-based smooth for Depth permitted to change between locations. The complexity of f was estimated as part of the fitting process. The interaction between site and depth was also included, i.e. allowing different f for the sites based on AIC (ΔAIC -40.72) suggesting that a

different smoothing function was needed for each location. Overall, 66.6% of the deviance was explained by the model.

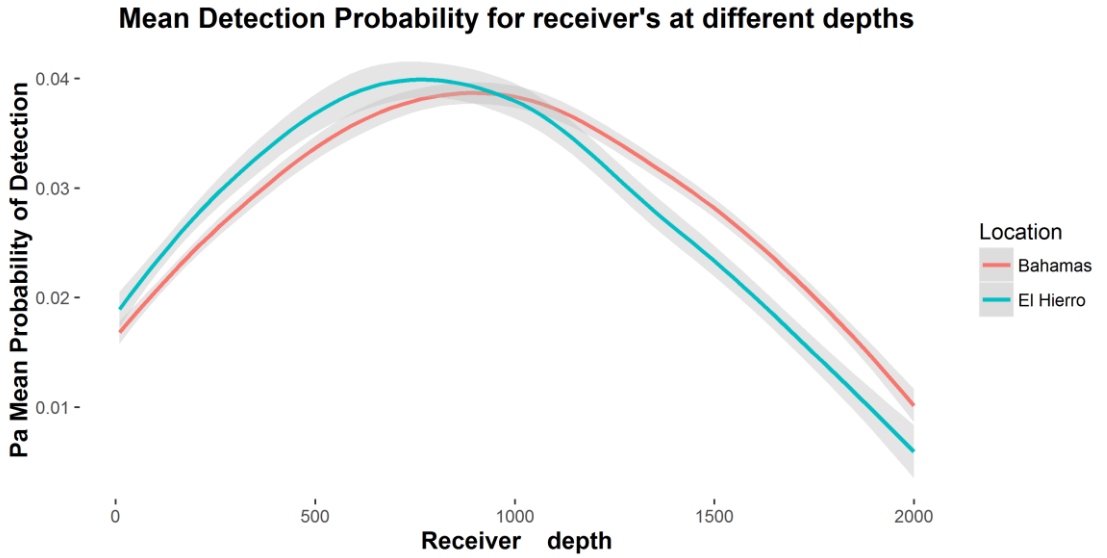

Figure 3.9 Average detection probability as a function of receiver depth for single echolocation clicks of Blainville's beaked whales, for the Bahamas (red line) and for El Hierro (blue line).

The average detection probability for El Hierro ranges from 0.004 for receivers at 2000m to 0.04 for receivers placed at 600m and 800m. For the Bahamas, the average detection probability range is between 0.005 for 2000m receivers up to 0.049 for receivers placed at 800m and 1000m depth (Fig. 3.9). Two different parameters of the detection function are the probability of detection at zero distance g(0), and the average probability of detection. This can be translated to effective radius, or effective area, for comparing detectability under different sets of parameters that may affect the probability of detection.

3.3.3 Click rates

The click rate is the number of clicks produced per unit time; as beaked whales perform deep dives followed by shallow silent dives, click rates are calculated by taking the full dive cycle of whales into consideration. Here, the click rate is estimated as the proportion of time spent clicking in relation to the full dive cycle divided by the estimated inter-click-interval. Duration during clicking is estimated from the start of clicking until the end of clicking through a foraging dive. For each full dive-cycle the proportion of vocal period in relation to the duration of the full dive duration is divided by the estimated ICI. The estimated ICI was

calculated by a weighted mean during the vocal sequences of a foraging dive. The click rates were calculated separately for the El Hierro and the Bahamas data (Fig. 3.10). Because full dive cycles are required to estimate the proportion of vocal activity in relation to the full dive cycle, the dives used were 67 in comparison to 71 used in the simulation, 38 for the El Hierro and 29 for the Bahamas dataset.

The mean click rate (weighted by the full dive duration) for El Hierro was estimated to be 0.41 per second (CV of 0.38) and for the Bahamas 0.41 per second (CV of 0.52). The two click rates were compared statistically with an unpaired Welch test, which failed to reject the null hypotheses (p=0.47) that the click rates come from the same distribution i.e. the mean click rates are statistically equivalent for the two sites.

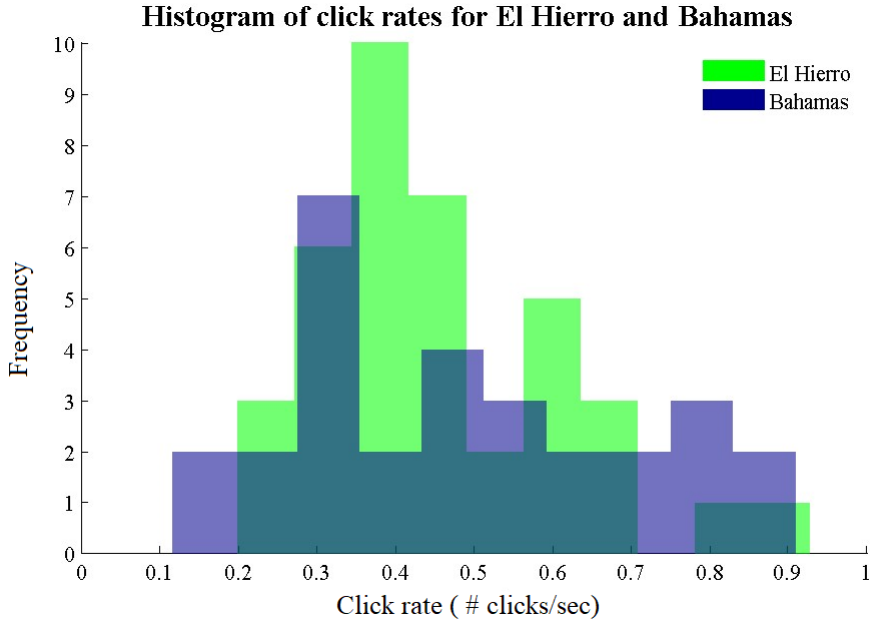

Figure 3.10 Histogram of click rate per dive-cycle for El Hierro, n=38, (green) and the Bahamas, n=29 (blue).

3.3.4 Click Scans

The click scan (CS_d) is defined as a series of clicks detected on the receiver with ICI smaller or equal to a predefined threshold. A threshold of 1 s was chosen to be in line with the definition of regular clicking as produced by the whale, where the time between regular clicking for Blainville's beaked whales range between 0.1 - 1 s (Johnson et al., 2006). The upper one-second threshold corresponds to approximately one to two clicks being missed from the produced click sequence as recorded on the DTAG.

Click sequences (or click trains) (CS_p) as produced by the whale and recorded on the DTAG are a series of regular clicks occurring between pauses of regular clicking, with inter-click-interval between regular clicking of 0.1-1s (Johnson et al., 2006; Madsen et al., 2013).

For the animals in El Hierro, the mean number of CS_p produced during a foraging dive was 62.3 (15.9 std) with a mean ICI of 0.43 and a mean inter-click sequence interval (ICS_pI) of 4.09 seconds. For the Bahamas dataset, the number of click sequences produced was 87.3 (32.1 std) per dive with a mean value of ICI 0.4 s and ICS_pI of 3.5 s. The length of the click scans was 58.4 (11.1 std) and 43.2 (23.6 std) for El Hierro and the Bahamas, all measures derived from the DTAG records.

Table 3 Number of click sequences (CS_p) detected on the DTAG audio recordings for animals from El Hierro and the Bahamas. A CS_p is defined as a click sequence for which the inter-click-intervals are smaller than or equal to 1 s. The columns indicate the number of click sequences per dive, Length of CS_p: the average number of clicks contained on a CS_p, mean ICI per CS_p and inter-Cs-interval (ICS_pI) in s.

Area	Animal id	Dive #	# CS Produced	Length CS	Mean ICI (s)	Mean ICSI (s)	Area	Animal id	Dive #	# CS Produced	Length CS	Mean ICI/CS	Mean ICSI
El Hierro	md03_284a	1	64	66.17	0.42	4.32	BAHAMAS	md06_296a	1	125	46.30	0.40	3.14
		2	64	67.19	0.43	4.19			2	109	44.86	0.41	3.30
		3	76	55.97	0.50	5.96			3	78	58.35	0.39	2.95
		4	54	44.30	0.45	6.23			4	122	61.94	0.42	3.12
		5	55	64.45	0.41	4.67		md07_227a	1	93	40.19	0.40	8.27
	md03_298a	1	52	63.56	0.43	3.12			2	68	62.70	0.37	2.17
		2	60	64.78	0.42	4.59			3	81	46.80	0.42	2.14
	md04_287a	1	65	59.54	0.39	3.30			4	61	55.70	0.42	2.06
		2	65	57.48	0.45	3.82			5	60	65.50	0.46	2.01
		3	57	61.75	0.40	3.59			6	107	41.40	0.39	2.18
		4	67	64.40	0.43	4.27		md07_245a	1	126	52.00	0.37	3.12
	md05_277a	1	59	60.37	0.44	3.98			2	59	48.00	0.43	2.53
		2	67	61.01	0.44	4.53			3	50	48.38	0.39	2.50
		3	52	64.94	0.41	4.09			4	122	33.99	0.37	2.85
	md05_285a	1	93	45.47	0.37	3.61		md07_248a	1	86	46.76	0.39	4.05
		2	60	57.13	0.47	2.91			2	101	41.03	0.35	3.02
		3	62	56.52	0.45	2.77			3	107	42.22	0.42	3.31
		4	78	58.82	0.28	3.76			4	102	43.07	0.45	3.69
	md05_294a	1	50	61.04	0.45	4.41		md07_248b	1	123	37.15	0.35	2.64
	md05_294b	1	43	60.93	0.40	4.77			2	120	51.92	0.40	3.16
		2	99	29.84	0.31	3.10			3	100	57.11	0.42	3.20
		3	57	58.81	0.47	3.17			4	151	41.94	0.37	3.43
	md08_136a	1	68	60.06	0.37	4.51		md08_289a	1	86	57.56	0.41	4.20
	md08_137a	1	95	41.52	0.47	3.63			2	63	69.79	0.44	4.65
		2	70	45.00	0.40	2.68			3	72	53.43	0.41	3.91
		3	98	35.41	0.50	3.81			4	66	68.45	0.47	3.98
		4	52	66.02	0.40	3.25			5	29	85.00	0.42	4.62
		5	56	71.00	0.42	3.54			6	17	64.71	0.34	5.29
		6	76	54.59	0.58	7.94			7	48	78.58	0.43	3.82
		7	87	47.82	0.45	3.59	**Mean**		**29**	**87.3**	**53.27**	**0.40**	**3.50**
	md08_142a	1	31	97.32	0.41	5.48							
	md08_148a	1	62	51.34	0.51	3.83							
		2	65	65.75	0.43	5.50							
	md10_146a	1	62	49.23	0.44	4.10							
	md10_163a	1	66	58.38	0.43	4.59							
		2	38	70.95	0.42	4.47							
		3	38	58.97	0.44	4.28							
		4	54	59.78	0.44	3.27							
		5	55	54.58	0.45	3.63							
		6	65	60.48	0.43	3.08							
		7	35	72.97	0.46	3.93							
		8	45	49.56	0.49	3.80							
Mean		**42**	**62.3**	**58.45**	**0.43**	**4.09**							

The click scans (CS_d) as recorded on the receivers varied considerably as a result of the movement of the animal in combination with the varying distance between the whale and the receiver.

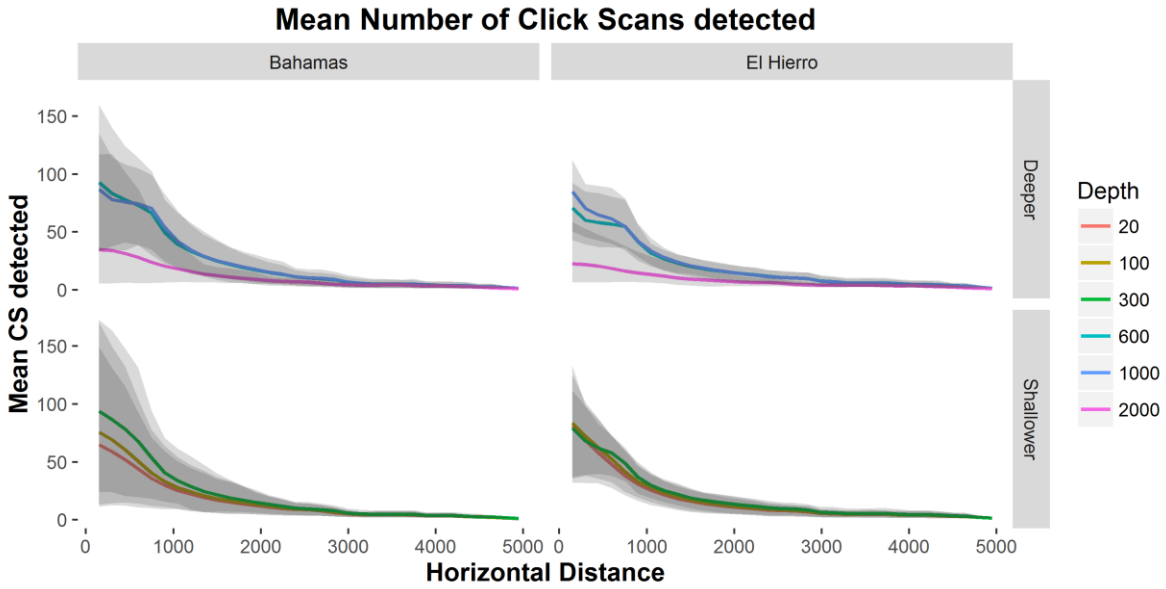

Figure 3.11 Mean number of click scans (coloured lines) as a function of horizontal distance, for receivers at different depths and 5 - 95 % (shadowed area). Shallower receivers were at depths of 20m, 100 m, 300m, and deeper receivers at depths 600m, 1000m and 2000 m.

The number of CS_d per dive varies with receiver depth and horizontal distance to the animal, with a decreasing mean value as the distance between the whale and the receiver increases. The CS_d is dependent on the movement of the animal, as the off-axis attenuation of the signal will lead to smaller received levels on the receiver. As expected, the length of the CS_d varies with distance from the receiver to the animal with larger CS_d to be found at smaller distances and shorter CS_d at distances further away (Fig. 3.11).

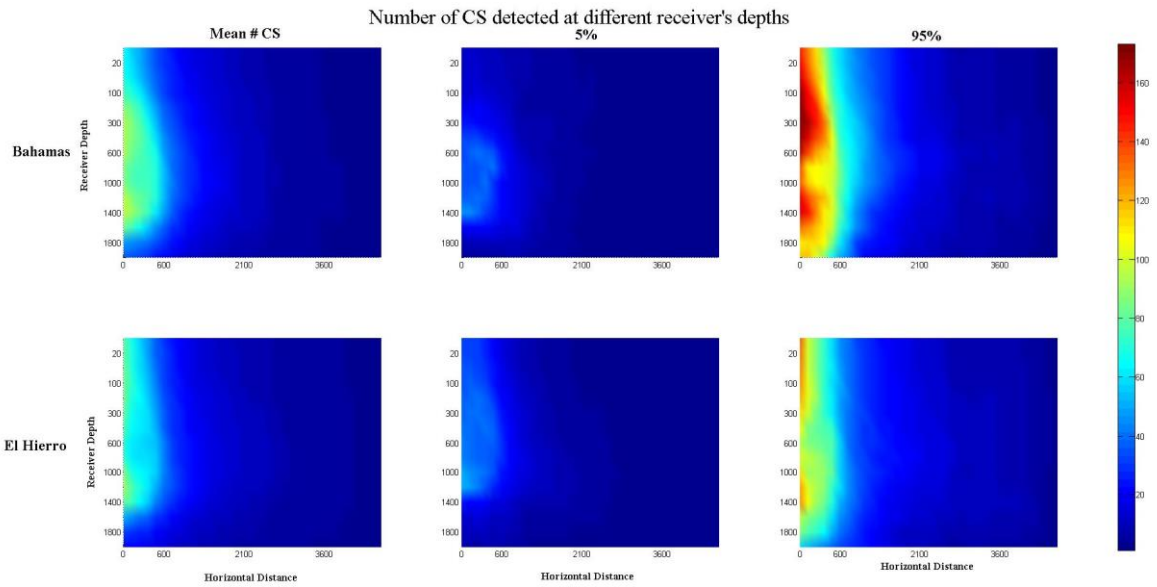

Figure 3.12 Mean number of click scans (CS_d) detected based on depth of the receiver and horizontal distance for the Bahamas and El Hierro dataset. The mean number of CS detected as well as the upper and lower 5% confidence surfaces, derived from 71 dives of Blainville's beaked whales (29 dives from Bahamas and 42 dives from El Hierro).

In addition to the distance dependence, the number of click scans detected is dependent as well on receiver depth (Fig. 3.12). The number of CS_d received at various depths differs, with smaller CS_d numbers detected at deep receivers (1600-2000 m) and larger number of CS_d per dive detected at receivers of 1000-1400 m depth. The number of CS_d detected per dive increase on the receivers that are shallower and/or deeper than the foraging depth of the animal. The mean size of click scans (number of clicks in a CS_d) increases for receivers that are closer to the foraging depth of the animal (Fig. 3.13).

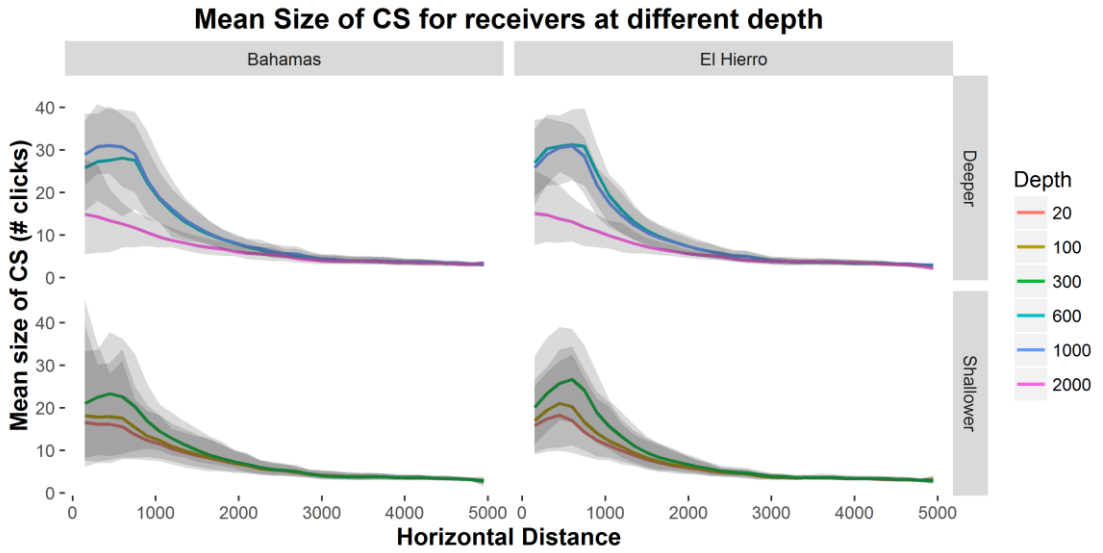

Figure 3.13 Mean Number of clicks per click scan (coloured lines) as a function of horizontal distance in receivers placed at different depths and 5-95% CI (shadowed area) for the two locations: the Bahamas and El Hierro. Shallower receivers shown are placed at 20m, 100m, 300m, and deeper receivers at 600m, 1000m and 2000m.

The average length (size) of a click scan increases for receivers up to 500m horizontal distance and then decreases with increasing distance between the animal and the receiver. At shorter distances between the receiver and the clicking whale (which is a function of depth and horizontal distance), the CS_d are larger than the CS_d at further distances away (Fig. 3.14). Changes in orientation of the animal at distances further away would lead to undetected clicks and hence the shorter CS_d length than of those closer to receiver. At larger distances, even small changes in orientation away from the axis of sound production will reduce the received level below the detection threshold. The mean number of CS detected changes as a function of depth (Fig. 3.15 – red line) with an average CS_d between 19 and 23 CS for receivers between 10 m and 1600 m and then a considerable drop to the mean number of CS detected for deeper receivers. The mean number of clicks per CS is around 6 for shallower receivers, increasing to approximately 12 clicks per CS for receivers around 600 to 1200 meters. For deeper receivers, the average number of clicks per CS decreases to approximately 6 to 7 clicks per CS (Fig. 3.15 – blue line). There is marked variability in the number of clicks per CS for receivers at different depths, with receivers at the foraging dive depth having fewer but longer CS and shallower and deeper receivers detecting more and shorter CS. This occurs because when the receiver is near the depth of the whale, it will detect longer runs of clicks in a click train, while at more distant depths, the click train is broken up into several shorter scans.

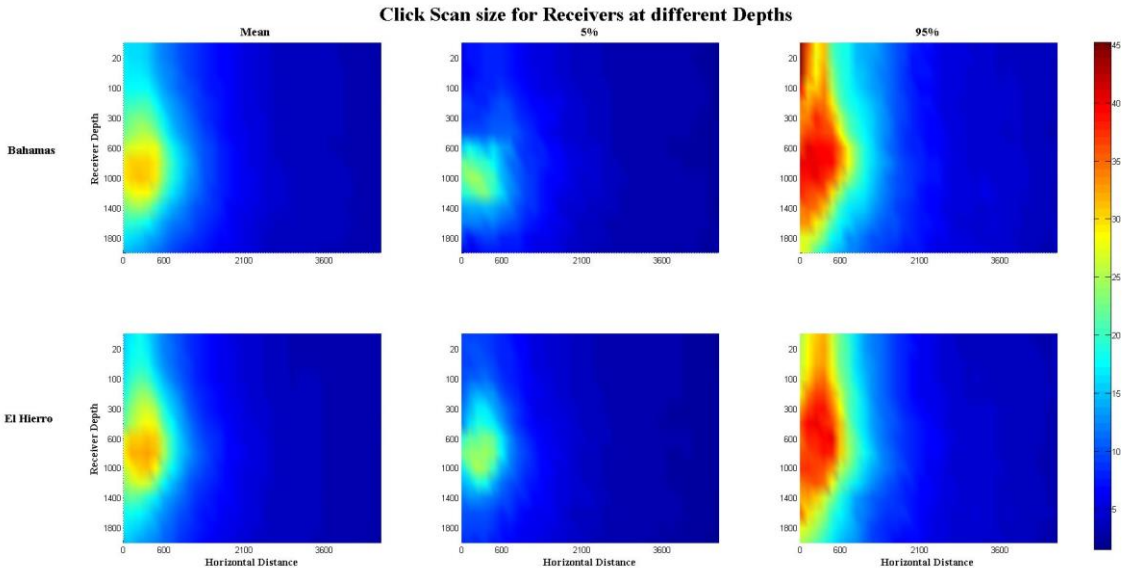

Figure 3.14 Mean size (number of clicks) of CS_d detected based on depth of the receiver and horizontal distance for the Bahamas and El Hierro datasets. The mean size is plotted in addition to 5% and 95% values of the CS_d detected derived from 71 dives of Blainville's beaked whales (29 dives from the Bahamas and 42 dives from El Hierro).

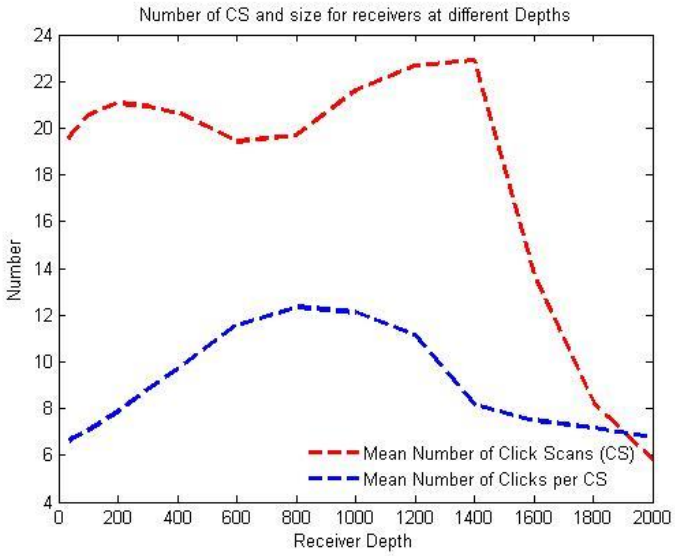

Figure 3.15 Mean Number of Click Scans (CS_d) for receivers at different depths (red dashed line). Mean number of Clicks per CS for receivers at different depths (blue dashed line).

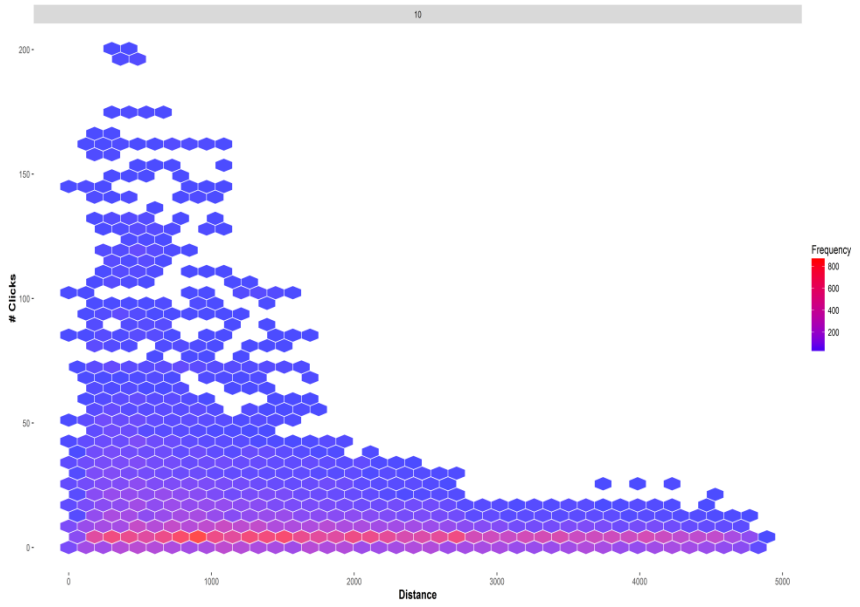

Figure 3.16 Number of clicks per click scan detected as a function of horizontal distance, for receiver at 10m depth.

While there is high variability for the number of clicks contained in each detected CS (Fig. 3.16) the most frequent length of CS is less than 5 clicks.

3.3.5 Click scan rates

The click scan rate is not straightforward to calculate, as in the case of click cue rate, because of partial detection of click trains produced by the whale, defined by pauses or buzzes (Fig. 3.17 - right).

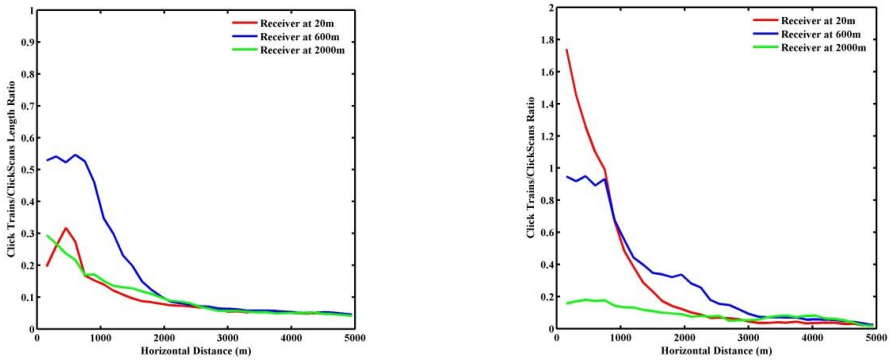

Figure 3.17 Ratio between click trains produced by the whale as recorded on the DTAG (CS_p) and click scans as recorded at the receivers (CS_d) (Right) and ratio of their corresponding size (Left).

If the click rate approach is intended to extract the click scan rate, then the click scan rate is the number of click trains produced by the whale (CS_p as recorded on the DTAG) in a unit of time. The click scan rate (number of click scans per second) is estimated as the number of

click trains produced during a full dive cycle divided by the duration of the dive cycle, a weighted mean based on the duration of full dive-cycle.

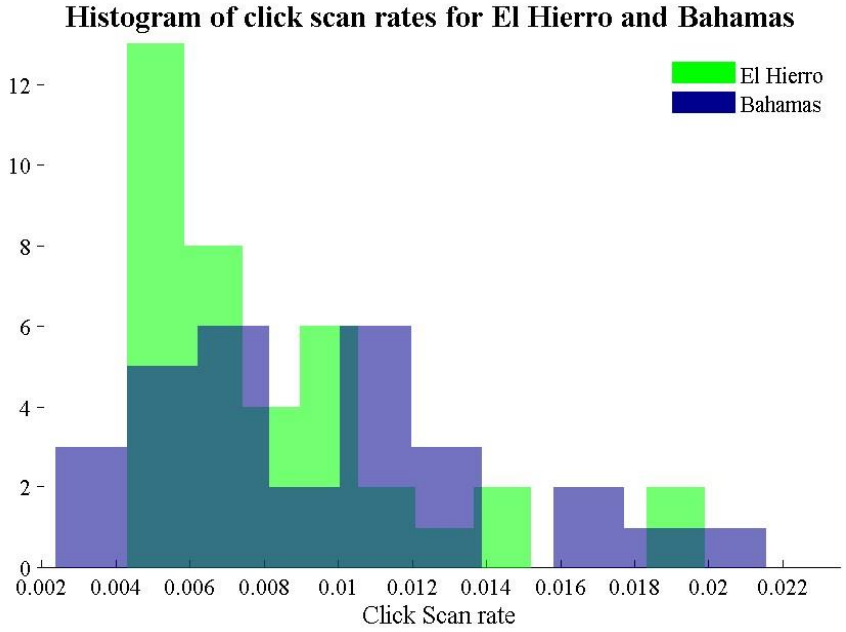

Figure 3.18 Histogram of click scan rate (number of click scans per second) for each dive-cycle for El Hierro, n=38, (green) and the Bahamas, n= 29 (blue).

The mean click scan rate (weighted by the full dive duration) for El Hierro is estimated to be 0.0073 per second and for the Bahamas 0.0083 per second (CV of 0.52) (Fig. 3.18).

3.3.6 Density Estimation using click and click scan cue counting

Density estimation using single clicks as a cue for a fixed sensor is estimated by $\hat{D} = \frac{n(1-f)}{\hat{p}a\hat{r}}$ where f is the proportion of false positive detections, p is the probability of detecting a cue given that it is produced within the area surveyed, a, and r is the cue production rate. The results show that p, the probability of detection of the cue is conditional on the depth of the receiver d, for the Blainville's beaked whales. The equation is transformed to $\hat{D} = \frac{n(1-f)}{a\hat{p}_d\hat{r}_g}$ where, p_d is the detection probability for a receiver at a depth d, and r is conditional to geographic location. In our case, f equals to zero as only regular clicks of Blainville's are considered, due to the nature of the simulation.

The cue rate for click counting can and has been extracted by the deployment of DTAGs on animals (Marques et al., 2009; Kusel et al., 2011), where the true number of clicks produced

by the animal can be counted. The click cue rate r_g represents the average number of clicks per unit time for a population g, and the $\hat{r}\hat{p}$ represents the expected number of clicks per unit of space and time for one individual.

In the click scan cue counting method, the click sequence produced as recorded on the DTAG cannot be used directly as a cue rate in the cue counting equation, due to partial detection of click trains (CS_p) produced by the animal. The expected click scan cue rate for a unit of time and space (which is the $\hat{r}\hat{p}$ term in click cue counting) is the integration of the mean number of CS_d detected as obtained from the simulation over the area sampled. The density then can be estimated by $\hat{D} = \frac{n_{cs}}{a\hat{r}_{cs}}$, where n_{cs} is the number of CS_d detected on the acoustic sensor, where $\hat{r}_{cs}$ is the expected number of CS_d per unit time per unit area and a is the area surveyed. The expected number of click scans detected for a receiver at a given depth is estimated by $\int_0^w CS_d \frac{2x}{x^2} dx$ divided by the time of full dive cycle and corresponds to the $\hat{r}\hat{p}$ of the click counting approach. *W* is the truncation distance and *x* is the horizontal distance from the receiver.

3.3.7 Application to field PAM data

While clicks are detected in click scan packages, the CS_d , the size/length of this CS_d is highly variable.

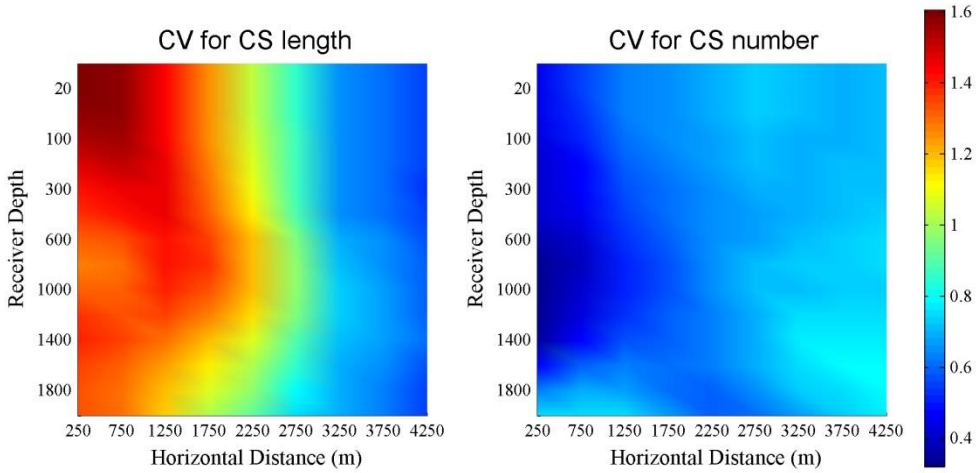

Figure 3.19 Coefficient of Variance (CV) of the length of click scans (CS_d) (Left) and of the number of CS (Right), for receivers at different depths and different horizontal distance from the animal.

The coefficient of variation (CV) of the CS_d's length shows that lengths of CS_d for receivers in shallow waters and in smaller distances are highly variable (Fig. 3.19). The variability decreases with increasing distance where the length of CS_d is more stable towards the more frequent length of CS_d found in all combinations of distances and depths, which is 3 clicks per CS_d. Figure 3.20 shows the proportion of CS_d of less or equal to size 1, 2, 3, 4 and 5 clicks per scan in relation to the total number of CS_d detected for receivers placed at different depth. A CS_d of length one click represents only 0.5% of the total CS_d detected, CS_d of length two, three, four and five clicks represent 18 %, 26.5 %, 6.8 % and 6.5% of the total number of CS_d detected.

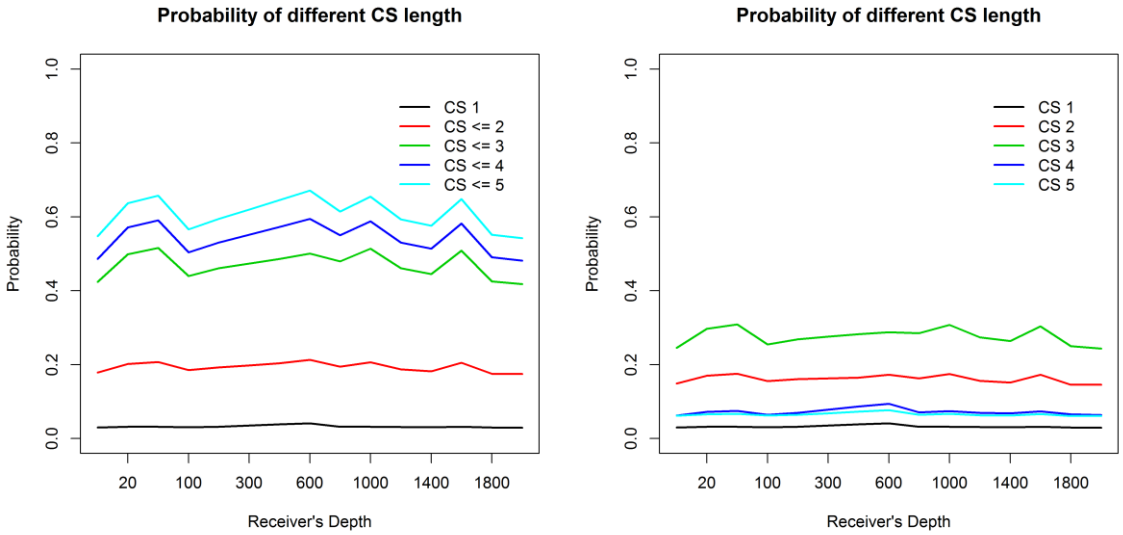

Figure 3.20 Proportion of click scans of length equal or smaller to 1 click up to 5 clicks for receivers at different depths (left) and proportion of click scans of length equal to 1,2,3,4,5 clicks. Black CS of length of 1 click, red line: CS of length 1-2 clicks, green line: CS of length 1-3 clicks, blue line: CS 1-4 clicks. and cyan line: CS 1-5 clicks.

While there is a very small probability of observing one click alone, click scans of length three are the most common of the CS_d (Fig. 3.20 right).

To minimize false detections, it is common to remove clicks that belong to CS_d of length of certain size. Here, we excluded click scans with minimum lengths of 1 click up to 5 clicks and the effect average detection probability for single click counting is shown on Fig. 3.21 for receivers at various depths.

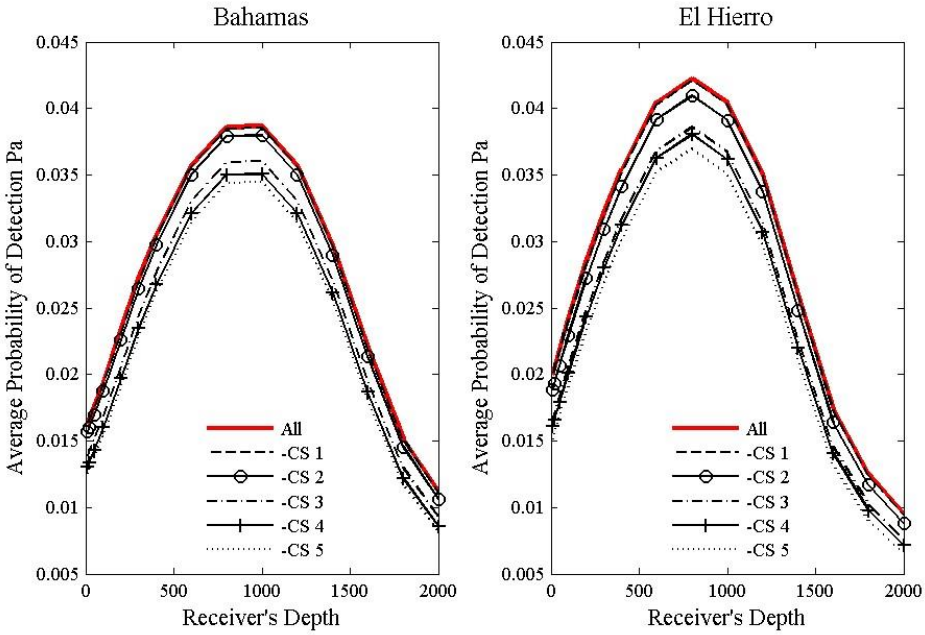

Figure 3.21 Average Detection Probability after the exclusion CS_d of length 1 (dashed line), smaller or equal 2 (circled line), smaller or equal of three (dot dash line), smaller or equal of four (cross mark line) and smaller or equal to five (dotted line) clicks per CS.

For the two different locations, the average detection probability is reduced by a mean of 0.5% - 17% across all depths depending on the length of CS_d excluded. When single clicks are removed, the Pa is reduced by 0.5% (0.3%-0.8%), for CS_d of size ≤2, the reduction is 3% (1.8%-4.9%), for CS of size ≤3, the reduction is 11% (6.7%-17%), for CS of size ≤4, the reduction is 15% (9.2%-23.3%) and for CS of size ≤5, the reduction is 17% (10.8%-27%).

3.4 Discussion

The cue counting approach for density estimation using acoustic data is a well-defined methodology for vocal animals with numerous applications. Acoustic cues have been used for marine mammals, either odontocetes (Kyhn et al., 2011; Marques et al., 2009) or mysticetes (Martin et al., 2013), land mammals (Kidney et al., 2015) and birds (Dawson & Eddord, 2009). While the definition of a cue is study specific (Marques et al., 2013), if the cue derives from a stereotyped behaviour then abundance estimates have the potential of being less biased in relation to cues that are produced under seasonally dependent behaviours such as mating for some species (Watkins et al., 2000). In cetaceans, while the vocalizations of baleen whales can differ seasonally, deep divers such as beaked whales echolocate in a predictable way during their foraging dives. In addition to the cue production bias based on

behavioural variability, other factors can introduce bias to density estimation methods that need to be identified in an effort towards unbiased population size estimations. In this chapter two different acoustic cues were investigated for density estimation of Blainville's beaked whales, those of a single click and a click scan. Factors that influence detectability of acoustic cues of beaked whales due to survey design specifications were also tested, such as receiver depth on detection of clicks and click scans. The data consisted of DTAG deployments from two different geographical locations in El Hierro and the Bahamas in the presence of a simulated network of receivers.

3.4.1 Detection function for regular clicks

The acoustic detection function for a regular click of Blainville's beaked whale is the probability of detection as a function of distance between animal and receiver (Buckland et al., 2001). Here, following standard usage in distance sampling, we present the detection probability as a function of horizontal distance. Detection probability functions have previously been estimated by Zimmer et al., (2008) and Kusel et al., (2011) using a passive sonar equation, Marques et al., (2009) using a localization analysis from passive acoustic tracking of a tagged whale using and array of bottom mounted hydrophones and in Chapter 2, combining passive acoustics from drifters with data from an acoustically tagged whale. Different studies deriving a depth- dependent detection function used different receiver depths, depending on the receiver depth where the data were collected: Zimmer et al., (2005) assumes a theoretical receiver at 100m depth, Kusel et al., (2011) an average of 2000m depth as in Marques et al., (2009) and receivers at 20m and 200-300m depth were assumed in Chapter 2. Here, to identify the number of clicks detected, the sonar equation was used to calculate the received energy signal at the theoretical receivers using data derived from the DTAG to sample the orientation and depth of the tagged whale as sequentially recorded on the tag during a foraging dive. The number of detections received on an acoustic sensor will be determined by the received signal energy in relation to the detection threshold. This study demonstrates the influence of receiver depth on the detectability of Blainville's beaked whale regular clicks and compares detection functions between different sites.

The difference in detectability of the clicks as a function of receiver depth is a result of foraging depth distribution in addition to pitch angle during clicking. The distance between the whale and the receiver is called the slant range and can be calculated as the difference in depth of source and receiver divided by sin(pitch angle). The narrow beam of a beaked

whale's signal loses energy due to transmission loss, as the slant range between whale and receiver increases, and off-axis attenuation, as the angle between the whale's orientation and receiver increases. Receivers closer to the foraging depth of the whales will detect clicks at larger slant ranges, and hence will have a higher detection function. Receivers close to the surface and in waters deeper than 1200 m are prone to fewer detections, as a result of the large slant range between the vocalizing animal and receiver, with the minimum possible slant range to be the difference in depth between the animal and receiver.

Beaked whales start producing regular clicks during their deep foraging dives in waters deeper than 200m (Johnson et al., 2006). Between the two different geographical locations, El Hierro and the Bahamas, beaked whales forage at slightly different depths. The Bahamas population forages in deeper waters (830m) than in El Hierro (700m). The difference in foraging depth distribution could correspond to differences in bathymetry between locations or differences in the three-dimensional distribution of prey, although these factors were not tested in the analysis. The detection function for regular clicks and for a receiver placed at a specific depth is mostly sensitive to the vertical movement of the animal and the foraging depth where the animal vocalizes. Chapter 2 showed that regular clicks from Blainville's beaked whales are less detectable by the shallow receivers (20m), in contrast to deeper receivers at 200-300m depth, which is a result of larger slant ranges, larger off-axis angles between whale and receiver, and increased ambient noise levels due to surface generated noise.

Beaked whales have a narrow beamwidth of sound production of their echolocation click, so the orientation of the animal during clicking influences the optimal depth of the receiver which can be at different depths than the foraging depth, depending on the orientation of the animal. The orientation of the whale is mostly horizontal during the maximum foraging depths (pitch angle around -10° to 10°), yielding larger attenuation of the signal for the increased off-axis angles between receivers that are placed near the surface and near the bottom (~ 2000m depth).

The probability of detection at zero horizontal distance also varies with depth of receiver, with maximum probabilities around 800-1000 m depth for both El Hierro and Bahamas. Barlow et al., (2013) also derived estimates for g(0) representing the availability of beaked whales to acoustic detection. To do so, Barlow et al., (2013) created a model which takes into account the "available for detection" time, which was the foraging time plus a time window of observation divided by the whole full dive cycle period.. A whole dive cycle corresponds

to the foraging time plus silent time during the silent phases of descent and ascent, surfacing and shallower dives. Barlow et al., (2013) assume that a hydrophone is towed behind a boat either for line or point transects; without taking into account the effect of long slant ranges between a towed hydrophone and the foraging depth of beaked whales. Large slant ranges between a surface-located hydrophone and a deep diver and the off-axis attenuation of the signal due to the whale's horizontal orientation during foraging lead to smaller detectability. The g(0) in the study here corresponds to the probability of detection at zero horizontal distance conditional to the animal clicking during a foraging dive (hence vocal), of a receiver at a particular depth. The probability at zero horizontal distance integrates all the possible slant ranges during the foraging dive of the animal and all the possible orientations in relation to the receiver. The multiplication of these two g(0) estimates, from Barlow et al., (2013) and this study would lead to the integrated maximum probability of detection at zero horizontal distance for any point in time for a receiver placed in a specific depth.

3.4.2 Average detection probability for regular clicks

In cue counting methods for estimating the density of animals, the average detection probability is a parameter that describes the probability of detection in the area effectively searched around the acoustic sensor (Buckland et al., 2001). The function describing the average detection probability along different depths of the receiver significantly differs for the two locations. The range of the model prediction for the average detection probability for El Hierro is 0.007 (for receivers at 2000m) - 0.040 (for receivers at 800m), and for the Bahamas is 0.01 (for receivers at 2000m) – 0.038 (for receivers at 800m). Marques et al., (2009) estimated an average detection probability of 0.036 (CV of 0.155) for the bottom-mounted hydrophones of AUTEC, which are mostly at depths of around 2000m.

The receiver depth influences detectability of individual clicks with maximum average detection probability (P_a) around 800 m depth for El Hierro and 1000 m depth for the Bahamas. The depth at which different populations of Blainville's beaked whales spend most of their time during the foraging period will affect the detection function, the detection function at zero horizontal distance g(0), and as a consequence the average probability of detection, P_a. To maximize the number of detections, receivers should be placed in water depths closer to the foraging depth of the animal, where the slant range between the animal and the receivers is smaller than for receivers placed near the surface or in waters much deeper than the maximum depth of the animals. This is especially important for species that

are not abundant or have low probability of acoustic detection due to narrow beam profile such as the beaked whales (Zimmer et al., 2005; Shaffer et al., 2013; Madsen et al., 2013). In cases where the receiver cannot be deployed at the optimal depth, appropriate parameters for the average detection probability at the selected depth should be used or density estimates may be biased. Acoustic platforms that pass through different depth layers, such as autonomous acoustic underwater gliders, must consider the varying depth-dependent detectability of beaked whales clicks during their survey.

3.4.3 Click rates

Click rates for Blainville's beaked whales were calculated based on a methodology in the literature (Kusel et al., 2009, Hildebrand et al.,2015), where the proportion of vocal time of a full dive cycle is divided by the estimated inter-click-interval. The vocal time is defined as the period of clicking excluding periods when the whale was either buzzing or pausing. The mean duration click rate for El Hierro weighted by the full dive-cycle was estimated to 0.41 (CV of 0.38) and for the Bahamas 0.42 (CV of 0.52). No significant difference in click rates was found between El Hierro and the Bahamas. Marques et al., (2009) found a click rate of 0.407 with CV of 9.8% for the Bahamas population. Kusel et al., (2011) found a click rate of 0.649 clicks/s with CV 15.86% using information from the literature regarding mean ICI, number of buzzes and number of pauses. Kusel et al., (2011) found a higher click rate for the Bahamas population in relation to Marques et al., (2009) and in the analysis here, which could be the result of using mean values from the literature for estimating the click rates.

3.4.4 Click scan cue counting

Regarding CS as a cue for the cue counting method, the partial detection of click trains introduces some bias in the definition of the click scan cue. The CS detected is sensitive to vertical movement of the whale as is the use of individual clicks for cue counting. The CS is also sensitive to horizontal movement of the beaked whales due to their narrow beam profile, which consequently causes the click trains produced by the whale to be divided into smaller click scans detected at the receiver. For relatively small distances, the number of click scans detected is 1.8 times greater than the number of click sequences produced by the animal, as recorded on the DTAG, showing the division of the click sequences to more than one click

scan detected. The number of CS detected at the receivers differs as a function of distance and as a function of receiver depth. This feature of CS is a problem for cue counting.

Because of the high variability of CS, a way to use this cue for density estimation would be to use a Bayesian cue counting approach where prior information regarding the distribution of the CS_d is known (Buckland, *personal communication*). The distribution of CS_d can be extracted with a simulation method, as per this study. In addition, other models taking into account probability of an event to occur such as Hidden Markov Models (Buckland, *personal communication*) would assist in the click scan cue counting approach.

This insight into the clustering nature of click detections, with a relationship between the number and the size of click scans as a function of distance and depth, gives an alternative perspective into the single click detections and the single cue counting methods. CS may give information on the number of animals present within detection range, as in group counting (Hildebrand et al., 2015) and coupled with knowledge about the inter click interval of a species may improve the classification of clicks to species and estimation of the number of individuals that are in the acoustic vicinity of the receiver.

In acoustic surveys, false detections play an important role either when the presence of an animal in an area is required to be assessed with some certainty, or in density estimation studies, where the number of detections must be corrected with the false alarm rate (Marques et al., 2013). However, it is often difficult to distinguish between detections that occur due to random noise or other species in the area and detected clicks that appear as single or few clicks in a specific observation period. Therefore, automated or semi-automated detectors under the supervision of an experienced observer usually require and make use of additional information in the detected clicks themselves. Additional information can be time between clicks, inter-click interval (Gerard et al., 2009), and number of clicks in close time proximity such as clusters of detected clicks. Here, we quantified the proportion of click scans of length 1 to 5 clicks, to assess the consequence of removal of click scans of specified lengths to the estimation of the parameters relative to the detection function g(0) and average detection probability P_a. The reduction of the average probability of detection for click counting is only 0.5% if single clicks removed from the analysis due to uncertain classification. If > 5 clicks per click scan is required to increase the certainty in density estimation of the species, then the average detection probability will be reduced by 10% to 27% dependent on receiver depth. Matsumoto et al., (2013), accepted click bouts (sequences of clicks) of size larger than 5 clicks, potentially throwing away 50% of the clicks detected (left cell of Fig. 3.20). Estimates of the probability of detection for receivers close to the foraging depth of the

animal, are relatively insensitive to the removal of click scans < 5 clicks in length. In contrast, the shallower or deeper receivers outside the foraging layers of Blainville's beaked whales, may experience up to a 17% reduction in the average detection probability.

Knowledge about CS and their probability of occurrence can assist in mitigation protocols where the existence of the animal in an area has to be confirmed with a given confidence threshold for a predefined searched area around the receivers. This application occurs in marine mammal monitoring surveys (e.g. mitigation for seismic surveys). False detections due to transient sounds or other species can trigger the detection algorithm, and a process for distinguishing the false detections with small size CS should be in place if possible. Hildebrand et al., (2015) in a density estimation for monitoring different species of beaked whales, eliminated encounters less than 75 s duration or 5 min time-bins with less than 5 clicks detected.

The detection threshold of the acoustic recorder will influence the detection function, average detection probability, and number and length of click scans detected. A low self-noise recorder will be able to detect clicks over longer distances and clicks with varying orientations between animal and receiver, and the number and length of CS will be larger in relation to a lower detection threshold.

The depth-dependent detectability of beaked whales illustrates the importance of applying the correct detection function relative to depth of receiver that future acoustic survey designs should account for. In addition, the different detectability at the two geographical locations indicates the necessity of extracting the detection function at the same place where density estimation studies are conducted, as previously proposed by Marques et al., (2013).

The results presented here are based on some assumptions regarding the sound production and source level of Blainville's beaked whale clicks, propagation modelling and the detection process. Sensitivity analysis for each parameter involved in the simulation would be desirable and could show the effect of variation in those parameters on the detection probability when this is derived from simulation methods such as the one presented here. Specifically, instead of one constant value for Blainville's beaked whales source level, a range of values could be used in the simulation. A more sophisticated propagation model could be used to calculate the range of received levels for the clicks detected on the acoustic receivers, including factors such as variation in ambient noise (Ward et al., 2011). Finally, the first criterion for detection of clicks and click scans is based on one threshold based on a simple energy detector. A theoretical analysis similar to that carried out by Ward et al. (2008) could be useful to account for different ambient noise levels at different depth layers.

3.5 References

Aguilar de Soto, N.A., Madsen, P.T., Tyack, P., Arranz, P., Marrero, J., Fais, A., Revelli, E. & Johnson, M. (2012) No shallow talk: Cryptic strategy in the vocal communication of Blainville's beaked whales. Marine Mammal Science, 28, E75-E92.

Arranz, P., de Soto, N.A., Madsen, P.T., Brito, A., Bordes, F. & Johnson, M.P. (2011) Following a foraging fish-finder: diel habitat use of Blainville's beaked whales revealed by echolocation. Plos One, 6, e28353.

Au, W.W.L.1993. The Sonar of Dolphins. Springer, New York

Barlow, J. (1999) Trackline detection probability for long-diving whales. Marine Mammal Survey and Assessment Methods, 209-221.

Barlow, J., Tyack, P.L., Johnson, M.P., Baird, R.W., Schorr, G.S., Andrews, R.D. & de Soto, N.A. (2013) Trackline and point detection probabilities for acoustic surveys of Cuvier's and Blainville's beaked whales. Journal of the Acoustical Society of America, 134, 2486-2496.

Buckland, S.T., Anderson, D.R., Burnham, K.P., Laake, J.L., D.L., B. & Thomas, L. (2001) Introduction to distance sampling: Estimating abundance of biological populations. Oxdord University Press, Oxford.

Caillat, M., Thomas, L. & Gillespie, D. (2013) The effects of acoustic misclassification on cetacean species abundance estimation. Journal of the Acoustical Society of America, 134, 2469-2476.

Gerard, O., Carthel, C. & Coraluppi, S. (2009) Classification of odontocete buzz clicks using a multi-hypothesis tracker. Oceans 2009 - Europe, Vols 1 and 2, 247-253.

Gillespie, D., Dunn, C., Gordon, J., Claridge, D., Embling, C. & Boyd, I. (2009) Field recordings of Gervais' beaked whales *Mesoplodon europaeus* from the Bahamas. Journal of the Acoustical Society of America, 125, 3428-3433.

Hildebrand, J.A., Baumann-Pickering, S., Frasier, K.E., Trickey, J.S., Merkens, K.P., Wiggins, S.M., McDonald, M.A., Garrison, L.P., Harris, D., Marques, T.A. & Thomas, L. (2015) Passive acoustic monitoring of beaked whale densities in the Gulf of Mexico. Scientific Reports, 5, 16343.

Johnson, M., Madsen, P.T., Zimmer, W.M.X., de Soto, N.A. & Tyack, P.L. (2004) Beaked whales echolocate on prey. Proceedings of the Royal Society B-Biological Sciences, 271, S383-S386.

Johnson, M., Madsen, P.T., Zimmer, W.M.X., de Soto, N.A. & Tyack, P.L. (2006) Foraging Blainville's beaked whales (*Mesoplodon densirostris*) produce distinct click types matched to different phases of echolocation. Journal of Experimental Biology, 209, 5038-5050.

Johnson, M.P. & Tyack, P.L. (2003) A digital acoustic recording tag for measuring the response of wild marine mammals to sound. IEEE Journal of Oceanic Engineering, 28, 3-12.

Kimura, S., Akamatsu, T., Li, S.H., Dong, S.Y., Dong, L.J., Wang, K.X., Wang, D. & Arai, N. (2010) Density estimation of Yangtze finless porpoises using passive acoustic sensors and automated click train detection. Journal of the Acoustical Society of America, 128, 1435-1445.

Kimura, S., Akamatsu, T., Wang, D., Li, S.H., Wang, K.X. & Yoda, K. (2013) Variation in the production rate of biosonar signals in freshwater porpoises. Journal of the Acoustical Society of America, 133, 3128-3134.

Kusel, E.T., Mellinger, D.K., Thomas, L., Marques, T.A., Moretti, D. & Ward, J. (2011) Cetacean population density estimation from single fixed sensors using passive acoustics. Journal of the Acoustical Society of America, 129, 3610-3622.

Madsen, P.T., de Soto, N.A., Arranz, P. & Johnson, M. (2013) Echolocation in Blainville's beaked whales (*Mesoplodon densirostris*). Journal of Comparative Physiology a-Neuroethology Sensory Neural and Behavioral Physiology, 199, 451-469.

Marques, T.A., Thomas, L., Martin, S.W., Mellinger, D.K., Ward, J.A., Moretti, D.J., Harris, D. & Tyack, P.L. (2013) Estimating animal population density using passive acoustics. Biological Reviews, 88, 287-309.

Marques, T.A., Thomas, L., Ward, J., DiMarzio, N. & Tyack, P.L. (2009) Estimating cetacean population density using fixed passive acoustic sensors: An example with Blainville's beaked whales. Journal of the Acoustical Society of America, 125, 1982-1994.

Martin, S.W., Marques, T.A., Thomas, L., Morrissey, R.P., Jarvis, S., DiMarzio, N., Moretti, D. & Mellinger, D.K. (2013) Estimating minke whale (*Balaenoptera acutorostrata*) boing sound density using passive acoustic sensors. Marine Mammal Science, 29, 142-158.

Matsumoto, H., Jones, C., Klinck, H., Mellinger, D.K., Dziak, R.P. & Meinig, C. (2013) Tracking beaked whales with a passive acoustic profiler float. Journal of the Acoustical Society of America, 133, 731-740.

Miller, P.J.O., Johnson, M.P. & Tyack, P.L. (2004) Sperm whale behaviour indicates the use of echolocation click buzzes 'creaks' in prey capture. Proceedings of the Royal Society B-Biological Sciences, 271, 2239-2247.

Moretti, D., Marques, T.A., Thomas, L., DiMarzio, N., Dilley, A., Morrissey, R., McCarthy, E., Ward, J. & Jarvis, S. (2010) A dive counting density estimation method for Blainville's beaked whale (*Mesoplodon densirostris*) using a bottom-mounted hydrophone field as applied to a Mid-Frequency Active (MFA) sonar operation. Applied Acoustics, 71, 1036-1042.

Rayment, W., Dawson, S. & Slooten, L. (2009) Trialling an automated passive acoustic detector (T-POD) with Hector's dolphins (*Cephalorhynchus hectori*). Journal of the Marine Biological Association of the United Kingdom, 89, 1015-1022.

Roch, M.A., Klinck, H., Baumann-Pickering, S., Mellinger, D.K., Qui, S., Soldevilla, M.S. & Hildebrand, J.A. (2011) Classification of echolocation clicks from odontocetes in the Southern California Bight. Journal of the Acoustical Society of America, 129, 467-475.

Shaffer, J.W., Moretti, D., Jarvis, S., Tyack, P. & Johnson, M. (2013) Effective beam pattern of the Blainville's beaked whale (*Mesoplodon densirostris*) and implications for passive acoustic monitoring. Journal of the Acoustical Society of America, 133, 1770-1784.

Tyack, P.L., Johnson, M., Soto, N.A., Sturlese, A. & Madsen, P.T. (2006) Extreme diving of beaked whales. Journal of Experimental Biology, 209, 4238-4253.

Ward, J.M., R. Moretti, D., DiMarzio N., Jarvis S., Johnson, M. Tyack, P. & White C. (2008) Passive acoustic detection and localization of *Mesoplodon densirostris* (Blainville's beaked whale) vocalizations using distributed bottom-mounted hydrophones in conjunction with a Digital Tag (DTag) recording. Can. Acoust., 36, 16.

Watkins, W.A., Daher, M.A., Reppucci, G.M., George, J.E., Martin, D.L., DiMarzio, N.A. & Gannon, D.P. (2000) Seasonality and distribution of whale calls in the North Pacific. Oceanography, 13, 62-67.

Watwood, S.L., Miller, P.J.O., Johnson, M., Madsen, P.T. & Tyack, P.L. (2006) Deep-diving foraging behaviour of sperm whales (*Physeter macrocephalus*). Journal of Animal Ecology, 75, 814-825.

Wood, S.N., 2006. Generalized Additive Models: An Introduction with R. Chapman & Hall/CRC, Boca Raton

Yack, T.M., Barlow, J., Roch, M.A., Klinck, H., Martin, S., Mellinger, D.K. & Gillespie, D. (2010) Comparison of beaked whale detection algorithms. Applied Acoustics, 71, 1043-1049.

Zimmer, M.X. (2011) Passive Acoustic Monitoring of Cetaceans. Cambridge University Press, New York.

Zimmer, W.M.X., Johnson, M.P., Madsen, P.T. & Tyack, P.L. (2005) Echolocation clicks of free-ranging Cuvier's beaked whales (*Ziphius cavirostris*). Journal of the Acoustical Society of America, 117, 3919-3927.

APPENDIX I

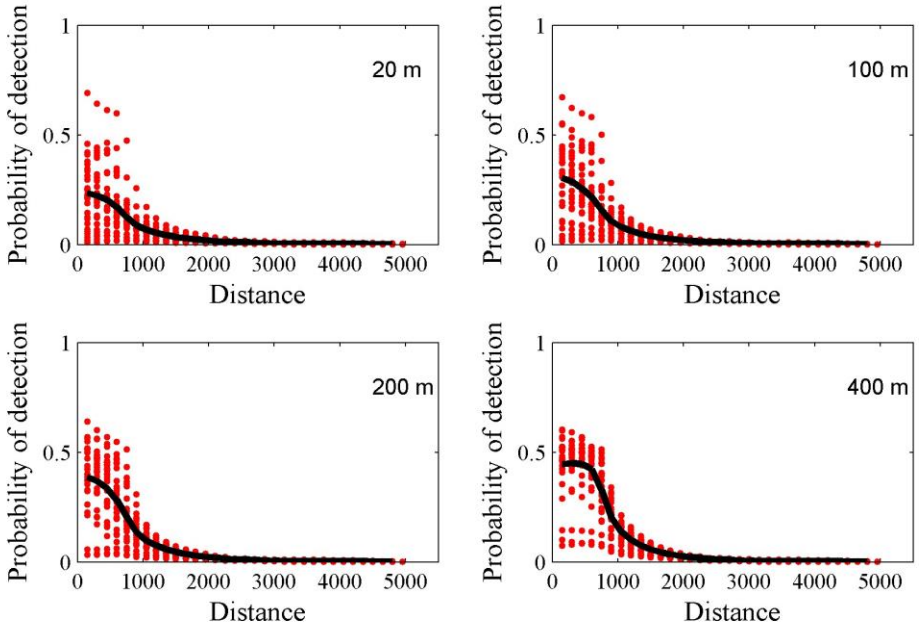

Figure A 3 Detection probability of a single Blainville's beaked whale echolocation click for receivers at 20, 100, 200 and 400 m for the Bahamas dataset. The red dots are observed ratio of clicks detected in relation to the ones produced by different individuals. The black line is the mean detection probability from all the individuals, n= 29 dives.

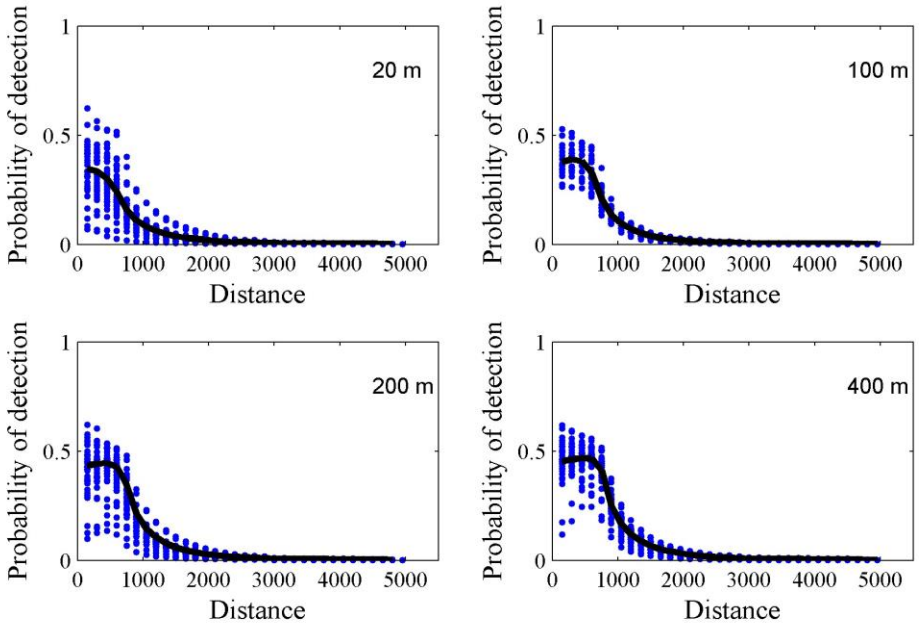

Figure A 4 Detection probability of a single Blainville's beaked whale echolocation click for receivers at 20, 100, 200 and 400 m for the El Hierro dataset. The blue dots are observed ratio of clicks detected in relation to the ones produced by different individuals. The black line is the mean detection probability from all the individuals, n= 42 dives.

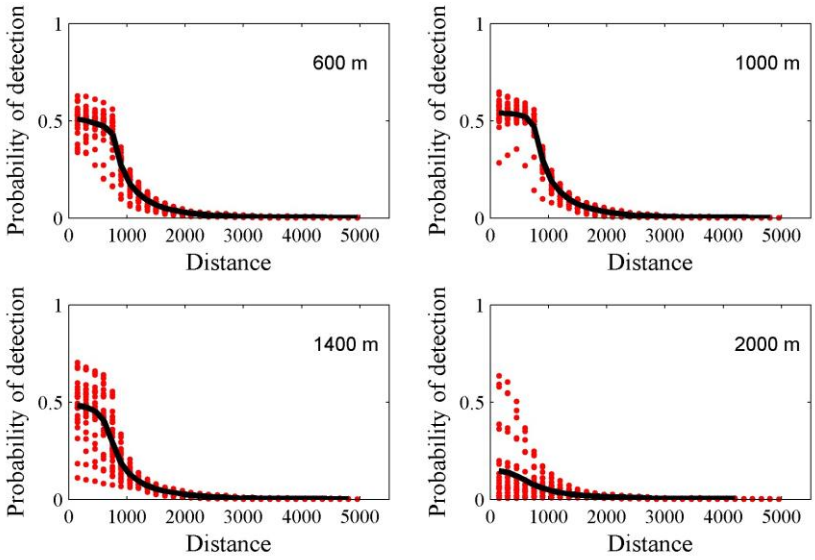

Figure A 5 Detection probability of a single Blainville's beaked whale echolocation click for receivers at 600, 1000, 1400 and 2000 m depth for the Bahamas dataset. The red dots are observed ratio of clicks detected in relation to the ones produced by different individuals. The black line is the mean detection probability from all the individuals, n= 29 dives.

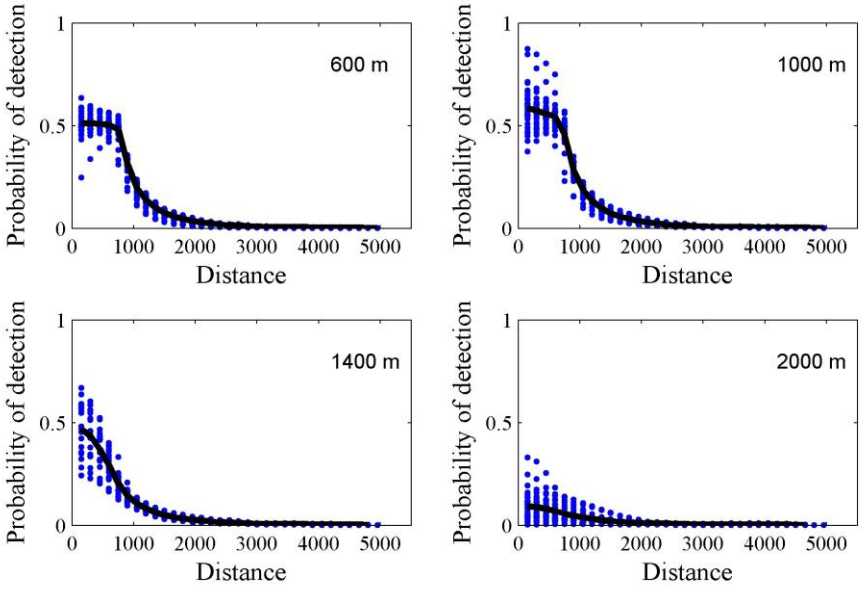

Figure A 6 Detection probability of a single Blainville's beaked whale echolocation click for receivers at 600, 1000, 1400 and 2000 m depth for the El Hierro dataset. The red dots are observed ratio of clicks detected in relation to the ones produced by different individuals. The black line is the mean detection probability from all the individuals, n= 42 dives.

Chapter 4

The underwater autonomous glider as a platform for acoustic survey for marine mammals: A simulation study to evaluate the suitability of gliders for PAM

4.1 Introduction

Autonomous underwater vehicles (AUVs) are increasingly used for sampling ocean data because of their low cost and persistent sampling of most of the water column. AUVs, such as Slocum gliders (http://www.teledynemarine.com/slocum-glider), are vehicles that can remain in the water for a long period of time while a dedicated pilot can control the route through web-based piloting tools and satellite telemetry links. This chapter explores the use of gliders for passive acoustic monitoring of marine mammals by detecting their vocalizations. They are a quiet platform (Suberg et al., 2014) favouring their use for passive acoustic monitoring. Underwater gliders sample oceanographic features in higher resolution than satellite sensing and unlike satellites, they can sample across various depths, which makes it possible to sample oceanographic variables at depths where many marine mammals spend most of their time. Gliders offer the opportunity to simultaneously sample environmental data with animal occurrence data, which may enable the identification of environmental parameters that can be used in habitat modelling for predicting a species' distribution (Aarts et al., 2008). The detailed information on environmental processes that occur under the sea surface, derived from the AUV's sensors, can also provide insight into the processes driving the presence of marine mammal prey, which is one of the main forces driving their foraging behaviour (Croll et al., 1998)

The efficiency of gliders as a platform for passive acoustic surveys still remains to be evaluated and there are some challenges regarding their use as an acoustic platform for marine mammal surveys. Some aspects of gliders, such as their slow speeds, can introduce biases in already well-established methodologies for abundance estimation using acoustic data.

Gliders with a horizontal speed of ~ 0.25m/s (Rudnick, 2016) are likely to be moving slower than marine mammals, which often swim at 1-2m/s (Sato et al., 2007). This slow relative speed may violate a main assumption of models generally used to analyse line transect data:

"objects are measured in their initial location, prior to any movement" (Buckland et al., 2001) – an assumption which limits the recounting of individuals. Movement of animals during the detections will introduce bias in density estimation, as the animal has moved from the initial location where it was detected and can enter or leave the survey area, resulting in double counting of individuals. The movement of animals results in an increased number of detections in comparison to an unbiased survey. Due to the nature of detection function - animals are detected closer to the observer/or detection system - then the detection function will be steeper resulting to an underestimation of the probability of detection and hence overestimation of the density (Thomas L. personal communication). The slow movement of the glider with respect to the animals may make double counting of individuals more likely if multiple calls are detected from the same individual, which would violate the assumption of independent detections, which is required for distance sampling (Buckland et al., 2001).

Another assumption of distance sampling is that "distances are measured accurately" (Buckland et al., 2001), which is a second assumption relating to the detection function estimation method. A glider with one acoustic sensor usually cannot estimate distance from the animal and this is why a separate survey in the study area where the glider will operate would be useful for estimating the detection function; an example of such a method is demonstrated in chapter 2.

The estimation of the detection function and its derived products allows for estimating the effective area over which an acoustic sensor is searching for animals - the sensor here being on a glider. For example, the effective radius, which is the distance at which as many animals were detected as were missed, is an important product of the detection function that makes it possible to estimate absolute density of animals. If this kind of product is required, the detection function should be estimated for the population of the area where the survey is going to be conducted but often must be estimated separate from the survey design (Marques et al., 2013). Similarly, acoustic cue rates should also be derived from the same population that will be surveyed with any acoustic platform (Marques et al., 2013), and this also applies to gliders.

The survey design for abundance estimation calls for tracks to be randomly placed and be representative of the environmental space. Randomization of tracks assists with minimizing the sampling bias for unknown environmental features and possible existing environmental gradients. Prior to a survey, a careful investigation of the environment and identification of any areas with special characteristics can assist in ensuring that the survey passes through all the possible values of the specific variable. For example, depth of the seafloor is an important

variable for many deep diving cetaceans (Canadas et al., 2005). If, for any reason, tracks sample more of a specific feature of the environment than is representative, then density estimates can be biased. The degree to which this bias affects density depends on the difference in density across the features. If the glider conducts a dedicated marine mammal survey, then the survey can be designed to meet the assumption of random placement of tracks. However, PAM on gliders often involves the addition of an acoustic sensor to collect data on surveys that are primarily motivated by oceanography; in this case, the survey is not designed for marine mammal abundance estimation and may fail the random placement assumption. If data derive from primarily oceanographic surveys, and there is reason to believe they do not obtain representative samples of marine mammal habitat, then observations can be treated as deriving from an opportunistic platform. Though, increased spatial and temporal effort would make data from PAM opportunistic gliders valuable for answering animal density questions, in a spatial distance sampling framework.

Previous density estimation studies that use acoustic methods for marine mammals have used hydrophone arrays towed from a boat, drifters or fixed bottom-mounted hydrophones. In previous studies, these platforms place each sensor at one predefined depth that is constant for the whole survey duration. In contrast, gliders must move up and down in the water column, and are capable of sampling at various depths, from the sea surface down to 1000m or more. This provides opportunities to sample the variety of layers where each species vocalises. Deep diving beaked whales tend to vocalise at depths ranging from 600m – 1000m where the animals echolocate to forage and navigate. Acoustic sampling at those depths can be difficult or impossible for moving platforms other than gliders or profiling drifters that sample different water depths. It is similarly difficult and expensive to achieve using vertical arrays of sensors fixed at those depths. By sampling the vocal depths of deep divers, such as beaked whales, gliders may have a larger number of detections, while at the same time being able to cover larger areas than acoustic receivers at fixed depths.

Underwater gliders combine a unique feature for surveying marine mammals, which is the vertical movement in combination with the large spatial coverage while moving with slow speed relative to the speed of the animal. As mentioned earlier, application of line-transect methodology is not straightforward due to the slow speed of the platform relative to the speed of the animal. Gliders operate with an approximate horizontal speed of $0.25ms^{-1}$ which is 4 to 8 times slower than the typical 1-2m s^{-1} speed of the animals. Some bias in density estimation could arise by violation of some basic assumptions due to (1) non-independent detections of the same individual, which leads to correlation of the detections, (2) ability of the relatively

highly mobile animals to enter and leave the survey area which will increase the number of detected animals. Also, it is not always possible to derive distance from the vocalizing animal from one acoustic receiver.

The slow speed of gliders with respect to the animals creates problems with applying line transect methods, but this characteristic gives the opportunity to apply methodologies for density estimation similar to ones that are applicable to fixed sensors with the advantage of increased spatial coverage. For example, click cue-counting methodology has been applied to clicks of echolocating animals (Küsel et al., 2011; Marques et al., 2009) using single receivers fixed at one location. Requirements for applying cue-counting methods are: knowledge about the cue rate of the animal of interest, a measure of detectability over space. total size of surveyed area that can be sampled with fixed acoustic receivers will be determined by the number of fixed receivers deployed in the area and the species-specific effective radius. For echolocating animals, the acoustic detectability varies from about few hundred meters for small cetaceans such as porpoises (Gillespie et al., 2005; Macaulay et al., 2017) to a couple of tens of kilometres for sperm whales. An underwater glider moving through the water can be thought of as a slow "fixed" receiver where the clicks of the animals that are in detection range are recorded, but the varying depth of the glider requires knowledge about the detectability of the species for each surveyed depth. Cue-counting approaches for glider surveys equipped with a single acoustic sensor require a measure of detectability as a function of space and as a function of time. A measure of detectability such as the detection function and the average detection probability can be used from a separate study, and the same can be adopted for click rates, which are required for converting number of clicks detected to number of individuals.

Chapter 2 and Chapter 3 describe how the detectability of acoustic cues can differ depending upon the depths where each species vocalizes and the depths at which the receiver is placed. As a glider moves underwater, passing through different depth layers, changes in the depth-dependent detectability need to be considered in the analysis. It follows that acoustic detections derived from gliders require a correction for detectability for each glider depth where each cue occurs. This can be achieved with the use of a continuous function of cue detectability as a function of depth. A function for click detectability as a function of depth has been presented in chapter 3 for two different beaked whale populations: that of El Hierro and that of the Bahamas, derived from DTAG datasets. Similar approaches for considering variation in detectability, based on a continuous variable, have been previously applied in other density estimation methods such as Spatially Explicit Capture Recapture models

(SECR), where detectability of jaguars varies as a function of hour within a day, resulting from the activity of the species itself (Borchers et al., 2014; Distiller, 2016 PhD-thesis). For line transects, detectability can change as a function of number of animals in a group.

Gliders use less power than propeller driven autonomous underwater vehicles, but acoustic glider deployments will encounter limitations in power availability over their long deployments, due to the restricted space and weight that the glider can afford for batteries. The glider mission duration is dependent on the maximum dive depth, piloting speed, the number of sensors used and their sampling frequency (Dumont Estelle (SAMS) personal communication). The maximum depth of the glider is preferred to be as deep as possible, because the longer the dive, the less energy is used by the pumps and the satellite communication on the surface (Dumont Estelle (SAMS) communication). For waters deeper than 1000m, a glider survey (using Slocum gliders) can last up to 7 months in comparison to a glider survey above the shelf (less than 200m) that conducts shallower dives, where operation may be limited to 2-3 months. The maximum glider dive depth is one of the main factors influencing energy consumption per unit time, with others being speed (faster is less efficient), vehicle hydrodynamics/drag, and the combination of ocean stratification with differences in compressibility between the glider hull and seawater (Rudnick et al., 2004). The difference in total operation time between deep water gliders and shallow water gliders relates to the consumption of power at the vertical turning points for each dive, meaning shallow water operations use more energy due to the larger rate of dives per unit of time. A 7 month deployment in deep waters, with a horizontal speed of 0.25m/s will give a survey track-line length of 4536 km in comparison to a maximum of 1950 km in shallow waters – for Slocum gliders. The piloting speed is determined by the weather conditions and current speeds. For example, in calm waters the horizontal speed is approximately 0.25 m/s and in high seas or around eddies where the water current is high, the speed can be increased to ~0.3 m/s. Eventually, the speed of the glider is a combination of piloting speed and the effect of the current (positive or negative). Finally, the duty cycle with which the sensors sample environmental parameters on board usually is determined after the deployment of the glider by remote sensing and following optimization planning adapted to the weather conditions and study requirements.

For a PAM glider, the duty cycle of the acoustic recorder, i.e. the fraction of time that a recorder is on, will be dictated by a variety of factors including the duration of the glider deployment and the amount of power available. The amount of power available to the acoustic recorder is affected by whether it will power itself from the glider's internal power

supply (whether acoustic recorder will power itself from the glider's internal power supply) or will be powered autonomously. The sampling frequency depends upon the frequency range of the calls of the species of interest. The on-time and off-time for each duty cycle, a predefined recording time interval of for example 10 seconds every minute with the recorder active and 50 seconds inactive (Barlow et al., 2014) and daily sampling regime may be set by the calling behaviour of the species of interest. For deep diving beaked whales, there is often a silent interval between deep foraging dives of 60-90 minutes (Tyack et al., 2006); when they are clicking during their foraging dive, the gaps between clicking are approximately every 4 seconds for some species (Chapter 3). Last but not least, the sampling may be determined by the assumptions of the methodology that is planned to undertake the analysis, where thinning of data to satisfy the independence assumption of detections can be used as a guide for the acoustic sampling strategy.

When continuous sampling is not possible due to power consumption and storage space in the case of long deployments, a strategy of limiting acoustic recording to periods with high probability of detection must be considered. Either a time-based strategy and/or a depth threshold trigger for the recorder can be used to make the best use of available power and storage space. For animals with diurnal patterns of calling, a time-of-day strategy may be called for. Depending on the species of interest, a depth threshold to activate the recorder can be introduced as in Klinck et al., (2012) and Suberg et al., (2014). Information on the amount of detections expected for each glider depth, regarding each species of interest, would assist decisions for allocating recorder time to different depths in glider surveys.

Finally, the number of acoustic elements deployed on a glider will determine the method used for estimating density from acoustic data. Most gliders deployed so far have one hydrophone (Baumgartner et al., 2008; Baumgartner et al., 2013; Klinck et al., 2012; Suberg et al., 2014). This limits the ability to estimate range to the calling animal, which can be problematic for methods of point-sampling and cue-counting (Marques et al., 2013). There are however autonomous vehicles that can tow a hydrophone array which can beamform the acoustic data to estimate the bearing to the sound source (Miller and Tyack 1998). If the sound source continues calling and moves slowly enough with respect to the glider, then changes in the bearing as the glider moves (target motion analysis) can additionally be used to estimate range to the calling animal. However, gliders move slowly compared to the typical speed of 1-2 m/s for [calling] cetaceans (Sato et al., 2007), reducing applicability, and a towed array increases drag and reduces mission duration and spatial coverage. An option to measure distance would be to use two or more gliders that operate in the same area and close enough

in order to detect and localize the same individual. A fleet of gliders each equipped with a single hydrophone can be used to localize animals that are in detection range from the fleet (Baumgartner et al., 2008). There will however be some uncertainty in a glider's position underwater, which propagates uncertainty to the estimation of the detection function and average detection of probability. Notably the difficulties arising from this uncertainty of glider position are only relevant sub-surface, as the gliders have GPS for surface locations. In addition to the uncertainty distance estimation from a fleet of gliders, there are naturally higher survey costs. The advantage of using multiple gliders for estimating distance and applying distance sampling methodologies is beyond the scope of this thesis.

In this chapter, the use of underwater gliders equipped for passive acoustic monitoring will be tested as a platform for density estimation of Blainville's beaked whales in a simulated survey. The different components of the simulation are as follows:

1) the horizontal distribution of the whales
2) the vertical movement of the whales
3) the sound production of the whales and
4) the glider movement.

The simulation uses the DTAG dataset from El Hierro and the Bahamas, which was used in Chapter 3, to simulate species vocal production and animal movement. A glider survey, equipped with one acoustic sensor, in a predefined area will be tested in the following scenarios:

1. single animals are fixed at a specific horizontal point – allowing only vertical movement and change in orientation based on DTAG data,
2. animals are clustered in groups and fixed at a specific horizontal point - allowing vertical movement and change in orientation based on DTAG data.

For these two scenarios, abundance estimation will use cue-counting based upon two different cues: single clicks and click scans (Chapter 3).

Objectives of this chapter are:

1) to provide a methodology for estimating abundance of vocal animals from acoustic data derived from a slow moving underwater vehicle,

2) to evaluate the method with a simulation study in different survey scenarios and animal densities

3) to estimate density from two acoustic cues for Blainville's beaked whales

4) to evaluate biases derived from the use of the average detection probability.

4.2 Material and Methods

4.2.1 Proposed Method for estimating density from underwater gliders

The detectability of beaked whale clicks varies as a function of depth of the clicking whales and of the receiver on the glider as it changes depth. Here I develop a new mathematical equation for analysing acoustic data deriving from acoustic platforms that pass through different acoustic layers where there is a change in detectability. These platforms include underwater autonomous gliders, but the method is applicable for any slow acoustic receiver that changes depth.

The equation for estimating density from acoustic cues from fixed sensors is

$$\hat{D} = \frac{n(1-\hat{f})}{TK\hat{p}a\hat{r}} \tag{4.1}$$

where *K* is the number of receivers, *T* is the period that each sensor is monitoring, $a = \pi w^2$ is the area (projected on the surface) surveyed around one receiver where w is the truncation distance, $\hat{r}$ is the estimated cue rate. The average probability of detection $\hat{p} = \int_0^w g(x)h(x)dx$, where w is the truncation distance, $g(x)$ is the detection function (probability of detection as a function of distance, *x*) and $h(x)$ is the probability density of cues for an area of radius *x* around the receiver. The probability density of cues, *h(x)*, is not dependent on depth as it is assumed to be uniform around a receiver regardless of depth. The depth distribution of the animal, and hence that of the cues, is taken in to account within the detection function, which is the average detection probability of a cue (randomly selected from a dive). Here we assume the glider has a single acoustic receiver that instead of being fixed at a location for the whole survey duration T is moving, so the number of acoustic sensors K equals 1.

Now, the $\hat{p} = \int_0^w g(x)h(x)dx$ changes as a function of depth as shown in chapter 3, and the equation becomes

$$\hat{p}_z = \int_0^w g(x,z)h(x)dx \tag{4.2}$$

for a receiver at a specific depth z, where $g_z(x,z)$ is the detection function conditional to the receiver's depth.

For a platform that changes depth throughout the survey duration T, the track averaged probability of detection $\hat{p}_{TR}$ becomes

$$\overline{p}_{TR} = \frac{1}{T}\int_1^T \hat{p}_z(z(t))dt \tag{4.3}$$

For each point in time during the glider survey, the probability of detection is the integration of the duration t that the glider remains on a specific depth. So the equation for estimating density for underwater autonomous gliders using cue-counting becomes

$$\hat{D} = \frac{n(1-f)}{T\hat{r}a\hat{p}_{TR}} \tag{4.4}$$

Click scan cue counting for gliders

The methodology for the integrated average detection probability of an acoustic sensor passing through different depths (Eq. 4.3) is also adapted for the click scan (CS) cue counting method. For CS cue counting the equation for density estimation is as follows:

$$\hat{D} = \frac{n}{Ta\hat{p}_{TR_{CS}}} \tag{4.5}$$

Note that in Eq. 4.5 there is not a CS rate as found in click cue counting. This is because the average detection probability of the CS is derived from the observed CS as detected on a single receiver in Chapter 3. The track-averaged detection probability $\hat{p}_{TR_{CS}}$ for CS cue counting represents the integrated average detection probability of expected CS, per unit of time (1 sec) and of area.

4.2.2 Evaluation of underwater gliders as a platform for density estimation for marine mammals

To evaluate the sea glider as a platform for abundance estimation of beaked whales, I simulated glider surveys in the open ocean and presence of animals in a static [x,y] location,

the animals are free to move only vertically in the water column and I use orientation and sound production data from Dtagged Blainville's beaked whales for relative changes in heading of the animals and production of regular echolocation clicks. DTAG data from two Blainville's beaked whale populations, El Hierro and the Bahamas, are examined separately due to the different detectability of the two populations (Chapter 3). The simulation gives the opportunity to evaluate different abundance estimation methods using acoustic data and to identify the potential biases with the use of the glider as a platform in comparison to other platforms such as a boat or drifters.

The different components of the simulation are as follows: 1) the horizontal distribution of the whales 2) the vertical movement of the whales 3) the sound production of the whales and 4) the glider movement. The glider survey is performed for different animal densities, where simulated animals are placed in the study area based on one of two horizontal distribution scenarios (uniform or "hot spot"). The simulated whale's diving behaviour and orientation are derived from DTAG deployments. Finally, a simulated acoustic glider samples the study area following a pre-determined path and records the time and the received level for each click for any whale that is in close proximity to the receiver. For all the iterations for each simulation, the abundance of whales is estimated based on a cue-counting method, and different ways of using the data are investigated.

Whale movement data, number of clicks produced, and their relative time as recorded on DTAGs, are used to inform the diving profiles for the simulated animals. Twelve DTAG deployments were used from the El Hierro population, and six DTAG deployments from the Bahamas population. For a description of the DTAG data see Chapter 3 – Material and Methods.

4.2.3 Horizontal density

A theoretical area of 64 km by 70 km was chosen for the simulation. These dimensions are similar to AUTEC to enable comparisons of different methodologies. Three levels of animal density, i) low ii) medium iii) high density are considered for the study area. The medium density was chosen from estimations based in the AUTEC area (Marques et al., 2009), and the low and high density a magnitude lower and larger than that. Two different scenarios are considered regarding spatial distribution for any given animal density: uniform and clustered. In the latter a non-uniform distribution of the animals in space is simulated, based on a spatial model.

4.2.4 Vertical movement

The simulation treats whales as horizontally stationary in initial positions defined by the horizontal density (uniform or hot-spot) and moving only vertically in time based on the DTAG data (as described in Chapter 3). The x and y position of each animal simulated in the survey is considered stable, as the dead-reckoning track that would be used from the DTAG data is not precise due to inability of the sensor to record the speed of the animal. So, here for simplicity, the animal is simulated as changing depth and body orientation based on real DTAG deployments, but ignoring changes in x and y position. Only full dive cycles (foraging dive and the consecutive shallow dives) are used for the simulation and each full dive cycle, which is assigned randomly to each animal, and sampled with replacement for the duration of the survey. The depth of the animal is taken from the DTAG data as recorded on the depth sensor, and the orientation of the whale at any point of the glider survey is calculated by the 3-d orientation matrix as described in Chapter 3. To randomize the process further, a random starting point along the dive profile is chosen which may occur at any time during the 'true' initial dive profile, in addition a random angle as a starting point for the orientation of the whale is assigned at the beginning of the dive which initialize all later orientations to be taken based on the random start.

4.2.5 Sound Production

To model the sound produced by the whales while foraging, a beam pattern is used to model the echolocation clicks of the Blainville's beaked whales, based on a flat circular piston oscillating in an infinite baffle (Au et al., 1978). The click beam pattern is described in Chapter 3. The number of clicks produced, and the depth when each regular echolocating click is produced, is extracted from the DTAG data.

4.2.6 Glider movement and detection of clicks

An acoustic survey was simulated using a single acoustic sensor attached to an underwater autonomous glider. The platform moves with a horizontal glider speed of 0.25 m/s with a 6 km horizontal displacement between two sequential surfacing points of the glider. For a 6 km horizontal displacement, the glider requires 6.6 hours to complete a dive to a maximum depth

of 1000m. The underwater distance covered by the glider with the current horizontal speed is 6.32 km and 3D underwater speed of 0.26 m/s with slope of 18° between the surface and the glider's orientation.

With the glider's horizontal speed of 0.25m/s and a 1000 m maximum glider dive depth, the platform requires a 30.27 days to sample the survey area of 4480 km^2 and horizontal track line of 654 km and an underwater track line of 689 km (Figure 4.1).

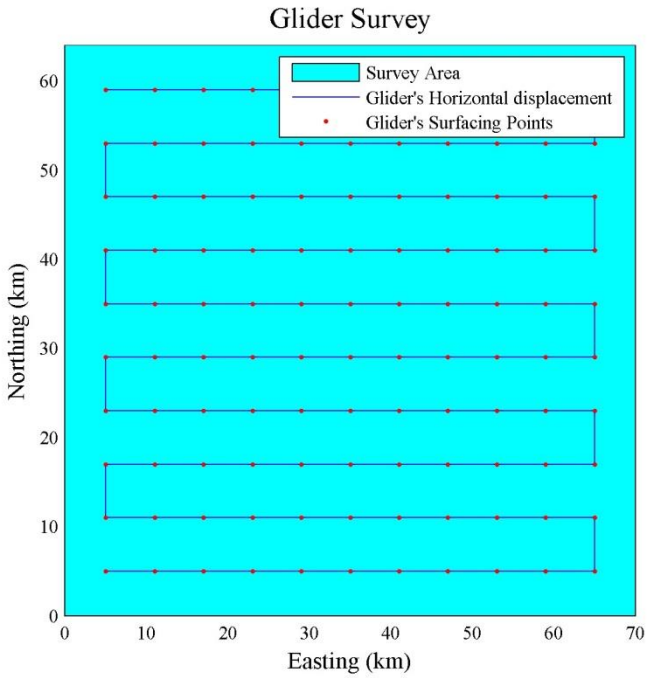

Figure 4.1 Glider survey design in a 64 km by 70 km area. The glider horizontal displacement is indicated by the blue line and the glider surfacing position by the red points. The duration of the simulated survey is 30.27 days where the simulated glider performed 109 dives to a maximum depth of 1000m.

As the glider moves through the survey area, the distance D_i between each animal producing the i^{th} click and the acoustic receiver is calculated. For the period that the glider is in close proximity to an animal, which here is defined as 5 km (due to truncation distance being 4.8 km), the received level for each click produced during that period is estimated as shown below

$$RL_i = SL + B(\theta) - 20\log_{10} D_i - aD_i \qquad (4.6)$$

where, SL_i is the source level of the Blainville's beaked whale, D_i is the direct distance (slant range) between the animal and the receiver for the time i of the regular click event, a is the absorption coefficient, θ is the angle between the animal orientation and the glider, and B(θ) is the decrease in level with respect to SL of the modeled beampattern at angle θ. The absorption coefficient a was calculated based on standard absorption curves (Kinsler & Frey,

pp. 159-160), and was estimated at 0.0075 using Ainslie et al., (2014), athough neglecting the bandwidth of echolocation clicks can introduce bias in propagation loss and eventually the estimation of population from single hydrophones (Ainslee et al., 2014). For all the clicks produced by each whale while the acoustic platform is in the acoustic field, defined as within 5 km around the receiver, the time of clicking received is recorded along with the RL_i.

4.2.7 Scenarios for animal placement

Abundance estimation is calculated based on a cue-counting method (Buckland et al., 2001). Four separate cue-counting methods are considered: i) an overall cue-counting method based on the total number of clicks detected throughout the glider survey, ii) a cue-counting approach stratified by glider dive iii) a cue-counting approach stratified by glider depth bin throughout the glider survey and iv) a cue-counting approach stratified by glider dive and depth bin.

Five different scenarios are considered regarding animal placement: **I. Random placement of individual animals -** each fixed at a single horizontal point, **II. Random placement of groups of animals -** with each individual in a group randomly placed in a circle of 10 meters around a randomly allocated point– i.e. individuals are clustered, **III. Hot spots of single animals –** Spatially dependent distribution of single animals, **IV. Hot spot of groups of animals –** Spatially dependent distribution of groups of animals. For all the scenarios listed above, the process is repeated for the two different DTAG and detection datasets, El Hierro and Bahamas.

I. Random placement of individuals fixed on a single point. The location of each animal is drawn from a uniform spatial distribution, with equal probability for each animal to be located anywhere in the study area. For the three different densities a resampling process from the DTAG deployments is allocated to define the diving and clicking behaviour of each animal participating in each simulation. Marques et al., (2009) estimated densities of Blainville's beaked whales at AUTEC of 22.5-25.3 / 1000 km^2, which is close to our medium density of 100/4480 km^2 = 22.3/1000 km^2. The low and high density is chosen to be a magnitude order lower than the estimate from Marques et al., (2009) and one magnitude higher for the high density.

II. Random placement of groups of animals. In this simulation, animals are found in groups. The location of each group is drawn from a spatially uniform distribution. The size of

each group is derived by a Poisson process with λ_E and λ_B parameters to represent the mean number of animals in a group found in El Hierro and the Bahamas respectively. The mean number of animals per group for El Hierro is at 4.1 animals (Reis et al., submitted) and for the Bahamas is 4 animals (Moretti et al., 2006). There are too few deployments of different individuals tagged simultaneously from the same group to use these to simulate group swimming behaviour. However, the limited data available demonstrates that beaked whales tend to synchronize their deep foraging dives (Dunn et al., 2017). In order to simulate this with available data, the tag record of one individual is used to represent the different animals in a group in order to produce similar swimming behaviour during the group foraging dive, though with different starting orientations for each individual in the simulated group. The individual representing each group is selected randomly from the DTAG pool deployments for each site. The synchronized diving and surfacing behaviour is simulated by repeating the same randomly allocated dive profile across the different number of individuals that participate in the group, randomising the initial orientation. The horizontal position of each individual participating in the group is allocated randomly within a radius of 10 meters about the central point of the group position.

III. Hot spot of single animals. A simulated density map was created by combining two multivariate density distributions for a range of longitudes and latitudes (Fig. 4.2). The locations of animals were simulated using a Poisson spatial process. A random Poisson number with λ parameter to be the probability of occurrence as defined by the density map is assigned to each cell of the study area. Then scaling the total number of animals derived from the Poisson spatial process dependent on the density scenario Low, Medium and High, which corresponds to 10, 100 and 1000 animals respectively for the entire study area.

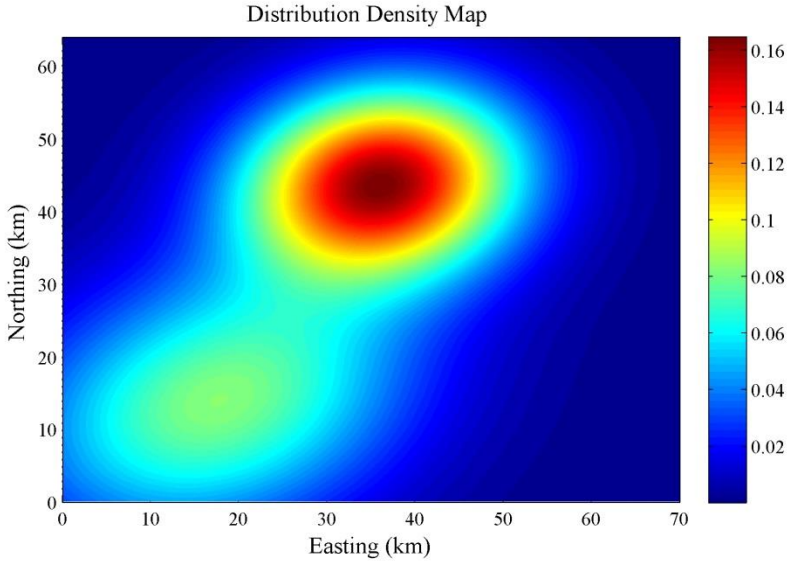

Figure 4.2 Distribution density map for simulations based on a simulated hotspot. Colours represent the probability of occurrence of an animal, single or group of animals depending on the scenario, red is high probability and blue is low.

IV. Hot spot of groups of animals. The location of each group of animals is defined by a spatially dependent distribution, and each group size is defined by a Poisson distribution as in **III** for individuals.

4.2.8 Abundance estimation

Different analytical methods of click cue-counting were applied to the results of the different animal placement scenarios: 1) Pooled Click cue counting, taking in to account the total number of clicks detected throughout the total duration of the survey; 2) Pooled Click scan cue counting, taking in to account the total number of CS detected throughout the survey; 3) Click cue- counting, stratified by glider dive and 4) a spatial model for density estimation, taking in to account the number of cues detected in each cell grid of the survey area. Each method is described below:

1. Acoustic detections derived from an acoustic underwater glider can be treated as similar to those derived from a fixed acoustic platform, where the number of acoustic cues detected can be treated as a point-sampling transect with cue-counting. In this case abundance estimates derived from a glider survey would take into account the total number of clicks detected over the whole area of the survey. Abundance estimates $\hat{D}$ derived with click cue-counting would follow the formula shown in 4.7:

$$\hat{D}_d = \frac{n}{Ta\hat{r}_g \frac{1}{T}\hat{p}_{TR}} \qquad (4.7)$$

where n is the number of clicks detected during the survey, T is the total duration of the glider survey, and $\hat{p}_z$ is the estimated average detection probability for a particular depth z. For a particular depth z, $\hat{p}$ equals $\int_0^w g(x|z)h(x)dx$, a is the area surveyed πw^2 and $\hat{r}_g$ is the estimated click rate for the population surveyed in the geographic area g. A GAM model was used to estimate the detection probability as a function of receiver depth (Chapter 3). Fig. 4.3, from Chapter 3, shows the average detection probability for receivers at different depths. For the simulation here, an integration of the probabilities up to 1000 meters depth was chosen to estimate the average tracked probability $\overline{p}_{TR}$.

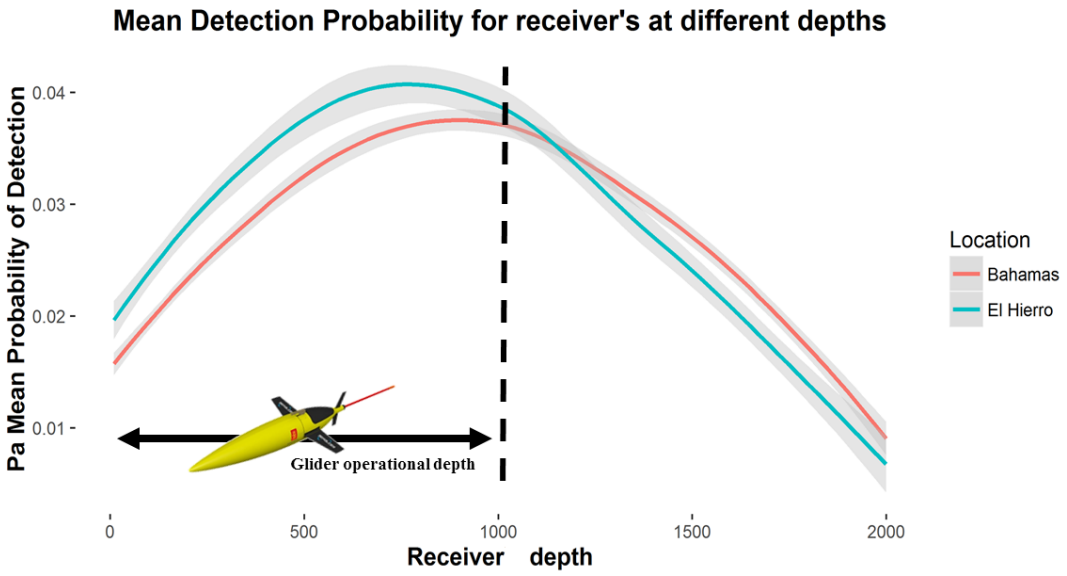

Figure 4.3 Average detection probability of individual regular Blainville's beaked whales click for receivers ranging from 10 meters to 2000m depth. As the glider surveys waters down to a depth of 1000m, an integration up to a maximum limit of 1000m depth was derived for the averaged tracked survey detection probability.

2. As a glider is a moving platform, this gives the opportunity to estimate density per glider dive, which defines a specific spatial area. As a glider dive is a well-defined feature of the survey design, then density can be estimated separately per dive. The density estimate per dive can be estimated using the following equation:

$$\hat{D}_d = \frac{n_d}{T_d k a \hat{r} \hat{p}_{TR}} \quad (4.8)$$

where n_d is the number of clicks detected during each dive d, T_d is the time spent on each glider dive, k is the number of dives, $\hat{p}_{TR}$ is the tracked averaged detection probability for the depths that the glider passed through, a is the area surveyed = πw^2 and $\hat{r}$ is the estimated click rate for the population surveyed.

3. The density of cues can be seen as well as the total densities of stratified estimates of density at different depth bins. As the acoustic platform, the glider, is passing through different depth layers, the density of animals can be stratified by a depth bin.

$$\hat{D} = \sum_S \frac{n_S}{T_v k a \hat{r} \frac{1}{T} \int_0^{z_{max}} \hat{P}(t \mid z) dz} \quad (4.9)$$

The ways of estimating the abundance in the 2nd and 3rd approaches described above stratified the data by dive or depth layer using the same data used in the first approach. Stratification of the data can be informative when there is heterogeneity in the area surveyed or in the detectability of the cues based on environmental or surveying parameters such as depth and other features that may influence detectability. A cue-counting stratification based on glider dive can give spatial information of more abundant areas if there is heterogeneity in the distribution of the animals as in the case with the Hot-Spot simulation. In addition, a cue-counting stratification based on depth bins gives the opportunity of identifying depths where the animals are more detectable. That information assists in decisions for when to record when recording space or available power is limited.

4. Abundance estimation based on a spatial model

As a glider is a moving platform, this gives the opportunity to estimate density and bundance based on a spatial model. Abundance estimation based on modelling approaches has been used for line transects and other survey designs (Buckland et al., 2001; Buckland et al., 2004; Miller et al., 2013). Here a Generalized Additive Model is used to model the number of clicks detected as a function of longitude and latitude, with a smooth parameter. Then for each cell for which the number of clicks is predicted from the model, the relative amount of glider time spent in the grid cell is used to account for effort.

4.3 Results

Glider surveys were simulated in twelve different scenarios for the Bahamas and similarly for the El Hierro dataset. Abundance estimates and variances were calculated for all the combinations of different density (Low, Medium, High), distribution (Uniform and Hot-Spot) and for solitary and grouped animals. The results presented here assume horizontally stationary animals, naturally an unrealistic assumption which will lead to smaller variances than would be found in practice. However, this assumption does allow evaluation of the general efficacy of the cue counting method without animal movement, as commonly assumed under line- and point-transect distance sampling (Harris, personal communication).

For all the scenarios, the glider survey duration, T, is 30.2 days and the glider performed 109 dives to a maximum depth, $z_{max,}$ of 1000m. The glider operates with a horizontal speed of 0.25 ms^{-1} and covers a horizontal distance of 6km per dive, with a total distance of 719.4 km for an area of 4480 km^2.

The animals that participated in the simulation were derived from DTAG deployments and used for depth distribution and relative click production times during the survey. The spatial location of the whales is chosen randomly based on a uniform distribution or based on a density map for the Hot-Spot scenario; for the whole period of the simulation, the whale position [x,y] remains constant while the depth is changing based on the DTAG depth recordings. For each whale participating in the survey, a distance between the animal and glider is calculated and then for positions of the glider and the whale that were smaller than 5000 km were examined further for clicking production by the whale. In cases where the whale was clicking during the period that the glider was in close proximity, as defined before, the orientation between the whale and glider was calculated based on the orientation matrix of the whale and the DTAG data and the source level was estimated for each click. Clicks which had a received level above 100 dB were noted as detected by the glider. Figure 4.4 shows the distances of detected clicks between the whale and the glider, the depth of the whales for those clicks, and the depth of glider during the detections.

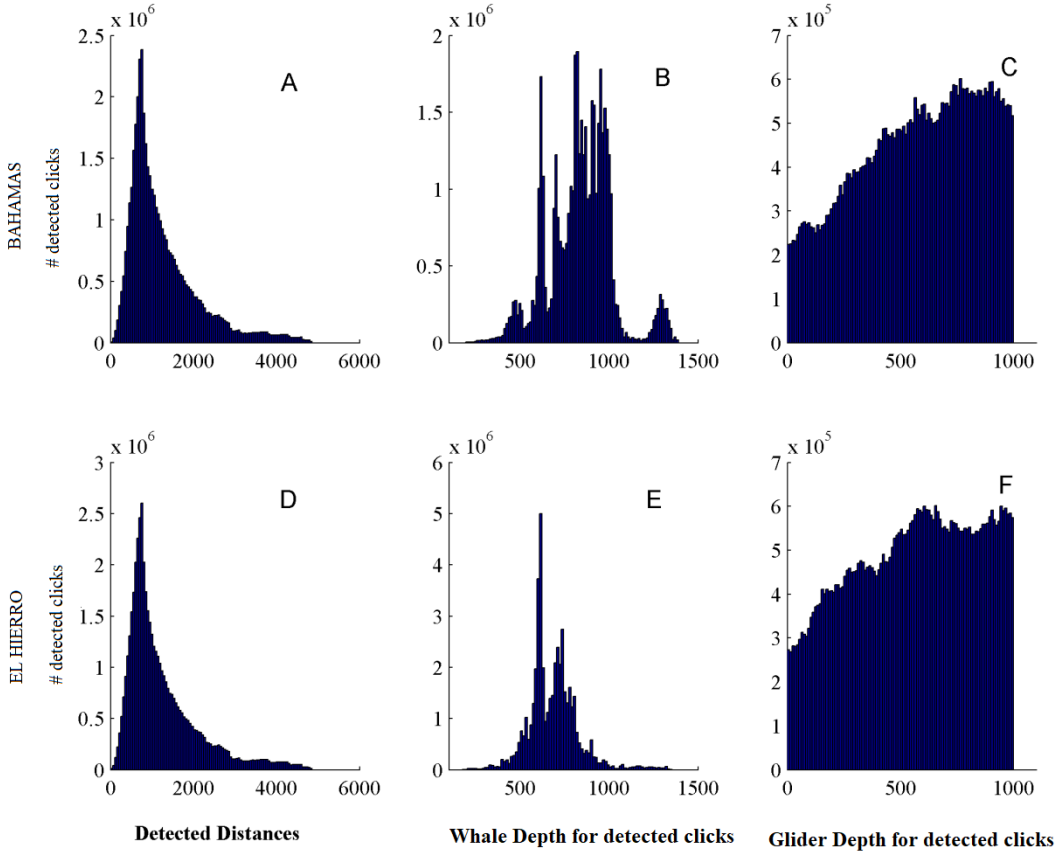

Figure 4.4 Results from 100 simulated animals drawn from a uniform distribution, showing the number of detected clicks for the two locations, Bahamas and El Hierro. A) and D) are the detected distances between the glider and the animals for the Bahamas and El Hierro respectively, B) and E) are the depth of the whale for their detected clicks and C and F is the depth of the glider for the detected clicks.

The maximum detected distance in the simulation is about 5 km (Fig. 4.4 A and D), the glider detected clicks for all of the receiver depths in the surveys with more clicks detected at glider depths > 500 m (Fig. 4.4 C and F). The depths where whales produce clicks that were detected ranged from 200m to 1400m, with the El Hierro dataset having a peak at 600m whereas the Bahamas had two peaks: one at 600m and the other ranging from 800m to 1000m. Many more clicks were detected at relatively short distances (less than 2km). The pattern in Fig. 4.4 A and 4.4 D results from the interaction between the shape of the detection function and the larger availability of animals (and hence cues) as the distance from the receiver increases.

4.4 Density estimation

1. Estimating the density of animals based on the single cue-counting method taking account the whole glider survey.

To estimate the density of animals for each glider survey based on click cue counting, all the clicks detected (clicks with received level larger than the detection threshold DT) during the whole survey, n_d are recorded. During the survey the glider performed 109 full dives of maximum depth 1000m for which the glider spent equal time at each depth, so the tracked survey average probability $\hat{p}_{TR}$ for El Hierro is 0.0292 (std. dev. 0.0005) and for the Bahamas is 0.0269 (std. dev. 0.0006).

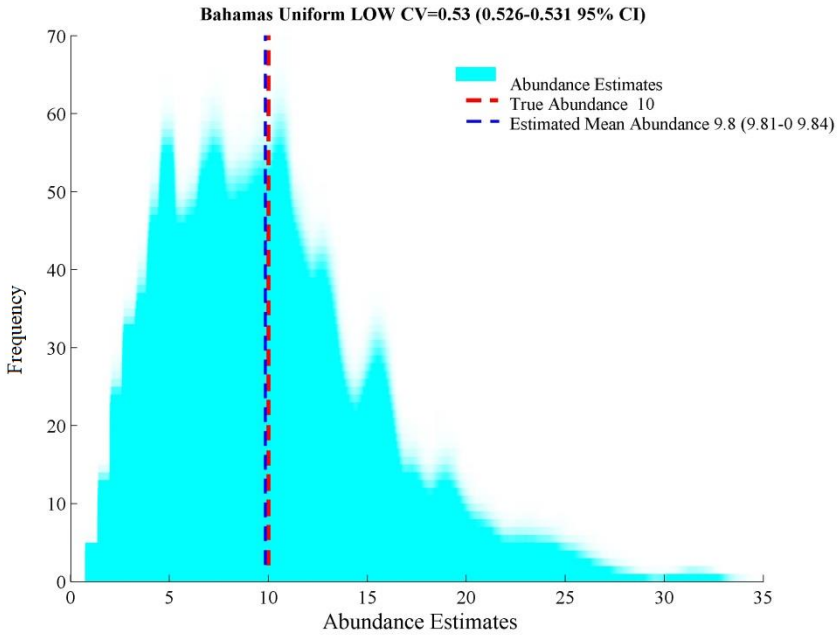

Figure 4.5 Histogram of abundance estimates for 1000 simulations for the Bahamas dataset based on a Hot-Spot distribution scenario and Low density. The dashed red line corresponds to the true animal abundance – the number of animals used in each simulation, which for the low density scenario corresponds to 10 animals. The blue dashed line corresponds to the mean estimated abundance taking in to account all the simulations.

The parameter $\hat{p}_{TR}$ in equation 1 corresponds to the integration of the average detection probability $P_{a.}$, where z is the depth at which the acoustic platform is at time t. The $\overline{p}_{TR}$ for the El Hierro dataset for depths 0 to Z_{max} that is the maximum glider depth was calculated at 0.03 and click rate of 0.4142. The parameters P_a and click rate were estimated in an independent simulation (Chapter 3).

Figure 4.5 shows the simulation results for the Bahamas population based on a hot-spot distribution scenario and low density. The results for animals distributed as single individuals for the different density scenarios in uniform and hot-sport environment for the Bahamas population can be seen in Fig. 4.6 and Fig. 4.7.

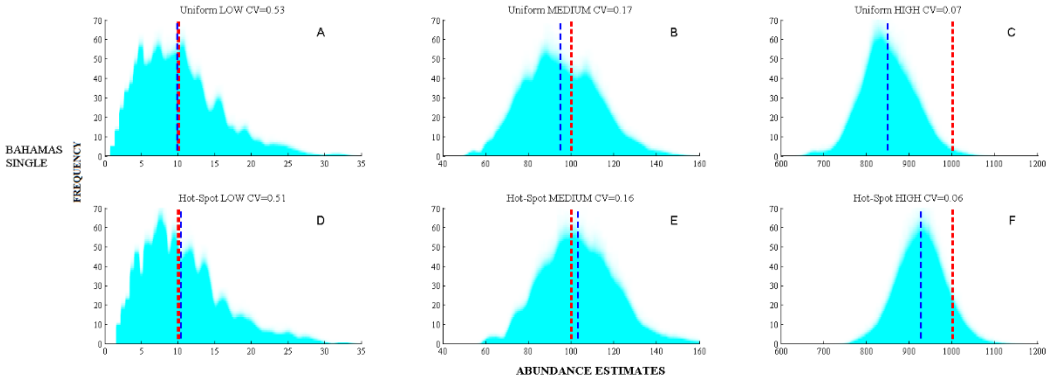

Figure 4.6 Abundance estimates for Blainville's beaked whales distributed as single individuals derived from 1000 simulated glider surveys. The red dashed line is the true abundance and the blue dashed line is the mean value of the simulations for each scenario. Uniformly distributed animals for A) Low B) Medium and C) High density animals and Hot-Spot distributed animals for D) Low E) Medium and F) High density animals.

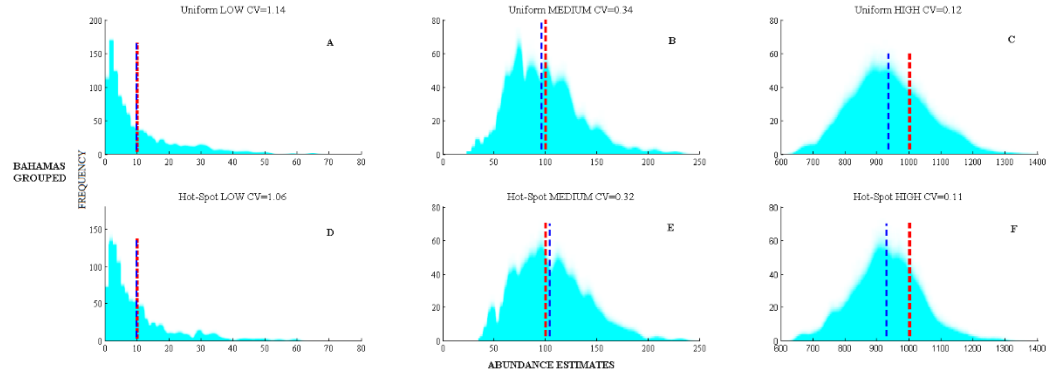

Figure 4.7 Histograms of abundance estimates for Blainville's beaked whales aggregated in groups for the area of Bahamas (red dashed line is the true abundance and the blue dashed line is the mean value of the simulations (1000 repetitions) for each scenario). Uniformly distributed animals during A) Low density B) Medium density C) High density. Hot-Spot distributed animals during D) Low density E) Medium density and F) High density.

Taking into account the total number of clicks detected during each survey in a cue-counting approach, during the uniform scenario, the mean abundance estimate was 10.1 (CV 0.47) and 99.2 (CV 0.15) animals for Low and Medium density for the El Hierro population Fig. 4.8 A-C. During the Hot-Spot scenario where animals were aggregated in an area with higher density the mean abundance estimate was 9.96 (CV 0.42) and 102.6 (CV 0.14) animals for Low and Medium density Fig. 4.8 D, E.

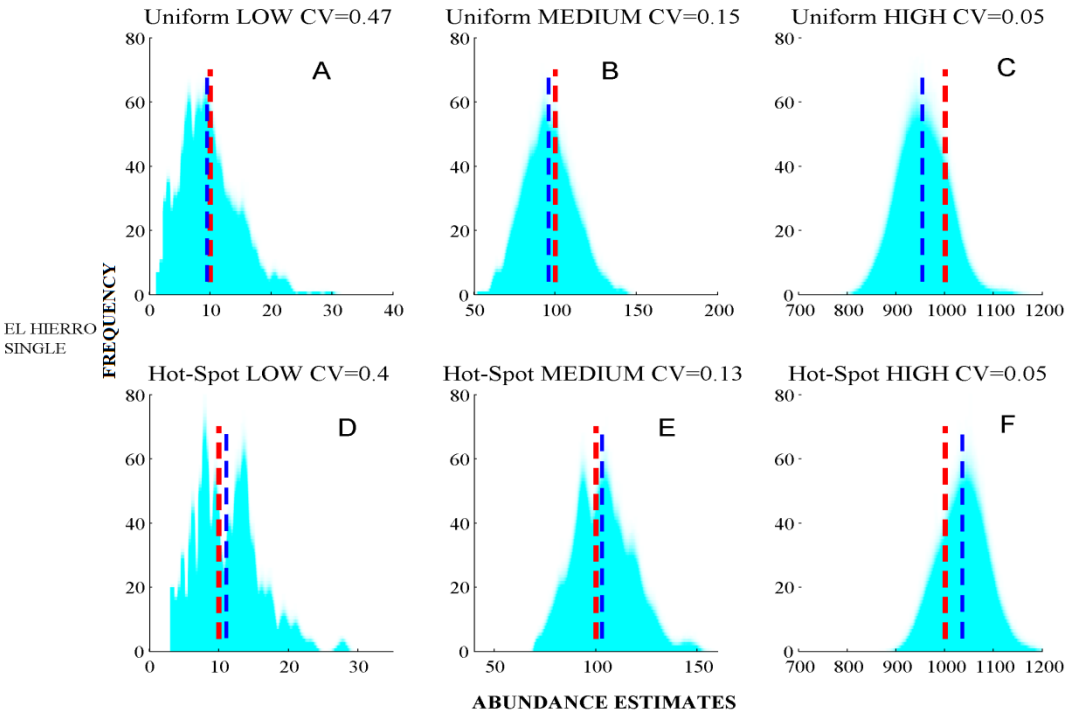

Figure 4.8 Histogram for abundance estimates for Blainville's beaked whales aggregated in groups for the area of El Hierro (Canary Islands) (red dashed line is the true abundance and the blue dashed line is the mean value of the simulations (1000 repetitions) for each scenario). Uniformly distributed animals during A) Low density B) Medium density C) High density. Hot-Spot distributed animals during D) Low density E) Medium density and F) High density.

For the scenarios where the animals were aggregated in groups and were uniformly distributed the mean abundance estimates were 9.9 (CV 0.94) and 101.8 (CV 0.30) animals for Low and Medium density for the El Hierro population (Fig. 4.9 A-C). For the grouped animals appearing in the Hot-Spot distribution, the mean abundance estimates were 10.1 (CV 0.87) and 101.8 (CV 0.27) animals for Low and Medium density (Fig. 4.9 D,E).

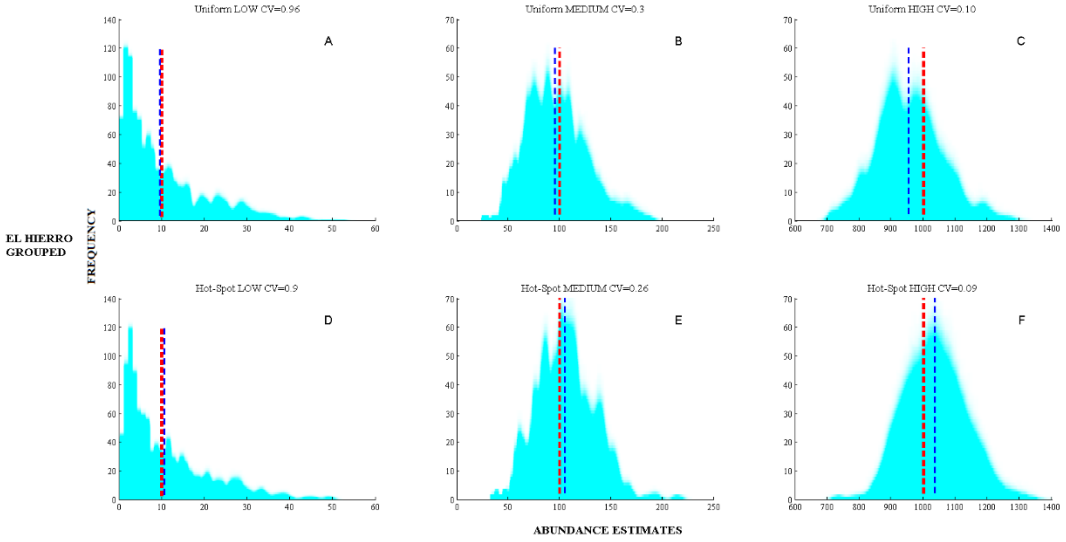

Figure 4.9 Histogram for abundance estimates for Blainville's beaked whales from the El Hierro dataset, aggregated in groups. The red dashed line is the true abundance and the blue dashed line is the mean value of the simulations (1000 repetitions) for each scenario. A) Uniformly distributed animals during Low density B) as A but Medium density C) Hot-Spot distributed animals – Low density D) as C but Medium Density.

Table 4 Abundance estimates and associated coefficient of variation (CV %) for all the 12 different scenarios for Bahamas and El Hierro dataset.

Area	Grouping Type	Distribution	Density	Abundance Mean (95% CI)	CV %
EL HIERRO	SINGLE	Uniform	L	**9.48** (9.47-9.50)	**47.37** (47.19-47.55)
			M	**95.8** (95.68-95.91)	**15.39** (15.27-15.52)
			H	**953.67** (952.61-954.78)	**5.17** (5.06-5.29)
		Hot-Spot	L	**11.03** (11.02-11.05)	**40.05** (39.9-40.2)
			M	**103.03** (102.91-103.15)	**13.48** (13.35-13.6)
			H	**1035.7** (1034.4-1036.9)	**4.51** (4.4-4.63)
	GROUPED	Uniform	L	**9.65** (9.63-9.66)	**95.78** (95.44 -96.16)
			M	**95.63** (95.5 -95.75)	**29.72** (29.56 -29.87)
			H	**954.07** (052.8 -955.32)	**10.26** (10.12 - 10.40)
		Hot-Spot	L	**10.54** (10.53-10.56)	**90.21** (89.0 -90.56)
			M	**105.45** (105.33-105.56)	**25.82** (25.68 -25.
			H	**1034.1** (1032.9-10354)	**9.02** (8.9 -9.14)
BAHAMAS	SINGLE	Uniform	L	**9.8** (9.91-9.84)	**52.9** (52.6-53.1)
			M	**94.9** (94.74-95)	**17.48** (17.33-17.63)
			H	**848.9** (847.65-850.11)	**6.81** (6.67-6.94)
		Hot-Spot	L	**10.37** (10.35-10.28)	**51.22** (50.97-51.46)
			M	**103.07** (102.93 -103.23)	**15.99 (15.85-16.16)**
			H	**926.25** (924.96 -927.51)	**5.78** (5.66 - 5.92)
	GROUPED	Uniform	L	**9.9** (9.88-9.926)	**110.55** (11.05-111.06)
			M	**99.8** (99.67-96.97)	**33. 77** (33.58-33.96)
			H	**933.74** (103.77-104.07)	**12.21**(12.07-12.37)
		Hot-Spot	L	**9.81** (9.79-9.83)	**106.12** (105.57-106.63)
			M	**103.93** (013.77 - 104.07)	**32.22** (32.04-32.41)
			H	**927.63** (926.34-928.95)	**10.84** (10.68-10.911)

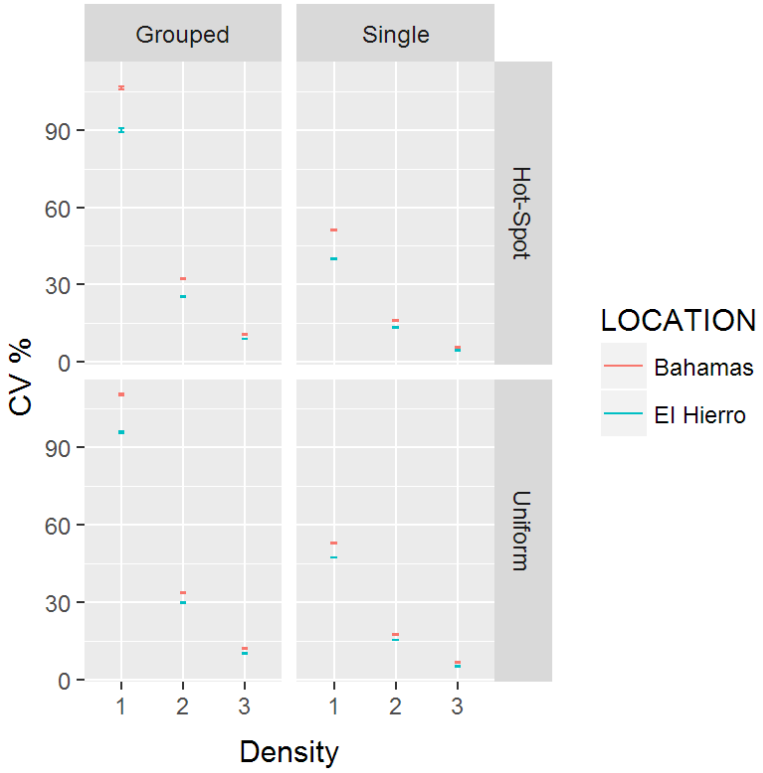

Figure 4.10 Coefficient of variation (CV %) of the abundance estimates based on different scenarios for El Hierro and the Bahamas based simulations. Blue points correspond to El Hierro based simulations and red to the Bahamas based simulations, for animals appeared as grouped and as single individuals distributed in a uniform and hot-spot type of distribution. The CV estimates derive from the standard deviation of all the abundance estimates divided with the mean abundance estimates from all the 1000 simulations for each scenario.

The coefficient of variation (CV) represents the dispersion of an estimated parameter and is calculated as the ratio of the standard deviation to the mean of an estimate, which here is the abundance estimate from each simulation. Fig. 4.10 shows the CV resulting from the simulations for the different scenarios shown here, Grouped vs Single and Hot-Spot vs Uniform for Low (1) and Medium (2) and High (3) density. Estimates derived from animals found in groups and distributed based on a patchy Hot-Spot environment (Fig. 4.10) are similar to the estimates for uniform distribution, this probably is a result of the size of the hotspot that is quite big in relation to the glider tracks separation. The CV for the simulations based on aggregation of animals is higher than the CV for single individuals, something that was expected as detections from grouped of animals are going to be clustered more than when animals are uniformly distributed.

The CV of the abundance estimates decreases as the density of animals increases, something that is expected as in low-density areas as the opportunity to miss an animal is higher than when density is high, hence there is higher variability of on the estimates.

Figure 4.11 shows how many surveys are required to achieve the same variability that would derive from cumulative surveys. The blue line corresponds to resamples of the simulation of the surveys from two up the maximum number of simulations for this particular scenario. Is shown that up to 200 surveys required to have the same variability in the estimates that the ones that derived from the results presented here.

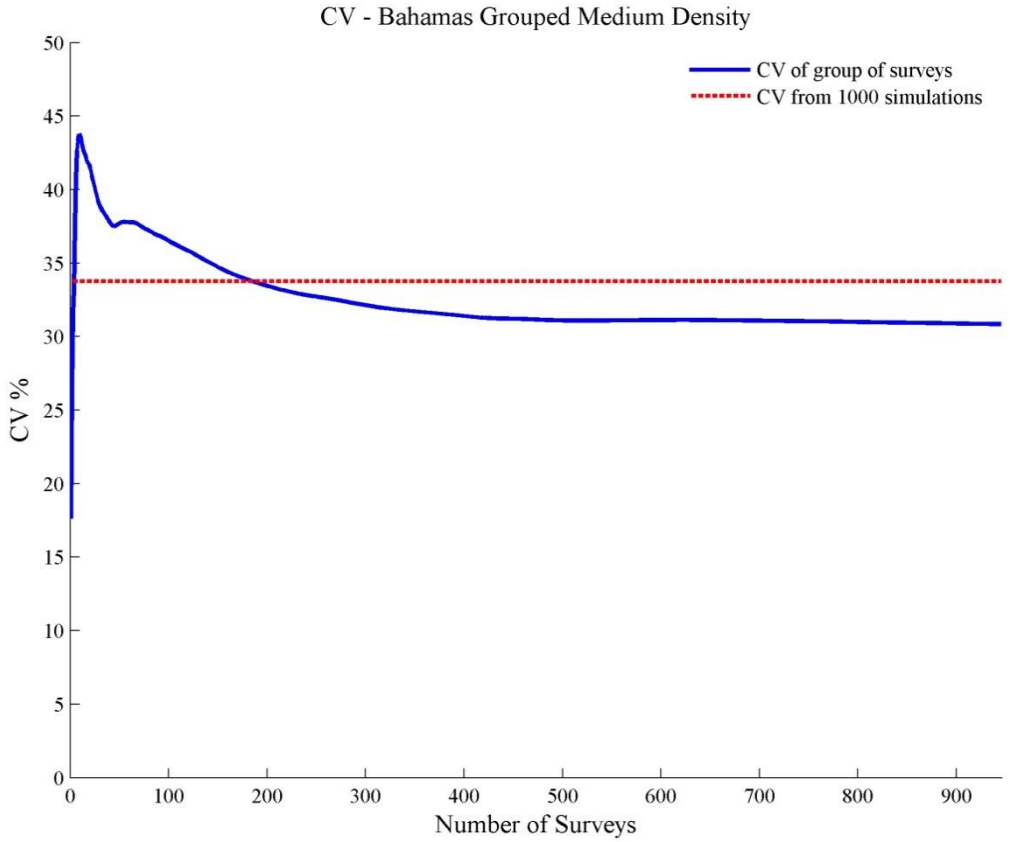

Figure 4.11 Calculation of Coefficient of variation (CV %) of sampling randomly from the repeated surveys for the Bahamas Uniform with animals aggregated in groups in a medium density scenario. The blue line represents the CV from a combination of two up to the maximum number of simulations. The red-dashed line represents the CV of 1000 simulations, by repeating each simulation 1000 times to account for variability in the estimates of the average tracked probability.

2. Density Estimation Based on Click–Scan cue counting

To estimate the density of animals for each glider survey, based on click scan cue counting methods, I first recorded all clicks that were detected, n_d (clicks with received level larger than the detection threshold DT) during the whole survey T. Then detected clicks with an ICI less than 1 s are grouped into CS and the total number of CS detected during the survey, $n_{d_{cs}}$ are used for the analysis.

During the survey, the glider performed 109 full dives of maximum depth 1000m, for which the glider spent equal time at each depth. The average probability for the CS cue counting method, similar to the click cue counting, is $\hat{p}_{TR_{cs}}$ across the whole survey, which for El Hierro is 0.001 (std dev. 0.0005204) and for the Bahamas is 0.000845 (std dev.0.000426).

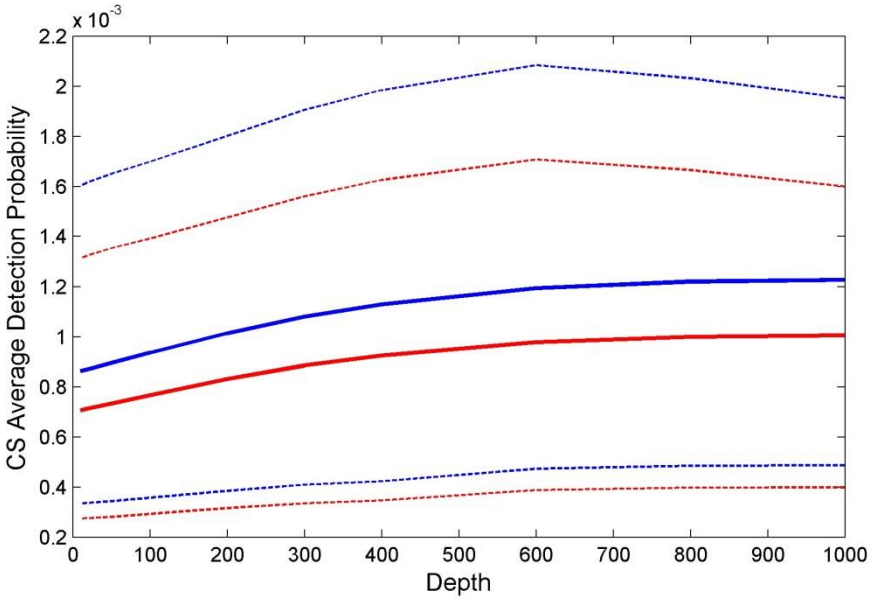

Figure 4.12 Click scan average detection probability used for the glider survey for depths up to 1000m depth. The red solid line is the average detection probability of CS for receivers at different glider depths and dashed red line are the lower and upper 95% quantiles for the Bahamas dataset. The blue solid line is the average detection probability of CS for receivers at different glider depths and dashed red line are the lower and upper 95% quantiles for the El Hierro dataset.

The results for the cue counting method based on CS as an acoustic cue are shown below in Figures 4.13 -16.

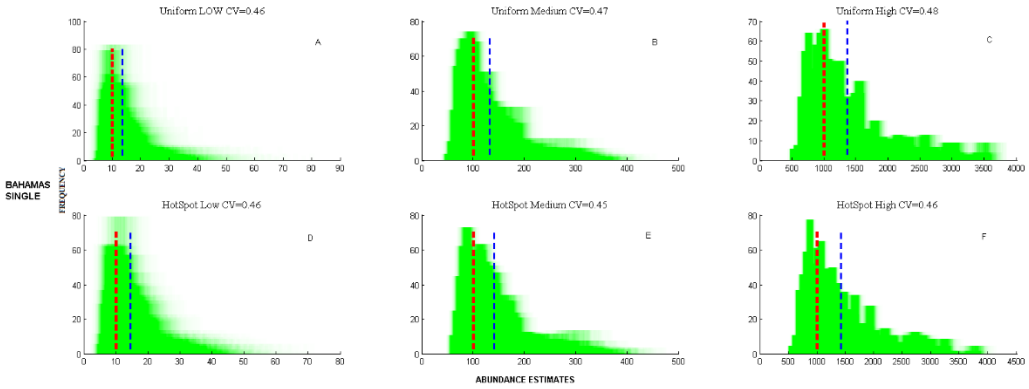

Figure 4.13 Histograms for abundance estimates derived from CS cue counting method for Blainville's beaked whales distributed as single individuals for the area of Bahamas (the red dashed line is the true abundance and the blue dashed line is the mean value of the simulations (1000 repetitions) for each scenario). Uniformly distributed animals during A) Low density B) Medium density C) High density. Hot-Spot distributed animals during D) Low density E) Medium density and F) High density.

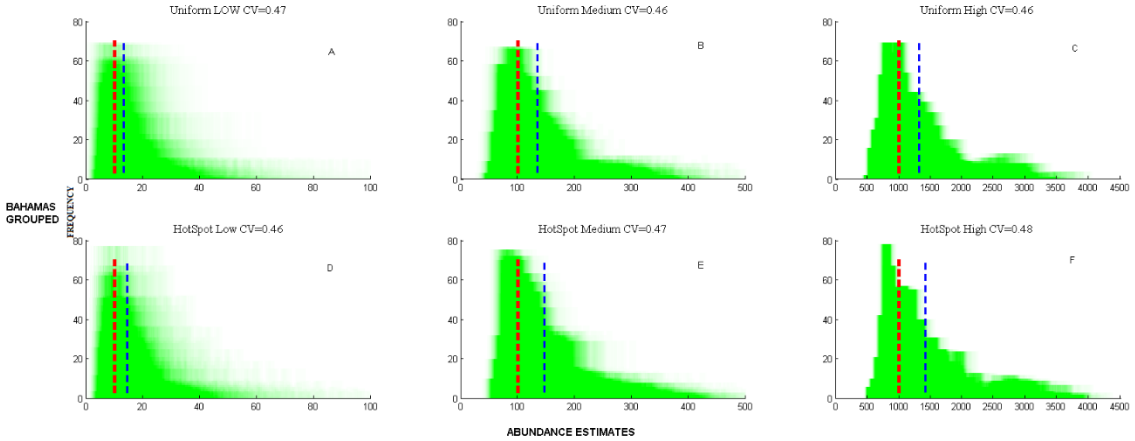

Figure 4.14 Histograms for abundance estimates derived from CS cue counting method for Blainville's beaked whales aggregated in groups for the area of Bahamas (the red dashed line is the true abundance and the blue dashed line is the mean value of the simulations (1000 repetitions) for each scenario). Uniformly distributed animals during A) Low density B) Medium density C) High density. Hot-Spot distributed animals during D) Low density E) Medium density and F) High density.

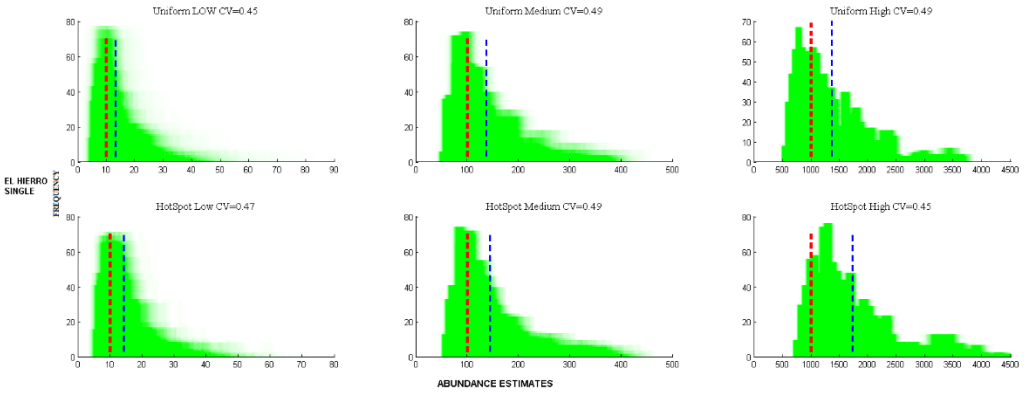

Figure 4.15 Histograms for abundance estimates derived from CS cue counting method for Blainville's beaked whales distributed as single individuals for the area of El Hierro (Canary Islands) (the red dashed line is the true abundance and the blue dashed line is the mean value of the simulations (1000 repetitions) for each scenario). Uniformly distributed animals during A) Low density B) Medium density C) High density. Hot-Spot distributed animals during D) Low density E) Medium density and F) High density.

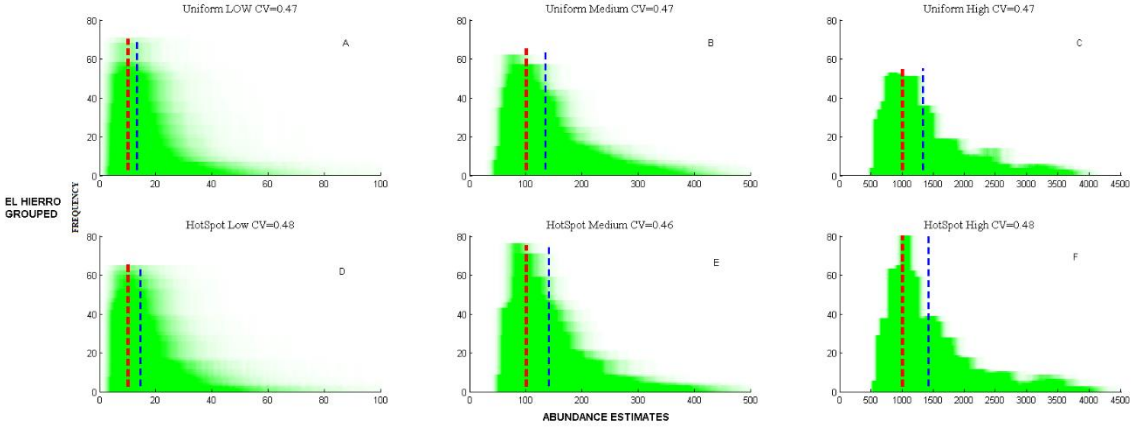

Figure 4.16 Histograms for abundance estimates derived from CS cue counting method for Blainville's beaked whales aggregated in groups for the area of El Hierro (Canary Islands) (the red dashed line is the true abundance and the blue dashed line is the mean value of the simulations (1000 repetitions) for each scenario). Uniformly distributed animals during A) Low density B) Medium density C) High density. Hot-Spot distributed animals during D) Low density E) Medium density and F) High density.

There is an approximately 30% - 40% regular overestimation of the number of animals using the CS cue counting approach (Table 2 and Fig. 4.13-16).

Table 5 Abundance Estimates based on the click scan (CS) cue counting method for the El Hierro and the Bahamas dataset.

Area	Grouping Type	Distribution	Density	Abundance Mean (95%)	CV %
EL HIERRO	SINGLE	Uniform	L	**13.29** (6.1-30.75)	**47.88** (25.11-74.87)
			M	**131.81**(59.86- 303.37)	**47.53** (39.98- 55.75)
			H	**1324** (634-3080)	**48.01** (45.38- 50.48)
		Hot-Spot	L	**14.64** (6.98-33.64)	**46.78** (29.45-68.50)
			M	**141.89** (65.36-331.81)	**49.31** (43.09-56.79)
			H	**1399.7** (639.5 - 3349.1)	**46.52** (44.24-48.62)
	GROUPED	Uniform	L	**13.25** (6.1-31.29)	**46.79** (61.90- 308.20)
			M	**134.39** (61.90-9 308.20)	**46.9** (32.63- 64.03)
			H	**1330** (670 -3195)	**47.5** (42.42- 53.16)
		Hot-Spot	L	**14.55** (6.66-34.72)	**47.51** (13.89 - 102.12)
			M	**141.28** (64.8 -328.38)	**46.35** (34.84-59.71)
			H	**1.421** (659 -3318)	**47.53** (43.33-51.83)
BAHAMAS	SINGLE	Uniform	L	**14.05** (6.42-32.23)	**48.33** (25.82- 76.82)
			M	**132.61** (62.47- 298.70)	**45.75** (38.45- 53.45)
			H	**1290** (577-2956)	**45.80** (43.27-48.88)
		Hot-Spot	L	**14.52** (6.86-32.53)	**44.94** (25.43-67.99)
			M	**143.37** (67.95 -325.46)	**47.74** (40.71- 55.44)
			H	**1421** (675.7 -3225)	**46.13** (43.45 - 48.61)
	GROUPED	Uniform	L	**13.21** (6.48- 29.99)	**45.98** (8.62-107.47)
			M	**132.85** (66.34- 315.10)	**48.05** (33.33-64.52)
			H	**1332** (622.8-2934.5)	**46.19** (41.37-51.39)
		Hot-Spot	L	**14.35** (6.68-31.72)	**46.64** (14.18- 103.52)
			M	**145.66** (68.65 - 329.33)	**46.75** (34.17-60.17)
			H	**1424.1** (695.2-3195.3)	**46.65** (42.54- 51.46)

3. Density Estimation Based on Glider Dive

The glider performed 109 dives per survey, with each glider dive lasting 6.6 hours with a maximum glider depth of 1000m. The number of animals is estimated for each glider depth (Fig. 4.17) and inter-dive variability can be seen as a time series of abundance estimates.

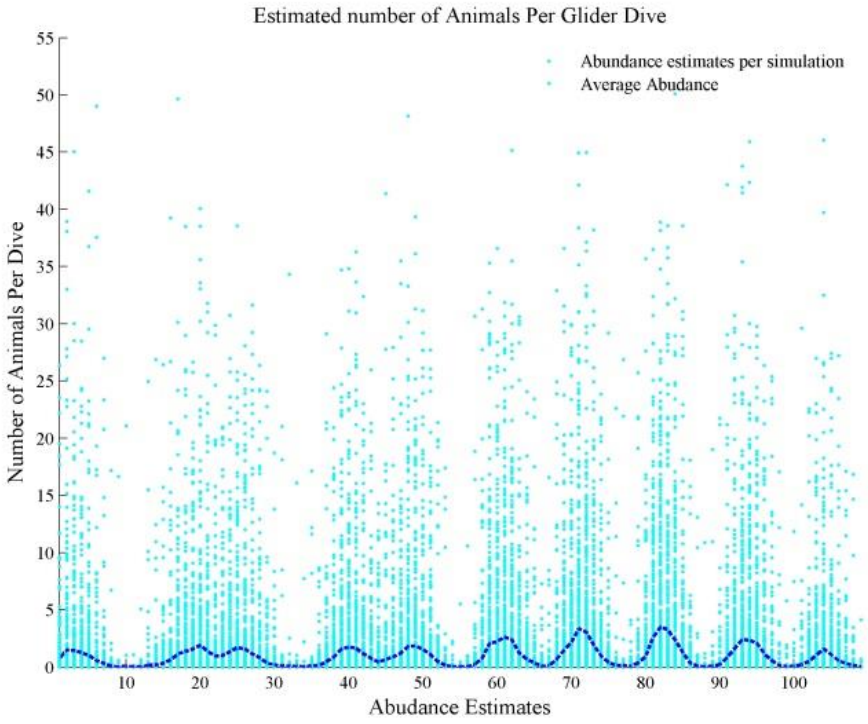

Figure 4.17 Estimated Number of animals per glider dive for the El Hierro Medium Density Hot-Spot scenario. Points show the variation in estimates from each simulation for each glider dive and the blue line is the mean abundance from the 1000 simulations.

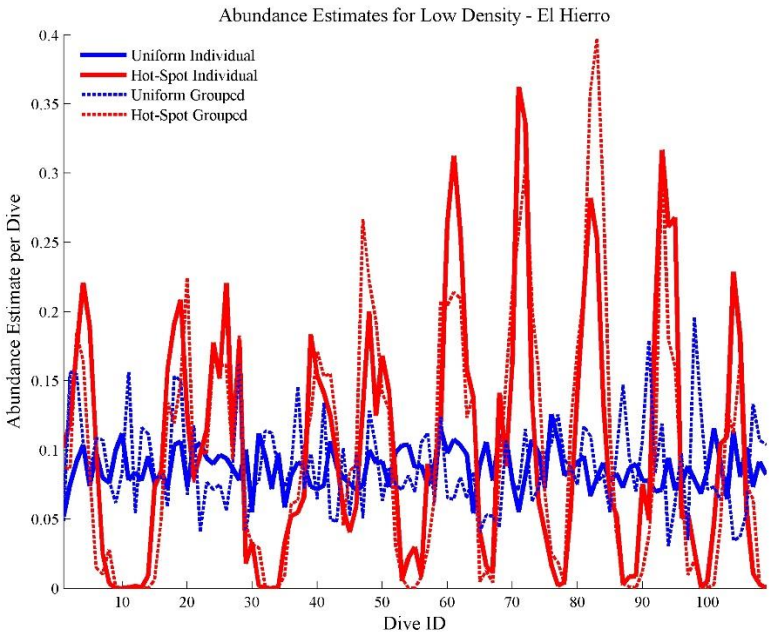

Figure 4.18 Abundance estimates per glider dive derived from LOW density El Hierro simulations based on the Uniform and Hot-Spot density scenarios and animals appearing as individuals or grouped. The red lines correspond to Hot-Spot scenarios (solid for individual animals and dashed for grouped animals. The blue line corresponds to uniform distribution scenarios (solid line for individual animals and dashed line for grouped animals).

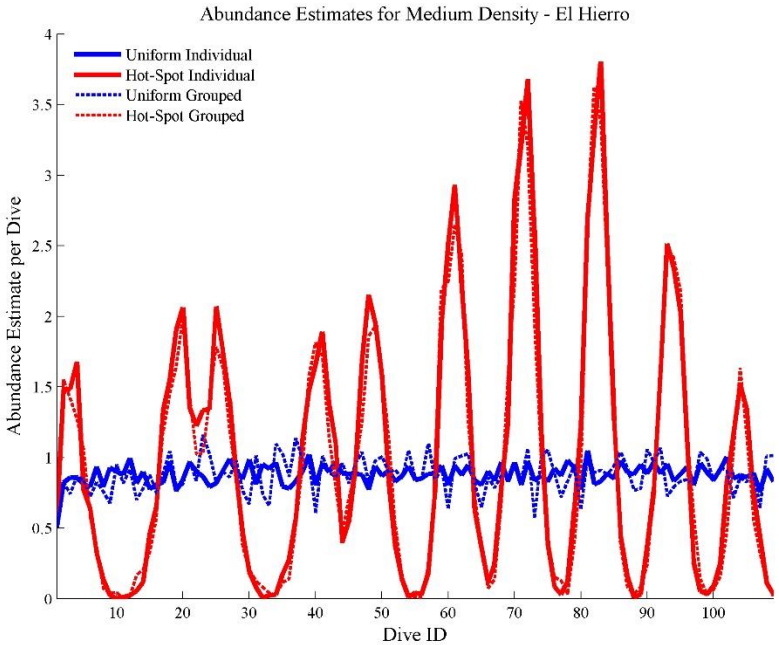

Figure 4.19 Abundance estimates per glider dive derived from MEDIUM density El Hierro simulations based on Uniform and Hot-Spot density scenario and animals appearing as individuals or grouped. The red lines correspond to Hot-Spot scenarios (solid for individual animals and dashed for grouped animals. The blue line corresponds to uniform distribution scenarios (solid line for individual animals and dashed line for grouped animals).

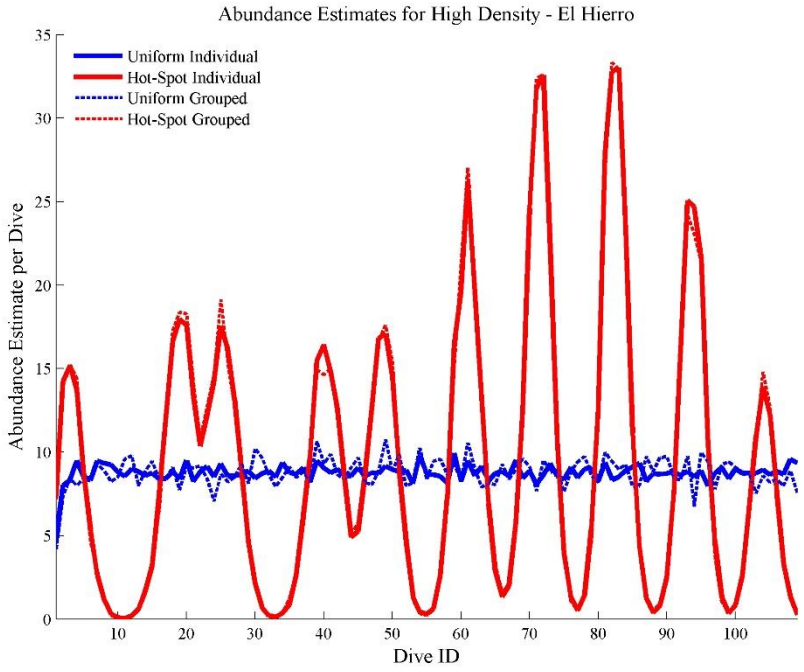

Figure 4.20 Abundance estimates per glider dive derived from HIGH density El Hierro simulations based on Uniform and Hot-Spot density scenario and animals appearing as individuals or grouped. The red lines correspond to Hot-Spot scenarios (solid for individual animals and dashed for grouped animals. The blue line corresponds to uniform distribution scenarios (solid line for individual animals and dashed line for grouped animals).

Abundance estimates in a patchy environment such as the scenario where there is a Hot-Spot in the area are translated into variability in the abundance estimates at each dive. Similarly when animals are aggregated in groups, as is the case with Blainville's beaked whales found in nature, abundance per glider dive is more variable than when animals are found as single individuals.

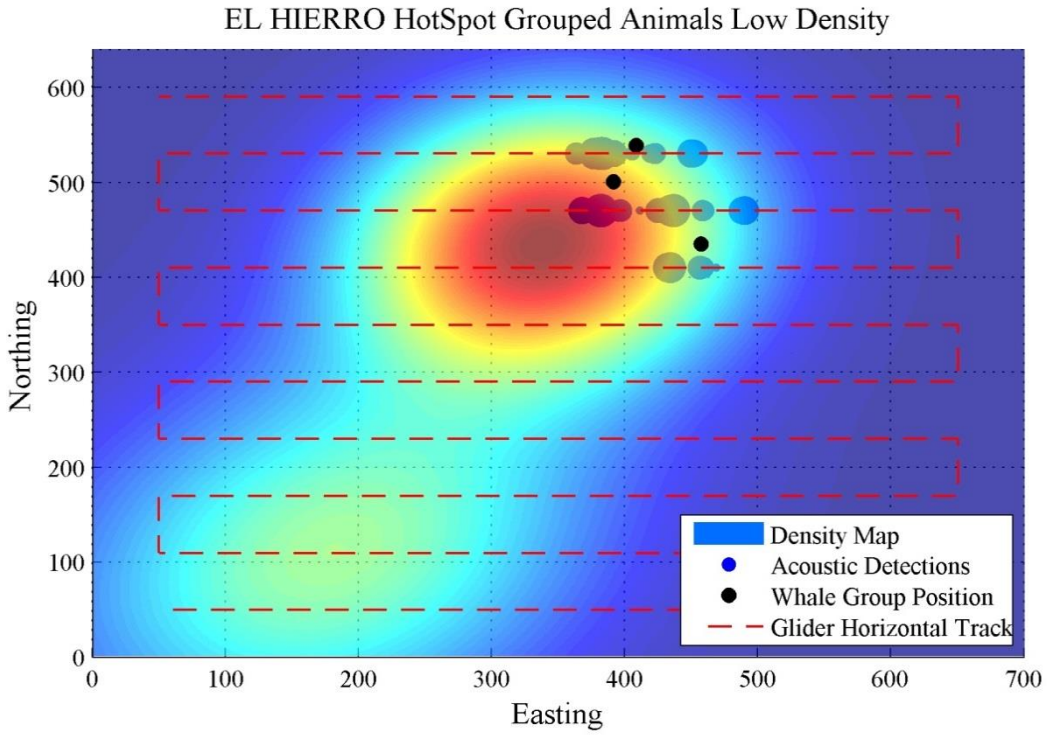

Figure 4.21 Acoustic detections along the the horizontal track of the glider, which is indicated by the red dashed line. The blue circles indicate the acoustic detections of Blainville's beaked whales three groups (for a total of 10 animals). The black dots mark the position of the animal groups during one simulation and the coloured surface plots the density map from which the animals were randomly chosen.

4. Density Estimation Based on Spatial Modelling

The number of clicks per unit area was predicted from each simulation as a function of longitude and latitude. The results for each simulation were fitted in a generalized additive model with an interaction smooth term between x and z. An average prediction of counts of clicks was then derived, taking into account the predictions of 1000 fitted models. For each prediction cell, the total amount of time that the glider spent observing, and the average tracked detection probability is taken in to account to estimate abundance for each cell. The total abundance is derived by summation of the abundances for each cell.

For each simulation results a GAM (Generalized Additive Model) model was fitted to the number of clicks detected at the glider to estimate the abundance of animals. The mgcv library in R (Wood, 2006) was used to fit a GAM model (Gaussian errors, log-link), modelling the number of clicks detected as a function gliders position (x_g, y_g) The systematic component is therefore:

$$\eta_t = \beta_0 + f(Lat_t) + f(Lon_t)$$

Where η provides the link-scale predictions, comprising of the intercept, β_0, and a spline-based smooth, f, for Latitude and Longitude. Figure 4.22 shows the mean predictions from 1000 simulations with the upper and lower 95% CI. An estimate of abundance based on the spatial model was 92.6 animals (8.3 -310.4 95% CI for the medium density for the Bahamas dataset. The rest of the scenarios were not tested.

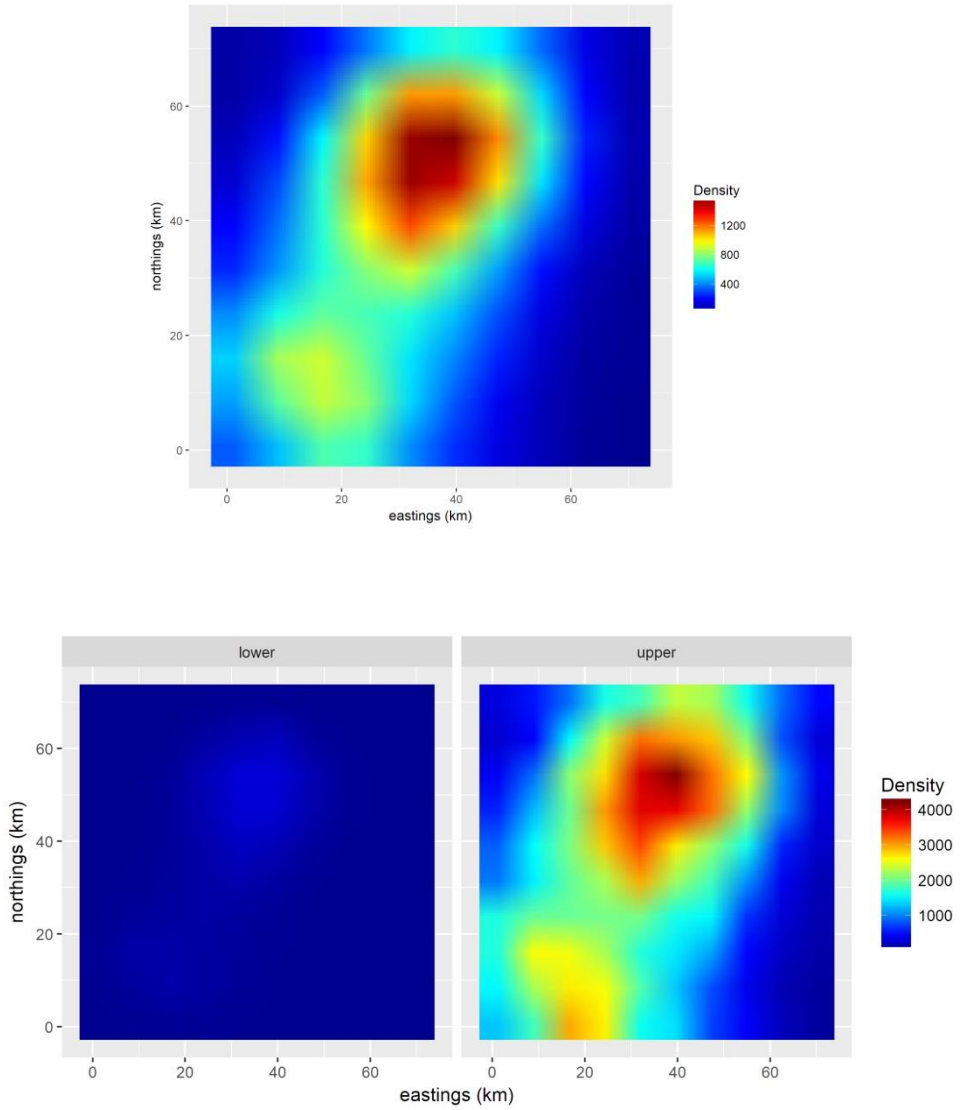

Figure 4.22 Average predictions from 1000 Generalized Additive Models (GAMs), each one derived from one simulation for the Bahamas Hot-Spot scenario (A). Animal density is the number of single animals per km^2. In B the lower CI is derived from the 1000 models and C shows the upper 95% CI. Each model was a GAM quasi-Poisson with number of clicks detected the response variable.

5. Bias

Biases in density estimation can arise from use of biased multipliers as well as due to survey design (Marques et al., 2013). In cue-counting methods, the multipliers used are the click rate for the animal of interest and the average detection probability. Here, we investigate two different populations, those of El Hierro and the Bahamas. The click rates for the two populations have been estimated to be 0.41, so biases due to different click rates are not going to be investigated further.

Biases deriving from the tracked average detection probability $\hat{p}_{RT}$: In the pooled cue counting method for estimating abundance from glider surveys, the average detection probability depends on the duration the glider spends in each depth, which determines the overall average tracked survey detection probability $\hat{p}_{RT}$. This parameter will influence the results of the survey, by integrating the appropriate duration the depths that the glider passes through. The average probability over the entire survey track is a function of the time spent by the platform at each depth. The integration of *Pa* over the different depths that glider passes through must take into account the time that the platform spends at each depth $\int_0^T P(t \mid z)dt$. For the El Hierro dataset, the mean average probability of detection is **0.03** for depth ranging between 0 and 1000m and an equivalent distribution of time at the different depths for the Bahamas dataset is **0.025**.

If a $\hat{p}_{RT}$ from a different location, for example the Bahamas, is applied to the data from, for example El Hierro, then this will result in an overestimation of the abundance of about 17%, and a 20% underestimation of population size when the tracked average probability of detection from El Hierro is applied to the Bahamas dataset.

4.5 Discussion

In this chapter, a methodology for estimating density from acoustic recordings made from an AUV platform is presented and tested in a simulation study, using real movement and sound production data derived from DTAG deployments on Blainville's beaked whales in two different habitats. The simulations indicate minimal biases in density estimation for this species using this approach with an underwater glider, with the potential of applicability to other species as well, though this has to be investigated further.

The abundance estimates presented here are derived from a simulation study for assessing the underwater autonomous glider as a platform for passive acoustic monitoring. Specifically, I present a new mathematical formulation for estimating abundance using cue-counting methods applied to slow-moving platforms that sample different depths. The method takes into account the changes in detectability of individual Blainville's beaked whale clicks as a function of receiver depth, using a continuous function. Estimates of variance and bias show that the method is dependent on knowledge from DTAG data for the species, conditional on the geographic location of the deployment, and on the survey design.

This chapter presents a new mathematical equation, an extension of the equation for estimating abundance from fixed acoustic sensors. The method is a variant of the click cue-counting method for beaked whales as derived by Marques et al., (2009). For the click cue-counting method, an estimated average probability (P_a) accounting for the average detectability in space is required along with an estimation of a click rate. For deep-diving cetaceans, the average detection probability $P_a(z)$ is conditional on the depth of the receiver z, as shown in Chapter 3. The new method takes into account the change in detectability as a function of receiver depth. For slow-moving platforms, such as underwater gliders, the platform can be conceived as a fixed acoustic sensor, which changes three-dimensional position in time. Here, an estimator for the average detection probability based on a continuous relationship with receiver depth is used to give estimates of abundance in different population densities.

The derivation of the continuous relationship $P_a(z)$ was possible only with the use of DTAG data, which includes depth information, acoustic data that can be used to measure the production time of clicks, and data on the orientation of the clicking whale. The use of DTAG data makes it possible to estimate the number of clicks produced by the animal, and hence to estimate the click rates for the DTAG tagged population (Warren et al., 2017). In addition, information on the depth distribution of clicks produced, derived from DTAG data, allows

the probability of detection to be estimated as a function of receiver depth. The average detection probability is a product of the detection function (Buckland et al., 2001); the ability to estimate this parameter as a function of depth gives the opportunity to apply a continuous function correcting for detectability conditional to depth.

If no DTAG data were available, variations in the depth distribution where animals click to forage would limit our ability to estimate the function of conditional probability of P_a as a function of depth. Large aperture drifting arrays can be used for three-dimensional tracking of animals, which can estimate the depth distribution of marine mammals during vocalization (Macaulay et al., 2017; Miller et al., 2009; Thode 2005). However, these localization data cannot replace the resolution and efficiency of the DTAG for sampling the whole dive including periods when the animal is not vocalizing. These data make it possible to correct for availability bias and to define the detection function at zero horizontal distance for each receiver at a predefined depth, the g(0,z), where z is the depth of the receiver. Furthermore, DTAG data provide unbiased information regarding orientation of the animals during foraging, which plays an important role in the estimation of the detection function and as a consequence in the average detection probability.

In addition to click cue counting, the click scan cue counting approach was used in similar simulations measuring the number of click scans detected, where a click scan is defined as sequences of clicks with less than one second inter-click interval.

Comparing the two different acoustic cues for density estimation, the click scan cue counting method is dependent on a separate simulation to derive the expected/observed number of CS as a function of distance and depth (Chapter 3). This method is dependent on additional assumptions that may not apply in the wild. For example, the expected number of CS in the detectable area around a receiver may differ from that in the environment that was simulated to derive the estimate. Click cue counting requires a click rate that can be estimated from different DTAG deployments. For the CS approach, click trains as recorded on the DTAG, cannot be used directly to estimate the CS rate in the cue-counting approach and the observed encounter rate is used instead.

The results presented here show that the CS cue counting approach has a steady positive bias for all the different scenarios of density (low, medium and high) of around 30%. This bias implies a possible error in the way that the integrated average detection probability of CS is calculated, or a violation of the assumptions used for this cue counting method. The CS as a cue in the cue counting method is somewhat problematic as the size of CS changes as a

function of distance and depth, while the click as an acoustic cue is a more robust cue and remains constant regardless distance and receiver depth.

To account for uncertainty of the tracked average detection probability of click scans, an approximation of the parameter's distribution was used. It could be that this approximation has an overall underestimation of the true values of the average detection probability for the CS, hence the overestimation of the abundance estimates.

Another potential source of bias is the definition of a CS, which is defined as a series of clicks with inter-click- interval of less than one second. As shown in Chapter 3, the length of the CS changes as a function of distance from the receiver and at different at receiver depths. By pooling all the detections together to estimate an overall abundance for the total survey, there is the potential for bias in the estimator.

Conclusion

Underwater gliders provide an opportunity for long-term aquatic sampling with relatively low cost, in comparison to other acoustic platforms such as boats. In addition, gliders can be programmed to sample at depths where beaked whales are vocalizing during foraging dives. The slow movement in combination with the large depth range allows for higher detectability of acoustic cues for deep-diving animals. More traditional platforms, such as boats, face low detection probabilities, as their acoustic element is usually towed behind the boat in depths of approximately 20-100 meters (Barlow and Taylor 2005). The speed of the boat is usually much higher than that of the glider (approximately 12-15 km per hour in relation to 0.9 km per hour). This high a speed does not maximise the probability of encountering a beaked whale due to the silent period during their shallow dives, parts of the descent, and most of the ascent phase of deep foraging dives. A passing boat may therefore easily fail to detect a group of whales that is not calling during the period of time for which the boat is in detection range. This problem is compounded by the species' tendency to dive, and hence vocalise, with a degree of group synchronicity (Aguilar de soto et al., 2012).

The results presented here derive from simulated gliders using real DTAG data derived from two different geographical locations for Blainville's beaked whales. The abundance estimates are linked to estimates of average detection probability for receivers at various depths. If the initial data used for deriving the detection function of individual clicks are biased, the bias will translate to biases in abundance estimates. Information on noise data derived from real glider deployments will help theoretical studies like this one to use more realistic parameters regarding the detection threshold. Here a click was counted as detectable if the energy of the

received click was more than 100 dB re 1 μPa. For sensitive acoustic receivers in environments with relatively low ambient noise, this may lead to overestimation of beaked whale abundance, as results here are under a particular level of system and background noise The converse (under-estimation) could be true for more noisy (system/ambient) situations, such as high sea states as considered by Ward et al., (2011).

When an acoustic survey is designed for a specific area, multipliers derived from the same population are desirable in order to avoid biases in density estimation (Marques et al., 2013). Here we show that biases due to different detectability due to the depth distribution of foraging behaviour of two different populations can lead to 17% - 20% of under- or over-estimation of the number of animals in an area. Animals in the Bahamas forage at deeper waters than the animals of El Hierro (Chapter 3), which translates to different probabilities of detections (Chapter 3). For density estimation using acoustic methods, where the acoustic receiver can be placed at different depths or sample various depths as is the case for AUVs, a prior knowledge of the depth distribution of the species' vocalization should be used to optimize detection and to avoid biases in the estimated number of animals. The depth at which animals produce echolocation clicks to forage changes as a result of prey distribution. DTAG data assist in deriving that information, and wherever it is possible, DTAG deployments should be considered at the time and place of any survey.

The simulation here presents a simplified version of reality regarding glider surveys. Here, I simulate a glider survey with constant horizontal and vertical speed, assuming no influence of water currents. In reality, different weather conditions and underwater currents influence the speed of the autonomous platform, which also affects the noise floor of the recordings. The horizontal displacement of a glider between two sequential surfacing points is not constant, which will be affected by the underwater speed (slope of the glider). When strong currents exist in the area, the relative movement of the underwater platform towards the direction of the current will influence the final speed and subsequent movement of the glider. The time a glider spends at each depth is going to be affected by the presence and strength of underwater currents in the area, consequently altering the time that glider spends at each depth and hence changes the overall detectability $\hat{p}_{RT}$. Gliders have pressure sensors from which the depth of the platform can be estimated, and hence the appropriate $\hat{p}(t(d))$ probability can be derived by estimating the time that glider spends at each depth.

The approach explored here depends heavily on data from DTAGs. Prior knowledge of the foraging depth of echolocating species can improve studies that use data derived from

underwater autonomous gliders to estimate abundance and density of vocalising animals. To take full advantage of this platform, DTAG deployments on different species could provide species-specific parameters, such as the probability of detection of a vocal cue as a function of horizontal distance and as a function of receiver's depth. For a long-term deployment glider that requires optimization of duty cycle, prior information of the species expected to be encountered and the depthas at which they vocalise can assist planning the dive patterns of the glider. Furthermore, cue rates are also essential for using acoustic detections to estimate density, and these can be estimated for many species through the deployments of DTAGs.

4.6 References

Aarts, G., MacKenzie, M., McConnell, B., Fedak, M. & Matthiopoulos, J. (2008) Estimating space-use and habitat preference from wildlife telemetry data. Ecography, 31, 140-160.

Aguilar de Soto, N.A., Madsen, P.T., Tyack, P., Arranz, P., Marrero, J., Fais, A., Revelli, E. & Johnson, M. (2012) No shallow talk: Cryptic strategy in the vocal communication of Blainville's beaked whales. Marine Mammal Science, 28, E75-E92.

Ainslie, M.A. (2013) Neglect of bandwidth of odontocetes echolocation clicks biases propagation loss and single hydrophone population estimates. J. Acoust Soc Am., 134, 3506-3512.

.

Barlow, J. & Taylor, B.L. (2005) Estimates of sperm whale abundance in the northeastern temperate Pacific from a combined acoustic and visual survey. Marine Mammal Science, 21, 429-445.

Baumgartner, M.F. & Fratantoni, D.M. (2008) Diel periodicity in both sei whale vocalization rates and the vertical migration of their copepod prey observed from ocean gliders. Limnology and Oceanography, 53, 2197-2209.

Baumgartner, M.F., Fratantoni, D.M., Hurst, T.P., Brown, M.W., Cole, T.V.N., Van Parijs, S.M. & Johnson, M. (2013) Real-time reporting of baleen whale passive acoustic detections from ocean gliders. Journal of the Acoustical Society of America, 134, 1814-1823.

Baumgartner, M.F., Van Parijs, S.M., Wenzel, F.W., Tremblay, C.J., Esch, H.C. & Warde, A.M. (2008) Low frequency vocalizations attributed to sei whales (*Balaenoptera borealis*). Journal of the Acoustical Society of America, 124, 1339-1349

Croll, D.A., Tershy, B.R., Hewitt, R.P., Demer, D.A., Fiedler, P.C., Smith, S.E., Armstrong, W., Popp, J.M., Kiekhefer, T., Lopez, V.R. and Urban, J., 1998. An integrated approach to the foraging ecology of marine birds and mammals. Deep Sea Research Part II: Topical Studies in Oceanography, 45, 1353-1371.

Dunn, C., Claridge, D., Durban, J., Shaffer, J., Moretti, D., Tyack, P. Rendell L. (2017). Insights into Blainville's beaked whale (*Mesoplodon densirostris*) echolocation ontogeny from recordings of mother-calf pairs. Marine Mammal Science 33, 356-364.

Gillespie, D., Berggren, P., Brown, S., Kuklik, I., Lacey, C., Lewis, T., Matthews, J., et al., (2005). Relative abundance of harbour porpoises (*Phocoena phocoena*) from acoustic

and visual surveys of the Baltic Sea and adjacent waters during 2001 and 2002. J. Cetacean Res. Manag., 7, 51.

Borchers, D., Distiller, G., Foster, R., Harmsen, B. & Milazzo, L. (2014) Continuous-time spatially explicit capture-recapture models, with an application to a jaguar camera-trap survey. Methods in Ecology and Evolution, 5, 656-665.

Buckland, S.T., Anderson, D.R., Burnham, K.P., Laake, J.L., D.L., B. & Thomas, L. (2001) Introduction to distance sampling: Estimating abundance of biological populations. Oxdord University Press, Oxford.

Canadas, A., Sagarminaga, R., De Stephanis, R., Urquiola, E. & Hammond, P.S. (2005) Habitat preference modelling as a conservation tool: proposals for marine protected areas for cetaceans in southern Spanish waters. Aquatic Conservation: Marine and Freshwater Ecosystems, 15, 495-521.

Gillespie, D., Berggren, P., Brown, S., Kuklik, I., Lacey, C. Lewis, T., Matthews, J., et al., (2005) Relative abundance of harbour porpoises (*Phocoena phocoena*) from acoustic and visual surveys of the Baltic Sea and adjacent waters during 2001 and 2002. J. Cetacean Res. Manage., 7, 51-57.

Klinck, H., Mellinger, D.K., Klinck, K., Bogue, N.M., Luby, J.C., Jump, W.A., Shilling, G.B., Litchendorf, T., Wood, A.S., Schorr, G.S. & Baird, R.W. (2012) Near-real-time acoustic monitoring of beaked whales and other cetaceans using a Seaglider (TM). Plos One, 7, e36128.

Macaulay, J., Gordon, J., Gillespie, D., Malinka, C. & Northridge, S. (2017) Passive acoustic methods for fine-scale tracking of harbour porpoises in tidal rapids. Journal of the Acoustical Society of America, 141, 1120-1132.

Marques, T.A., Thomas, L., Martin, S.W., Mellinger, D.K., Ward, J.A., Moretti, D.J., Harris, D. & Tyack, P.L. (2013) Estimating animal population density using passive acoustics. Biological Reviews, 88, 287-309.

Marques, T.A., Thomas, L., Ward, J., DiMarzio, N. & Tyack, P.L. (2009) Estimating cetacean population density using fixed passive acoustic sensors: An example with Blainville's beaked whales. Journal of the Acoustical Society of America, 125, 1982-1994.

Moretti, D., DiMarzio, N., Morrissey, R., Ward, J. & Jarvis, S. (2006) Estimating the density of Blainville's beaked whale (*Mesoplodon densirostris*) in the Tongue of the Ocean (TOTO) using passive acoustics. Oceans 2006, Vols 1-4, 313-317.

Palka, D.L. & Hammond, P.S. (2001) Accounting for responsive movement in line transect estimates of abundance. Canadian Journal of Fisheries and Aquatic Sciences, 58, 777-787.

Rudnick, D.L. (2016) Ocean research enabled by underwater gliders. Annual Review of Marine Science, 8, 519-541.

Sato, K., Watanuki, Y., Takahashi, A., Miller, P.J.O., Tanaka, H., Kawabe, R., Ponganis, P.J., Handrich, Y., Akamatsu, T., Watanabe, Y., Mitani, Y., Costa, D.P., Bost, C.A., Aoki, K., Amano, M., Trathan, P., Shapiro, A. & Naito, Y. (2007) Stroke frequency, but not swimming speed, is related to body size in free-ranging seabirds, pinnipeds and cetaceans. Proceedings of the Royal Society B-Biological Sciences, 274, 471-477.

Thode, A. (2005) Three-dimensional passive acoustic tracking of sperm whales (*Physeter macrocephalus*) in ray-refracting environments. Journal of the Acoustical Society of America, 118, 3575-3584.

Tyack, P.L., Johnson, M., Soto, N.A., Sturlese, A. & Madsen, P.T. (2006) Extreme diving of beaked whales. Journal of Experimental Biology, 209, 4238-4253.

Ward, J., Jarvis, S., Moretti, D., Morrissey, R., DiMarzio, N., Johnson, M., Tyack, P., Thomas, L. & Marques, T. (2011) Beaked whale (*Mesoplodon densirostris*) passive acoustic detection in increasing ambient noise. Journal of the Acoustical Society of America, 129, 662-669.

Wood, S.N., 2006. Generalized Additive Models: An Introduction with R. Chapman & Hall/CRC, Boca Raton.

Chapter 5

General discussion

5.1 Synthesis

Density estimation is a key aspect of ecological studies that assess anthropogenic impacts on wild animal populations. Traditionally studies relied upon sighting animals to estimate their density, but alternative cues can also be useful. Many animal species produce sounds in order to communicate with conspecifics, hunt and navigate in their environment. Marine environments are relatively opaque visually, but transparent acoustically, increasing the importance of sound as a potential cue for detecting an animal. Many marine mammal species take advantage of long range propagation of sound in the ocean for foraging, communication and navigation, suggesting the utility of acoustic, rather than visual, detection methods for estimating their density.

We focus here on the navigation and foraging behaviour of deep divers as a means for acoustic detection of the animals, due to their stereotyped acoustic behaviour. Stereotyped vocal behaviour can lead to cue rates with smaller variance than a cue originating from a behaviour, such as mating, which may be seasonally dependent or just produced by one age/sex class. In applications where cues form the basis for later density estimation, lower variance in calling rates ought to provide greater precision in the subsequent density estimates. Here I focus on echolocation clicks of beaked whales which are produced every time a beaked whale forages. The detection probability of an echolocating animal is dependent on many characteristics of the sound produced: frequencies, directionality of the signal, the animal's movement, orientation and depth during its foraging dive, but also the receiver's characteristics, including its depth. Detection probabilities must be estimated if we are to scale up the observed cues to numbers and densities of animals locally, and for estimates over broader areas.

Such complexities require detailed data collection on animals to model detection probabilities. The use of DTAGs on deep divers provides detailed information on sound production and movement behaviour from the animal's perspective that is very hard to sample otherwise. Information derived from these devices has already assisted greatly in generating methodologies for abundance estimation from acoustic surveys (Marques et al., 2009; Marques et al., 2013; Moretti et al., 2010) in addition to knowledge about bioacoustics,

behaviour and habitat use of the species. Determining the factors affecting the detectability of a species is important to avoid biased estimates of density and to make the best use of data collected during an acoustic survey. With the advancing effectiveness of acoustic systems regarding storage capacity, range of acoustic platforms and advanced mooring systems, there is an increasing opportunity for long-term sampling of water depths that were previously hard to survey.

5.2 Outcomes of the thesis

This thesis has presented methods to derive parameters used in density estimation of marine mammals using acoustic cues from underwater autonomous gliders equipped with one acoustic sensor. It has applied these methods on Blainville's beaked whales from two different geographical locations, El Hierro (Canary Islands) and the Bahamas. The thesis used a simulation study to assess the performance of underwater gliders using cue-counting methods, with regular echolocation clicks as acoustic cues and has created a simulation framework to assess and compare acoustic platforms. Diving behaviour, including foraging depths and click production, which was used in the thesis, was derived from DTAG deployments on 18 animals, 12 animals from El Hierro and 6 animals from the Bahamas.

In **Chapter 2** a methodology was developed for deriving an acoustic detection function for echolocating animals in the field, with a combined biologging and passive acoustic monitoring experiment. The methodology was used to derive the acoustic detection function of Blainville's beaked whales of the island of El Hierro in the Canary Islands (Spain). The acoustic detection function of Blainville's beaked whales differs from receivers placed at different depths, with deeper receivers (200-300m) having 35% higher detectability for single regular clicks than shallower receivers (20m). Finally, a comparison of five different detectors for Blainville's beaked whales was presented. The comparison of five different click detectors for Blainville's beaked whales showed that the energy ratio detector had lower efficiency than two correlation detectors and two energy detectors.

In **Chapter 3** the acoustic detection functions of two acoustic cues for Blainville's beaked whales (individual clicks and click scans) were derived from a theoretical study and the use of DTAG data. The mean click rate was 0.41 clicks per second for both the Bahamas and the

El Hierro populations. Click scan rates for the Bahamas and the El Hierro populations are 0.417 and 0.414 respectively. Blainville's beaked whales of the Bahamas population forage deeper than El Hierro animals, based on DTAG data. The average detection probability of a regular echolocation click at a single receiver changes as a function of depth of the receiver, and depends on the foraging depth of the species and the orientation of the animals while producing vocal cues. The most frequent length of click scans detected on a single receiver at any depth is 3 clicks, though this result is very much linked to the definition of click scan. In the thesis here, the click scan is defined as a series of clicks detected on a passive acoustic recorder with ICI between 0.0 to 1 s. The maximum detectability of a single click is at a receiver depth of 1000 meters for the Bahamas population and 800 meters for the El Hierro population.

In Chapter 4 methods were developed for deriving animal density from slow moving underwater gliders based on cue-counting and accounting for changes in detectability based on the depth of the glider. An estimator used in the proposed methodology for density estimation of deep-diving echolocating cetaceans was derived by testing the method in a simulated glider survey in different animal densities. A spatial model for deriving the abundance of Blainville's beaked whales, modelling the number of clicks detected on the glider as a function of longitude and latitude and considering the detectability and effort of the platform derived similar abundance estimates (a mean abundance estimate of around 8% difference from the true density for the Bahamas dataset) to those derived with click cue-counting methodology. Though the spatial modelling can be greatly improved adapting existed spatial distance sampling approaches (Miller et al., 2013). It is important to use parameters such as the detection function and the average detection probability derived from the site where the survey is being conducted. Biases of up to 20% overestimation for density estimation for the Blainville's population of Bahamas arise if the average detection probability from El Hierro is used. An underestimation of 17% of the population of the El Hierro if the average detection probability from the Bahamas is used.

5.3 Limitations

There are several limitations in the thesis presented here, and these can be grouped by data availability, species applicability, modelling assumptions, choice of parameters used in the simulation for glider survey and methodological limitations for density estimation.

5.3.1 Data availability

The data used in Chapter 2 derived from 5 DTAG deployments from two different years, 2008 and 2010. As the estimation of the detection function derived from the available distances between the echolocating tagged animal and the acoustic receiver, the detection function is highly correlated to those distances. A greater availability of field experiments to expand the dataset would enable estimation of a more precise detection function. In addition, a larger experimental dataset during more varied weather conditions would allow for detectability to be estimated as a function of changes ambient noise induced by different weather conditions. Variability in the ambient noise could allow testing the performance of click detectors in different conditions than the low ambient noise levels of the data presented here. This weather dependent variation in ambient noise is important as it affects the detectability of cues (Ward et al., 2008) and as a consequence the density estimations when parameters of the detection function are used.

The variation in detectability of the acoustic cues of Blainville's beaked whales as a function of receiver depth was estimated based on 18 DTAG deployments containing full foraging dives (out of 19 DTAG deployments), 12 from El Hierro and 6 from the Bahamas and the detectability was estimated based on theoretical network of receivers. This approximates what would happen with real receivers under real environmental conditions. The effect of depth on ambient noise levels can alter the results presented here in a non-linear way, as in this study a threshold detector was used at a fixed 100 dB threshold. Receivers with a self-noise level lower than 100 dB have the potential to detect signals at lower received levels in reduced ambient noise. Much ambient noise is caused by sound sources such as vessels and breaking waves that are located at the sea surface. If this causes ambient noise to vary as a function of depth, then the depth dependent detection probability could have a different shape than the one presented here. Testing this would require measurements of ambient noise at different depths at the site of the survey. Other elements of the detection function are also affected by the choice of detection threshold. The studies in this thesis were designed for

general applicability to Blainville's beaked whales. More examination of the estimated functions in different threshold choices can give a more meaningful result for different acoustic systems and different ambient noise levels. Developers who are implementing such systems for specific species in specific sites should certainly explore these parameters in detail.

5.3.2 Assumptions

In this thesis I made some assumptions regarding the sonar production of Blainville's beaked whales. The beamwidth of the echolocation signal was estimated by fitting a broadband piston model. Small errors in the predictions of the piston model could lead to errors in received levels at off-axis angles between the animal and the receiver. These errors could potentially affect the modelled received level of clicks on single receivers and the detection function of acoustic cues. This is important especially in studies that estimate the detection function from theoretical studies such as in Chapter 3 and other studies as in Zimmer et al., (2005).

The detection function of other acoustic cues such as the click scans presented here, also depend on the estimated beam pattern of the species. Simulation studies that make use of a piston model will affect the results on the length of clicks scans detected, especially for narrowbeam species such as the beaked whales.

5.3.3 Glider simulation method

In this thesis I present a simulation study for glider surveys designed to estimate abundance of deep diving animals. The parameters of the simulation, such as three-dimensional underwater speed, horizontal speed, slope of the glider, time on the surface, time on the bottom can affect the total number of detections and hence the density estimation of animals. Information regarding the effect of underwater currents on horizontal displacement of the glider in the study area can assist the choice of speed and tracklines for glider surveys. An even more realistic scenario for simulation survey would be to use information of surface and underwater currents in the study area, so that the effect of these on the glider tracks can be

investigated and how these deviations from the survey plan may affect abundance estimates using cue counting methods.

A strong assumption made in the simulations is the stationary location of the animals, individuals or groups, at their [x,y] position. This assumption is not realistic as animals move horizontally during their deep foraging dives. The modelling of animals as horizontally stationary, would underestimate the relative speed between the animal and the platform if animals were moving away from the platform and would overestimate the relative speed of the animals if animals would move along with similar direction of the platform. Horizontal movement of an animal in relation to the moving acoustic receiver would result in fewer detections of clicks when the animal is swimming in the opposite direction of the glider, and larger amount of detections in case the animal moves in a similar direction as the platform. This would lead to greater variance in the estimates of abundance, though the average estimate probably would remain the same as in the case of our study here.

5.3.4 Species applicability

The thesis focuses exclusively on Blainville's beaked whales. The method for estimating the detection function can be applied to other echolocating species as well in cases where their signal can be extracted with an automated detector, and the efficiency of those detectors can be tested with a similar methodology. Depending on how frequently the species vocalizes, drifting receivers can be placed accordingly to achieve coverage of different distance ranges for extracting the acoustic detection function of the species; the variability at the recorded distances would result as well from the relative movement of the anima during the duration of the experiment i.e. if the animal never gets close to the receiver then the detection function will not be estimated at those distances.

5.3.5 Combination of different platforms

The results presented here focus mostly on detections at one single receiver, either stationary (Chapter 3) or moving platforms such as underwater gliders (Chapter 4). The depth dependent detectability of acoustic cues as a function of receiver's depth that was found here for Blainville's beaked whales, can be applied to other platforms that are deployed at predetermined depths. For example, wave gliders remain at the surface but can deploy

hydrophones at a fixed depth under the sea-surface; these gliders present similar speeds and the long survey duration typical of underwater gliders.

5.3.6 Comparing clicks vs click scans as cues

When click scans are used as cues, the cue counting method has increased variance compared to individual clicks, and the results depend more on the behaviour of the animal. Chapter 4 showed that the click scan cue counting approach overestimated the density by about 30%, which may stem from a potential error in estimating the average detection probability of the CS or from other assumptions for using this method for estimating number of animals. However, the distributions of click scans presented in this chapter along with information from the receiver can be used in a hidden Markov model approach to extract the probability of the click scan being a particular distance from the receiver, and as such a combination of distance sampling and cue-counting approach can be used be used (Buckland, personal communication). Hidden Markov models can also assist as well with assigning probabilities of number of individuals existing in a sequence of clicks where multiple animals are present.

5.4 Applications

Coordinated groups of autonomous underwater vehicles (AUVs) can provide significant benefit to a number of applications including ocean sampling, mapping, surveillance, and communication (Fiorelli et al., 2006). If those glider fleets are equipped with acoustic sensors, the combined data on acoustic densities from each glider can provide a reduced uncertainty of acoustic estimates if more platforms sample the same area, increasing the duration of cumulative effort in the area or reducing the time the platforms require to retrieve the same information. If glider fleets can be coordinated so that the receivers on multiple gliders can detect the same call, measurement of time differences of these arrivals can be used to derive an estimate of distances between the receivers and the animal. However, it is difficult to obtain accurate positions of the glider when it is submerged, which would make this estimation difficult and uncertain. The effect of measurement error for the distance between the animal and the receiver has been investigated by Marques (2003) and Borchers et al., (2010). Designers of surveys using fleets of gliders glider must plan the distance separating the gliders. This requires consideration of the effective acoustic radius of the

species of interest; when a survey is targeting more than one species, optimising the separation distance between platforms should consider the effective acoustic radii of all of the species. The simultaneous deployment of a fleet of acoustic gliders provides an opportunity of applying methodologies such as Spatially Explicit Capture Recapture Models (SECR). These SECR methods require simultaneous detection of an acoustic cue at multiple receivers, where the idea of "recapture" is accomplished when the same signal is detected on the different gliders. Time difference of arrival methodology then can be used to estimate the approximate distance from the animal to the receivers. This method has been used with a fixed microphone array for the density estimation of vocal animals (Stevenson et al., 2015). Even though the SECR methodology has been applied to stationary microphones, moving platforms with known locations provide "trap" occasions that can be thought of as changing position in time.

Furthermore, when it is possible to identify individuals through individually distinctive vocal cues, then recapture of the same individual can be considered when a single acoustic receiver such as an acoustic glider equipped with one acoustic sensor detects the same animal making the same call at different times and places. Recapture histories of the same individual can be assessed at different positions of the acoustic glider and so the effective sampling area (ESA) can be extracted. The depth dependent detectability of cues can be incorporated into the SECR methodology by taking into account the smooth function of detectability change in the algorithms of SECR as in Distriller et al., (2015). As the SECR methodology requires recapture of a signal, for acoustic cues that are not individually distinctive the only way to have recapture of the same signal is for it to be recorded at the same time by two different hydrophones. This can be achieved by a fleet of gliders operating in the same area and with more than one receiver close enough to detect the call (always relative to the species of interest).

Mitigation protocols for minimizing the impact of anthropogenic effects on marine mammals are of scientific interest and conservation concern. Acoustic methods are especially relevant for activities that produce noise that has the potential to impact the behaviour and physiology of the animals in the area of the activity. The size of the area of potential impact on animals depends on the type of activity and the noise levels produced. If the predicted impact zone is stationary and small enough then stationary acoustic buoys can cover the area. If the area that requires mitigation is very large compared to the detection range, gliders can provide a tool for large relative spatial coverage. The duration of the activity, the duration of any expected responses and the duration of expected return to baseline will define how long the activity

needs to be surveyed and the required duration for monitoring prior to and following the activity. A combination of fixed acoustic receivers and underwater gliders can give a better spatio-temporal sampling coverage of the area, by providing local points of ground truth regarding detections at specific spatial points.

Habitat preference studies for marine mammals have the potential to be improved by surveying marine mammals from underwater gliders, due to the real time environmental data that can be sampled throughout the water column by these platforms. Glider surveys with oceanographic sensors can identify oceanographic processes at different scales throughout the water column. Spatial modelling for habitat preferences for marine mammals has been well established (Miller et al., 2013). The environmental data used in these studies usually derives from satellite sensing which gives information mostly on the surface environment of the oceans. Most marine mammal species feed in waters deeper than the surface. Environmental data are sparse for the depths where they feed and these data usually don't coincide with the presence of animals during the survey. Gliders provide an opportunity to extract environmental data at the depths and locations where marine mammals are detected to be foraging. This provides better data for testing relationships between the presence of animals and the oceanographic processes existing at that particular time and place. These models may be expected to show a marked improvement over those incorporating only surface data. In addition, the use of more relevant data as covariates to cetacean abundance will allow stronger ecological inferences to be made than from previous models which were sometimes limited to selecting less relevant covariates because they were the only ones available.

5.5 Further work

Acoustic data are increasingly used for density estimation methods in marine mammal science. There are potential areas of future research that would assist our understanding of the nature of the animal's sonar and the interaction between echolocation behaviour and detection at the receivers. As a consequence, this understanding would allow for more precise estimates of the density and abundance of vocal animals.

More measurements of the transmit beampattern of echolocating animals would improve our estimates of off-axis attenuation, which would improve estimates of detection probabilities at off-axis angles. Thus far, models taking into consideration the beam profile of animals predict off-axis attenuation of the signal based upon fitting piston models to a few

measurements in the field. However, at least for the species presented here, more detailed data on beampattern exist (Shaffer et al., 2013). The latter study derived from bottom mounted hydrophones that were placed around 800m deeper than the foraging layer of the animals, this large range means that errors in estimating transmission loss will lead to uncertainty in the estimated source level. A 360° beam pattern for beaked whales would improve estimates for the detection function g(0) as well as products of the detection function such as the average detection probability. This in turn would improve estimates of abundance. This can be achieved by a methodology based on the one presented in chapter 2, with more receivers around the animal.

The detectability of different beaked whale populations as a function of receiver depth could be investigated further using DTAG deployments to provide this valuable information. The relationship between diving profiles of beaked whales and bathymetry can assist in predicting the optimal/foraging depth for populations that haven't been tagged and this can facilitate estimation of the P_a as a function of depth based on bathymetric information. For example, the depth distributions of the whales from the Bahamas and El Hierro for the data presented here can be used to identify if there is any pattern regarding foraging depth and bathymetry that can be tested on other datasets. Other variables that can predict the depth of Blainville's beaked whale prey could be used as well as a proxy for Blainville's foraging distribution. That would require information of prey species for different geographical locations and habitat preference studies for prey species. Stomach contents of dead beaked whales on different location can assist predicting the foraging depth of the whales if depth distribution of prey species found in the stomachs is available.

There are many vocal marine mammal species for which detectability is unknown or at least not statistically defined. For these populations, it is difficult to measure the area being surveyed acoustically, so abundance estimates are hard to extract. In an ocean environment with big changes and intense anthropogenic impact, detecting and quantifying the size of the populations is the first step towards quantifying our impact. Extraction of acoustic detection probabilities for other species using the methodology presented in chapter 2 can be applied if it is possible to tag the animals.

Available DTAG data from other species can be used in the same glider simulation methodology presented here to derive detection probabilities conditional on depth for glider surveys. For future surveys using gliders in a specific area, knowledge about the vocal behaviour of the species occupying the area can assist the optimization of the duty cycle for acoustic recordings, and the analysis of acoustic detections. In addition, the species-

detectability as a function of depth can assist classification algorithms taking in to account the probability of detection of each species as a function of depth in a Bayesian approach for a particular area. If knowledge of the species occupying an area exists, in addition to information about their detectability, then a cue counting approach based on a Bayesian approach could be applied. In that way, the false alarm rate, which would be derived from misclassifications from other species in the area, would be a function of depth as a result of the different depth detectability of the different species in the area.

Gliders should be used for habitat modelling of species, as they provide unique opportunities for sampling oceanographic data throughout the water column providing data simultaneous with whale detections to derive information on oceanographic processes such as thermal fronts, which are highly dynamic oceanographic features accumulating high nutrients that can drive the distribution of cetaceans and their prey. Furthermore, oceanographic data recorded on gliders can assist in predicting sound speed profiles. In cases where sound propagation models are used to estimate the distance from the vocalizing animal to the recorder then sound speed profiles can improve the estimation of distances and extract a more reliable acoustic detection function dependent on the species specific detectability and glider's spatial coverage.

Methods for analysing acoustic detections from gliders that have more than one hydrophone can provide opportunities for distance estimation and hence derive the detectability during the survey. This is a positive point as the detection function can change due to foraging behaviour and changes in animal depth distribution and clicking rate that are due to prey availability and prey depth distribution. In addition, the type of prey available at the time and consumed by the animal can affect parameters used in density estimation from acoustic cues. For example, if animals are feeding on denser prey during that particular time and place where the acoustic glider operates, this could lead to a higher number of buzzes and the pauses that follow the foraging attempt that could lead to lower clicking rates at the time of the survey. In addition, if animals at the particular time when the survey is conducted have a different depth distribution, that would affect the average detection probability as a function of glider depth. By being able to extract the distances from the animal to the receiver, the function of depth dependent detectability could be corrected and be unbiased for those particular survey methods to be used.

5.6 Conclusions

Density estimation of vocal animals is heavily dependent on extraction of parameters such as the vocalizing rate of the species, the detectability of the vocal cues as a function of distance between the animals and the receiver, and accurate distance estimation between the animals and the receivers. Depending on the platform used, different methodological approaches can be applied, although methodologies that are dependent on prior knowledge of parameters of species vocalization and depth distribution should confirm, if possible, that an effective way of deriving the parameters is chosen. For example, Warren et al., (2017) investigated click rates for two different beaked whale species and described spatio-temporal variation in click rates for Cuvier's beaked whales. DTAG deployments at different seasons and areas of the same species along with habitat preferences studies can assist density estimation of vocal animals.

5.7 References

Borchers, D., Marques, T., Gunnlaugsson, T. & Jupp, P. (2010) Estimating distance sampling detection functions when distances are measured with errors. Journal of Agricultural Biological and Environmental Statistics, 15, 346-361.

Distiller, G. & Borchers, D.L. (2015) A spatially explicit capture-recapture estimator for single-catch traps. Ecology and Evolution, 5, 5075-5087.

Marques, T.A., Thomas, L., Martin, S.W., Mellinger, D.K., Jarvis, S., Morrissey, R.P., Ciminello, C.A. & DiMarzio, N. (2012) Spatially explicit capture-recapture methods to estimate minke whale density from data collected at bottom-mounted hydrophones. Journal of Ornithology, 152, S445-S455.

Miller, D.L., Burt, M.L., Rexstad, E.A. & Thomas, L. (2013) Spatial models for distance sampling data: recent developments and future directions. Methods in Ecology and Evolution, 4, 1001-1010.

Shaffer, J.W., Moretti, D., Jarvis, S., Tyack, P. & Johnson, M. (2013) Effective beam pattern of the Blainville's beaked whale (*Mesoplodon densirostris*) and implications for passive acoustic monitoring. Journal of the Acoustical Society of America, 133, 1770-1784.

Warren, V.E., Marques, T.A., Harris, D., Thomas, L., Tyack, P.L., de Soto, N.A., Hickmott, L.S. & Johnson, M.P. (2017) Spatio-temporal variation in click production rates of beaked whales: implications for passive acoustic density estimation. The Journal of the Acoustical Society of America, 141, 1962-1974.